Schulich
MEDICINE & DENTISTRY

Oncology Research & Education Day 2025

Plenary Speaker:

Dr. Diwakar Davar
Hematologist and Medical Oncologist, UPMC.

Thursday, June 12, 2025

8.30 AM - 5.00 PM

BEST WESTERN LAMPLIGHTER INN

Register now at :

https://www.schulich.uwo.ca/oncology/index.html

TRAINEE SPEAKER LINEUP

SPEAKER 1

Edward Wang
MD/PhD Candidate

SPEAKER 2

Petra Samardzija
PhD Candidate

SPEAKER 3

Tiffany Cheung
MSc. Candidate

SPEAKER 4

Shengjie Ying
MD/PhD Candidate

SPEAKER 5

Michael Touma
Research Assistant

SPEAKER 6

Zainab Zahra
Undergraduate Student

SPEAKER 7

Leslie Ogilvie
Post Doc Associate

SPEAKER 8

Saurav Verma
Clinical Fellow

Schulich MEDICINE & DENTISTRY | London Health Sciences Centre Research Institute | LAWSON Research Institute ST. JOSEPH'S HEALTH CARE LONDON | Western Centre for Translational Cancer Research

21st Annual Oncology Research & Education Day

Co-Chairs: Daniel Breadner MD. FRCPC. and Saman Maleki PhD.

Thursday, June 12, 2025 8:30 AM – 5:00 PM

(Breakfast starts at 7:45 am)

Best Western Lamplighter Inn, Crystal Ballroom, Regency Room, Chelsea Room, and Atrium
591 Wellington Rd. S., London, Ontario, N6C4R3

AGENDA

7:45 – 9:00	**REGISTRATION AND OPENING REMARKS** ***Atrium & Crystal Ballroom***
7:45	**Registration and Breakfast** Please register and enjoy a light breakfast while networking with colleagues.
8:30	**Welcome and Opening Remarks** Daniel Breadner MD. FRCPC. and Saman Maleki PhD. - Conference Co-Chairs Robert Bartha PhD – Vice Dean, Research and Innovation, Schulich School of Medicine & Dentistry John MacFarlane - President & CEO, London Health Sciences Foundation Michael Ott MD. FRCSC. - Department of Oncology Chair and Physician Executive Oncology LHSC Kirk Baines – Philanthropist & Founder, Baines Centre for Translational Cancer Research
9:00 – 10:00	**MORNING ORAL PRESENTATIONS** **Judges: Drs. Alison Allan, Diwakar Davar, and Lisa Porter** ***Crystal Ballroom***
9:00	**1**. Towards an Open Source Fully Automated Treatment Planning Pipeline for Multi-Target Lung Stereotactic Ablative Body Radiotherapy. Edward Wang MD/PhD Candidate
9:15	**2.** Examining calcium signaling pathways in PDAC using patient-derived organoids and cancer-associated fibroblasts. Petra Samardzija PhD Candidate
9:30	**3.** Unintended Immunosuppression: Antibiotic Disruption of Gut Microbiota in Mismatch Repair-Deficient Tumours. Tiffany Cheung MSc. Candidate
9:45	**4.** Single cell characterization of head and neck cancer reveals the association of T cell exhaustion and cytotoxicity with disease recurrence and chemoradiation exposure. Shengjie Ying MD/PhD Candidate
10:00 – 11:30	**POSTER AND NETWORKING SESSION (Odd Numbers)** ***Regency and Chelsea Conference Rooms & Atrium***
10:00 - 11:30	**Poster Viewing and Judging (Regency and Chelsea Conference Rooms)** **Please enjoy refreshments and light snack (Atrium)**
11:30 – 12:30	**KEYNOTE LECTURE – Crystal Ballroom** **"Uncovering metagenomic signatures of response, and resistance to immunotherapy; the Rosetta Stone of our age"** **Diwakar Davar MD. MS.** **Objectives: 1. Understanding metagenomic signatures of response, resistance and irAE development in ICI treated melanoma; 2. Understanding that metagenomic signatures are ICI-regimen specific, 3. Using AI and ML to more accurately identify ICI-responders.**
12:30 – 1:30	**LUNCH** ***Crystal Ballroom & Atrium***

1:30 –2:30	**AFTERNOON ORAL PRESENTATIONS** **Judges: Drs. Alison Allan, Diwakar Davar, and Lisa Porter** ***Crystal Ballroom***
1:30	**5.** Examining Factors Affecting Clinical Trial Enrolment in the Clinical Trials Navigator Program. Michael Touma MD, Research Assistant.
1:45	**6.** Quantification of respiratory-induced errors in Stereotactic Ablative Radiotherapy for lung cancer using 4D-CT imaging. Zainab Zahra Undergraduate Student.
2:00	**7.** Novel anti-angiogenic compound elicits anti-tumour lymphocyte response in peripheral blood and ascites leading to disease regression in advanced-stage epithelial ovarian cancer. Leslie Ogilvie Postdoctoral Associate.
2:15	**8.** Impact of Stereotactic Ablative Radiotherapy (SABR) on Detection of ctDNA in Patients with Early-Stage Lung Cancer – Interim Findings from the Prospective SABR-DETECT Trial. Saurav Verma MD, Clinical Fellow.
2:30 – 3:00	**Panel Discussion** ***Enhancing Translational Research in London: Building Bridges Between Science and Medicine*** ***Moderator: Saman Maleki*** ***Features: Daniel Breadner, Rohann Correa, Diwakar Davar, Nicole Dearing, Sarah Mattonen, Anthony Nichols***
3:00 – 4:30	**POSTER & NETWORKING SESSION – (Even Numbers)** ***Regency & Chelsey Conference Rooms & Atrium***
3:00 – 4:30	**Poster Viewing and Judging (Regency and Chelsea Conference Rooms)** **Please enjoy refreshments and light snack (Atrium)**
4:30 – 5:00	**Award Ceremony**
4:30	**Presentation of Awards** Michael Ott - *Department of Oncology, Excellence in Academic and Teaching Awards (5)* Morgan Black - *Denise Power Cancer Research Staff Award of Excellence* Daniel Breadner and Saman Maleki - *Oral and Poster Presentation Awards*
5:00	**Concluding Remarks, Adjournment and Introduction of 2026 event co-leads** Daniel Breadner and Saman Maleki

**This program has received an educational grant or in-kind support from: Gold Sponsors: AstraZeneca, GSK, Lilly, Novartis. Silver Sponsors: AbbVie, Amgen, Astella, Bristol Myers Squibb, Daiichi-Sankyo AstraZeneca, EMD Serono, Eisai, Knight Therapeutics, Pfizer Oncology, Recordati Rare Diseases, Servier. Bronze Sponsors: Ipsen, Johnson & Johnson Innovative Medicine, Roche, Takeda.*

Poster Numbers (Alphabetical Order)

Poster	First Name	Last Name	Poster	First Name	Last Name	Poster	First Name	Last Name
43	Fatema	Abdullatif	72	Charles	Jia	8	Jeri	Spilberg
61	Laurice	Arayan (Creation….)	34	Tiffany	Johnston	55	Dan	Stefan
64	Laurice	Arayan (Standard...)	71	Leah	Kanee	58	isabella	Tait
47	Kelly	Baines	30	Rehanna	Kanji	11	Cornelia	Tolg
17	Fatemeh	Behjati Ardakani	12	Isabel	Kannampuzha	40	Emily	Tomas
80	Sari	Belzycki	35	Chanpreet	Kaur Riarh	65	Christina	Trieu
104	Pratibha	Bhai	62	Saqib	Khan	73	Kyla	Trinh
87	Noah	Blackburn-Hum	27	Bartlomiej	Kolendowski	33	Maria	Uribe Estrada
10	Mickenzie	Blayne Martin	89	Sarah	Konermann	2	Alejandra	Varela Jimenez
36	Alyssa	Bogle	26	Yee Wing	Kwok	76	Francesco	Vito
31	Natasha	Bruce	105	Carolyn	Lauzon-Young	9	Jack	Webb
28	Adrian	Buensuceso	54	Stephanie	Leighton	22	Alyssa	Wu
5	Joseph William	Butler	57	Ginnian	Leung	48	George	Xie
81	Erica	Chi Yan Lo	44	Sylvia	Lin Cheng	70	Inci	Yaman Bajin
96	Farley	Chicilo	50	Milan	Lobana	18	Kasha	Yan Mansour
91	Cristian	Ciciretto	101	Alana	Lopes	102	Justin (Haechan)	Yang
20	Chloe	Davidson	32	Vera	Luo	88	Timothy	Yau
98	Danny	De Sarno	74	Sarah	Ma	13	Tony	Zhang
86	David	DeVries	82	Celeste	MacDonald	100	Helen (Jiahai)	Zhou
14	Stephanie	Dinescu	59	Mahnoor	Malik			
66	Mina	Djuketic	3	Jeffery	Martin			
1	Anamika	Dutta	60	Amn	Marwaha			
63	Muhammad	El-Kassem	24	Sarah Elaine	McArthur			
67	Abdulla	Elsaleh	25	Liam	Mcfarlane			
56	Andris	Evans	90	Marcus	Milantoni			
37	Elizabeth	Fenton	93	Ahmed	Mohamed			
95	Nitara	Fernando	16	Fatemeh	Mousavi			
38	Bianca	Garlisi	49	Nhi	Nguyen Le			
46	Blane	Gebreyes	39	Maria	Nica			
92	Shahin	Ghaseminejad	4	Huilin	Niu			
45	Andrei	Glogov	68	Mathew	Oirschot			
19	Anayra de Fatima	Goncalves Santiago	78	Ria	Patel			
41	Brianna	Gonga-Cave	7	Urvi	Patel			
97	Emma (Haoyue)	Guo	15	Joana	Ribeiro Pinto			
69	Danial	Hadi	51	Vanessa	Riolo			
52	Oneeb	Hassan	42	Noor	Rizvi			
99	Sophie	Heinrich	85	Owen	Rodrigues			
79	Olla	Hilal	84	Raman	Sambhi			
21	Megan	Hong	83	Joseph	Samuel			
77	Amir	Hossein Karimi	94	Christine	Santiago			
29	Matthew	Huver	75	Anorin	Shadi Ali			
6	Erin	Iredale	23	Ye	Shen			
53	Behnam	Jabbarizadeh	103	Alexa	Smith			

Towards an Open Source Fully Automated Treatment Planning Pipeline for Multi-Target Lung Stereotactic Ablative Body Radiotherapy

Edward Wang,[1] Timothy Yau[1], Pencilla Lang,[2] Sarah A. Mattonen[1,3]

[1]Department of Medical Biophysics, Western University, [2]Verspeeten Family Cancer Centre, London Health Sciences Centre, [3]Department of Oncology, Western University

Introduction: Stereotactic ablative body radiotherapy (SABR) delivers high dose, hypofractionated radiation and is used in the treatment of metastatic cancer, either treating multiple synchronous lesions or in the retreatment setting. Multi-lesion treatment entails substantially increased treatment planning resources, as they often require plans with multiple isocenters and different fractionations across all targets. With growing adoption, reducing planning workload is essential. A widely investigated approach of treatment planning automation is to use a machine learning model to predict a 3-dimensional dose distribution, which is then used as the optimization target in inverse planning (IP). However, these techniques are predominantly limited to single lesion plans and rely on proprietary software. In this work, we present a fully open-source pipeline for automated treatment planning in the metastatic setting.

Methods: Radiation treatment plans were collected for patients who received single lesion and multi-lesion lung SABR at a single tertiary institution. Multi-lesion plans consisting of treatments to multiple-isocenters were decomposed to their individual isocenter components. For dose prediction, we trained a generative adversarial network (GAN) that utilized three channels as input: the planning CT scan, a structure map containing organs at risk (OARs) and all planning target volumes (PTVs) from previous treatments and simultaneous treatments, and a binary mask of current isocenter PTV(s) scaled with their prescriptions. The per-isocenter multi-lesion dataset was divided into 80% for training, and 20% for testing, with patients confined to a single split. All single-lesion plans were used in training. We modified the open-source treatment planning system matRad to perform IP for co-planar 2-arc volumetric modulated arc therapy using the predicted dose distributions as the optimization target. IP was performed separately for each isocenter plan for a given patient, and the resulting optimized doses were summed to create a cumulative fully automated dose (FAD) for each patient.

Results: In total, 244 single lesion plans and 257 multi-lesion plans were collected. The multi-lesion plans were separated into 531 single-isocenter plans (training n=423, testing n =108). The 108 single-isocenter test plans corresponded to 53 patient cases. The average mean absolute differences and gamma pass fractions between the test-set GAN predicted and clinical dose distributions were <1 Gy and >90 % across all OARs respectively. 51% of the treatment plans generated using the fully automated pipeline met all dose constraints, increasing to 55% when only considering hard constraints. Notably, only 60% of clinical plans met all constraints. As shown in Figure 1, the FAD improved on the clinical dose in some cases.

Discussion:

We present an open-source pipeline for fully automated treatment planning of multi-lesion lung SABR. To our knowledge this work is the first application of this approach in the multi-target metastatic setting. The presented pipeline has the potential to significantly decrease the human resources required in treatment planning, alleviating resource burden. Currently, the dose constraint pass rates of the FAD are slightly lower compared to clinical plans. Future work to improve the quality of the FAD include training more accurate prediction models, as well as incorporating clinical constraints into IP.

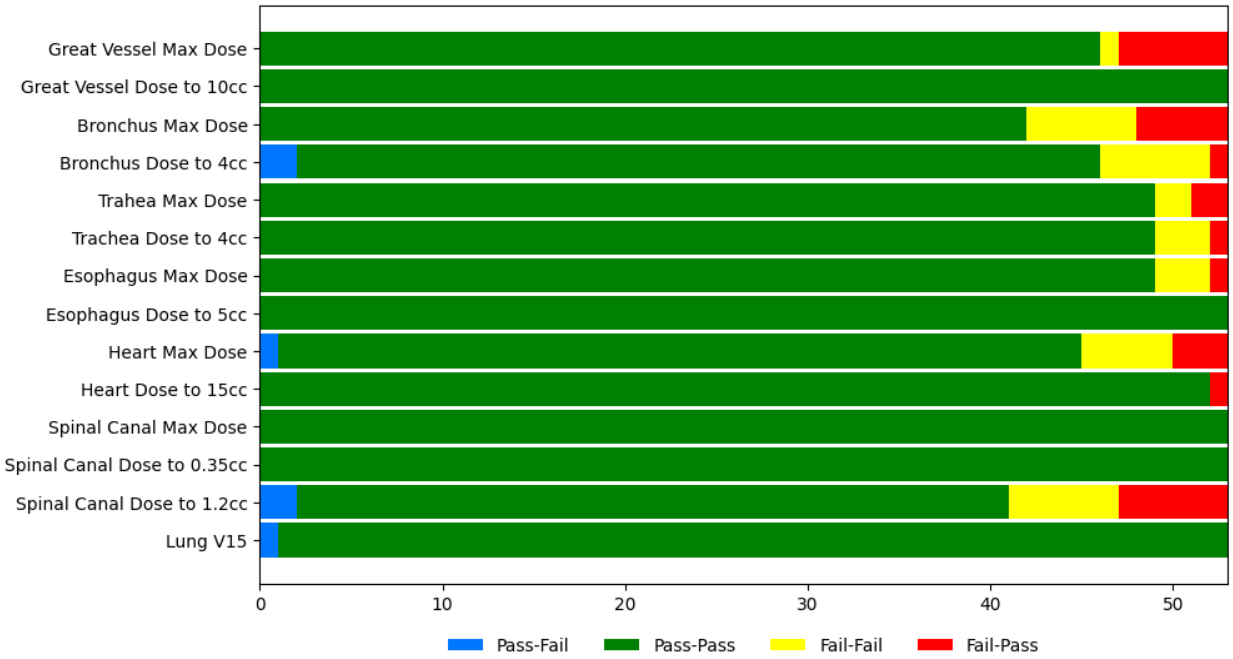

Figure 1: The number of passing and failing optimized constraints for the 53 test-set plans are shown. Blue indicates fully automated dose (FAD) meeting the constraints while the clinical dose fails. Green represents both meeting constraints, yellow indicates both failing, and red shows the FAD failing while the clinical dose meets constraints.

Oral #2

Examining calcium signaling pathways in PDAC using patient-derived organoids and cancer associated fibroblasts

Petra Samardzija[1], Emilie Jaune-Pons[1,4], Fatemeh B. Ardakani[4], Courtney Brooks[1,4], Peter B. Stathopulos[1], Christopher L. Pin[1-4].
Departments of [1]Physiology and Pharmacology, [2]Oncology, and [3]Paediatrics, Schulich School of Medicine and Dentistry, University of Western Ontario, [4]Verspeeten Family Cancer Centre and Baker Centre for Pancreatic Cancer, Lawson Health Research Institute, London, Ontario, Canada.

Introduction: Pancreatic ductal adenocarcinoma (PDAC) is the 3rd leading cause of cancer-related death in Canada, with a five-year survival rate of ~12%. The poor prognosis of PDAC is largely due to late detection and poor response to chemotherapy. Therefore, there is a critical need to identify novel biomarkers and therapeutic targets that could be used in a patient-specific fashion. Calcium (Ca^{2+}) is an essential second messenger required for integrating signals from the extracellular environment with regulation of signaling proteins, transcription factors and enzyme secretion. In cancer, elevated Ca^{2+} influx through ORAI1 channels at the plasma membrane via both store-operated (SOCE) and store-independent Ca^{2+} entry (SICE) pathways drives cell migration, proliferation and chemoresistance. While SOCE and SICE have emerged as promising therapeutic targets in various cancers, their specific roles in PDAC remain poorly understood. We hypothesize that SOCE and SICE promote increased aggressiveness and resistance in PDAC tumours.

Methods: The expression of SOCE and SICE modulators, ORAI1, STIM1, SPCA2 and CCDC47, were examined using RNA sequencing in wild-type mouse pancreatic acinar cells, pancreatic organoids derived from mice expressing oncogenic KRAS (*Ptf1a*$^{creERT/+}$*Kras*$^{G12D/+}$), the Cancer Genome Atlas (TCGA) database, patient-derived organoids (PDOs) and cancer associated fibroblasts (CAFs) derived from endoscopic biopsies of pancreatic cancer patients. Immunofluorescence staining on PDOs grown in Matrigel™ domes was performed to visualize protein expression of the Ca^{2+} regulators. Plasmids encoding CCDC47 and SPCA2 were electroporated into PDOs and growth was assessed. Ratiometric Fura2 imaging was used to examine SICE and SOCE in CAFs with and without cancer cells.

Results: RNA sequencing revealed a change in the expression of SOCE between normal pancreatic tissue and *Ptf1a*$^{creERT/+}$*Kras*$^{G12D/+}$ including the expression of full-length SPCA2 and increased expression of CCDC47 and ORAI1. PDOs displaying a more classical and ductal phenotype showed increased expression of SPCA2 compared to organoids with a more basal and mesenchymal phenotype. Preliminary analysis of CAFs with and without cancer cells showed differences in Ca^{2+} handling suggesting intercellular communication within tumours affect Ca^{2+} signalling.

Conclusions: These results suggest expression of SOCE and SICE mediators is increased during progression from normal to neoplastic cells. We also show variations in Ca^{2+} handling between patient samples that could be affected by intercellular communication. This information is critical if targeting Ca^{2+} signaling pathways are to be used for potential diagnostic and therapeutic targets in PDAC.

Oral #3

Exploring gut microbiota-related changes in antitumour immune response induced by antibiotic use in mismatch repair-deficient tumours

Tiffany Cheung[1], Gholami H[1], Jabbarizadeh B[2], Figueredo R[3], Baines KJ[1], Hong MMY[1], Davidson C[1], Maleki Vareki S[1,2,3,4]

[1] Department of Pathology and Laboratory Medicine, Western University

[2] Verspeeten Family Cancer Centre, Lawson Health Research Institute

[3] Department of Oncology, Western University

[4] Department of Medical Biophysics, Western University

Introduction: Immune checkpoint inhibitors (ICIs) treat cancer by enhancing the host's existing antitumour T-cell responses. However, antitumour immunity is influenced by the host gut microbiota, as certain commensal species and their metabolites have been linked to ICI response or nonresponse. Antibiotic use induces gut dysbiosis and has been linked to worse outcomes in ICI patients in multiple cancer types. Our lab has previously found that antibiotics promote tumour growth in a preclinical model of neuroblastoma, a pediatric cancer of the nervous system. This occurred in parallel with reduced T cell infiltration and increased intratumoral T cell dysfunction and exhaustion. However, it is unknown whether the enrichment of opportunistic species or the depletion of beneficial species following antibiotic depletion are driving ICI resistance. We hypothesized that antibiotics modulate the gut microbiota to hinder antitumour immunity and aim to validate the effect on tumour growth in a preclinical model of colorectal cancer.

Methods: Mice were administered an antibiotic cocktail (vancomycin, neomycin, ampicillin, metronidazole) or vehicle control for 10 days followed by subcutaneous injection of neuroblastoma (Neuro-2a) or colorectal cancer (MC38) cells. Stool samples were collected at baseline, 10 days and 29 days post-antibiotic treatment for shotgun metagenomic sequencing and taxonomic profiling with MetaPhlan4. Tumour and spleen tissues were processed into single-cell suspensions for T cell profiling by flow cytometry analysis.

Results: Antibiotics induced sustained changes in the gut microbiota composition of neuroblastoma tumour-bearing mice, reducing alpha diversity and shifted beta diversity up to 1-month post-treatment. This also resulted in the sustained depletion of many commensal species, while some opportunistic species persisted. Interestingly, many species characterized by MetaPhlan4 were novel species that were not previously identified by the NCBI Taxonomy Database. Additionally, antibiotics exacerbated colorectal cancer growth similarly to the neuroblastoma model, though there was no impact on intertumoral T-cells.

Discussion: These findings reveal the impact of antibiotics on gut microbiota composition while underscoring the need for further characterization of the mouse gut bacterial species to understand their metabolic functions in the gut. The difference in immune profiles between different tumour models suggest that the effect of antibiotics on antitumour immunity varies between cancer types and mouse strains. Given that cancer patients are more susceptible to infections, which increases the likelihood of antibiotic use, these results emphasize the judicious use of antibiotics in cancer patients.

Keywords: antibiotics, gut microbiota, neuroblastoma, immunotherapy, metagenomics, immune checkpoint inhibitors

Single cell characterization of head and neck cancer reveals association of T cell exhaustion and cytotoxicity with disease recurrence and chemoradiation exposure

Authors: **Shengjie Ying**[1,2], Peter YF Zeng[1,2], John W Barrett[1,2], Halema Khan[1,2], Krista Joris[1,2], Amir Karimi[1,2], Nhi Le[1,2], Matthew J Cecchini[1,2], Kevin Fung[1,2], Joe Mymryk[1], Anthony C Nichols[1,2]

1. Department of Otolaryngology – Head & Neck Surgery, Western University, London, Ontario, Canada
2. Department of Pathology and Laboratory Medicine, Western University, London, Ontario, Canada

Introduction: Head and neck squamous cell carcinoma (HNSCC) is the seventh most common malignancy worldwide, and a subtype related to human papillomavirus (HPV) infection is the fastest rising cancer in Canada. Current standard of care involves surgical resection of the primary tumour and/or chemoradiation therapy, with anti-PD1 immunotherapy approved only in the recurrent/metastatic setting. Previous single cell analyses have characterized heterogenous cell type compositions in HNSCC, however, have not compared clinical outcomes or standard treatment effects. We aimed to assess differences in the tumour microenvironment at a single cell resolution in HNSCC tumours of patients with recurrent and non-recurrent disease obtained before and after chemoradiation treatment (Figure 1A).

Methods: We performed single nucleus RNA sequencing using Chromium 3' reagent kits (10X genomics) for 28 frozen primary tumour samples of oropharyngeal HNSCC (n=26 HPV+, n=2 HPV-). Reads were aligned using CellRanger v9 followed by ambient RNA removal using CellBender. SCANPY was used to perform quality control, normalization, clustering, and cell type annotation. Cell type proportions were compared using a Wilcoxon signed-rank test.

Results: 28 primary tumour samples were categorized into three groups, comprising of samples obtained prior to the treatment of the initial tumour from patients who had non-recurrent disease ("pre-treatment non-recurrent"; pre-tx-NR; n=16) and who later developed recurrent disease ("pre-treatment recurrent"; pre-tx-R; n=4), and samples obtained from the recurrent tumour of patients who received prior chemoradiation therapy ("post-treatment recurrent"; post-tx-R; n=8) (Figure 1A). Following stringent quality control 183,388 nuclei were retained. Comparison of major cell types found that the pre-tx-NR and pre-tx-R groups had significantly greater abundance of B cells, plasma cells, and dendritic cells compared to the post-tx-R group (all $p<0.05$) (Figure 1B and C). To investigate the potential relevance of immune checkpoint receptor expression, we re-clustered the CD8 T cells and identified four subtypes (Figure 1D) characterized by, Cluster 0) a non-exhausted phenotype with high expression of granzyme K (c0_TNEx_GZMK), Cluster 1) high expression of exhaustion markers (PD-1, LAG-3, TIM-3) and cytotoxicity markers (granzyme B, interferon-gamma) (c1_TEx_ctxHi), Cluster 2) relatively lower expression of exhaustion and cytotoxicity markers (c2_TEx_ctxLo), and Cluster 3) a proliferative phenotype with high expression of Ki-67 (c3_TEx_CtxPro). We found that the pre-tx-R group had a higher proportion of c0_TNEx_GZMK compared to the pre-tx-NR ($p=0.08$) and post-tx-R ($p<0.01$) groups, and was depleted for both c1_TEx_ctxHi and c2_TEx_ctxLo subtypes (Figure 1E). Interestingly, compared to the pre-tx-R group, the post-tx-R group was enriched for c2_TEx_CtxHi cells ($p<0.01$) whereas the pre-tx-NR group was enriched for c1_TEx_CtxLo cells ($p=0.06$) (Figure 1E).

Discussion: We identified differences in the composition of major cell types and CD8 T cell subtypes in patients with HNSCC related to disease recurrence and treatment exposure. A granzyme K positive, non-exhausted CD8 T cell phenotype was most abundant in pre-treatment samples from patients who later developed recurrence. In contrast, higher co-expression of exhaustion and cytotoxicity signatures were

identified in the pre-treatment non-recurrent and post-treatment samples. These findings have implications for selection the of HNSCC patients for immunotherapy and optimal timing of immunotherapy administration.

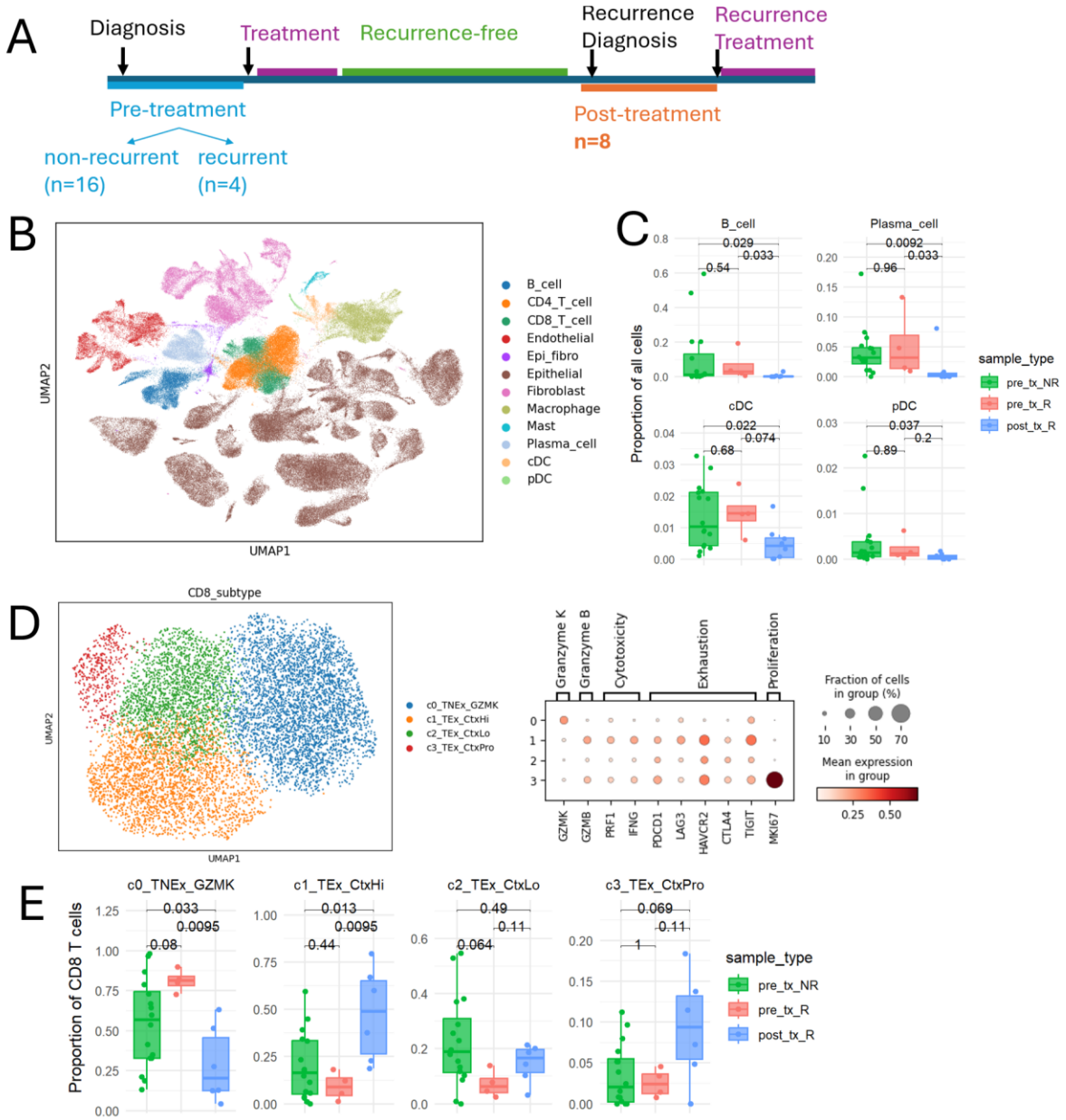

Figure 1. A) Overview of samples collected for snRNAseq from patients with HNSCC (n=28) with recurrent and non-recurrent disease, pre- or post-chemoradiation treatment. **B)** UMAP of 183,388 single nuclei annotated with major cell types. **C)** Major cell types with significantly different abundance between sample types. **D)** CD8 T cell subtypes defined based on immune checkpoint receptor/exhaustion, cytotoxicity, and proliferation markers. **E)** Comparison of CD8 T cell subtype abundance between sample types, among samples with >10 CD8 T cells.

Oral #5

Examining Factors Affecting Clinical Trial Enrolment in the Clinical Trials Navigator Program

Govana Sadik[1], Michael Touma[2], Renee Nassar[2], Milica Paunic[3], Mahmoud Hossami[2], Olla Hilal[4], Roaa Hirmiz[2], Depen Sharma[5], Anthony Luginaah[6], Pratham Gupta[4], Swati Kalia[2], Christina Trieu[7], Salah Alhajsaleh[7], Anaam Jaet[7], Ria Patel[7], Gregory Charalambos Anagnostopoulos[6], Megan Delisle[8,9], Laurice Togonon Arayan[10], Caroline Hamm[2,7,10]

1. Department of Biological Sciences, University of Windsor 2. Clinical Trials Navigator Inc, Windsor ON 3. Faculty of Medicine, University of Toronto 4. Department of Medical Sciences, Western University 5. Faculty of Medicine, University of Ottawa 6. Faculty of Medicine, Western University 7. Department of Biomedical Sciences, University of Windsor 8. Department of Surgery, University of Manitoba, Winnipeg, MB 9.Paul Albrechtsen CancerCare Manitoba Research Institute, Winnipeg, MB 10. Department of Oncology, Western University, Windsor Campus, Windsor ON

Introduction: Oncology clinical trial accrual rates are estimated to be around 5%, despite the potential benefits patients could receive on a clinical trial. Many factors contribute to whether a patient is successfully enrolled onto a clinical trial. The Clinical Trials Navigator (CTN) Program helps oncology patients identify clinical trials. We analyzed program and patient characteristics to determine features of successful enrollment.

Methods: A retrospective study was conducted. From March 2019 to April 2024, 411 records from the CTN program were analyzed. Of the 411, 73 were referred to a clinical trial. 14 of the 73 were enrolled onto a trial. The characteristics evaluated for the 14 enrolled and the 59 non-enrolled patients were: age, distance from home center to clinical trial site, CTN processing time, and time of initial CTN application to death. For the non-enrolled, the reason for non-enrollment was recorded. For the enrolled, the type of trial, trial phase and discipline were recorded. All comparative values were analyzed using a Welch's T-test.

Results: Comparison of the data between the enrolled and non-enrolled revealed that the average age was similar between both groups with the enrolled being 61 years, and non-enrolled being 57 years (p=0.154). The mean distance from home center to clinical trial site was 332.9 kilometers (km) for enrolled and 407.6 km for non-enrolled (p= 0.152). The CTN processing time for the enrolled group had a mean time of 4.1 days and the non-enrolled had a mean time of 12.5 days (p= 0.002). The time of initial CTN application to death for the enrolled group had a mean of 17.4 months and the non-enrolled had a mean 7.9 months. (p= 0.0051). For the non-enrolled group, the reason for non-enrollment was centre specific (60.1%) or patient specific (39.9%). The centre specific reasons included: non-eligibility (45%), trial no longer available (31%), centre declined (16%), COVID-19 delays (5%), not accepting patients (3%). The patient specific reasons included, the patient: passed away during the process (48%), sought alternative treatment (19%), declined (24%), lost to follow up (9%). For the enrolled group, the trial types were interventional (71%) and next generation sequencing (NGS) (29%). Enrollment of patients by phase of trial were as followed: three phase I (21.4%), two phase I/II (14.3%), three phase II (21.4%), one phase II/III (7.1%), one phase III (7.1%), and four NGS (28.6%).

Conclusion: These findings highlight some of the unique barriers and opportunities for patients in patient-centered clinical trials enrollment. The importance of the efficiency of the CTN program is highlighted. Almost one-third of patients were enrolled in phase I or phase I/II trials, demonstrating patient's willingness to travel for early phase trials. Early referral in the patient journey, inclusion of all phases of trials and efficient patient processing will lead to higher clinical trials accrual.

Quantification of respiratory-induced errors in Stereotactic Ablative Body Radiotherapy for lung cancer using 4D CT imaging

Zainab Zahra[1,2], Timothy Yau[1,2], Stewart Gaede[1,2]
[1]Western University; [2]London Health Sciences Centre

Introduction: Currently, stereotactic ablative body radiotherapy (SABR) is typically prescribed for inoperable early-stage lung cancer patients due to its improved survival outcomes.[i] When using radiation therapy for tumours exhibiting moderate motion in lung cancer, a motion encompassment technique is often used to treat the total extent of tumour motion over the patient's entire breathing cycle (Internal target volume). However, treatments are planned on a static time-averaged CT dataset, which do not account for tumour motion and assumes instantaneous delivery of the entire treatment to the volume encompassing the total tumour motion. For treatment deliveries using volumetric modulated arc therapy (VMAT), the interplay between the nonuniform photon fluence and tumour motion may lead to reduced tumour coverage.[ii] To quantify the discrepancy between prescribed doses relative to actual tumour coverage, this retrospective analysis investigates the interplay effects of 3D-CT based planning by comparing it to recalculated dose distributions derived from 4D CT imaging.

Methods: Eight patients with early-stage non-small cell lung cancer (NSCLC) previously treated with wide-amplitude gated SABR, characterized by 5–14mm of tumour motion, were analyzed in this study. Patients were anonymized through MIM v7.2.8 An in-house MATLAB script generated six sub-plans corresponding to each phase of the patient's free breathing cycle.[iii] These subplans were used to calculate phase-specific dose distributions across the full 4D-CT dataset using AcurosXB in Eclipse v15.6, to simulate dose delivery with respiratory motion. To account for anatomical changes across different phases, a deformable image registration technique was applied using MIM. The dose distributions were then summed onto two reference CT scans – at end-inhale and end-exhale – to compare against the prescription dose distribution. Dose-Volume Histograms were generated for both original and recalculated plans, evaluating D_{95}, the minimum dose received by at least 95% of the GTV. Additionally, GTV to IGTV ratios and mean Hounsfield Unit (HU) values were evaluated across cases.

Results: The recalculated dose distributions yielded comparable results to the original 3D dose distributions. Among the eight patients analyzed, the observed D_{95} ratio (recalculated D_{95}/original D_{95}) for both end-inhale and end-exhale accumulated dose varied across cases, from 0.86 to 1.08. Notably, two cases exhibited substantial reductions in D_{95} (≤0.93), suggesting cold spots in tumour coverage, while patients with values over 1.05 indicate areas receiving higher-than-prescribed dose, potentially increasing the risk of tissue toxicity (Fig.1). Further analysis of target volumes revealed a wide range in recalculated GTV to original ITV volumes (25%–93%). Mean CT tissue densities of the GTV to the ITV ranged from 0.3% to 58%. While some correlations can be drawn, these findings demonstrate that no one factor solely influences the changes to dose distribution.

Conclusion: The results of this study indicate both potential underdosing and overdosing due to respiratory motion, reflecting interplay effects on dose accumulation using 4D-CT based planning. Dose recalculations resulted in errors greater than 10% with variation between end-inhale and end-exhale dose accumulation. By incorporating respiratory motion, 4D-CT-based dose analysis can be utilized for quantifying dose discrepancies and enabling more precise evaluation of interplay effects in VMAT SABR treatment planning.

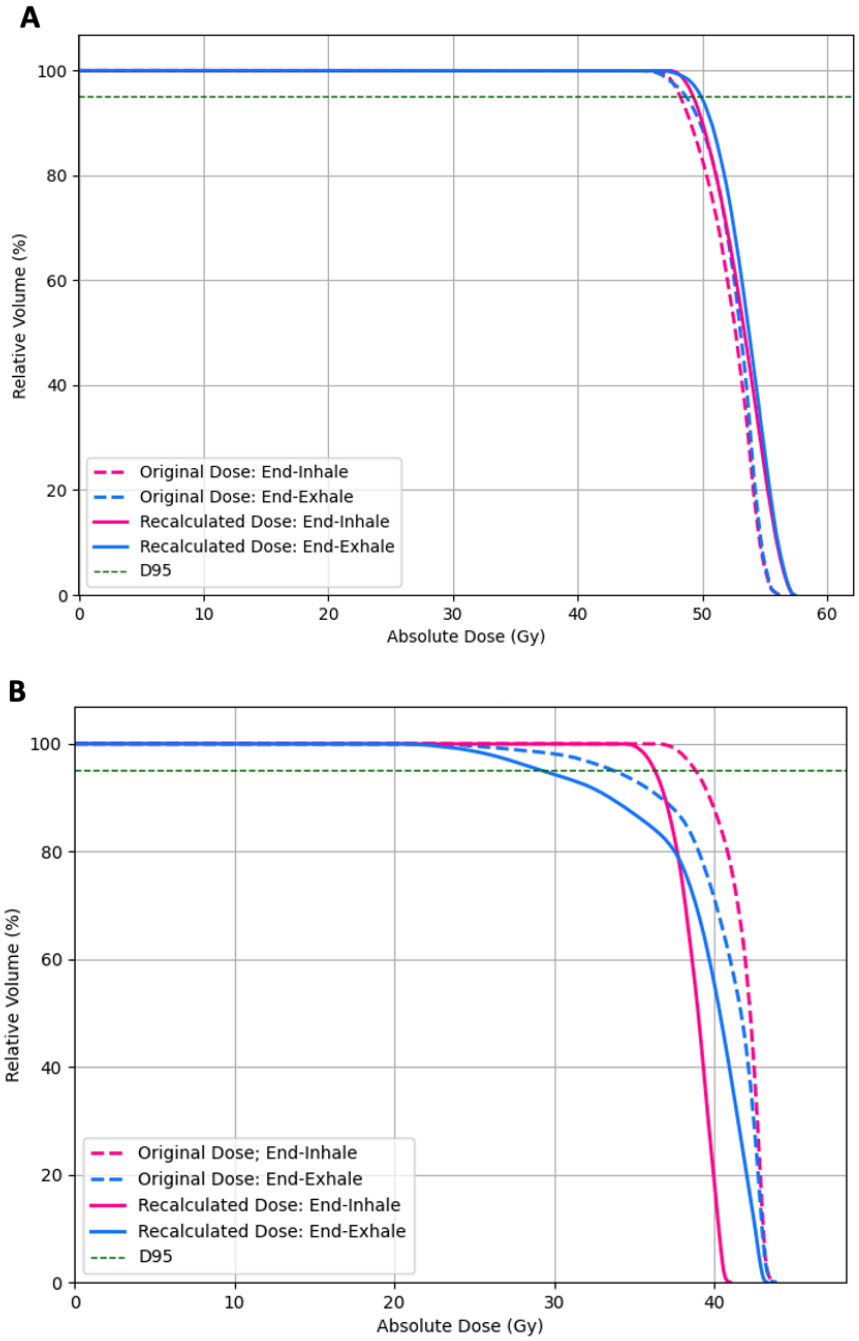

***Figure 1**: Dose-volume histograms of two patients' relative gross tumour volumes (GTV) of original and recalculated dose distributions at the end-inhale and end-exhale of their breathing cycles. Patient A demonstrates overdosing while patient B's DVH suggests underdosage. Minimum dose covering at least 95% of the volumes is represented by the green dotted line (D95).*

[i] Shamp SJ, Sheikh S, Chang T, et al. Stereotactic body radiotherapy (SBRT) for T2N0 (>3 cm) non-small cell lung cancer: Outcomes and failure patterns. *Journal of Radiosurgery and SBRT*. 2021;7(4):271. Accessed March 9, 2025. https://pmc.ncbi.nlm.nih.gov/articles/PMC8492054/

[ii] Keall PJ, Kini VR, Vedam SS, Mohan R. Motion adaptive x-ray therapy: a feasibility study. *Physics in Medicine and Biology*. 2000;46(1):1-10. doi:https://doi.org/10.1088/0031-9155/46/1/301

[iii] Yau T, Kempe J, Gaede S. A four-dimensional dynamic conformal arc approach for real-time tumor tracking: A retrospective treatment planning study. *Journal of Applied Clinical Medical Physics*. 2023;25(3). doi:https://doi.org/10.1002/acm2.14224

Oral #7

Novel anti-angiogenic compound elicits anti-tumour lymphocyte response in peripheral blood and ascites leading to disease regression in advanced-stage epithelial ovarian cancer

Leslie Ogilvie[1], Michael Westerveld[2], Alexa King[1], Bianca Garlisi[1], Caroline Aitken[1], Samuel Workenhe[2], Jim Petrik[1]
[1]Department of Biomedical Sciences, Ontario Veterinary Sciences, University of Guelph, Guelph, ON, Canada
[2]Department of Pathobiology, Ontario Veterinary Sciences, University of Guelph, Guelph, ON, Canada

Introduction: Ovarian cancer is the most lethal gynecologic malignancy and treatment strategies have remained largely unchanged for decades. Therapeutic efficacy is challenged by a hostile tumour microenvironment, including impaired tumoral blood flow, hypoxia, and the suppression of anti-tumour immunity. Our group has shown that Fc3TSR, a peptide fragment of the thrombospondin-1 protein, eliminates dysfunctional tumoral blood vessels, resulting in improved blood flow and normoxia, which could reduce immunosuppression in the tumour microenvironment. Our objective is to determine whether Fc3TSR treatment stimulates anti-tumour immunity in a murine model of advanced-stage epithelial ovarian cancer.

Methods: Ovarian tumours were induced by the surgical injection of $1x10^6$ murine ovarian surface epithelial cells (ID8) under the ovarian bursa of syngeneic mice. In this model, 60 days post-tumour cell implantation (PTI), mice develop large ovarian masses, numerous peritoneal lesions, and abdominal ascites, consistent with clinical features of stage III ovarian cancer. At this point, mice are administered two weekly injections of Fc3TSR (0.158mg/kg) or phosphate-buffered saline as a control. Retro-orbital blood and abdominal ascites fluid were collected at 24-hours, or 3-, 6-, 8-, or 11-days post-treatment. Cells were incubated with Fc block and stained with fluorophore-conjugated antibodies against various extracellular antigens. Data were acquired with a Cytek Northern Lights flow cytometer to enumerate T cell and NK cell populations in peripheral blood and ascites, and analyzed using FlowJo software. Following euthanasia, mice were assessed for primary tumour mass and peritoneal metastasis.

Results: Fc3TSR treatment increased activated ($NKp46^+$) NK cells in peripheral blood and ascites at 3 days post-treatment. Total CD8 T lymphocytes increased at 24-hours and 3-, 6-, and 8-days post-treatment in peripheral blood. We observed a population of CD44lo CD8 T cells representing an early activated subset, which was elevated at 24-hours and 3 days-post-treatment, and a population of CD44hi CD8 cells representing a highly differentiated and activated effector subset, which increased at 24-hours and 3-days post-treatment in peripheral blood. In the ascites, CD8 T lymphocytes were enriched at 3-days post-treatment—non-significant increases in CD44hi, CD44lo, and total CD8+ T cells were observed at 24-hours, 6-, and 8-days post-treatment. Total CD4 T lymphocytes increased in peripheral blood at 3-, 6-, and 8-days post-treatment. Interestingly, in the ascites of Fc3TSR-treated mice at 8-days post-treatment, we observed an increase in total CD4 T lymphocytes and a heightened population of $CD44^{hi}PD1^+$ CD4 T cells, representing a highly differentiated, effector subset of antigen-stimulated T lymphocytes. Fc3TSR therapy reduced primary tumour mass by more than 50% at 9- and 11-days post-treatment. Peritoneal metastasis also decreased with Fc3TSR treatment compared to controls.

Conclusions: We demonstrate that anti-angiogenic compound, Fc3TSR, stimulates anti-tumour immunity. Fc3TSR treatment increased effector subsets of NK cells, CD8, and CD4 T lymphocytes in peripheral blood and ascites, ultimately leading to disease regression. We believe Fc3TSR can address main barriers to therapeutic success in the ovarian tumour microenvironment and augment the efficacy of immune-based therapies in a combination approach for improved treatment of advanced-stage ovarian cancer.

Impact of Stereotactic Ablative Radiotherapy (SABR) on Detection of ctDNA in Patients with Early-Stage Lung Cancer – Interim Findings from the Prospective SABR-DETECT Trial

Saurav Verma[1], Sympascho Young[1], Thomas Kennedy[2], Morgan Black[1], Britney Messam[1], Emma Churchman[1], Joanna Laba[1], George B Rodrigues[1], Yee Ung[3], May Tsao[3], Christopher Goodman[1], Melody Qu[1], Pencilla Lang[1], Brian P Yaremko[1], Andrew Warner[1], Ningyou Li[3], Ruoying Yu[3], Alexander V. Louie[2], David A Palma[1], Daniel Adam Breadner[1].
[1]Verspeeten Family Cancer Centre, Schulich School of Medicine and Dentistry, Western University, London, ON; [2]Odette Cancer Centre, Sunnybrook Health Sciences Centre, University of Toronto, Toronto, ON; [3]Nanjing Geneseeq Technology Inc., Nanjing, China.

Introduction: Stereotactic ablative radiotherapy (SABR) is the preferred curative treatment for inoperable patients with stage I/IIA non–small-cell lung cancer (NSCLC). In cases where the tumor is inaccessible or biopsy carries a high risk of complications, SABR is offered even in the absence of a tissue diagnosis, based on a high likelihood of malignancy as calculated by validated predictive models. In these situations, a blood based liquid biopsy detecting circulating tumor DNA (ctDNA) can serve as an aide to confirm malignancy and allow molecular testing. However, low ctDNA yield in early-stage NSCLC presents a challenge for diagnosis. This study hypothesizes that ctDNA detection rates will improve by combining assessment of pre- and post-SABR plasma samples.

Methods: This is a multi-institutional study including two cohorts: 1) patients with suspected stage I/IIA NSCLC, with a pretreatment likelihood of malignancy of ≥60% on Herder or Brock models, and 2) patients with biopsy-proven NSCLC. SABR was delivered according to standard guidelines. Plasma was collected for ctDNA analysis before and 24-72 hours following the first fraction of SABR. SHIELDING™ ULTRA MRD panel of hotspot regions in 2365 cancer-related genes with ultra-high sensitivity was used for ctDNA analysis (mutation + fragment profile + CNV). In this pre-planned interim analysis, we report on the secondary objective: to assess the impact of SABR on detection rates of ctDNA.

Results: Paired plasma samples (pre- and post-SABR) were tested for 69 patients. After quality control analysis, 66 paired samples were analyzed and included in this interim analysis. The median age was 76 years (range; 56-89) and 36 (54%) were male. The median concentration of circulating free DNA (ng/mL) did not increase from pre- (5.5, interquartile range (IQR): 3.3-8.1) to post-SABR (5.7, IQR: 4.1-7.6) (P=0.82). The ctDNA detection rate in pre-SABR samples was 22.7% versus 27.3% in post-SABR samples (Table). Interestingly, in 10 patients (15.2%), ctDNA became detectable in post-SABR samples and in 7 patients (10.6%) the ctDNA was no longer detectable in the post-SABR samples. The ctDNA remained undetectable in 41 patients (62.1%). 37.9% of patients had detectable ctDNA either before or after SABR.

Conclusions: The diagnostic yield of ctDNA for confirming malignancy in early-stage NSCLC is improved by testing both the pre- and the post-SABR samples, collected within 24-72 hours after the first fraction of SABR. This approach may improve the diagnostic rates of liquid

biopsies for patients with presumed NSCLC undergoing SABR, warranting further investigation of ctDNA detection before and shortly after treatment.

Table - ctDNA detection rates (N=66)

Pre-SABR	Post-SABR	n (%)
detected	detected	8 (12.1%)
not detected	detected	10 (15.2%)
detected	not detected	7 (10.6%)
not detected	not detected	41 (62.1%)

Poster #1

Kindlin-2 modulates proliferation and migration of metastatic cSCC cells.

A. Dutta*, M. Calder*, and L. Dagnino*†.
*Department of Physiology and Pharmacology, Children's Health Research Institute, London Health Sciences Research Institute, and †Department of Oncology, University of Western Ontario, London, Ontario, N6A 5C1.

Introduction: Kindlin-2 is a member of a scaffold protein family with three orthologs in mammals (Kindlins 1-3, encoded, respectively, by the *FERMT1*, *-2* and *-3* genes). Epidermal keratinocytes express Kindlins 1 and 2, which play critical roles in epidermal function and homeostasis. In humans, loss-of-function mutations in *FERMT1* give rise to Kindler syndrome, a blistering disease characterized by epidermal fragility and increased susceptibility to cutaneous squamous cell carcinoma (cSCC). Kindlin-2 is expressed early in development and is essential for embryo implantation, cardiovascular formation, integrin activation, and formation of cell-extracellular matrix adhesion complexes. However, the functions of Kindlin-2 in normal or transformed epidermal keratinocytes remain poorly understood due, in part, to a lack of suitable models.

Methods: To address this knowledge gap, we used siRNA approaches to generate Kindlin-2-deficient cells that model cSCC progression stages. PM1, MET1, and MET4 cells were isolated, respectively, from a precancerous lesion, a primary SCC, and a metastatic lesion of the latter.

Results: Of note, whereas MET1 cells express both Kindlin-1 and -2, Kindlin-1 was not detectable in PM1 and MET4 cells. *FERMT2* silencing hindered the ability of PM1 cells to adhere to culture surfaces and reduced directional migration rates by 30-50% in the three cell types. Kindlin-2 deficiency decreased proliferation and spreading of PM1 and MET4 cells, and altered focal adhesions, F-actin, and microtubule cytoskeletal organization.

Discussion: We conclude that Kindlin-2 is important in modulating proliferation of PM1 and MET4 cells, as well as motility, focal adhesion assembly and cytoskeletal organization in PM1, MET1 and MET4 cells.

Supported with funds from the Canadian Institutes of Health Research, the Natural Sciences and Engineering Research Council and the London Regional Cancer Centre.

Poster #2

Kindlin-1 modulation of Cytoskeletal Organization and Nuclear Morphology in Squamous Cell Carcinomas

A. Varela and L. Dagnino

[1] Departments of Physiology and Pharmacology, and Oncology, Children's Health Research Institute, LHSC Research Institute, Western University, London, ON N6A 5C1, Canada

Introduction: Kindlin-1 is a scaffold protein expressed in epidermal cells and contributes to integrin activation and mechanotransduction. Loss-of-function mutations in the *FERMT1* gene, which encodes Kindlin-1, cause Kindler Syndrome, a disease characterized by skin fragility, blister formation, and elevated incidence of epidermal squamous cell carcinomas (cSCC). These tumours constitute the fifth most prevalent malignancy globally and arise from malignant transformation of epidermal keratinocytes.

Methods: To investigate the role of Kindlin-1 in mechanotransduction in squamous cell carcinoma, we generated two monoclonal Kindlin-1-deficient populations derived from SCC-13 cSCC cells, using CRISPR/Cas9-mediated *FERMT1* editing, hereafter termed Kin1-KO.

Results and Discussion: Unlike Kindlin-expressing cells, Kin1-KO cells display a disorganized microtubule network, with apparently branched filaments. In addition, whereas thick cortical actin bundles and stress fibers are present in Kindlin-1-expressing cells, they are largely absent in the majority of Kin1-KO cells. The absence of Kindlin-1 is also associated with decreased abundance of focal adhesions. The alterations in focal adhesions may be due to abnormal integrin signal transduction, as exogenous expression of wild-type Kindlin-1, but not a Kindlin-1 mutant unable to bind integrins, restores focal adhesion abundance in Kin1-KO cells. Kin1-KO cells also exhibit alterations in nuclear morphology, including reduced nuclear height, and roundness, compared to Kindlin-1-expressing cells. Further, whereas the nuclei of Kindlin-1 expressing cells display continuous lamin A/C staining, those in Kin1-KO cells show a discontinuous pattern of lamin A/C immunoreactivity. Collectively, these data indicate that Kindlin-1 is necessary for focal adhesion formation, F-actin and microtubule organization, and maintenance of normal nuclear morphology in epidermal cells. Disrupted cytoskeletal organization and nuclear mechanotransduction by Kindlin-1 deficiency suggests Kindlin-1 may be a potential target for novel therapeutic strategies.

Supported with funds from CIHR, NSERC and the London Regional Cancer Program (LRCP).

Poster #3

A Novel Platform to Monitor and Prevent Prostate Cancer Progression

Jeffery Martin[1], Elizabeth Fidalgo Da Silva[1], Lisa A. Porter[1,2]
[1]Biomedical Sciences Department, University of Windsor. [2]St. Joseph's Health Care London

Introduction: Prostate cancer (PC) is the second most common cancer in men worldwide, affecting 76 men daily in Canada. As treatment options continue to evolve, disease management and overall patient outcomes have improved. While effective, these treatments can sometimes pressure PC cells to transdifferentiate into a more aggressive, treatment resistant type of PC, known as neuroendocrine prostate cancer (NEPC). Treatment options for NEPC are limited as it is resistant to all current therapies, leading to an overall poor prognosis with an estimated survival of less than one year. Furthermore, the PC to NEPC transdifferentiation mechanism hasn't been well understood, with few markers being used to study progression. Our lab has identified a class of cell cycle regulatory proteins elevated in NEPC, with evidence supporting that these proteins have the potential to drive progression to this drug-resistant form of disease.

Methods: This project aims to establish a PC to NEPC platform of disease progression to elucidate the role of cell cycle regulatory proteins during PC transdifferentiation. To establish this platform, we will utilize LNCaP cells, a cell line model for the first stage of PC, Adenocarcinoma PC (AdPC). These cells will be pressured to differentiate into the common second stage of PC, castration resistant PC (CRPC), by utilizing charcoal stripped serum. Finally, these CRPC phenotype cell lines will be pressured to differentiate into an NEPC phenotype, the final stage of PC progression, by treating the cells with an androgen receptor inhibitor, Enzalutamide. Samples will be collected at every stage of progression and analyzed by western blotting, qRT-PCR, immunofluorescence, flow cytometry, and proliferation assays. After determining the timing of cell cycle regulatory proteins upregulation/downregulation, we will utilize CDK1/2 inhibitor drugs that can inhibit these proteins and test whether these drugs can treat and/or prevent the progression of disease to NEPC. The therapeutic potential of these drugs will further be tested by utilizing zebrafish as an in vivo model. Additionally, markers of disease progression will be analyzed using human samples. Cell-free RNA will be extracted from blood, urine, and saliva from patients with recurrent PC. and analyzed for cell cycle markers using next-generation sequencing.

Results: This project is ongoing, but our current results thus far demonstrate an early upregulation of cell cycle regulators such as Cyclin A, Cyclin B1 and Spy1 as PC progresses from AdPC to NEPC. Further, we have preliminary data to support that Dinaciclib, a CDK 1/2 inhibitor, can prevent the progression of PC to NEPC.

Discussion: Preventing the progression of AdPC to NEPC and identifying markers of NEPC remains one of the greatest challenges in this field. Through identifying the timing of cell cycle regulatory protein upregulation/downregulation with this novel platform, and then treating the cells with specific CDK inhibitors at that time, we expect to prevent PC disease progression. Overall, we have strong rationale and data to support this being a promising direction that could make a meaningful impact for PC patients.

Poster #4

Transcriptomic and Genomic Profiling Reveals Distinct Molecular Features of Metastatic Myxoid Liposarcoma

Huilin Niu[1], Irene L. Andrulis[2,3], Yael Babichev[2], Brendan C. Dickson[4], Rebecca Gladdy[2,4], Nalan Gokgoz[2], Kim M. Tsoi[5,6], Jay S. Wunder[5,6], Tallulah Andrews[1,7]

[1] Department of Biochemistry, Schulich School of Medicine and Dentistry, University of Western Ontario, London, ON, Canada
[2] Lunenfeld-Tanenbaum Research Institute, Sinai Health System, Toronto, ON, Canada
[3] Department of Molecular Genetics, University of Toronto, Toronto, ON, Canada
[4] Department of Laboratory Medicine and Pathobiology, Temerty Faculty of Medicine, University of Toronto, Toronto, ON, Canada
[5] Division of Orthopaedic Surgery, Department of Surgery, University of Toronto, Toronto, ON, Canada
[6] Musculoskeletal Oncology Unit, Sinai Health System, Toronto, ON, Canada
[7] Department of Computer Science, University of Western Ontario, London, ON, Canada

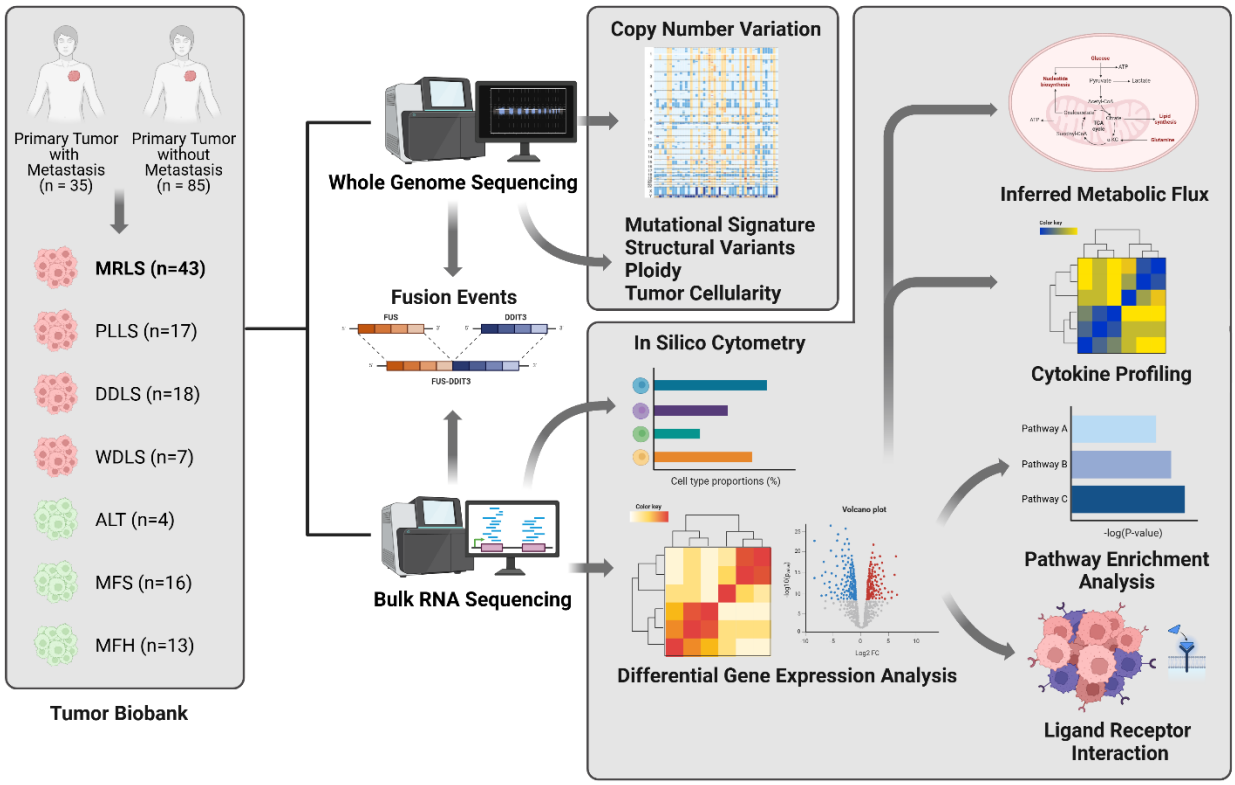

Background: Metastasis, the spread of primary tumor cells to distant sites, is the leading cause of cancer-related mortality. Liposarcoma, a rare mesenchymal soft tissue sarcoma, typically metastasizes to the lung. However, an aggressive subtype, myxoid liposarcoma (MRLS), exhibits a distinct extrapulmonary metastatic pattern. While primary MRLS tumors respond well to radiation

therapy and surgical resection, metastatic tumors are resistant to both radiation therapy and chemotherapy, leading to a 5-year survival rate of less than 10%. To improve patient outcomes and develop new therapeutic strategies, it is critical to understand the distinct molecular alterations of the MRLS and the mechanisms underlying its unique metastasis pattern.

Methods: To investigate the molecular mechanisms underlying MRLS metastasis, we performed whole-genome sequencing (WGS) and bulk RNA sequencing (bulk RNA-Seq) on a newly assembled cohort of 130 mixed liposarcoma tumor samples. WGS data were used to identify copy number variations, structural variants, mutational signatures, and tumor ploidy. Differential gene expression and pathway enrichment analyses were performed to identify molecular changes between metastatic and non-metastatic MRLS primary tumors. CIBERSORT was used to deconvolve immune infiltration, and METAFlux was used to infer metabolic flux. Cytokine profiling was performed by analyzing cytokine/chemokine-related gene expression.

Preliminary Results: Both WGS and bulk RNA-seq confirmed the presence of the FUS-DDIT3 fusion gene in 86% of clinically diagnosed MRLS samples. Sample distance heatmap analysis showed that MRLS samples cluster together, distinguishing them from other liposarcoma subtypes and clinically similar tumors, suggesting a unique gene expression profile. Metabolic flux analysis showed that most MRLS tumors exhibit low metabolic activity across all pathways. CIBERSORT deconvolution found heterogeneous immune infiltration levels across samples.

Differential gene expression analysis identified key molecular alterations in metastatic MRLS. Primary MRLS tumors that metastasize showed downregulation of ANKRD26, KCNA2, EGFL6, MPP3, RGS6, and ADAM33, genes involved in tumor suppression, cell adhesion, and metastasis regulation. Notably, EGFL6, a known promoter of epithelial-mesenchymal transition (EMT) and angiogenesis, was downregulated, suggesting a shift in metastatic mechanisms. Conversely, metastatic MRLS tumors exhibited upregulation of PPP1R1B, C4A, NEBL, SLC2A5, SPOCK1, and BBOX1, genes implicated in cancer progression and immune modulation. PPP1R1B, linked to oncogenic fusion events in gastric cancer, may contribute to tumor signaling, while C4A, a complement system protein, has been associated with immune evasion. Additionally, upregulation of LGR5 (a Wnt pathway-associated stem cell marker) and EGLN3 (a hypoxia response regulator) suggests metabolic and signaling adaptations in metastatic MRLS. Pathway analysis revealed key dysregulations in metastatic MRLS tumors. Wnt signaling, adipogenesis, and amoeboid-type cell migration were significantly downregulated, suggesting a shift away from traditional metastatic mechanisms. Conversely, pathways related to glycolysis, gluconeogenesis, mitochondrial protein degradation, amino acid metabolism, and hypoxia response were upregulated, indicating a shift toward a metabolically aggressive phenotype. Activation of ubiquitin-mediated protein degradation, p53-independent DNA damage response, and NF-kB signaling may further contribute to tumor survival and treatment resistance.

Conclusion: These preliminary findings highlight unique genomic and transcriptomic alterations in metastatic MRLS, particularly in metabolism, EMT, and tumor-immune interactions. Further research is needed to clarify MRLS's distinct biology and extrapulmonary metastasis.

Poster #5

Unravelling complex associations of genetic variation and tumor microenvironments for clonal expansion in breast cancer with metastasis

Joseph Butler[1], Cornelia Tolg[2], Kathleen A. Hill[1*], Eva A. Turley[2]
[1]Department of Biology, Western University
[2]Cancer Research Laboratory Program, Lawson Health Research Institute, Victoria Hospital; Departments of Oncology, Biochemistry, and Surgery, Western University

Introduction: Breast cancer (BrCa) is highly heterogeneous, with multiple distinct subtypes associated with variable clinical outcomes and high intra-tumor clonal diversity. This clonal diversity is caused by genomic instability, microenvironmental factors, and tumor cell plasticity. Intra-tumor clonal diversity has been linked to poor clinical outcomes including aggressive, recurrent, and treatment resistant tumors and progression to metastases. Somatic mutations that induce transcriptomic alterations and genomic instability, in combination with the harsh tumor microenvironment, shape the heterogeneity and expansion of intra-tumor clones. We identified RHAMM, which has pro-inflammatory functions in response-to-injury processes, as a contributor to BrCA cell heterogeneity. RHAMM is expressed in tumor and host cells and Rhamm-loss in these cell compartments strongly reduces clonal heterogeneity detected by single nucleotide variants used as endogenous barcodes. Our evidence predicts that a RHAMM-ve microenvironment exerts selective pressure permitting the emergence of dominant clones in lung metastases that carry specific oncogenic mutations. Our goal is to probe the interplay between clonal heterogeneity and the tumor microenvironment in the emergence of dominant intra-tumor clones.

Methods: Next-generation DNA sequencing technologies now offer a two-pronged approach to the analysis of genetic heterogeneity. Long-read genome sequencing enables discovery of large structural variants and short-read, deep sequencing achieves highly accurate detection of ultra-rare single nucleotide variants.

Discussion: The interplay of clonal dynamics and the tumour microenvironments in the development of heterogeneous BrCa tumours can be teased apart to better understand the causative processes underlying the metastatic and treatment-resistant nature of these tumours, with discovery of potential genetic determinants relevant to cancer management.

Poster #6

Intracranial Electrotherapy for Glioma Treatment In Vivo

Erin Iredale[1], Niveen Fulcher[1], Elizabeth Fenton[2], Susanne Schmid[2], Terry Peters[3,4], Eugene Wong[3,5], Matthew O. Hebb[1,2].
Department of [1]Clinical Neurological Sciences, [2]Anatomy and Cell Biology, [3]Medical Biophysics, Schulich School of Medicine and Dentistry, [4]Robarts Research Institute, Department of [5]Physics and Astronomy, Western University, London, ON, Canada.

Introduction: Glioblastoma (GBM) remains the most fatal form of primary brain cancer, with a median survival of 14 months despite standard treatments of surgical resection, chemotherapy, and radiation. Anti-cancer electrotherapy is showing potential as a new option for aggressive brain cancers, using low-intensity electric fields (1 V/cm) of intermediate frequency (200 kHz). Internal delivery of these fields from multiple bioelectrodes, called Intratumoral Modulation Therapy (IMT), has the potential to provide a sustained, localized GBM treatment approach. The objectives of this study are to evaluate the impact of dynamic IMT on GBM growth in vivo and validate treatment planning simulations.

Methods: A 3-electrode preclinical IMT apparatus was implanted into the left hemisphere of the Fischer rat brain (n=22), and F98 glioma cells injected at the center of the pedestal. Bioluminescence imaging (BLI) was performed on post-operative day 4 for each animal pair, prior to the initiation of dynamic IMT stimulation (200 kHz, ±2V amplitude sine waves equally phase shifted). Paired rats received either IMT or sham (no stimulation) treatment for 7 days with continuous voltage and current delivery monitoring. Endpoint BLI was performed on post-operative day 11 (n=11 pairs), and ex vivo 15.2T magnetic resonance imaging (MRI) utilized for analysis of the tumor volume (n=10 individuals). Tumor volume analysis and electric field simulations were performed on our custom IMT preclinical planning system platform.

Results: Tumor volume from ex vivo MRI linearly correlated with endpoint BLI signal (n=10, $p<0.01$). For treated rats with MRI (n=5), an average 1.71±0.07 V was delivered over the 7 days, with patient specific simulations yielding 100% coverage of the visible tumor volume with 1 V/cm IMT field. The measured electrical current was 5.8±1.3 mA, matching the predicted values from simulations of 5.4±1.1 mA. Over the 7 days, sham tumor burden grew 118.6-fold, while IMT only grew 13.5-fold, an 8.8 times reduction in tumor growth with IMT (n=11, $p=0.006$).

Discussion: This study provides key preclinical evidence of the efficacy of dynamic IMT against GBM. These results support the translation of IMT to clinical trials, to evaluate safety and efficacy in the human brain.

Poster #7

Therapeutic targeting of extracellular vesicles in breast cancer metastasis

Urvi Patel[1], Braeden Medeiros[1], Austyn Roseborough[1], David Goodale[3] and Alison L. Allan[1,2,3,4]
Department of [1]Anatomy and Cell Biology and [2]Oncology, Schulich School of Medicine and Dentistry, Western University; [3] Verspeeten Family Cancer Centre, London Health Sciences Centre; and [4]London Health Sciences Centre Research Institute, London ON, Canada.

Introduction: Breast cancer is a prominent cause of cancer diagnosis and death in women worldwide. The triple negative (TN) subtype has the poorest prognosis due to its lack of receptor expression and limited treatment options. It is highly aggressive and metastatic in nature, with an increased tendency to metastasize to the lung. Previous studies in our lab have demonstrated that extracellular vesicles (EVs) from the primary breast tumour can help to establish a pre-metastatic niche at the lung. These EVs can deliver cargo to the lung to induce changes that facilitate metastasis such as remodelling of the extracellular matrix and altering soluble components of the lung microenvironment. There is also evidence suggesting that tumor-derived EVs can influence metastatic processes such as angiogenesis (the formation of vasculature) to support tumor growth and dissemination by regulating proliferation and migration of endothelial cells at the primary site and distant secondary sites. Therefore, we hypothesized that TN breast cancer-derived EVs contain cargo that induce molecular and functional changes in the lung microenvironment, and that therapeutic inhibition of EV production/release reduces metastatic properties in TN cells.

Methods: Breast cancer-derived EVs were isolated using ultracentrifugation from non-malignant breast epithelial cells (MCF10A) and TN breast cancer cells (SUM159, MDA-MB-231, 231-LM2, 231-BoM). Breast cancer-derived EVs were validated using immunoblotting for EV markers, nanoflow cytometry and electron microscopy. To inhibit EV production/release, TN (SUM159, MDA-MB-231, 231-LM2) cells with increased propensity for lung metastasis were treated with tipifarnib or vehicle control. Following treatment, migratory capacity and expression of EV proteins were assessed through scratch-wound assays and immunoblotting, respectively.

Results: Preliminary data showed that treatment of TN breast cancer cells with tipifarnib resulted in an inhibition of EV release *in vitro* and reduced lung metastasis *in vivo* relative to vehicle control. Tipifarnib treatment significantly reduced migration of SUM159 and 231-LM2 TN cells *in vitro*. To explore the molecular mechanisms by which this inhibition occurred, we assessed the expression of proteins involved in EV production including ALIX (ESCRT-dependent), nSMase2 (ESCRT-independent) and Rab27a (secretion). Expression of nSMase2 and Rab27a was significantly decreased in response to tipifarnib treatment in SUM159 and 231-LM2 cells while no change was observed in ALIX expression.
Ongoing work is focused on assessing the influence of tipifarnib on proliferation and invasion. We are also working to elucidate the cargo within these EVs by identifying differentially expressed miRNAs through RNAseq analysis.

Conclusions: These results indicate that tipifarnib has an influence on cell behaviour, specifically migration. Additionally, inhibition of EVs through tipifarnib may be mediated by interference with ESCRT-independent production and secretion of EVs. By understanding factors mediating lung metastasis, a foundation can be built for the development of new biomarkers and/or therapies. This work explores the inhibition of production/release of EVs from the primary breast tumor to determine whether that can hinder pre-metastatic niche formation and delay metastasis. The fundamentals discovered through this study may ultimately lead to opportunities to improve TN patient outcomes.

Poster #8

Investigating the role of hypoxia-induced integrin expression on organotrophic breast cancer metastasis

Jeri Spilberg[1], David Susman[1], Alison L. Allan[1,2,3,4]
Department of [1]Anatomy and Cell Biology and [2]Oncology, Schulich School of Medicine and Dentistry, Western University; [3]Verspeeten Family Cancer Centre, London Health Sciences Centre; and [4]London Health Sciences Centre Research Institute, London ON, Canada.

Introduction: Breast cancer is the second leading cause of death in Canadian women, with metastasis accounting for >90% of breast cancer-related deaths. Breast cancer commonly metastasizes to the lung, liver, brain, and bone. This organotropism is determined by molecular characteristics of both breast cancer cells and the microenvironments they interact with in primary and distant sites. Our recent studies have investigated global differences in the proteome of triple negative breast cancer (TNBC) cells with different organ-specific preferences for metastasis. In addition, we compared cells cultured under normal vs. low oxygen (hypoxic) conditions, since hypoxia is also known to enhance metastasis. Under hypoxia, we observed 3 clusters of strongly connected protein nodes related to hypoxia signaling, integrins, and exosomes. The integrin family of proteins is comprised of cell surface receptors that facilitate cell-matrix interactions and have been shown to enhance cancer cell adhesion, migration, invasion, and metastasis. In the current study, we hypothesize that breast cancer cells with different organotrophic tendencies exhibit distinct patterns of hypoxia-induced integrin expression, leading to enhanced metastatic behavior.

Methods: Integrin profiles of parental MDA-MB-231 TNBC cells and their bone (231-BoM), lung (231-LM2), and brain (231-BR) metastatic variants are being assessed under normoxic (20%) and hypoxic (1%) conditions using CHEMICON® Alpha/Beta Integrin-Mediated Cell Adhesion Arrays. These arrays enable rapid, quantitative analysis of 14 alpha and beta integrins. Flow cytometry will be used to validate specific integrins with hypoxia-induced expression changes identified from the arrays. Blocking antibodies targeting differentially expressed integrins (based on organotropism and/or oxygen conditions) will be used to inhibit integrin function, relative to IgG controls. Differences in metastatic cell behavior will be evaluated *in vitro* via standard adhesion, proliferation, migration, and invasion assays.

Results: Previous work in the lab comparing parental MDA-MB-231 cells to bone-seeking 231-BoM cells revealed that in response to hypoxia, 3 integrins (ITGα5, ITGαV, and ITGβ4) were increased in parental 231 cells, whereas 7 integrins (ITGα1, ITGα2, ITGα3, ITGα6, ITGβ1, ITGβ3, and ITGβ5) were increased in bone-seeking 231-BoM cells. Completion of the integrin assay for parental MDA-MB-231 cells revealed upregulation of ITGα5, ITGα3, ITGβ1, and ITGβ4 under hypoxia. Notably, all integrins followed the hypoxia-induced upregulation trend predicted by the proteomic analysis. However, ITGα3 and ITGβ1 showed significant upregulation in array experiments, a finding not previously identified in the earlier analyses. Ongoing work is aimed understanding hypoxia-mediated changes in organ-specific 231 variants.

Conclusion: Investigating integrin expression across different metastatic organotropisms under hypoxic conditions will deepen our understanding of how cancer cells adapt to hostile environments. This knowledge has the potential to identify novel biomarkers or biotherapeutics for preventing and treating breast cancer metastasis.

Poster #9

ULK1-mediated regulation of mitochondrial homeostasis in ovarian cancer spheroids

Jack D. Webb[1,2], Matthew J. Borrelli[1,2], Owen Hovey[3], Shawn S-C Li[3], and Trevor G. Shepherd[1,2,4,5]

1. The Mary & John Knight Translational Ovarian Cancer Research Unit, Verspeeten Family Cancer Centre, London, ON, Canada.
2. Department of Anatomy & Cell Biology, Schulich School of Medicine & Dentistry, Western University, London, ON, Canada.
3. Department of Biochemistry, Schulich School of Medicine & Dentistry, Western University, London, ON, Canada.
4. Department of Oncology, Schulich School of Medicine & Dentistry, Western University, London, ON, Canada.
5. Department of Obstetrics & Gynaecology, Schulich School of Medicine & Dentistry, Western University, London, ON, Canada.

Introduction: Epithelial ovarian cancer (EOC) is the most lethal gynecologic malignancy, largely due to late-stage diagnosis and chemoresistance. During metastasis, EOC cells form multicellular spheroids in the peritoneal cavity, relying on adaptive mechanisms to survive in suspension. Our previous research identified ULK1, a key autophagy regulator, as essential for spheroid viability and metastatic progression. Herein, we aim to identify non-canonical functions of ULK1 in EOC progression.

Methods: To identify biological processes and metabolic pathways altered by ULK1 loss, we performed proteomic mass spectrometry followed by western blot validation. Mitophagy was assessed using a mCherry-GFP-$FIS1_{101–152}$ reporter. ATP content and redox potential in spheroids were measured using CellTiter-Glo and alamarBlue assays, respectively, while mitochondrial ROS levels were quantified with mitoSOX. Mitochondrial morphology in adherent cells was evaluated by immunofluorescence staining for TOM20 and visualized using fluorescence microscopy.

Results: ULK1 loss led to significant decreases in proteins involved in oxidative phosphorylation and glycolysis, although ATP levels remained unchanged, suggesting metabolic compensation. Proteomic data also revealed changes in mitochondrial degradation, synthesis, and gene expression. Mitophagy analysis showed enhanced mitochondrial clearance in OVCAR8 *ULK1*KO spheroids, but impaired clearance in HEYA8 *ULK1*KO spheroids, indicating cell line-specific regulation. Notably, increased mitophagy in OVCAR8 ULK1KO spheroids correlated with decreased mitochondrial ROS levels, whereas decreased mitophagy in HEYA8 *ULK1*KO spheroids was associated with elevated ROS. These findings suggest that mitochondrial degradation may be ULK1-dependent yet occur independently of canonical mitophagy pathways, potentially via lysosomal mechanisms. Furthermore, ULK1 loss dysregulated fission/fusion signaling, though no significant changes in mitochondrial morphology were observed in adherent culture.

Discussion: Our data suggest that ULK1 plays a critical role in maintaining mitochondrial homeostasis in EOC spheroids by regulating mitochondrial metabolism, turnover, and dynamics. The differential responses between cell lines highlight context-dependent functions of ULK1, and suggest alternative, mitophagy-independent mitochondrial degradation pathways may support spheroid survival.

Poster #10

Activating Transcription Factor 3 directly affects the tumour microenvironment in promoting pancreatic cancer initiation and progression

Mickenzie Martin[1,3-5], John DiGulglielmo[1,3], Christopher Pin[1-5]
Departments of [1]Physiology & Pharmacology, [2]Paediatrics, and [3]Oncology, Schulich School of Medicine and Dentistry, University of Western Ontario; [4]Baker Centre for Pancreatic Cancer; [5]Verspeeten Family Cancer Centre, London, Ontario

Background:
Pancreatic ductal adenocarcinoma (PDAC) is the third leading cause of cancer-related deaths in North America, with a five-year survival rate of ~12%. PDAC tumors are characterized by a dense tumor microenvironment (TME), composed predominantly of extracellular matrix (ECM), fibroblasts, and immune cells. While the TME contributes to therapeutic resistance, it also imposes stressors such as hypoxia and nutrient deprivation, triggering the unfolded protein response (UPR). Activating Transcription Factor 3 (ATF3), a UPR mediator, is expressed in multiple cell compartments during PDAC progression. Our previous work revealed differences between global and cell-targeted deletion of ATF3 in the context of PDAC progression suggesting multiple, and even contradictory roles for ATF3. This study investigates the requirement for ATF3 in non-epithelial cells within the TME, specifically fibroblasts. We hypothesized that ATF3 functions in the stroma to restrict tumor progression.

Methods:
To dissect ATF3's function in the pre-malignant pancreas, we compared fibroblasts and immune cells between $KRAS^{G12D}$-expressing mice with (*Ptf1a*$^{creERT/+}$*KRAS*$^{G12D/+}$) or without global ATF3 deletion (*Atf3*$^{-/-}$ *Ptf1a*$^{creERT/+}$*KRAS*$^{G12D/+}$; APK). A mouse model allowing acinar-specific *Atf3* deletion and $KRAS^{G12D}$ expression (*A*^{acinar}*PK*) was also included. Fibroblast abundance and activation were evaluated using immunohistochemistry (IHC) for α-smooth muscle actin (αSMA) and vimentin and immune cell composition was analyzed by flow cytometry. To investigate fibroblast-intrinsic roles for ATF3, fibroblasts were isolated from injured *APK* and *Ptf1a*$^{creERT/+}$*KRAS*$^{G12D/+}$ pancreata and assessed *in vitro* following TGF-β stimulation. To test the effects of stromal ATF3 loss on tumor growth, pancreatic tumor cells were orthotopically transplanted into wildtype and *Atf3*$^{-/-}$ recipient mice.

Results:
Histological comparisons revealed ATF3 loss reduced fibroblast activation and collagen deposition without affecting fibroblast abundance. Consistently, *Atf3*$^{-/-}$ fibroblasts showed impaired TGF-β-induced activation *in vitro*. Flow cytometry analysis indicated no change in total immune infiltration but a selective reduction in $CD4^+$ T cells upon ATF3 loss. Despite these stromal alterations, orthotopic transplantation showed ATF3 deficiency in the TME did not prevent tumor formation.

Conclusions:
These findings suggest ATF3 regulates fibroblast activation and influences immune cell composition during early PDAC development. While fibroblast-intrinsic ATF3 drives activation, its effect on immune infiltration may involve epithelial-derived cues. Importantly, loss of ATF3 in the TME does not block tumor growth, suggesting its role evolves during PDAC progression. Future studies will explore whether targeting ATF3-regulated genes enhances chemotherapeutic responses in PDAC.

Poster #11

Hyaluronan blocks UVB-induced skin cancer: A role for *Trp53*

C. Tolg[1], V. Liu[2], H. Pavanel[3], C. Taylor[3], D. Chen[3], K. Cousteils[2], K.A. Hill[3] E.A. Turley[1,4]
[1.] Verspeeten Family Cancer Center, LHSC, Victoria Hospital, London ON, CA; [2.] Dept. Biochemistry, Schulich School of Medicine and Dentistry, Western University, London, ON, CA; [3.] Dept. Biology, Faculty of Science, Western University, London ON, CA; [4.] Depts Oncology, Biochemistry and Surgery, Schulich School of Medicine and Dentistry, Western University, London ON, CA.

Introduction
Although UVB-induced mutations accumulate in skin with increasing age, not every mutant clone will initiate keratinocyte tumors, suggesting a tumor-suppressing effect of the host microenvironment. High molecular weight hyaluronan (HA), which is a skin polysaccharide that decreases with age and UVB-exposure, is one potential microenvironmental tumor resistance factor. To directly assess the effect of HA on UVB-induced keratinocyte tumor initiation, we developed a skin-penetrating HA formulation (HAPE) and applied it to a UVB-exposed mouse model of UVB-induced cutaneous basal (BCC) and squamous (SCC) cell carcinoma susceptibility (*Hr*$^{-/-}$:*Ptch1*$^{+/-}$).

Methods
Hr$^{-/-}$:*Ptch1*$^{+/-}$ mice were exposed to UVB twice/week for 26 weeks and treated 5X/week with an application of HAPE using vehicle cream as a control. UVB-induced DNA damage and mutations were characterized by 8-Oxo-DG/CPD ELISAs and whole exome sequencing. 10X genomics spatial transcriptomic platform was used to probe the effect of HAPE on skin cell transcriptomes. IHC/IF was used to confirm effects of HAPE on cell proliferation, apoptosis and oncogenic driver pathway activation. The immortalized human keratinocyte cell line HaCaT, which contains TP53 gain-of-function mutations, was used to model the effect of HAPE on the survival of tumor-initiating Krt15+ cells bearing TP53 mutations.

Results
HAPE prevented BCC and SCC initiation. This anti-tumor effect associates with inhibition of oncogenic driver pathways, and maintenance of epidermal quiescence and polarity. DNA damage and mutation load is similar in both HAPE and control UVB-exposed skin. Whole exome sequencing identified the presence of mutated driver oncogenes in both control and HAPE treated skin with the notable exception of Trp53 mutations, which were lacking in HAPE-treated skin. Spatial transcriptomics and IHC/IF showed that HAPE treatment suppressed Trp53 mRNA and protein expression and promoted apoptosis of CD44+/Krt15+/mutant *Trp53+* stem cells that are tumor-initiating in *Hr*$^{-/-}$:*Ptch1*$^{+/-}$mice. To directly assess the effects of HA on survival of CD44+/Krt15+/mutant *Trp53+* stem cells, HA was added to human keratinocytes (HaCaT) with gain-of-function TP53 mutations. In this model, knockdown of TRP53 expression by ShRNA transfection induces cell apoptosis. HA suppressed TP53 mRNA and protein expression and specifically induced apoptosis of CD44+/Krt15+/Trp53+ keratinocyte subpopulations.

Conclusions
These results show that HAPE suppresses tumor initiation by culling tumor-initiating cells bearing a mutant *Trp53*. In future experiments clonal analyses will be performed using the highly sensitive, error corrected DNA sequencing method CarcSeq to confirm these results and to identify additional changes in clonal heterogeneity of tumor initiating cells resulting from HAPE treatment.

Poster #12

Targets of Radiotherapy and CFI-400945 identified using a Whole Transcriptomic Analysis in Triple Negative Breast Cancer

Isabel Kannampuzha[1], Armen Parsyan[2,3,4,5], Alison Allan[2,3,4]

1. Department of Biochemistry, Western University, 2. Department of Anatomy and Cell Biology, Western University, 3. Department of Oncology, Western University, 4. Verspeeten Family Cancer Centre, London Health Sciences Centre, 5. Department of Surgery, St. Joseph's Health Care and London Health Sciences Centre

Introduction: Among the different subtypes of breast cancer, triple negative breast cancer (TNBC) is one of the most aggressive forms, characterized by the lack of estrogen, progesterone, and human epidermal growth factor receptor 2 (HER2). In its later, more aggressive stages, TNBC has the propensity to develop resistance to common treatments including radiotherapy (RT). Combined with the lack of known biomarkers, this treatment resistance highlights that TNBC requires further investigation to elucidate potential targets and biomarkers important for patient management and drug development. The novel drug CFI-400945 (CFI), a selective inhibitor of Polo-Like Kinase 4 (PLK4), shows promise in clinical trials and is reported to disrupt centriole duplication leading to genomic instability and anticancer effects. As RT similarly targets centriole duplication and causes genomic instability, combination treatment with CFI has been investigated as a treatment avenue for TNBC. Previously, treatment with radiotherapy (RT) and CFI has been observed to result in increased anti-proliferative effects in *in vivo* models of TNBC in comparison to single agent treatments. To further understand the mechanisms underlying the response to combination treatment, RNA-sequencing analysis was performed and differentially expressed genes in the single agent and combination treatments were identified. In the current study, we hypothesized that validation of differentially expressed genes from the RNA sequencing data would identify potential targets of the mechanism of action in RT and CFI combination treatment.

Methods: Based on the RNA-seq data, differentially expressed genes in the single agent and combination treatment compared to the control were characterized using DAVID bioinformatics and narrowed using PubMed searches; 16 genes were chosen validation using RT-qPCR. Of these, 4/16 genes encoding for MMP1, IL8, IL1RL1 and ICAM1 were further validated at the protein level using immunoblotting. Finally, due to these gene's involvement in the senescence, senescence-associated β-galactosidase assays were conducted to determine differences in levels of senescent cells in response to single agent and combination treatment.

Results: Several genes including those encoding for MMP1, IL8, IL1RL1, and ICAM1 demonstrated increased mRNA expression in response to combination treatment relative to untreated controls. Further validation was conducted at the protein level using immunoblotting to assess MMP1 and ICAM1, however a similar significant increase in protein expression was not observed. Using β-galactosidase assays, the number of senescent cells was significantly increased in the combination condition compared to the control.

Discussion: These findings give insight to TNBC's response to the anticancer effects of RT and CFI combination treatment, laying the groundwork for identifying potential novel biomarkers and drug targets. Ongoing investigation of MMP1, IL8, IL1RL1, and ICAM1 is underway, and future analysis of the RNA-seq dataset will contribute to the identification of other key targets and pathways at play in the response mechanism.

Poster #13

Patient-Derived Xenografts in Immunodeficient SRG Rats as a Novel Orthotopic Model of Glioblastoma

Tony Zhang[2], Elizabeth Fenton[1], Niveen Fulcher[2], Lohiny Balendran[2], Rehanna Kanji[1], Abdulla Elsaleh[3], Cleusa De Oliveira[1], Susanne Schmid[1], Matthew O. Hebb[1,2]
Departments of [1]Anatomy and Cell Biology, [2]Clinical Neurological Sciences, [3]Physiology and Pharmacology, Western University, London, ON, Canada

Introduction:
Glioblastoma multiforme (GBM) is the most aggressive and prevalent primary malignant brain tumor in adults, characterized by rapid progression, extensive heterogeneity, and limited therapeutic options. Despite advancements in surgical resection, radiotherapy, and chemotherapeutic regimens, patient prognosis remains dismal, with median survival rarely exceeding 15 months. This underscores a critical and ongoing need for translational preclinical models that more accurately reflect the human disease. The Sprague Dawley-Rag2/Il2rg Knockout Rat (SRG Rat™), a recently developed immunodeficient rodent model, offers a promising platform for intracerebral xenograft studies. Its lack of mature T, B, and NK cells enables robust engraftment of human tumor cells, making it a potentially powerful model for evaluating novel therapeutic strategies in GBM.

Methods:
Patient-derived GBM cells (GBM17, GBM23, and GBM93), obtained from surgical resections, were transduced to express tdTomato-luciferase. These GBM cell lines were subsequently used for stereotaxic implantation. Adult SRG RatsTM were anesthetized with isoflurane and placed in a stereotaxic frame. A unilateral burr hole was drilled at the following coordinate from bregma: anteroposterior + 1.2 mm, lateral + 3.0 mm, dorsoventral - 6.5 mm. Animals received 1 × 106 GBM17 or GBM23 cells in 10 µL PBS—injected unilaterally at a rate of 0.2 µL/min using a 10 µL Hamilton syringe. Tumor growth was monitored using bioluminescence imaging (BLI) for up to 13 weeks. At endpoint, brains were extracted, and post-mortem MRI was performed to confirm tumor presence.

Results:
GBM17 and GBM23 cells were implanted into cohorts consisting of n = 2 male and n = 2 female SRG Rats™ per cell line (total n = 4 per group). Of the GBM17 group, two animals exhibited steadily increasing BLI signals indicative of tumor growth, which was subsequently confirmed by post-mortem MRI. The remaining two rats in this group did not show increased BLI signal, suggesting either failed engraftment or minimal tumor proliferation. In contrast, all four animals implanted with GBM23 cells demonstrated progressive increases in BLI signals. Post-mortem MRI confirmed the presence of established tumors in three out of four cases. Implantation of GBM93 cells was recently completed, and early-stage data are currently being collected.

Conclusions:
These preliminary findings suggest that the SRG Rat™ supports successful intracerebral engraftment of patient-derived GBM cells, positioning it as a valuable model for preclinical glioblastoma research. The consistent tumor growth observed in the GBM23 cohort demonstrates the model's potential reliability, whereas the variability observed with GBM17 underscores the influence of tumor-intrinsic factors such as cellular heterogeneity and differing tumorigenic capacities among primary GBM lines. Further studies employing larger sample sizes, multiple GBM subtypes, and extended longitudinal follow-up are essential to evaluate the model's robustness and reproducibility. Validation of this system could bridge critical gaps in translational neuro-oncology by offering a more physiologically relevant platform for therapeutic testing, ultimately improving the pipeline for advancing candidate treatments into clinical trials.

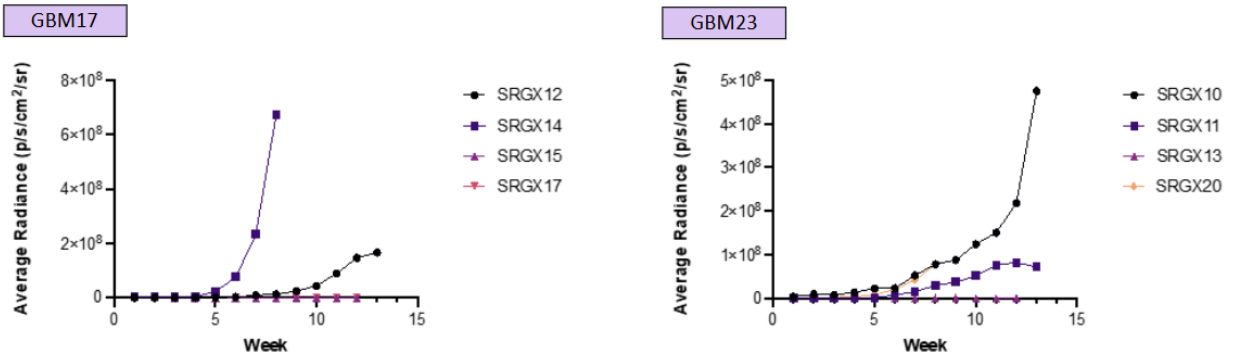

Figure. Longitudinal monitoring of intracerebral tumor growth via bioluminescence imaging in SRG Rats™ implanted with GBM17 or GBM23 cells. Average radiance (p/s/cm²/sr) was measured weekly using bioluminescence imaging (BLI) following intracerebral implantation of 1×10^6 patient-derived glioblastoma multiforme (GBM) cells into SRG Rats™. **Left panel:** BLI signal from rats implanted with GBM17 cells (n = 4; SRGX12, SRGX14, SRGX15, SRGX17) revealed heterogeneous tumor growth, with only two animals (SRGX12 and SRGX14) showing substantial increases in signal. **Right panel:** BLI signal from rats implanted with GBM23 cells (n = 4; SRGX10, SRGX11, SRGX13, SRGX20) demonstrated more consistent tumor progression, with all rats showing sustained radiance increases over time (SRGX13 increase not visible).

Poster #14

The Cyclin-Like Protein Spy1 Overrides Senescence in Glioblastoma (GBM)

Stephanie Dinescu[1], Dorota Lubanska[1], Lisa Porter[1,2]
[1]University of Windsor, [2] St. Joseph's Health Care London

Introduction: Glioblastoma (GBM) is the most frequent and aggressive primary malignant brain tumour with a poor prognosis despite intensive conventional therapies. A key challenge in treating GBM is its ability to resist treatment, with a subset of tumour cells surviving and entering cellular senescence, a state of irreversible cell cycle arrest. While senescence initially halts tumour growth, prolonged senescence can lead to an altered tumour microenvironment, which in turn can lead to tumour recurrence. Spy1, an atypical cell cycle regulator elevated in GBM, has been shown to be implicated in senescence. This cyclin-like protein activates cyclin-dependent kinases (CDKs) even in the presence of conditions that would normally cause cell cycle arrest. Spy1 has also been shown to override reprogramming-induced senescence by suppressing critical senescence-inducing CDK inhibitors (CKIs), leading to increased and uncontrolled cell proliferation. We hypothesize that Spy1 promotes GBM tumour growth and progression by enabling cancerous cells to evade senescence.

Methods: Using in vitro and in vivo systems, this project will explore Spy1's influence on senescence in GBM and assesses whether Spy1 targeting can enhance the effectiveness of therapies targeting senescent cells. Spy1 will first be knocked down in GBM cell lines, and the levels of senescence will be evaluated through senescence-associated β-galactosidase staining and transcriptional analysis of senescence markers. These assessments will be replicated in Spy1-knockdown GBM cell lines subjected to temozolomide (TMZ), the conventional treatment for GBM. Furthermore, this project will explore the combination of Spy1 inhibition with senolytic drugs, which are designed to eliminate senescent cells. The therapeutic efficacy of this combination will be evaluated through cell viability assays to assess cell death.

Results: Spy1 has been shown to be override cellular senescence of GBM. We have demonstrated that endogenous levels of Spy1 increase up to 14 days post therapy-induced senescence induction with TMZ. Furthermore, GBM cells were sorted into senescent and non-senescent populations, revealing differential Spy1 mRNA expression between the two groups. Spy1 knockdown, both in vitro and in vivo, led to a significant increase in senescence. Lastly, combining senolytic treatment with Spy1 targeting in GBM cells treated with TMZ enhanced cell death, indicating a potential combinatorial therapeutic strategy.

Discussion: We have demonstrated that targeting Spy1 leads to an increase in the number of senescent cells in GBM, and importantly, these senescent populations can be effectively eliminated using senolytics. Further investigations are needed to determine the optimal timing and duration for administering TMZ, Spy1-targeting, and senolytic therapies. Future studies should further explore these therapeutic combinations using *in vivo* models. Continued research into Spy1 and its involvement in senescence of GBM may open new avenues for the development of personalized treatments aimed at preventing the onset and progression of GBM.

Poster #15

DNA methylation patterns in patient-derived organoids distinguish basal-like vs. classical phenotypes

Joana Ribeiro Pinto[1,6], Fatemeh Behjati[4] and Christopher Pin[1-3,5-6]

Departments of Physiology and Pharmacology[1], Oncology[2], Paediatrics[3], Pathology and Computer Science[4], Schulich School of Medicine & Dentistry at Western University; Baker Centre for Pancreatic Cancer Research[5] and Verspeeten Family Cancer Centre[6], London ON, Canada

Introduction: Pancreatic ductal adenocarcinoma (PDAC) is predicted to become the second leading cause of cancer-related deaths by 2040 with a 5-year survival rate of ~12%. This dismal outcome is linked to late diagnosis and rapid adaptative response to chemotherapy regimens, which are composed of either gemcitabine-Abraxane or the poly-agent FOLFIRINOX. These treatments are given based on patient fitness rather than the tumour's molecular characteristics which does not always reflect how the tumour will respond to treatment. Therefore, there is a need to develop patient-specific strategies to overcome this obstacle, which should be based on the tumour's molecular characteristics. The consensus PDAC subtypes are "classical" and "basal-like", characterized by the expression of pancreatic developmental genes or mesenchymal genes, respectively. While basal-like tumors are classified as more aggressive than classical tumors, this stratification does not provide insight into PDAC's adaptability mechanisms. Rapidly acquired resistance is thought to involve epigenetic reprogramming leading to the repression of pathways involved in chemosensitivity. Therefore, identifying epigenetic profiles that correlate to tumor subtypes will improve tumour subtyping and possibly elucidate potential adaptative mechanisms associated with these subtypes. We hypothesize that DNA methylation profiles provide a stable definition of tumour subtypes in patient-derived organoids (PDOs), which can be used for further tumour characterization of tumour samples for better stratification in a clinical setting.

Methods: DNA was isolated from PDOs derived from the COMPASS and Prosper-PANC cohorts (n=66). Global DNA methylation was assessed using Illumina Human EPIC v2 Methylation array. DNA methylation profiles associated with basal-like and classical subtypes were determined by Differential Methylation Analysis to identify subtype-specific CpGs. DNA methylation profiles were assessed in TCGA-PAAD samples to determine global DNA methylation patterns of bulk tumour from patients.

Results: DNA methylation patterns clustered PDOs based on differentially methylated CpG sites representative of basal-like vs classical. Basal-like tumours showed more consistent methylation patterns compared to classical tumours, suggesting targeted hypermethylation occurs in this subtype. Similar hypermethylation events were observed in bulk tissue when comparing subtypes, suggesting DNA methylation patterns distinguish PDAC subtypes. This data also identified potential targetable hypermethylation events in basal-like subtype.

Conclusions: PDOs have been established as a reliable model for targeted therapeutic studies as they consistently maintain patient characteristics, however transcriptomic analysis shows variance between patient and PDOs in culture. DNA methylation identify a more stable and expandable categorization method of cancer cells and suggests epigenetic profiles may be linked to specific clinical features. These results support the hypothesis that PDAC epigenetic programs are stable and can be used for better PDAC classification and additional therapeutic target testing *in vitro.*

Poster #16

ATF3 mediates the epigenetic reprogramming in KRAS^{G12D}-dependent pancreatic cancer

Fatemeh Mousavi[1,5,6], Parisa Shooshtari[1,3], Christopher Pin[1,2,4,5,6]

Departments of [1]Physiology & Pharmacology, [2]Paediatrics, [3]Pathology and Lab Medicine and [4]Oncology, Schulich School of Medicine and Dentistry, University of Western Ontario; [5]Baker Centre for Pancreatic Cancer and [6]Verspeeten Family Cancer Centre, London, Ontario

Introduction: With a five-year survival rate of ~12%, Pancreatic Ductal Adenocarcinoma (PDAC) is the 3rd leading cause of cancer-related deaths in North America. Over 90% of PDAC patients harbour gain of function *KRAS* mutations, most notably *KRAS^{G12D}*. However, additional genetic or environmental events are required for *KRAS* mutations to promote PDAC. Our laboratory has been examined cell stress pathways and identified Activating Transcription Factor 3 (ATF3) as a key contributor to KRAS^{G12D}-dependent pancreatic cancer initiation and progression. Mechanistically, ATF3 can promote histone deacetylation at genes that stabilize a mature cell phenotype, which leads to gene repression and allow progression to high grade pancreatic intraepithelial neoplasias and PDAC. However, the mechanisms ATF3 affects to promote PDAC remain unknown. Based on previous studies, I hypothesize that ATF3 affects pancreatic tumorigenesis by promoting histone deacetylation and repressing genes that affect KRAS signalling.

Methods: Organoid lines were established from neoplastic pancreatic tissue in mice expressing KRAS^{G12D} with (*ATF3$^{+/+}$KRAS$^{G12D/+}$*) or without ATF3 (*ATF3$^{-/-}$KRAS$^{G12D/+}$*). Following at least five passages to ensure only neoplastic cells remained in the cultures, morphologic, transcriptomic, and epigenetic landscapes were assessed 5 and 7 days after organoid passaging. Global gene expression (RNA-seq), H3K27 histone acetylation (chromatin immunoprecipitation; ChIP-seq), and chromatin accessibility (Assay for transposase-accessible chromatin; ATAC-seq) were assessed in multiple *ATF3$^{+/+}$KRAS$^{G12D/+}$* and *ATF3$^{-/-}$KRAS$^{G12D/+}$* organoid lines. Sequenced datasets were aligned to the mm10 genome using STAR (RNA-seq) or Bowtie2 (ChIP-seq, ATAC-seq). Differential expression and binding analyses were performed using DESeq2 (RNA-seq) or Bedtools (ChIP-seq, ATAC-seq). Experimental validation of targets was performed via Western Blotting.

Results: *ATF3$^{-/-}$KRAS$^{G12D/+}$* organoids showed widespread increases in histone acetylation and chromatin accessibility preferentially at distal regions of the chromatin, indicating ATF3 coordinates KRAS^{G12D}-induced acetylation programming. At 7 days after passaging, *ATF3$^{-/-}$KRAS$^{G12D/+}$* organoids start collapsing and dying, which is associated with widespread loss of acetylation at gene promoters. Distal acetylation remains high in the absence of ATF3, suggesting ATF3 actively stabilizes acetylation over time. Interestingly, ATF3 seem to outcompete other transcription factors for certain open chromatin regions to transcriptionally repress them, and a significant portion of these repressed regions affect oncogenic KRAS signaling. ATF3 directly targets *Dusp10* and *Ptprr*, two phosphatases that inhibit KRAS signaling, which was confirmed by reduced ERK phosphorylation in *ATF3$^{-/-}$KRAS$^{G12D/+}$* organoids. This suggests a role for ATF3 in directly mediating oncogenic KRAS signaling during pancreatic cancer development.

Conclusion: These findings indicate ATF3 plays multiple roles in affecting KRAS-drive pathways in PDAC. ATF3 is a crucial mediator of histone deacetylation driven by KRAS^{G12D} to preferentially inhibit gene expression. In addition, ATF3 targets specific genes that repress KRAS signaling. These results identify ATF3 as a central link between stress response pathways and chromatin regulation in PDAC and highlight its potential as a therapeutic target to disrupt KRAS-driven epigenetic programming.

Poster #17

Interpretable Deep Learning Integration of Multi-Omic data in Pancreatic Cancer

Fatemeh Behjati[3,5,6], Emilie-Jaune Pons[1,5-7], Brian Yan[2,6], Michael Sey[2,6], Jennifer Campbell2,[6,7], Nadeem Hussain[2], Ken Leslie[2,4-7], Zaharacy Klassen[1,6-7], Christopher Pin[1,5-7] and Parisa Shooshtari[3,5-7]

Departments of [1]Physiology and Pharmacology, [2]Medicine (Division of Gastroenterology), [3]Pathology, [4]Surgery, and Laboratory Medicine, and [5]Oncology, Schulich School of Medicine and Dentistry, Western University, [6]Baker Centre for Pancreatic Cancer, [7]Verspeeten Family Cancer Center, London Health Sciences Centre, London, Ontario, Canada

Introduction: Pancreatic ductal adenocarcinoma (PDAC) is a highly lethal cancer in Canada, characterized by inter- and intra-patient heterogeneity and resistance to current treatments. This complexity is partly due to the influence of cancer-associated fibroblasts (CAFs), particularly the inflammatory (iCAF) and myofibroblastic (myCAF) subtypes, which play crucial roles in shaping the tumor microenvironment and drive tumor progression. However, the specific epigenetic mechanisms by which CAFs affect tumor cells remain unclear.

Methods: To address this, our laboratory generated multi-modal data from patient-derived organoids treated with conditioned media from iCAF or myCAF enriched samples, or human feeding media (HFM), and profiled them with RNA-seq, ATAC-seq, DNA methylation, and whole-exome-sequencing (WES). We have access to clinical data to link molecular characteristics with patient outcomes (Fig1.a).

We developed a novel two-channel attention-based variational autoencoder (VAE) to integrate CAF subtype-specific chromatin accessibility data to identify and prioritize regulatory regions influencing gene expression, providing new insights into the molecular drivers of PDAC heterogeneity and CAF-tumor interactions (Fig1.b).
We employed 1D convolutional layers to capture spatial genomic dependencies. We represent iCAF and myCAF profiles as separate channels into the model, encouraging it to integrate this data into a shared latent space.
Results: Our model achieved a prediction correlation of approximately \$0.44±0.02 (P-value < 0.001) on the test dataset (Fig1.c). By interrogating attention weights, we are able to identify regulatory regions for any given gene. An example is Figure1d, which illustrates attention weights and true ATAC signal for *KRAS*, a key regulator in PDAC, and their product as a proxy for regulatory region importance.

Conclusions: Our proposed VAE equipped with an attention mechanism and regression head provides interpretable weights, highlighting chromatin regions most predictive of gene expression for each CAF treatment. Comparing results with HFM-treated organoids allows us to pinpoint CAF-specific regulatory elements. Our interpretable deep learning

framework enhances understanding of PDAC biology and supports precision oncology by linking molecular subtypes to therapeutic response.

Figure1 Schematic overview of the data and VAE model. **a)**Patient-derived organoids (PDOs) were established to profile the genetic and epigenetic landscape of tumors in the presence or absence of conditioned media from CAFs. ATAC-seq read counts from iCAF and myCAF samples served as input for training **b)** a two-channel variational autoencoder (VAE). The model's regression segment predicts gene expression for both iCAF and myCAF samples. **c)** Scatter plot illustrating the correlation between predicted and true gene expression in the test set (correlation coefficient = 0.46). d**)** Attention weights and ATAC-seq signal for \emph{KRAS} are visualized to highlight regulatory regions related to identified by the model for this gene.

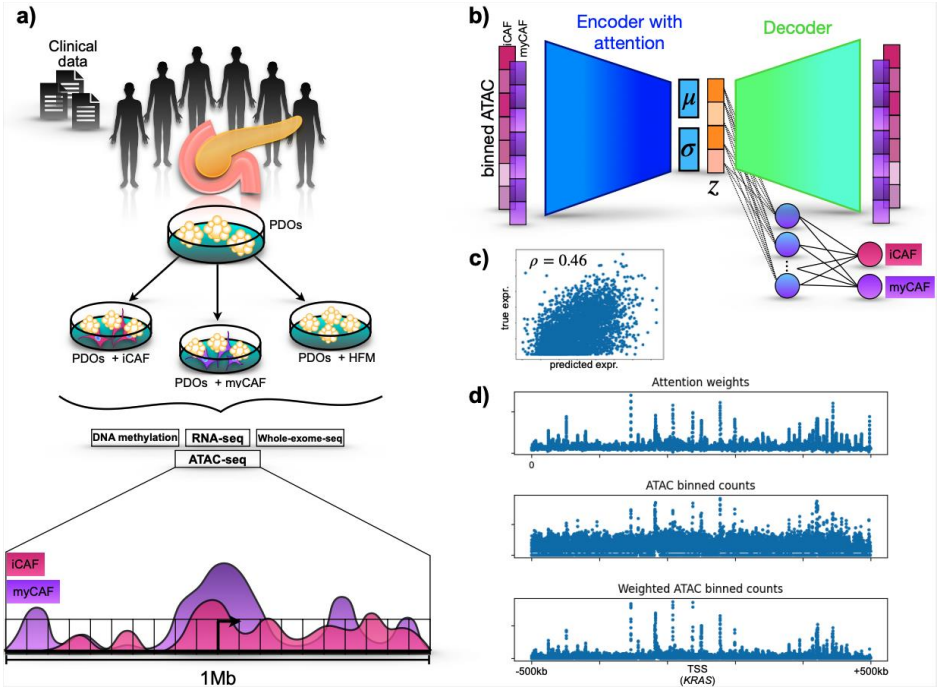

Poster #18

Exploring cell fate conversion during glioma initiation and progression

Kasha Y. Mansour[1,2,5], Yan Jiang[2,5], Jasper Wu[1,2,5], Qi Zhang[4] and Nathalie G. Bérubé[1,2,3,5]

[1]Department of Anatomy and Cell Biology, [2]Pediatrics, [3]Oncology, and [4]Pathology and Laboratory Medicine Western University, London ON, Canada; [5]Division of Genetics and Development, Children's Health Research Institute, London ON, Canada

Introduction: Mutations in the alpha-thalassemia intellectual disability (*ATRX*) and tumour protein 53 (*TP53*) genes are prevalent in cancer, particularly in gliomas. ATRX encodes a chromatin remodelling protein crucial for genome stability, gene expression regulation, and DNA repair. We previously demonstrated that perinatal ATRX ablation in oligodendrocyte precursor cells (OPCs) leads to a fate switch towards astrocyte-like phenotype. Here, we investigated whether concurrent loss of ATRX and TP53 in OPCs promotes tumour progression and astrocytoma-like tumour formation through a similar fate switch.

Methods: We generated a genetic model of glioma in mice using inducible Cre-dependent ATRX and TP53 ablation, along with tdTomato expression (tdTom+) in Sox10+ neural crest-derived cells. Tumours are dissected, sectioned and subject to immunohistological analysis by staining for markers of OPCs, oligodendrocytes, and astrocytes. Primary cell cultures will be established from the tumours and immunofluorescence staining will be performed to assess similar markers.

Results: We found that ATRX and TP53 double knockout (dKO) mice develop tdTom+ masses in the brain and periphery, leading to an end-of-life between 6-16 months. Notably, we observed a significant sex-based disparity in survival rates: female dKO mice exhibited a markedly shorter median survival (308 days) compared to their male counterparts (409 days). Immunohistochemical analysis revealed tumour heterogeneity, with regions expressing OPC markers and others expressing astrocyte markers, indicating clonal expansion after fate conversion. Primary cells from a tdTom+ brain lesions also showed high astrocyte marker expression and genomic instability (multinucleated cells, micronuclei), supporting the notion that ATRX and TP53 loss in OPCs initiates tumour formation accompanied by a conversion to an astrocytic lineage.

Conclusions: We have confirmed that loss of ATRX and p53 leads to the development of tumours, in the brain and periphery. Preliminary analysis of the tumours reveals regions of the tumour that express markers of astrocytes, with low expression of oligodendrocyte markers indicating a fate switch. This provides a model system for investigating tumourigenesis mechanisms associated with ATRX/TP53 loss, which can be leveraged in the future to identify novel therapeutic targets for gliomas.

Poster #19

Exploring Molecular and Tumour Immune Microenvironment Alterations in Pathogenesis of Triple-Negative Breast Cancer Using Spatial Proteomics

Anayra Goncalves[1], Vasudeva Bhat[1,2,3], Emily Goebel[2,3], Carl Postenka[2], Muriel Brackstone[4,6] Alison Allan[1,2,4], Armen Parsyan[1,2,4,5,6]

[1]Department of Anatomy and Cell Biology, Schulich School of Medicine and Dentistry, Western University, London, ON, Canada; [2]Verspeeten Family Cancer Centre, London Health Science Centre, London, ON, Canada; [3]Department of Pathology and Laboratory Medicine, Western University, London, ON Canada; [4]Department of Oncology, Schulich School of Medicine and Dentistry, Western University, London, ON, Canada; [5]Department of Surgery, Schulich School of Medicine and Dentistry, Western University, London, ON, Canada; [6]St. Joseph's Health Care London, London, ON, Canada and London Health Sciences Centre

Introduction: Triple-negative breast cancer (TNBC) is an aggressive subtype with poor outcomes and limited biomarkers and targeted therapies. Axillary lymph nodes (ALN) are a central gateway for metastasis and the interplay between cancer cells and the immune tumour microenvironment (iTME) is a major contributor to this metastatic progression. Understanding this process may reveal novel biomarkers and therapeutic targets. We hypothesize that region-specific alterations in tumour cells and the surrounding iTME within heterogeneous TNBC tissues contribute to ALN metastasis.

Materials and Methods: Formalin fixed paraffin embedded tissue blocks from 50 treatment-naïve TNBC patients (with ALN metastases and no distant metastases), including primary tumours, metastatic ALNs, and normal breast tissue were selected. Hematoxylin & Eosin staining was performed on tissue microarrays to identify regions of interest (ROI) including tumour location and tumour infiltrating lymphocytes (TIL). Spatial proteomics was performed using GeoMx Digital Spatial Profiler, with areas within the ROIs selected using PanCK (tumour cell marker) and CD45 (immune cell marker) fluorescent antibodies. The nCounter immuno-oncology panel was used to evaluate the impact of immune system on ALN metastases.

Results: Our preliminary in silico analysis revealed perturbation of proteins in primary breast tumour tumour compared to normal tissue. We found significant upregulation of proteins such as S6, p53, and an anti-apoptotic marker BCLXL in tumour cell (PanCK+) enriched areas. Additionally, we found an abundance of the phosphorylated form of MEK1 (S217/S221). Interestingly, proteins upregulated in PanCK+ cells in the primary tumour, such as S6, BCLXL, and the activated form of MEK1 (phosphor-MEK1) were also found to be upregulated in PanCK+ cells found in the ALN compared to normal tissue. Furthermore, we also found upregulation of PARP, Histone H3, and phosphorylated AKT (S473) PanCK+ cells in ALN compared to normal tissue. Our analysis revealed an abundance of phosphorylated proteins related to survival, proliferation, and therapy resistance including AKT1 (S473), and JNK (T183/Y185) in PanCk+ cells within high TIL regions of primary breast tumours compared to normal breast tissue. Our analysis revealed that changes in the protein expression profiles in PanCK+ cells in primary breast tumour and ALN suggested their role in tumour progression and enhanced metastatic burden. In CD45+ immune cell-rich areas, we observed a potential upregulation of markers associated with different immune cells including CD11c (dendritic cells), CD4 (T helper cells), and CD68 (macrophages). We also observed upregulation of immune checkpoint protein, VISTA (associated with suppressing T cell function), in primary breast tumour compared to control. We also observed upregulation of HLA-DR, markers linked to enhanced responses to immunotherapy indicating a more active and immunogenic iTME. Ongoing analysis is expected to reveal additional molecular and iTME alterations for downstream validation.

Conclusion/Discussion: Our preliminary findings highlight distinct molecular and immune signatures associated with TIL-high regions in breast tumours when compared to normal breast tissues. The presence of phosphorylated AKT1 (S473) and JNK (T183/Y185) in tumour cells may contribute to therapeutic resistance and disease progression. Together, these insights may support the identification of spatially-resolved biomarkers and inform the development of target therapeutic strategies in TNBC.

Poster #20

Dendritic cells orchestrate immune response to anti-PD-1 therapy in MMR-deficient colorectal cancer

Chloe Davidson[1], Hong MMY[1], Baines KJ[1], Figueredo R[2], Jabbari Zadeh B[3], Cheung T[1], Maleki S[1,2,3,4]

[1] Department of Pathology and Laboratory Medicine, Western University, [2] Department of Oncology, Western University, [3] Verspeeten Family Cancer Centre, Lawson Health Research Institute, [4] Department of Medical Biophysics Western University

Introduction: The DNA mismatch repair (MMR) pathway corrects errors in base pairing during DNA replication. A deficiency (dMMR) in this pathway leads to heightened presence of tumour neoantigens, increased tumour immunogenicity, and likeliness to respond to immune checkpoint inhibitors (ICIs) like anti-programmed cell death protein 1 (PD1) therapy. However, less than half of dMMR colorectal cancer (CRC) patients respond to anti-PD1 therapy. This signifies the importance to identify factors beyond tumour mutational burden that influence ICI response. One possible factor is the role dendritic cells (DCs) in the tumour microenvironment. DCs can recognize tumours and present tumour-specific antigens to T-cells which can then initiate an anti-tumour immune response. The role of each unique DC subset in activating and recruiting tumour-specific T-cells within dMMR CRC tumours is not well understood. We hypothesize that anti-PD1-sensitive and -resistant dMMR tumours differentially mature and recruit DCs, which will ultimately impact T-cell infiltration and responsiveness to anti-PD1 therapy.

Methods: We used naturally occurring dMMR MC38 and induced dMMR CT26 cell lines to investigate differential immune profiles within the tumours along with their ability to respond to anti-PD1 therapy. dMMR CRC cells were injected into mice and the tumours growth was measured. Tumours were treated with three injections of anti-PD1 treatment or isotype control. The endpoint was reached when tumour volumes exceeded 1500 mm^3. Tumours were then harvested, stained with antibodies for maturation and activation markers, then analyzed using flow cytometry. The Cancer Genome Atlas was also utilized to assess RNA expression level of cytokines and chemokines within human CRC tumours to examine any differences that may influence anti-PD1 response between MMR-deficient and -proficient (pMMR) tumours.

Results: Our results confirm that MC38 tumours are responsive to anti-PD1 therapy due to limited tumour growth while dMMR CT26 tumours are resistant to anti-PD1 as the tumours receiving treatment were not affected. Anti-PD1-sensitive tumours contained a higher abundance of DCs with more maturation while anti-PD1-resistant tumours had more T-cells present. MMR-deficiency also increased the expression of DC regulatory chemokines and cytokines as compared to pMMR CRC in patient samples.

Conclusions: Despite dMMR tumours having increased immunogenicity, specific cytokine and chemokine expression patterns may influence DC recruitment and maturation in the tumour microenvironment, ultimately affecting response to anti-PD1.

Poster #21

Macrophages as key determinants of immune checkpoint inhibitor response in DNA mismatch repair-deficient tumours

Megan M Y Hong[1], Rene Figueredo[3], Saman Maleki Vareki[1-4]

[1]Department of Pathology and Laboratory Medicine, University of Western Ontario, London, Ontario, Canada
[2]London Regional Cancer Program, Lawson Health Research Institute, London, Ontario, Canada
[3]Department of Oncology, University of Western Ontario, London, Ontario, Canada
[4]Department of Medical Biophysics, University of Western Ontario, London, Ontario, Canada

Introduction: Immune checkpoint inhibitors (ICIs), such as anti-PD1 and anti-CTLA-4, enhance patients' anti-tumour immune responses to eliminate cancer cells. Patients with DNA mismatch repair-deficient (dMMR) tumours have a greater response to anti-PD1 therapy than those with MMR-proficient (pMMR) tumours, a difference attributed to the elevated T-cell infiltration commonly observed in dMMR tumours. However, over half of these patients do not respond to anti-PD1 therapy, suggesting that T-cell abundance alone is not a reliable predictor of therapeutic success. Macrophages, the most abundant immune cells in solid tumours, can promote or suppress anti-tumour T-cell responses. Yet, their role in the therapeutic response to ICIs in dMMR cancers remains poorly understood. This study investigates how MMR deficiency affects the composition and function of macrophages in tumours and its consequent impact on the response to ICIs.

Methods: MMR repair deficiency was induced in ICI-resistant pMMR murine neuro-2a, 4T1, and CT26 cell lines by knocking out Mlh1 expression using CRISPR/Cas9. pMMR or dMMR tumours were grown in immunocompetent syngeneic mice and treated with anti-PD1 or anti-CTLA-4 once tumours became palpable. Macrophages were depleted using clodronate liposomes or anti-CSF1R to assess their effects on ICI response. Tumour growth was measured with callipers, followed by immune profiling by flow cytometry.

Results: dMMR neuro-2a, CT26 and 4T1 tumours exhibited greater T-cell infiltration than their pMMR tumour counterparts, yet response to anti-PD1 therapy varied among these models. MMR deficiency sensitized 4T1 tumours to anti-PD1 therapy, whereas dMMR neuro-2a and CT26 tumours remained resistant. Immune profiling revealed that anti-PD1-sensitive dMMR 4T1 tumours had an increase of pro-inflammatory macrophage subsets—specifically $Ly6c^{High}$, $MHCII^{+}$, and M1-like macrophages—compared to pMMR tumours. In contrast, this shift in macrophage composition towards a pro-inflammatory phenotype was not observed in anti-PD1-resistant dMMR CT26 tumours compared to pMMR tumours. This divergence suggests that specific macrophage populations may drive anti-PD-1 sensitivity, independent of T-cell infiltration. Depletion of immunosuppressive macrophages with anti-CSF1R sensitized dMMR CT26 and neuro-2a tumours to anti-PD1 therapy and increased $CD8^{+}$ T-cell activation. Notably, while dMMR neuro-2a tumours were resistant to anti-PD1 therapy, they became sensitized to anti-CTLA-4 therapy. The therapeutic efficacy of anti-CTLA-4 depended on $Ly6c^{High}$ macrophages that depleted regulatory T-cells through Fc-dependent mechanisms.

Discussion: These findings highlight macrophages as critical modulators of ICI response in dMMR tumours. While macrophages in dMMR tumours confer resistance to anti-PD1 therapy, certain subsets can be leveraged to enhance Fc-dependent therapies like anti-CTLA-4. Understanding how the tumour immune microenvironment shapes ICI response will enable more strategic therapeutic selection, ultimately improving patient outcomes.

Poster #22

STAT3 Signalling Orchestrates Actin Cytoskeleton Remodelling and Oncogenic Transformation

Alyssa Wu[1], Chenelle Flores[1], Evan Wang[1], Tomonori Kaneko[1], Shawn S. C. Li[1,2]
[1]Department of Biochemistry, [2]Oncology, Schulich School of Medicine and Dentistry, Western University

ABSTRACT

Introduction: Signal Transducer and Activator of Transcription 3 (STAT3) is a constitutively activated transcription factor in many human cancers, driving tumorigenesis, proliferation, metastasis, and chemoresistance. While canonical STAT3 activation pathways have been extensively investigated, a comprehensive understanding of all upstream regulators, downstream targets, and interacting partners, particularly in the context of non-canonical signalling and feedback mechanisms, remains incomplete. This knowledge gap hinders the development of truly effective and specific STAT3-targeted therapies.

Methods: We employed a multi-faceted proteomic and phosphoproteomic approach using mass spectrometry to analyze changes in protein expression and phosphorylation upon STAT3 modulation via CRISPR-Cas9 knockout. This allowed us to identify novel STAT3-regulated proteins and characterize non-canonical STAT3 phosphorylation events. F-actin immunofluorescence, wound healing, transwell assays, and 3D colony formation in soft agar validated functional consequences.

Results: Proteomic and phosphoproteomic analyses revealed thousands of differentially expressed proteins and phosphosites upon STAT3 modulation, suggesting a broader regulatory role than previously recognized. Beyond confirming a small subset (<200) of known STAT3 transcriptional targets, we identified novel putative STAT3-regulated proteins and pathways, including those associated with actin filament-based processes, wound healing, and extracellular matrix (ECM) remodeling. Furthermore, we characterized non-canonical STAT3 phosphorylation events impacting mitochondrial function and cellular metabolism. These findings point to a potential role for STAT3 in metastasis and suggest compensatory feedback mechanisms involving STAT3 activation upon inhibition of other signalling pathways, including upregulation of ECM-related genes and cell adhesion markers.

Conclusions: Our findings provide insights into molecular mechanisms underlying STAT3-driven cancer. This thorough investigation aims to generate a comprehensive list of proteins, phosphoproteins, and signalling pathways regulated by STAT3. The identified novel interactions, phosphorylation events, and downstream targets will provide a more complete picture of STAT3's pleiotropic roles and may reveal new vulnerabilities for therapeutic intervention in STAT3-dependent cancers, with the potential to overcome current limitations in targeted therapy.

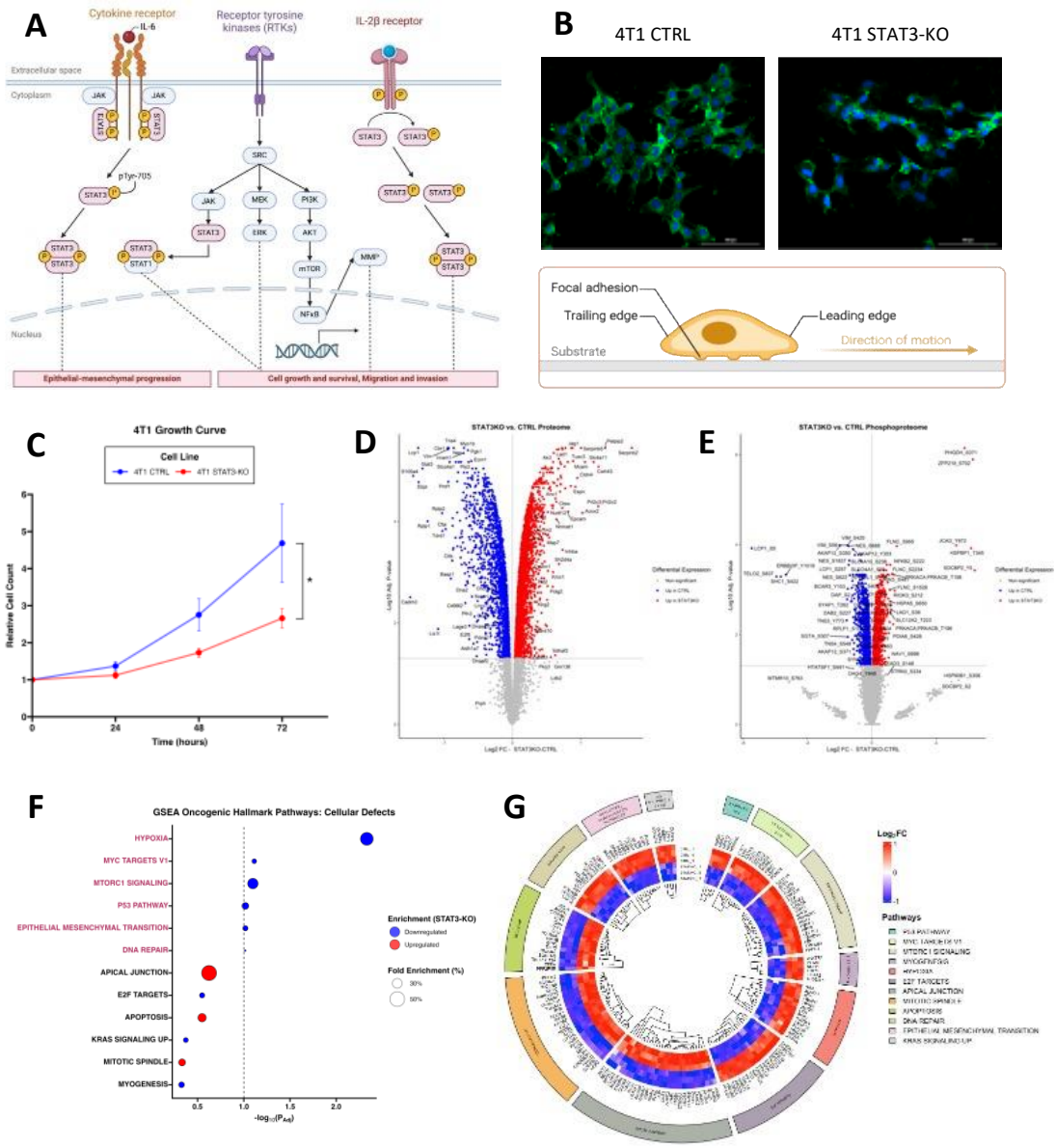

Figure 1. Effects of STAT3 knockout in triple-negative breast cancer cells. **(A)** Schematic representation of the STAT3 signalling pathway. **(B)** Fluorescent microscopy images of 4T1 CTRL and STAT3-KO cells stained for F-actin (Phalloidin iFluor-488, green) and nuclei (Hoechst 33342, blue). **(C)** Growth curve of 4T1 STAT3-KO compared to 4T1 CTRL. Data are presented as mean ± SD. Statistical significance is shown as *$p < 0.05$. **(D-E)** Volcano plots showing differentially expressed genes for **(D)** proteome and **(E)** phosphoproteome. Red dots represent upregulated proteins, while blue dots represent downregulated proteins. Grey dots represent proteins/phosphosites that did not meet the significance threshold. **(F)** Dot plot showing the enrichment of GSEA oncogenic pathways in 4T1 STAT3-KO cells. Dot size corresponds to gene ratio, converted to fold enrichment. **(G)** Annotated circular heatmap showing the differentially-expressed proteins (DEPs) involved in the oncogenic pathways. Heatmap shows the protein abundances according to log fold-change (Log_2FC) > 1 and adjusted p-value < 0.05. All experiments with done using biological triplicates (n = 3).

Poster #23

Examining the Unfolded Protein Response in Radiation Resistance of Pancreatic Ductal Adenocarcinoma

Ye Shen[1,2,7], Emilie Jaune-Pons[1,2,7], Sophie Heinrich[3], Eugene Wong[3,4,5], Christopher Pin[1,2,5,6,7]

Departments of [1]Physiology and Pharmacology, [3]Physics & Astronomy, [4]Medical Biophysics,[5]Oncology, and [6]Paediatrics, Schulich School of Medicine and Dentistry, University of Western Ontario, [7]Baker Centre for Pancreatic Cancer, [2]Verspeeten Family Cancer Center, London, Ontario, Canada

Introduction: Pancreatic ductal adenocarcinoma (PDAC) is one of the deadliest malignancies, with a five-year survival rate of around 12%. At the time of diagnosis, 25%–30% of cases are characterized as either borderline resectable or locally advanced PDAC, where the tumor is confined to the pancreas but invades surrounding vascular structures, complicating the possibility of surgical resection. For these cases, chemoradiotherapy can be used to shrink the tumor preoperatively, but its clinical benefit remains controversial. Recent studies highlight the unfolded protein response (UPR) as a potential contributor to chemoradiotherapy resistance in PDAC. UPR is a signaling pathway activated in response to accumulation of unfolded or misfolded proteins in the endoplasmic reticulum (ER) during cell stress. The UPR consists of three pathways - PERK, IRE1, and ATF6 – and are all regulated by the ER chaperone BiP/GRP78. BiP/GRP78 is frequently overexpressed in various cancers, where it supports survival and is linked to poor prognosis and chemoresistance. Therefore, we hypothesize that high activity of BiP/GRP78 promotes radio-resistance in PDAC cells.

Methods: Radiation sensitivity was assessed in three patient-derived 2D PDAC cell lines (PDAC021T, PDAC001T, and PDAC013T) and three patient-derived 3D PDAC organoids (EUS107, EUS124, and EUS137), using cell proliferation and clonogenic assays to determine. Cell growth was assessed using an Incucyte system for live cell imaging. To evaluate DNA damage, immunofluorescence staining for γ-H2AX was performed at 24 and 72 hr post-irradiation. UPR activity was analyzed via Western blotting of key UPR signaling mediators at 0.5, 4, and 24 hr following exposure to 4 Gy radiation. To assess whether inhibiting BiP/GRP78 alters cancer cells' responses to radiation, PDAC cell lines were treated with the BiP inhibitor HA15, alone or in combination with 4 Gy radiation.

Results: Cell proliferation assays revealed distinct radiation response profiles among the three PDAC cell lines - PDAC021T exhibited radioresistance, PDAC013T was radiosensitive, and PDAC001T showed an intermediate response. The three patient-derived PDAC organoids also displayed variable responses to radiation therapy, underscoring the heterogeneity of treatment responses in PDAC. Immunofluorescence staining for γ-H2AX indicated increased DNA damage repair activity across all cell lines post-irradiation. Notably, BiP/GRP78 protein levels varied among the lines and correlated with their radiation sensitivity. Time-course Western blot analysis demonstrated the radiosensitive PDAC013T line exhibited rapid PERK activation following radiation exposure. Preliminary experiments combining the BiP/GRP78 inhibitor HA15 with radiation therapy suggested enhanced anti-tumor effects on cell growth compared to single treatment.

Discussion: Our data shows diversity in the radioresponse of cell lines, reflecting an inherent heterogeneity between PDAC tumours. Although induces DNA damage in all three lines, the activation and resolution of DNA breaks did not correlate with radiosensitivity. The inverse correlation of BiP/GRP78 expression and radiation sensitivity suggests BiP/GRP78 may be a viable target in combination with several different therapies. Understanding the role of UPR will be crucial for developing targeted strategies to overcome radiation resistance and improve treatment outcomes in PDAC.

Poster #24

Pharmacological inhibition of LKB1-NUAK1 signaling in a spheroid model of ovarian cancer metastasis

Sarah McArthur[1,2], Yudith Ramos Valdés[1] Ahmed Abdelhameed[3], Babu Joseph[3], Methvin Isaac[3], Radek Laufer[3], David E. Uehling[3], Trevor G. Shepherd[1,2,4,5]

[1]The Mary & John Knight Translational Ovarian Cancer Research Unit, Verspeeten Family Cancer Centre, London, ON, Canada.

[2]Department of Anatomy and Cell Biology, Schulich School of Medicine and Dentistry, Western University, London, ON, Canada.

[3]Drug Discovery Program, Ontario Institute for Cancer Research, MaRS Centre, Toronto, ON, Canada.

[4]Department of Oncology, Schulich School of Medicine and Dentistry, Western University, London, ON, Canada.

[5]Department of Obstetrics and Gynaecology, Schulich School of Medicine and Dentistry, Western University, London, ON, Canada.

Introduction: Epithelial ovarian cancer (EOC) is a lethal gynaecologic cancer, usually only diagnosed after widespread metastasis throughout the peritoneal cavity. EOC metastasis is unique, spreading via multicellular aggregates known as spheroids. Previously, we demonstrated Liver kinase B1 (LKB1) to be critical for the survival of EOC cells during metastasis. In response to bioenergetic stress invoked during metastasis, LKB1 activates NUAK1, which promotes spheroid integrity, reattachment, and fibronectin production. Using genetics-based CRISPR deletion cell lines, we have solid evidence that LKB1-NUAK1 signalling plays crucial roles in EOC metastasis, establishing them as new therapeutic targets. In collaboration with the OICR, we have developed several new small molecule LKB1-specific inhibitors, whereas NUAK1 can be inhibited by the commercially-available compound ON123300/Narazaciclib. Herein, we will investigate the effects of pharmacologic inhibition of LKB1-NUAK1 on metastatic properties of EOC spheroids, with the hypothesis that LKB1 ablation will have a greater impact on EOC metastasis as compared with NUAK1 blockade.

Methods: An initial screen of the OICR kinase library (n=720) was done against LKB1 in complex with its complex proteins, STRADA and MO25, to obtain promising LKB1 inhibitors. ASC-069 and Dinaciclib were the two compounds chosen and over 200 derivatives have been generated to further improve LKB1 specificity. Current lead compounds from cell-based NanoBRET and CETSA assays are 38964 (ASC-069 derivative), and 40482 and 40543 (Dinaciclib derivatives). Dose-response curves and spheroid reattachment assays were performed to evaluate LKB1-NUAK1 inhibition on spheroid cell viability and cell dispersion, respectively. Mesothelial clearance assays and Transwell migration/invasion assays will be performed to further evaluate LKB1/NUAK1 inhibition on metastatic properties of EOC spheroids in culture. On-target LKB1-NUAK1 inhibitory activity of ON123300 in EOC spheroids was verified by western blotting.

Results: Spheroid viability and dispersion following reattachment were more potently reduced following treatment with the LKB1 inhibitors compared to ON123300. Specifically, the ASC-060 derivative 38964 was more potent than both Dinaciclib derivatives, 40482 and 40543, to reduce spheroid cell viability and reattachment. Although ON123300 had little effect on spheroid cell viability, fibronectin expression was potently reduced in cultured spheroids and during reattachment following ON123300 treatment. Indeed, treatment with ON123300 resulted in a spheroid phenotype distinct from LKB1 inhibitor effects possibly by direct fibronectin reduction impacting spheroid integrity.

Discussion: We are the first to develop and characterize potential LKB1 small molecule inhibitors. These inhibitors will be important tools for the field as well as potential anti-cancer therapeutics alone or in combination with first-line chemotherapy. This project will continue to provide new insights into LKB1-NUAK1 as a crucial stress signalling mediator during advanced EOC disease.

Poster #25

The effect of pharmacological inhibition of endogenous hydrogen sulfide production on bladder cancer gemcitabine resistance

Liam McFarlane[1,2], Alp Sener[1,2,3,4]

[1]Matthew Mailing Center for Translational Transplant Studies, London Health Sciences Center, Western University, London, ON N6A 5A5, Canada

[2]Department of Microbiology & Immunology, Schulich School of Medicine & Dentistry, University of Western Ontario, London, ON N6A 5C1, Canada

[3]Department of Surgery, Division of Urology, London Health Sciences Center, Western University, London, ON N6A 5A5, Canada

[4]Multi-Organ Transplant Program, London Health Sciences Center, University Hospital, London, ON N6A 5A5, Canada

Introduction

Intravesical gemcitabine (GEM) and sequential GEM-docetaxel are emerging alternatives to Bacillus Calmette-Guérin (BCG) for intermediate- and high-risk non-muscle invasive bladder cancer (NMIBC), respectively. GEM is also used in BCG-unresponsive and BCG-refractory cases. Hydrogen sulfide (H_2S), an endogenously produced gaseous signaling molecule, is elevated in bladder tumors and correlates with tumor grade. Inhibition of H_2S synthesis has been shown to sensitize cancer cells to various chemotherapies. We investigated the effects of D-L-propargylglycine (PAG), an inhibitor of the H_2S-producing enzyme cystathionine γ-lyase (CSE), on the proliferation, migration, and GEM sensitivity of human NMIBC cells.

Methods

5637 bladder cancer cells were treated with varying concentrations of PAG, and cell proliferation was assessed using a CCK-8 assay over 72 hours. Migration was evaluated via scratch-wound assay with/without 100 µM PAG, imaged every 12 hours. GEM (1 µM) was added to the media with/without PAG, and expression of H_2S producing enzymes, intracellular H_2S levels, intracellular reactive oxygen species (ROS) level, and cell viability was analyzed using qPCR and flow cytometry at 24 and 48 hours.

Results

PAG treatment significantly attenuated 5637 cell proliferation and migration. GEM alone induced upregulation of CSE and consequently resulted in elevated intracellular H_2S levels as well as an increase in intracellular ROS. Co-treatment with PAG attenuated this increase of intracellular H_2S and exacerbated the GEM-induced increase of ROS. Cells treated with both GEM and PAG exhibited significantly reduced viability compared to GEM alone.

Discussion

These findings suggest that targeting CSE may be an effective strategy in enhancing GEM's cytotoxicity in NMIBC. Considering the well-established role of H_2S as an antioxidative agent, H_2S may act as a protective factor in NMIBC cells by buffering ROS induced by gemcitabine. Our study highlights the therapeutic potential of combining H_2S inhibition with standard chemotherapy approaches in the treatment of NMIBC.

Poster #26

TGFβ Induced Epithelial to Mesenchymal Transition in PDAC cells

Yee Wing Kwok and John DiGuglielmo
Physiology and Pharmacology, Schulich School of Medicine, Western University, London, ON, Canada

Introduction: Pancreatic cancer is one of the deadliest forms of cancer, with its most common form pancreatic ductal adenocarcinoma (PDAC), accounting for 90% of all pancreatic cancer cases. PDAC is the 4th highest cause of cancer mortality, with a five-year survival rate of 5%. This can be attributed to several factors: late diagnosis, aggressive metastasis, and treatment resistance. One process that can contribute to treatment resistance is epithelial-to-mesenchymal transition (EMT). EMT involves the transformation of epithelial cells into mesenchymal cells through the loss of their cell-to-cell adhesion. One of the inducers of EMT is transforming growth factor beta (TGFβ), a multifunctional cytokine that serves as a tumor suppressor in normal cells and a tumor promoter in cancerous cells. We aim to identify which pathway(s) and specific protein: SMAD4 and TRAF6/TAK1/p38, are required for TGFβ dependent EMT in PDAC *in vitro*. For the SMAD4 pathway, SMAD4 and SMAD3 have been studied for their effects on EMT. It was determined that a deletion of SMAD4 has no effect on TGFβ induced EMT. SMAD3 deletion alone was found to inhibit EMT in SMAD4-expressing pancreatic tumor cells. But more research needs to be conducted to confirm its role in EMT specifically in the absence of SMAD4, as a SMAD4 mutation is common in pancreatic cancers. Concerning the TRAF6/TAK1/p38 pathway, TRAF6 is overexpressed in PDAC and an inhibition of TRAF6 induces a reduction of EMT in head and neck squamous cell carcinoma.

Methods: Our research will determine the effects of SMAD4 and TRAF6/TAK1/p38 pathway on TGFβ induced EMT via Western blotting for the respective proteins and EMT markers using a 2D PANC-1 model, a PDAC cell line. siRNAs and inhibitors will also be used to inhibit specific pathways and determine the importance of each pathway in TGFβ induced EMT.

Results: Based on the findings, the individual and combined inhibition of the SMAD2, SMAD4, TRAF6 and TAK1 does not seem to effectively inhibit EMT. However, SMAD3 inhibition has exhibited significant suppression of SNAIL, a mesenchymal marker, and a suppression in E-Cadherin, an epithelial marker, suggesting its potential significance in TGFβ induced EMT. Lastly, a combined inhibition of the SMAD4 and TRAF6/TAK1/p38 pathway has shown a greater reduction in SNAIL and E-Cadherin levels suggesting that the other proteins may play a minor, but supporting role to SMAD3.

Discussion: Further research is needed to explore the effects of these inhibitions on the cellular structure. This will be done through immunofluorescence to observe the changes to the actin filaments and microtubules in the cell. Additionally, a transwell migration assay will be conducted to assess migration and invasion in 2D PANC-1. Finally, the findings from the 2D cell experiments will be validated using 3D cell models, spheroids and organoids, to determine whether the results are consistent in systems that more closely mimic the tumour microenvironment.

Poster #27

Transcriptomic analyses of ovarian clear cell carcinoma spheroids reveal distinct proliferative phenotypes and therapeutic vulnerabilities

Kolendowski B[1,2], Cheng S[1,2,] Ramos Valdes Y[1,2], Shepherd TG[1,2,3,5,6], DiMattia GE[1,2,3,4]

[1] Mary & John Knight Translational Ovarian Cancer Research Unit, London Regional Cancer Program, London, ON, Canada;[2] Lawson Health Research Institute, London, ON, Canada; [3] Department of Oncology, Western University; [4] Department of Biochemistry, Western University; [5] Department of Anatomy & Cell Biology, Western University; [6] Department of Obstetrics & Gynaecology, Western University

Introduction: Ovarian clear cell carcinoma (OCCC) cells disseminate throughout the peritoneal cavity by forming three-dimensional spheroids, which exhibit resistance to anoikis and conventional therapies, significantly contributing to metastatic disease. We hypothesize that spheroid formation induces distinct proliferative states, proliferative or dormant, that are driven by unique transcriptional and regulatory mechanisms. Identifying these mechanisms and vulnerabilities could inform new therapeutic strategies, addressing the current lack of effective treatments for OCCC.

Methods: RNA sequencing (RNA-seq) was employed to comprehensively characterize the global transcriptional profiles of two human OCCC cell lines, 105C (dormant phenotype) and KOC-7c (proliferative phenotype), under monolayer and spheroid culture conditions. Differential gene expression, principal component analysis (PCA), gene set enrichment analysis (GSEA), and pathway enrichment analysis were performed. Key G2/M checkpoint regulators (Wee1, CDC25C, CDK1, PLK1) identified from RNA-seq data were validated at the protein level using western blotting across multiple OCCC cell lines. Therapeutic vulnerability to Wee1 inhibition was assessed using the inhibitor AZD1775, determining drug sensitivity (EC50), spheroid reattachment capability, and evaluating DNA damage and apoptosis markers.

Results: Transcriptomic analyses revealed substantial and reproducible differences in gene expression profiles between dormant 105C and proliferative KOC-7c spheroids. Principal component analysis underscored significant distinctions in transcriptional programs related to the G2/M checkpoint, autophagy, cellular stress responses, DNA repair pathways, and metabolic reprogramming. Dormant spheroids exhibited pronounced downregulation of critical G2/M checkpoint regulators including Wee1, CDC25C, CDK1, and PLK1 at both the transcript and protein levels. Conversely, proliferative KOC-7c spheroids maintained elevated expression levels of these G2/M regulators, enabling continued cell-cycle progression despite suspension conditions.

Therapeutically, these distinct proliferative states correlated with differential sensitivity to Wee1 kinase inhibition by AZD1775. Proliferative spheroids showed increased sensitivity to Wee1 inhibition characterized by pronounced DNA damage (γH2AX), disrupted mitotic progression and induction of apoptosis (cleaved PARP and cleaved Caspase-3). In contrast, dormant spheroids were inherently resistant to AZD1775, exhibiting negligible changes in DNA damage markers, mitotic entry, and apoptosis, even at high drug concentrations. Furthermore, spheroid reattachment assays demonstrated that proliferative spheroids lost viability and reattachment potential after AZD1775 treatment, whereas dormant spheroids maintained their viability and reattachment abilities, reinforcing their resistance phenotype.

Conclusions: Distinct transcriptional and regulatory mechanisms underpin the divergent proliferative behaviors of OCCC spheroids, significantly impacting therapeutic responsiveness. Proliferative spheroids sustain an active G2/M checkpoint, rendering them highly susceptible to Wee1 inhibition, whereas dormant spheroids downregulate these checkpoint regulators, resulting in robust therapeutic resistance. These findings highlight critical biomarkers and vulnerabilities within OCCC spheroids, offering novel insights into therapeutic targeting strategies aimed at disrupting metastatic disease and overcoming treatment resistance in ovarian clear cell carcinoma.

Poster #28

Phospho-Proteomic Characterization of Stress Kinase Ablation in a Spheroid Model of Epithelial Ovarian Cancer

Adrian Buensuceso[1], Yudith Ramos Valdes [1], Matthew J. Borrelli[1], Jack D. Webb[1], Owen Hovey[5], Shawn Shun-Cheng Li[5], Trevor G. Shepherd[1,2,3,4]

[1]The Mary & John Knight Translational Ovarian Cancer Research Unit, Verspeeten Family Cancer Centre, London, Ontario, Canada. Departments of [2]Anatomy & Cell Biology, [3]Oncology, [4]Obstetrics & Gynaecology, [5]Department of Biochemistry, and, Schulich School of Medicine & Dentistry, The University of Western Ontario, London, Ontario, Canada

Introduction: Epithelial ovarian cancer (EOC) ranks among the most lethal gynecologic malignancies in the developed world. High-grade serous ovarian cancer (HGSOC) accounts for the majority of EOC cases and is frequently diagnosed at an advanced stage, characterized by metastasis to peritoneal sites beyond the ovaries. Most patients initially respond well to the standard treatment for HGSOC, which involves a combination of primary debulking surgery and cytotoxic chemotherapy. However, relapse with chemo-resistant disease is common and fewer than 30% of patients with metastatic HGSOC survive beyond five years. Thus, improving outcomes will require new ways of limiting metastasis. Mounting evidence implicates multicellular clusters, or spheroids, as important mediators of metastasis in EOC. Building on this, we have demonstrated that ablation of key stress-associated kinases — including STK11, NUAK1, ULK1, and CAMKK2 — results in perturbed spheroid biology. We sought to profile the post-translational signaling networks regulated by these kinases within EOC spheroids.

Methods: Phospho-proteomic profiling was performed by tandem mass tag (TMT) mass spectrometry on spheroids of OVCAR8 cells, and CRISPR-mediated deletion lines OVCAR8-*STK11*KO, OVCAR8-*NUAK1*KO, OVCAR8-*CAMKK2*KO, and OVCAR8-*ULK1*KO. Differential expression analysis was performed using the LIMMA R package. Pathway level analysis was performed using Post-Translational Modification-Signature Enrichment Analysis (PTM-SEA).

Results: PTM-SEA revealed 39, 61, 40, and 56 significantly altered signatures in OVCAR8-*STK11*KO, OVCAR8-*NUAK1*KO, OVCAR8-*CAMKK2*KO, and OVCAR8-*ULK1*KO spheroids, respectively, compared to OVCAR8 controls. Among these, a core set of 15 signatures was significantly downregulated across all KO models compared to controls. These were dominated by mitogen-activated protein kinase (MAPK)-associated signatures but also include receptor tyrosine kinase (RTK) signaling and stress response pathways. Furthermore, 4, 17, 8, and 11 signatures, respectively, were unique to each corresponding knockout model. Signatures covering a broad range of biological functions (RTK signaling, cellular stress, cell cycle, adhesion) were uniquely altered in OVCAR8-*NUAK1*KO spheroids, while signatures associated with cell cycle control and broad stress response were altered in OVCAR8-*ULK1*KO spheroids. OVCAR8-*CAMKK2*KO spheroids were characterized by alteration of several signatures associated with DNA repair. Additionally, signatures associated with small-molecule compounds impinging on the mammalian target of rapamycin (mTOR) pathway were altered in OVCAR8-*STK11*KO spheroids. Notably, signatures associated with fibronectin and AMP-activated protein kinase alpha 1 were significantly downregulated in OVCAR8-*NUAK1*KO and OVCAR8-*CAMKK2*KO spheroids, respectively, consistent with our previous immunoblot data.

Conclusions: Stress-associated kinases have notable roles in EOC, but the precise signaling networks they regulate have not been elucidated in the context of a spheroid metastasis model. The results presented here provide a preliminary characterization of the post-translational signaling effects associated with ablation of *STK11*, *NUAK1*, *CAMKK2*, or *ULK1* in EOC spheroids. Ongoing experiments aim to validate and interrogate signaling pathways identified by this study that support EOC metastasis.

Poster #29

Pannexin 1 as a cell signaling pathway interactor in glioblastoma multiforme

Matthew Huver[1], Danielle Johnston[1], Rehanna Kanji[1], Carlijn Van Kessel[1], Matthew Hebb[2,3], and Silvia Penuela[1,3]

[1]Department of Anatomy and Cell Biology, Schulich School of Medicine and Dentistry. The University of Western Ontario, London, ON, Canada,
[2]Department of Clinical Neurological Sciences, Schulich School of Medicine and Dentistry. The University of Western Ontario, London, ON, Canada,
[3]Department of Oncology; Division of Experimental Oncology, Schulich School of Medicine and Dentistry. The University of Western Ontario, ON, Canada.

Introduction: Glioblastoma multiforme (GBM) is the most prevalent and aggressive malignant brain tumour, with a median survival of fourteen months despite conventional therapies. Pannexin 1 (PANX1) is upregulated in GBM compared to normal brain tissue, and CRISPR-Cas9-mediated knockout (KO) of PANX1, as well as its inhibition, reduces GBM growth in vitro.

Methods: PANX1 expression was assessed in patient-derived GBM cell lines and CRISPR/Cas9-mediated PANX1 KO cells. RNA sequencing and Kyoto Encyclopedia of Genes and Genomes (KEGG) pathway analysis identified differentially expressed pathways. PANX1 was inhibited using Probenecid (PBN) and Spironolactone (SPIR) to evaluate changes in expression of key cancer pathway proteins. qPCR was performed to measure mRNA expression of notable genes and protein changes were analyzed by immunoblotting and immunofluorescence microscopy. An ex vivo Chick-Chorioallantoic Membrane (Chick-CAM) assay tested the effect of PBN and SPIR on GBM tumour size in 3D.

Results: KEGG pathway analysis revealed differential expression of the Hippo and Wnt signaling pathway in PANX1 knockout cells. Yes1 Associated Protein (YAP) and β-Catenin, two members of these pathways, were decreased in PANX1 KO GBM cells compared to controls, but neither inhibitor changed their expression. Immunofluorescence microscopy showed β-Catenin localization was impacted by both inhibitors, and PBN reduced CTNNB1, the gene coding for β-Catenin, transcript levels as determined through qPCR analysis. Use of a xenograft Chick-CAM model demonstrated that both PBN and SPIR reduced tumour progression, as evidenced by a significant reduction in tumour weight in the treatment groups compared to controls.

Conclusions: These findings suggest that PANX1 inhibition, through genetic KO and pharmacological agents PBN and SPIR, reduces GBM growth by modulating key signaling pathways, such as the Hippo and Wnt pathways. These results support the potential of targeting PANX1 as a therapeutic strategy for glioblastoma treatment.

Poster #30

Pannexin 1 as a potential therapeutic target for glioblastoma multiforme

Rehanna Kanji[1], Danielle Johnston[1], Matthew Huver[1], Niveen Fulcher[2], Elizabeth Fenton[1], Andrew Deweyert[1], Matthew Hebb[2,3], and Silvia Penuela[1,3].
[1]Department of Anatomy and Cell Biology, Schulich School of Medicine and Dentistry. The University of Western Ontario, London, ON, Canada, [2]Department of Clinical Neurological Sciences, Schulich School of Medicine and Dentistry. The University of Western Ontario, London, ON, Canada, [3]Department of Oncology; Division of Experimental Oncology, Schulich School of Medicine and Dentistry. The University of Western Ontario, ON, Canada.

Introduction: Glioblastoma multiforme (GBM) is the most common malignant brain tumour in the central nervous system (CNS). Despite the current standard of care, the median survival time is 14 months, highlighting the need for new therapeutic interventions. PANX1 is a channel-forming glycoprotein that is overexpressed in GBM relative to non-neoplastic brain. This study investigates the expression of PANX1 and the effects of its inhibition in GBM, while also investigating preclinical models of GBM to study PANX1 inhibitors.

Methods: GBM tumour fragments (N=7) and patient-matched non-neoplastic brain tissue (N=6) were stained for PANX1 using immunohistochemistry (IHC). Pharmacological PANX1 inhibitors, PBN and SPIR, were tested in combination with the standard chemotherapeutic agent temozolomide (TMZ) to evaluate their effects on GBM cell growth and viability. In addition, PANX1 expression was examined in the rat glioma cell line F98 to investigate its suitability for syngeneic allograft models, followed by PANX1 IHC staining in Fischer brains with F98 implants and SRG brains with patient-derived GBM xenografts.

Results: PANX1 had variable expression in GBM tumours and was expressed in patient-matched non-neoplastic brain. Treatment with SPIR and PBN reduced GBM cell growth and did not alter the effects of TMZ *in-vitro*. SPIR and PBN trended toward exhibiting fewer toxic effects than TMZ. In F98s, PANX1-25K, a novel isoform of PANX1, was predominantly expressed, and only SPIR significantly reduced cell growth. *In-vivo*, PANX1 was detected in patient-derived GBM xenografts but showed low expression in F98 allografts.

Conclusions: Our findings show that PANX1 is variably expressed in GBM, potentially reflecting its differential regulation in the tumour microenvironment. PANX1 inhibition reduced GBM cell growth, did not alter the effects of TMZ and trended toward exhibiting fewer toxic effects, highlighting their potential to be used as safe therapeutic options. Additionally, we saw that PANX1-25K is the dominant isoform expressed in F98 rat glioma and SPIR but not PBN, reduced F98 cell growth, potentially due to binding the C-terminus. Finally, PANX1 expression in patient-derived xenografts in SRG rats more closely mimicked human presentation than F98 allografts, underscoring the need for careful model selection. Overall, these results support continued investigation of PANX1 as a potential therapeutic target in GBM.

Poster #31

Evaluation of novel LKB1 inhibitors as new therapeutics against ovarian cancer histotypes

Evaluation of novel LKB1 inhibitors as new therapeutics against ovarian cancer histotypes
Natasha Bruce1,2, Yudith Ramos Valdés1, Babu Joseph3, Ahmed Abdelhameed3, Methvin Isaac3, Radek Laufer3, Dhananjay Joshi3, Laurent Hoffer3, Richard Marcellus3, Rima Al-Awar3, Elton Zeqiraj4, David E. Uehling3, Trevor G. Shepherd1,2,5,6
1The Mary & John Knight Translational Ovarian Cancer Research Unit, Verspeeten Family Cancer Centre, London, ON, Canada
2Department of Anatomy and Cell Biology, Western University, London, ON, Canada.
3Drug Discovery Program, Ontario Institute for Cancer Research, Toronto, ON, Canada
4Astbury Centre for Structural Molecular Biology, University of Leeds, Leeds, United Kingdom
5Department of Oncology, Western University, London, ON, Canada
6Department of Obstetrics and Gynecology, Western University, London, ON, Canada.

Introduction: Epithelial ovarian cancer (EOC) is a highly aggressive disease with an 80% relapse rate following surgery and combination chemotherapy, highlighting the urgent need for more efficacious therapeutic strategies. EOC is classified into five histotypes, each genetically and phenotypically unique, yet they all follow a common metastatic mechanism. Malignant cells disseminate from the primary ovarian tumour, form spheroids, then migrate to secondary sites throughout the peritoneum. Our lab has demonstrated that Liver Kinase B1 (LKB1) and its downstream target AMP-activated protein kinase (AMPK) are crucial for EOC spheroid survival and metastasis. No commercially available LKB1 inhibitors exist, which prompted our lab to collaborate with the Ontario Institute for Cancer Research to pursue their development. We have now identified and optimized several LKB1-targeting compounds (derivatives of ASC-069 and Dinaciclib parent molecules) that have been initially assessed using in vitro kinase and cell-based assays. We propose that LKB1 inhibition will reduce spheroid viability and metastatic potential among EOC histotypes as spheroids are a universal mechanism for disease spread.

Methods: Using EOC cell lines representing three distinct histotypes—high-grade serous (n=6), low-grade serous (n=2), and clear cell carcinoma (n=4)—12-point dose-response curves as well as Trypan Blue exclusion assay were used to assess each compound on spheroid cell viability. On-target activity was confirmed by immunoblotting for phospho-AMPK T172, and substrates for potential off-target activity (e.g., CDK2 substrates). Markers for apoptosis and cell cycle/proliferation was quantified in LKB1 inhibitor-treated EOC cells and spheroids.

Results: Early results demonstrate consistent sensitivity to LKB1 inhibitors in adherent models of both high-grade serous and clear cell carcinoma cell lines. In contrast, spheroid models exhibit variable responses, indicating heterogeneity in sensitivity to LKB1 inhibition. In the high-grade serous cell line OVCAR8, treatment with ASC-069 and its derivative 38964 resulted in on-target inhibition of LKB1, as evidenced by reduced phospho-AMPK (T172) signaling. Additionally, LKB1 inhibition induced apoptotic marker expression without affecting proliferative marker level.

Discussion: LKB1 inhibitor evaluation among EOC histotypes will deepen our understanding of their broader therapeutic potential for future clinical application in treating this complex and deadly disease.

Poster #32

Electric field versus temperature effects of intratumoral modulation therapy (IMT) on glioblastoma cell culture

Vera Luo[1], Erin Iredale[2], Abdulla Elsaleh[3], Tony Zhang[2], Susanne Schmid[4], Terry M. Peters[5, 6], Matthew O. Hebb[2,4], Eugene Wong[5, 7]

Departments of [1]Physiology and Pharmacology, [2]Clinical Neurological Sciences, [4]Animal and Cell Biology, [5]Medical Biophysics, [6]Robarts Research Institute, [7]Physics and Astronomy, Western University, London, ON, Canada; [3]Temerty Faculty of Medicine, University of Toronto, Toronto, ON, Canada

Introduction: Glioblastoma (GBM) is a brain cancer with a median survival of 15 months, needing new treatment options. A proposed treatment termed intratumoral modulation therapy (IMT) involves applying low-intensity electric fields to inhibit tumour growth. While in vitro and in vivo studies have demonstrated IMT's anti-tumoral effects, the heat given off by the current in the media due to the electric fields, an unavoidable effect when applying electric fields, raises the temperature in vitro. The objective of the study was to determine both the electric field effects and the temperature effects of in vitro IMT treatment on GBM cells.

Methods: Patient-derived GBM cells transfected with luciferase underwent 3-day treatments: conventional IMT (heat and fields present); fields-only IMT (37°C), or heat-only treatments (39°C, 40°C and 41°C). The incubator temperature is lowered for the fields-only IMT (to maintain cultures at 37°C) and is raised for the heat-only treatments. A custom printed circuit board delivered electric fields to GBM cells in a 24-well plate with temperature probes centred in wells. Fields (1.0, 1.25 and 1.5 V/cm intensity, 200 kHz frequency) were produced by a 4-channel waveform generator. After 3 days' stimulation, cell viability was assessed through bioluminescence imaging. The cell viability after IMT treatment was normalized to sham controls (IMT hardware present but no fields) at 37°C. Normalized cell viability values were displayed as the mean ± SEM, and a one-way ANOVA was performed for statistical analyses.

Results: Cell viability results for fields-only experiments, normalized to shams (n = 24), were 0.55 ± 0.04 at 1.0 V/cm (n = 8), 0.51 ± 0.04 at 1.25 V/cm (n =7), and 0.47 ± 0.05 at 1.5 V/cm (n = 4). For heat-only experiments, temperatures were chosen to match with those of our experimental IMT intensities: 37°C with 0 V/cm IMT, 39°C with 1.0 V/cm IMT, 40°C with 1.25 V/cm IMT, and 41°C with 1.5 V/cm IMT. The heat-only viability results, normalized to controls (n = 24), were 0.41 ± 0.02 at 39°C (n = 6), 0.19 ± 0.02 at 40°C (n = 12), and 0.12 ± 0.02 at 41°C (n = 6). With conventional IMT treatment (with both heat and fields), cell viability results normalized to shams (n = 21) were lower than viability results for heat or fields individually: 0.28 ± 0.01 at 1.0 V/cm (n = 12), 0.14 ± 0.02 at 1.25 V/cm (n = 3), and 0.08 ± 0.02 at 1.5 V/cm (n = 3). The differences between treatment groups and controls were all found to be significant ($p < 0.0001$).

Conclusions: The results indicate that the electric field effects of IMT alone have a significant effect on lowering GBM viability, while demonstrating the significant role of heat during in vitro electric field application, which has not previously been studied. This study is the first step to providing insights on the mechanism(s) by which electric fields exert their anti-cancer effects, which are currently uncertain, by providing an improved method to study the isolated effect of electric fields in vitro.

Poster #33

The role of IKZF3 and its induced degradation by lenalidomide in B cell leukemia.

Maria F. Uribe Estrada and Rodney DeKoter
Department of Microbiology & Immunology, Western University, Canada

B cell leukemia is a rare blood cancer, including chronic lymphocytic leukemia (CLL) and precursor B cell acute lymphoblastic leukemia (pre-B-ALL). CLL involves transformation of mature B cells with dysregulated signaling pathways involving the B-cell receptor (BCR). Pre-B-ALL involves transformation of immature precursor B cells and is dependent on interleukin-7 signaling. Mutations in the IKZF3 gene encoding Aiolos have been detected in both CLL and pre-B-ALL. IKZF3, a transcription factor involved in the regulation of B cell proliferation and differentiation; through its zinc-finger domains it binds to specific DNA sequences. The L162R “hotspot” mutation in Zinc finger 2 of IKZF3 is crucial for driving B cell neoplasia and transcriptional dysregulation in CLL. This mutation upregulates genes involved in BCR signaling and associated kinases. In pre-B-ALL, the H196Y mutation in IKZF3's third DNA-binding zinc finger alters its DNA-binding specificity, contributing to transcriptional dysregulation.

Lenalidomide an immunomodulatory drug causes selective degradation of IKZF3 through binding to CRBN. CRBN is the substrate adaptor of the CRL4CRBN E3 ubiquitin ligase complex that targets proteins for their ubiquitination and degradation. CRBN is responsible for recognizing and binding target proteins; it has a groove in which lenalidomide acts as a "molecular glue" and binds to CRBN. This binding induces conformational changes modulating its substrate specificity making it target IKZF3. The induced proximity between CRBN and IKZF3 triggers the ubiquitination process, degrading IKZF3.

The goal of my research is to understand the role of IKZF3 in B cell development, as well as using lenalidomide-induced degradation of IKZF3 to elucidate IKZF3 mutation’s function in CLL and pre-B-ALL pathogenesis and how lenalidomide induced degradation causes gene expression changes in leukemia cells. I hypothesize that IKZF3 is a critical regulator of pre-BCR signaling and overexpression of various IKZF3 mutants will alter gene expression in a manner that promotes CLL and B-ALL. Lenalidomide-induced degradation of IKZF3 mutant proteins will restore dysregulated signaling pathways. Collectively, this evidence leads to the hypothesis that IKZF3 is a critical regulator of BCR signaling and overexpression of various IKZF3 mutants will alter gene expression in a manner that promotes CLL and B-ALL. Lenalidomide-induced degradation of IKZF3 mutant proteins will reduce leukemogenesis.

Lentiviral vectors encoding wild-type and mutant IKZF3 have been constructed and the H196Y mutant vectors have been transduced into REH cells, where lenalidomide successfully promoted IKZF3 degradation (Fig. 1). The next steps include analyzing gene expression and signaling changes and cell death assays to evaluate the effects of the different IKZF3 mutations in different cell lines.

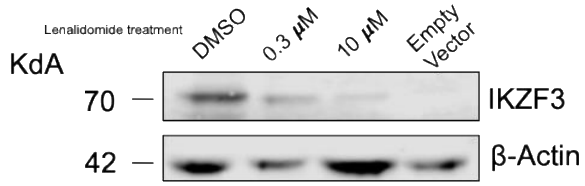

Figure 1. Western blot analysis of H196Y IKZF3 expression in REH cells following lenalidomide treatment and 8 hours.

My work will provide critical insights into the potential of lenalidomide as a treatment for IKZF3-related leukemias, extending its therapeutic application beyond its established use. Additionally, this research will elucidate the mechanisms by which IKZF3 regulates B cell development, offering a deeper understanding of its role in normal and malignant B cell biology.

Poster #34

The History and Success of the Ovarian Tumour Biobank at the Mary and John Knight Translational Ovarian Cancer Research Unit (TOCRU)

Tiffany P. A. Johnston[1,2], Yudith Ramos Valdés[1], Emily Tomas[1,4], Renée Resendes[1], Stephen Welch[5], Jacob McGee[2,5], Gabriel E. DiMattia[1,3], Trevor G. Shepherd[1,2,4,5]

[1] Mary and John Knight Translational Ovarian Cancer Research Unit, Verspeeten Family Cancer Centre
[2] Department of Obstetrics and Gynecology, Schulich School of Medicine and Dentistry, Western University
[3] Department of Biochemistry, Schulich School of Medicine and Dentistry, Western University
[4] Department of Anatomy and Cell Biology, Schulich School of Medicine and Dentistry, Western University
[5] Department of Oncology, Schulich School of Medicine and Dentistry, Western University

Introduction: Epithelial ovarian cancer (EOC) is the most lethal gynecologic malignancy in the developed world. EOC comprises diverse histological subtypes with distinct molecular and clinical features. High-grade serous ovarian cancer (HGSOC), the most common histotype, is marked by *TP53* mutations and genomic instability, resulting in significant heterogeneity that complicates treatment and research modeling. Rarer histotypes, like low-grade serous and clear cell carcinoma, are often chemoresistant and lack well-established research models. To address these challenges, the TOCRU has been actively developing a living biobank of patient-derived models that span a broad range of EOC histotypes to enhance preclinical research.

Methods: Longstanding collaboration among the TOCRU, gynecologic oncologists, the Ontario Tumour Bank, and pathology staff at London Health Sciences Centre, has established an efficient pipeline for patient biospecimen collection. Since 2007, ascites samples (n= 486) have been collected during surgery or therapeutic paracentesis, processed to isolate cancer cells, and used to generate ascites-derived iOvCa cell lines (n=52). iOvCa cell lines were genomically profiled using the Oncomine Hotspot panel and CytoScan HD assays and characterized under 3D culture conditions as spheroids and organoids to model tumour growth and metastasis in vitro. Since 2019, solid tumour tissues collected during debulking surgery or diagnostic laparoscopy have been processed as PDOs (n= 98). Clinical data were extracted from electronic medical records and maintained in REDCap, enabling integrated analyses that align cell-based model characteristics with patient disease profiles.

Results: We have established a living biobank of 52 ascites-derived iOvCa cell lines, 3 established PDOs and over 20 PDOs that have reached at least five passages. These models primarily represent HGSOC, with some examples of rare EOC histotypes, and reflect a range of clinical backgrounds from treatment-naïve to heavily pre-treated patients. Genomic profiling confirmed key mutation drivers consistent with tumour histopathology, supporting their clinical and translational relevance. *In vitro* therapeutics testing on seven iOvCa cell lines representing HGSOC revealed distinct responses to standard and investigational therapies, mirroring intrapatient heterogeneity. Our biobanking activities have enabled broad collaborative engagement, including participation in the multi-centre BioDIVA clinical trial. Ongoing partnerships include the development of patient-derived xenograft (PDX) models with the University of Guelph and single-cell RNA sequencing of PDOs with researchers at the University of Ottawa.

Conclusion: This growing repository is a valuable resource for advancing translational EOC research and fostering cross-institutional collaboration. We are excited to build on this foundation to deepen biological insights, drive innovation, and improve outcomes for EOC patients.

Poster #35

Novel transcription factor binding sites and their regulatory role in Activation-Induced Cytidine Deaminase in the context of Pre-B Acute Lymphoblastic Leukemia

Chanpreet K. Riarh[1], Allanna C.E. MacKenzie[1], Rodney P. DeKoter[1]
[1]Department of Microbiology and Immunology, Schulich School of Medicine & Dentistry, Western University, London, Ontario, Canada.

Introduction: Activation-induced cytidine deaminase (AID), encoded by the *Aicda* gene, is a mutagenic enzyme expressed at high levels in germinal centre B cells. AID is also expressed at lower levels during early B cell development; however, its role is less well understood. Evidence suggests that AID may play a role in inducing driver mutations that lead to pre-B acute lymphoblastic leukemia (pre-B-ALL). Despite advances in treatments, Pre-B-ALL remains the highest mortality count amongst pediatric cancers. The transcription factor (TF) PU.1 has been identified as a negative regulator of *Aicda*. Recent data has suggested that PU.1 suppresses *Aicda* expression through a negative regulatory binding site (R2-1 of Intron 1). A second TF binding site with an octamer motif has been identified upstream of the PU.1 site as well. We thus hypothesize that the TFs PU.1 and Oct-2 directly regulate *Aicda* via the R2-1 regulatory region.

Methods: An existing pre-B 38B9 murine cell line with a CRISPR-Cas9 mutation disrupting both TF binding sites was used for this study. We compared the mutant with WT cells upon LPS stimulation and qPCR was used to determine changes in *Aicda* RNA expression. We used ChIP-qPCR to measure protein-DNA interaction and demonstrate that both PU.1 and the Oct-2 TFs associate with the GGAA motif and the octamer motif respectively. We stimulated *Aicda* RNA expression with LPS and measured the protein-DNA interaction with ChIP-qPCR again. Anti-H3K27ac ChIP was performed to determine the chromatin structure at R2-1.

Results: In a pre-B 38B9 murine cell line with a heterozygous mutation disrupting both binding sites, qPCR analysis revealed a significant increase in *Aicda* mRNA transcript levels in the mutated cells compared to WT. Under unstimulated conditions, we observed decreased binding of Oct-2 but similar levels of PU.1 binding to R2-1, compared to wild-type (WT). Under LPS stimulation, there was a significant reduction in binding to R2-1 for both PU.1 and Oct-2, in both WT cells and the mutant. Anti-H3K27ac ChIP showed that despite the increased *Aicda* expression levels in the mutant clone, there is no difference in the enrichment for H3K27ac between the mutant and wild-type, also indicating the TFs do not function by chromatin remodeling.

Conclusions: PU.1 or Oct-2 directly bind to and regulate *Aicda* expression and disrupted binding to the negative regulatory region R2-1 may lead to transcriptional dysregulation of *Aicda*. The data suggests that the regulatory mechanism of these TFs could be at the level of transcription. Further research into the mechanisms of action could provide novel therapeutic targets for the treatment of pre-B-ALL.

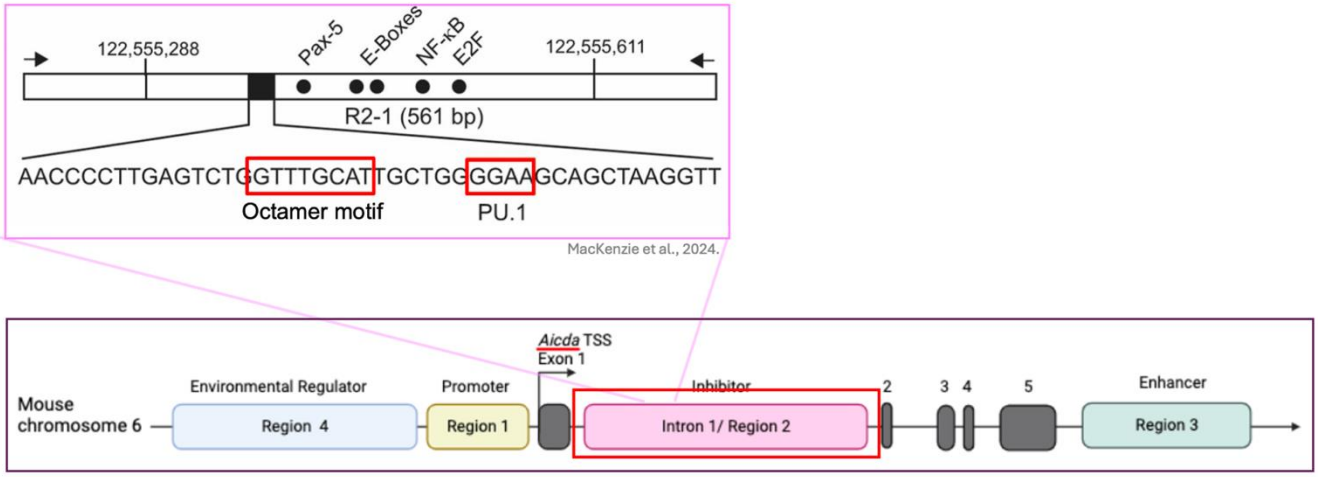

Figure 1. Schematic representation of mouse *Aicda* gene locus and representation of transcription factor distribution in R2-1, near the PU.1 and Octamer binding motifs. Regulatory regions 1-4 and their known function is identified (coloured boxes). The dark grey boxes represent the exons and the space outside the boxes is intronic DNA (horizontal black line). The pink box contains the region of interest R2-1 containing the transcription factor binding sites for PU.1 and Oct-2 (red boxes). Adapted from MacKenzie et al., 2024.

Poster #36

Assessing OrfV's Oncolytic Activity in an Orthotopic KPC Pancreatic Cancer Model

Alyssa E. Bogle, Jacob G. E. Yates, James J. Petrik, Sarah K. Wootton.
Affiliations: Dept. of Pathobiology and Biomedical Sciences, University of Guelph

Introduction

Pancreatic cancer remains one of the deadliest cancers, with limited clinical advancement over the years. This high rate of mortality can be attributed to the desmoplastic tumor microenvironment (TME) associated with pancreatic cancer which makes it difficult for traditional treatments such as chemotherapy to penetrate the tumor. Novel therapeutics are needed to combat this difficult to treat cancer. Our lab focuses on developing oncolytic viruses (OVs) to treat cancer. OVs are viruses that can infect and replicate in tumor cells, leaving healthy cells unharmed. Through immune system activation, OVs can elicit tumor-specific immune responses, enhancing antitumor immunity. These properties position OVs as a promising therapeutic modality in cancer treatment.

Methods

Parapoxvirus ovis (OrfV) is a member of the *Poxviridae* family that naturally infects sheep, causing lesions around the lips and muzzle. A modified version of OrfV, with deletion of the veg-f gene, has been developed as an OV and vaccine vector. Previously, we demonstrated that intraperitoneal administration of OrfV significantly increased survival and reduced ascites fluid accumulation in an orthotopic mouse model of epithelial ovarian cancer. Here, we investigate the therapeutic potential of OrfV in an orthotopic model of pancreatic ductal adenocarcinoma (PDAC). KPC cells were surgically implanted into the pancreas of C57BL/6 mice (4 males and 4 females per group), and after 14 days, mice received intraperitoneal administration of 5×10^7 PFU of OrfV or PBS every other day for three doses.

Results

ORFV treatment led to a significant extension of survival ($P < 0.001$), with no observed sex-based differences. These findings provide evidence for the potential of OrfV as an oncolytic therapy in PDAC and warrant further investigation into its immunomodulatory effects.

Conclusions

To elucidate the underlying mechanisms, we will assess the impact of OrfV on the tumor microenvironment using flow cytometry to analyze immune responses in tumors and tumor-draining lymph nodes, focusing on dendritic cells and T-cell subsets. Based on the insights from this study, we plan to engineer a recombinant OrfV designed to specifically enhance its ability to stimulate an immune response in pancreatic cancer. In the meantime, we have engineered three recombinant viruses created to enhance the immune stimulatory properties of OrfV. Two of the immune inhibitory genes (viroceptors) of OrfV, mainly the viral interleukin-10 (vIL-10) and the chemokine binding protein (CBP), were knocked out individually and in combination. We hypothesize that deleting these anti-inflammatory genes from OrfV will increase immune cell infiltration into the TME ultimately leading to an improved anti-tumor immune response. We will conduct a survival study to evaluate all engineered recombinants, identifying which one offers the greatest survival benefit and whether it's linked to its ability to stimulate a greater immune response. This will guide further optimization of OrfV as a potential therapeutic for pancreatic cancer.

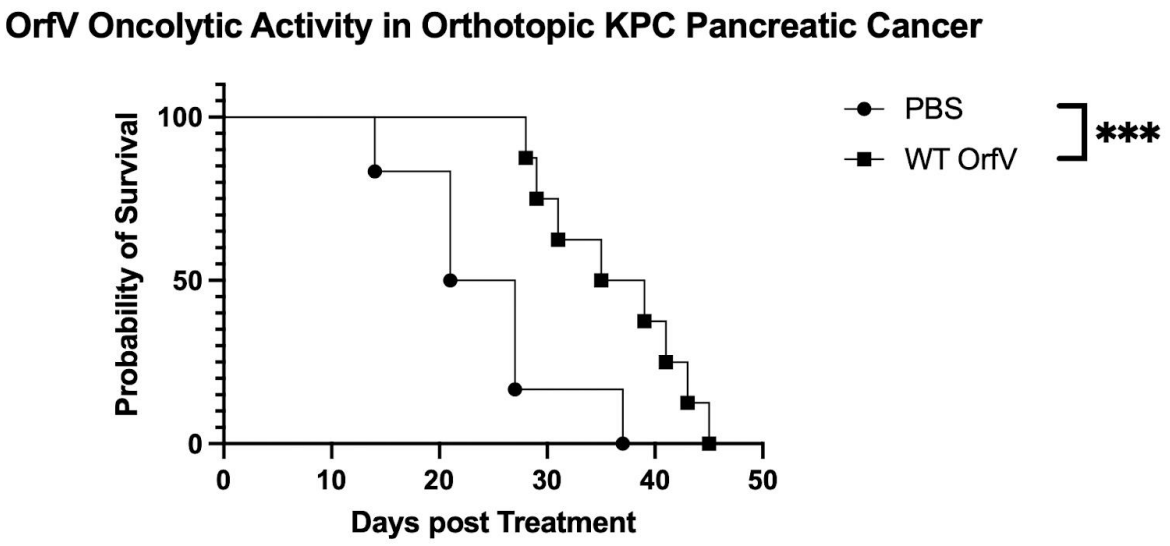

Figure 1. Kaplan-Meier Survival analysis of mice with KPC tumors treated with Wild-type OrfV and PBS. Mice treated with WTOrfV significantly prolonged survival (P>0.001) compared to PBS-treated mice.

Poster #37

Assessing heat shock transcription factor 1 as a therapeutic target in high-grade glioma

Elizabeth Fenton[1], Niveen Fulcher[2], Rehanna Kanji[1], Abdulla Elsaleh[3], Cleusa D'Oliveira[1], Susanne Schmid[1], Matthew O. Hebb[1,2]
Departments of [1]Anatomy and Cell Biology, [2]Clinical Neurological Sciences, [3]Physiology and Pharmacology, Western University, London, ON, Canada

Introduction: High-Grade Gliomas (HGG), including Glioblastoma Multiforme (GBM) in adults and Diffuse Midline Glioma (DIPG) in children, are highly aggressive and treatment-resistant tumors with poor prognoses. The heat shock response, regulated by Heat Shock Transcription Factor 1 (HSF1), has emerged as a promising therapeutic target in various cancers; however, its specific role in HGG progression remains poorly understood. This research aims to evaluate the therapeutic potential of HSF1 inhibition in HGG tumorigenesis *in vitro* and develop an optimized preclinical model for testing HSF1-targeting therapies.

Methods: Patient-derived GBM and DIPG cell lines were treated with DTHIB, an HSF1 inhibitor, at various concentrations to assess its impact on tumor growth and viability. Cell proliferation was monitored using IncuCyte® live-cell imaging, while viability was assessed via bioluminescence imaging and MTT assays. Downstream effects of HSF1 depletion were examined through qPCR analysis of heat shock protein expression. For *in vivo* studies, patient-derived GBM and DIPG cells were implanted into the striatum of Sprague Dawley-Rag2/Il2rg Knockout Rats, an emerging immunodeficient model for oncology research. Tumor growth was tracked using bioluminescence imaging, with post-mortem MRI used to confirm tumor presence and volume. Brain tissue was further analyzed through immunohistochemistry to quantify HSF1 expression.

Results: In vitro, DTHIB treatment reduced GBM cell growth *(n=3 each cell line; p=0.0005 & p=0.0042)* and viability *(n=3 each cell line; p<0.0001)* in a dose-dependent manner, while DIPG cells exhibited more variable responses. The qPCR analyses confirmed that DTHIB decreased expression of HSF1 target genes in GBM cells, including HSPB1 *(n=3; p=0.0173)*, HSPA1A *(n=3 each cell line; p=0.0236 & p=0.0007)*, and HSP90AA1 *(n=3 each cell line; p=0.0035 & p=0.0358)* after 24 hours. *In vivo,* tumors were detected via bioluminescence imaging and MRI, with tumors exhibiting higher HSF1 expression than contralateral brain *(n=5 paired samples; p<0.0001)*.

Discussion: These findings highlight the therapeutic potential of HSF1 inhibition in HGG tumorigenesis and further support its investigation as a treatment strategy. Additionally, the use of Sprague Dawley-Rag2/Il2rg Knockout rat xenografts enhances preclinical modeling, providing a valuable tool for further testing HSF1-targeted therapies in vivo.

Poster #38

Fc3TSR Remodels the Tumour Microenvironment to Enhance Efficacy of Immune Checkpoint Inhibitors and Facilitate Immune Cell Migration in a Murine Model of Pancreatic Ductal Adenocarcinoma.

Garlisi, B[1]., Aitken, C[1]. Lauks, S[1]., Lockington, C[1]., Lawler, J[2]., Petrik, J[1].

[1]Department of Biomedical Sciences, University of Guelph, Canada.
[2]Beth Israel Deaconess Medical Center and Harvard Medical School.

Introduction: Pancreatic Ductal Adenocarcinoma (PDAC) has a poor survival rate due to late diagnosis where metastasis has often occurred. Angiogenesis, the process by which new vessels form from pre-existing vasculature, is crucial for tumor growth and metastasis. Tumors aggressively upregulate expression of pro-angiogenic factors, stimulating rapid vessel formation. These vessels often lack pericyte coverage and have dysfunctional morphology, reducing perfusion and contributing to high interstitial fluid pressure (IFP). This vascular dysfunction can impede therapy uptake inhibit immune cell migration to the tumor and tumor draining lymph nodes. Fc3TSR is a novel fusion protein derived from the type I repeat region of the endogenous angiogenic inhibitor thrombospondin 1, which we have shown can reduce tumor size and normalize vasculature in ovarian tumors, significantly enhancing therapy uptake. Here, we evaluated Fc3TSR's ability to remodel the tumor microenvironment (TME) to induce tumor regression and to enhance efficacy of immune checkpoint inhibitors.

Methods: We developed an orthotopic syngeneic murine model of PDAC, whereby we surgically injected $2.5x10^4$ murine PDAC cells (KPC) into the tail of the pancreas of C57BL/6 mice. Tumors were allowed to progress for 14 days before intraperitoneal (IP) administration of Fc3TSR (0.158mg/kg) or PBS (control) on day 14 and 21 to induce TME remodelling. Immune checkpoint inhibitors (anti-CTLA-4 and anti-PD-L1 (25ug)) IP injections were administered on day 23 and 26. Mice were euthanized on day 30 and tumours were weighed and collected. Tumors were cryo-preserved, sectioned, and stained using immunofluorescence and immunohistochemistry for apoptosis (cleaved caspase-3), proliferation (ki-67), hypoxia (Hypoxyprobe), blood and lymphatic vasculature (CD31, alpha-smooth muscle actin (a-SMA), LYVE-1), and immune cell markers (CD4, CD8, CD11c, CD68, CD138, NKG2D, FoxP3).

Results: Fc3TSR significantly reduced tumour weights compared to PBS controls. Fc3TSR + anti-CTLA-4, but not anti-PD-L1, significantly reduced tumour weights compared to Fc3TSR monotherapy. Fc3TSR increased the proportion of mature blood vessels, decreased hypoxic area, and increased the presence of tumor lymphatic vessels compared to PBS controls. Fc3TSR alone significantly increased the presence of cleaved-caspase 3, CD4, CD8, CD11c, CD68, CD138 and NKG2D in tumors, and there was a further increase with the combination of Fc3TSR + anti-CTLA-4 or anti-PD-L1. Combination therapy with Fc3TSR and checkpoint inhibitors resulted in a decrease in the immunosuppressive marker FoxP3. Lymph nodes were collected and are also being optimized for staining of these immune cells and TME markers.

Conclusion: Our data suggests that normalizing the TME can enhance the uptake and efficacy of immune checkpoint inhibitors, which have shown limited efficiency *in vivo* for PDAC patients. Enhanced perfusion through normalization of blood and lymphatic vasculature could facilitate the migration of activated immune cells and may enhance immune responses in PDAC patients. Here we demonstrate a novel approach to optimize therapeutic efficacy and immune cell migration in advanced stage PDAC.

Selective HDAC5 inhibition as a combinatorial strategy to overcome gemcitabine-resistant PDAC

Maria Nica[1,3], Fatemeh Behjati[1,3], Emilie Jaune-Pons[1,3], and Christopher Pin[1,2,3]
Department of Physiology and Pharmacology[1], Department of Oncology[2], Schulich School of Medicine & Dentistry, Western University; Baker Centre for Pancreatic Cancer, Verspeeten Family Cancer Centre[3], London, Ontario, Canada

Introduction: Pancreatic ductal adenocarcinoma (PDAC) remains one of the most lethal cancers diagnosed in Canada. While several cancers have seen an improvement in survival rates, current PDAC therapies have resulted in a dismal 5-year survival rate of ~12%. PDAC is primarily treated with either gemcitabine-based regimens or the combination therapy FOLFIRINOX. However, PDAC is highly resistant to chemotherapy, highlighting the need for novel approaches to increase sensitivity of PDAC cells to these agents. Epigenetic repressors are often over-expressed in PDAC and may therefore be involved in reprogramming cancer cells to increase resistance. Consequently, broad spectrum histone deacetylase (HDAC) inhibitors Givinostat and Dacinostat were observed to enhance cytotoxic T lymphocyte killing of PDAC cells. However, toxicity has been observed when using these inhibitors in clinical trials, potentially resulting from their off-target profiles. Consequently, we will investigate whether selective HDAC inhibition can sensitize PDAC to first-line therapeutics. HDAC5 is one such candidate that is only expressed in pathological states such as pancreatitis. Therefore, we hypothesize that inhibition of HDAC5-mediated epigenetic repression will increase sensitivity to chemotherapy.

Methods: To determine whether inhibiting HDAC5 increases sensitivity in PDAC, patient-derived organoids (PDOs) derived from PDAC patients will be treated with LMK-235, a highly specific inhibitor for HDAC5, for 5 days to prevent histone deacetylation. We will identify the optimal doses of LMK-235 on PDOs that promote histone acetylation without promoting cell death. The effect of LMK-235 on HDAC5 function will be evaluated at the level of histone H3 acetylation. Histones will be extracted and western blot analysis performed for histone acetylation marks. Once optimal doses are determined, we will examine the dose-dependent sensitivity of PDOs to gemcitabine alone and gemcitabine given pre-treatment with the optimal dose of LMK-235 for 7 days. Cell viability and growth will be assessed using the Incucyte system and Alamar Blue.

Results: The findings showed that treatment with LMK-235 increased histone acetylation in PDOs compared to controls. Furthermore, LMK-235 did not significantly reduce cell death across all conditions. In a resistant PDO line, the dose-response curve for the combined treatment of LMK-235 and gemcitabine shifted to the left, and the IC50 was decreased compared to gemcitabine alone.

Discussion: The results demonstrate that the impact of LMK-235 on H3K27ac varies between PDOs, but overall, LMK-235 increases histone acetylation in PDAC PDOs without reducing cell viability. Additionally, LMK-235 enhances gemcitabine sensitivity in resistant PDOs. Our findings will provide evidence that LMK-235 could potentially improve the treatment of gemcitabine-resistant PDAC.

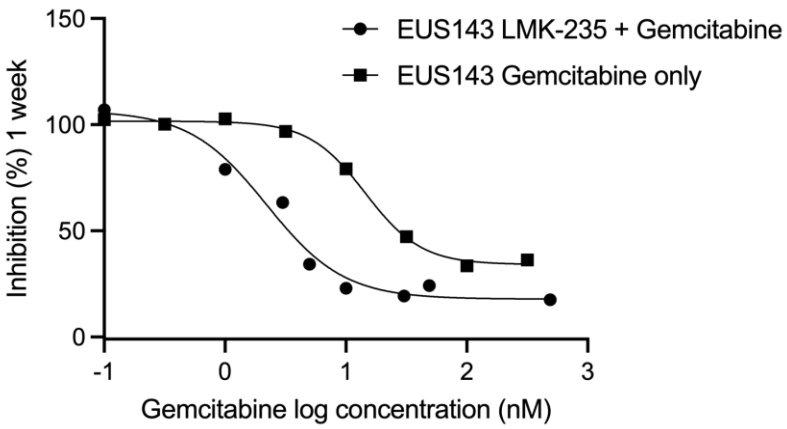

Figure 1. Dose-response curve of cell viability of PDO EUS143 with respect to treatment with different concentrations of gemcitabine for 7 days. The circle symbol indicates the combination therapy LMK-235/gemcitabine. The square symbol represents the gemcitabine only treatment.

Poster #40

Investigating the role of Snail independent of TGFβ signaling in epithelial ovarian cancer

Emily Tomas[1,2], Jennifer Davis[1], Yudith Ramos Valdes[1], Gabriel E DiMattia[1,3,4], Trevor G Shepherd[1,2,3,5]
[1]The Mary and John Knight Translational Ovarian Cancer Research Unit, Verspeeten Family Cancer Centre, London, ON, Canada; [2]Anatomy & Cell Biology, Western University, London, ON, Canada; [3]Oncology, Western University, London, ON, Canada; [4]Biochemistry, Western University, London, ON, Canada; [5]Obstetrics & Gynaecology, Western University, London, ON, Canada

Introduction: Epithelial ovarian cancer (EOC) metastasizes uniquely by spreading as spheroids within the peritoneal cavity. Our extensive research on EOC spheroid pathobiology has revealed dynamic changes in cell signaling that enable stress adaptation and survival, although the mechanisms remain unclear. Present work characterizing EOC spheroids versus organoids demonstrated differential signaling pathways confirming our speculations that cells undergo biological switching behaviours during metastasis. Additionally, prior studies identified elevated transforming growth factor beta (TGFβ) signaling in spheroids, facilitating epithelial-to-mesenchymal transition (EMT) for cell survival. However, recent transcriptomic analysis of seven patient ascites-derived (iOvCa) cell lines confirmed increased TGFβ signaling in spheroids compared to organoids; however, EMT was elevated in organoids compared to spheroids, presenting a paradox.

Methods: In this study, iOvCa cell lines were used to generate spheroids in suspension on Ultra-Low Attachment plates and organoids using modified patient-derived organoid culture conditions. RT-qPCR and immunoblotting of key markers for the TGFβ signaling pathway and EMT were conducted on spheroids in comparison to organoids. Manipulation of TGFβ signaling was performed by using the SB-431542 inhibitor and TGFβ1 ligand. siRNA knockdown of *SNAI1* was completed on adherent and spheroid cultures to demonstrate the influence of Snail on EMT markers.

Results: Genes relevant to the TGFβ signaling pathway (i.e. *ATF3, ID2, KLF10* and *PPP1R15A*) confirmed elevated levels in spheroids. In terms of EMT, high Snail levels, yet low levels of Vimentin and inconsistent levels of E-cadherin were observed in iOvCa spheroids in comparison to organoids. This means that Snail did not influence the classical EMT markers, E-cadherin and Vimentin. TGFβ inhibition and activation further demonstrated TGFβ's selective regulation of EMT proteins, with iOvCa cells exhibiting a hybrid EMT phenotype regardless of biological state. After expanding to other EMT markers, our results showed that Snail, rather than TGFβ signaling, may strongly influence N-cadherin and Claudin-1 protein expression, suggesting a connection to EMT but in a non-canonical way. Loss of *SNAI1* in iOvCa cell lines confirmed that Snail may increase N-cadherin expression and decrease Claudin-1 expression indicating potential regulation of these markers during metastasis. Treatment with Entinostat on adherent and spheroid cultures demonstrates that increasing global H3K27Ac may play a role in increased Snail transcript expression levels in spheroids.

Conclusions: This contradictory TGFβ signaling and Snail activity within our spheroids and organoids may provide new insight into EMT and how it assists in EOC metastasis. Of course, additional experiments need to be completed to determine the exact mechanism of Snail regulation in EOC spheroids compared to organoids. Therefore, our findings emphasize the significance of using three-dimensional models to study disease progression and uncover novel therapeutic targets, especially for EOC.

Poster #41

Loss of RanBP9 cooperates with p53 deficiency to promote sarcomagenesis

Brianna C. Gonga-Cavé[1,2], Gabriel Onea[1,2], Xu Wang[1], Sean-Cregan[3], Patti Kaiser[4], Caroline Schild-Poulter[1,2,5]

[1]Robarts Research Institute, University of Western Ontario, London, ON N6A 5B7, Canada, [2]Department of Biochemistry, Schulich School of Medicine and Dentistry, University of Western Ontario, London, ON N6G 2V4, [3]Neuroscience Program, Department of Physiology and Pharmacology, Schulich School of Medicine and Dentistry, University of Western Ontario, London, ON N6G 2V4, [4]Department of Pathology, Schulich School of Medicine and Dentistry, University of Western Ontario, London, ON N6G 2V4, [5]Department of Oncology, Schulich School of Medicine and Dentistry, University of Western Ontario, London, ON N6G 2V4

Introduction: RAN binding protein 9 (RanBP9) is a scaffolding protein that is essential for the formation of the C-terminal to LisH (CTLH) complex. This multi-subunit E3 ubiquitin ligase regulates various biological processes including cell cycle, cell proliferation, and metabolism. In the context of cancer, several studies have demonstrated that RanBP9 functions as a tumour suppressor, but no studies have investigated the outcome of RanBP9 deficiency on tumour development in a mouse model.

Methods: Here, we investigated the tumour suppressive role of RanBP9 in C57BL/6 mice. Bulk RNA sequencing (RNA-seq) analysis of RanBP9 knockout ($R9^{KO}$) mice liver identified an upregulation of several oncogenic signalling genes. Although $R9^{KO}$ mice displayed a shortened lifespan, these mice did not develop spontaneous tumours suggesting that additional genetic perturbations are required for tumour development. To establish whether the loss of RanBP9 could promote tumour formation in a p53-deficient background, we generated mixed heterozygous ($R9/p53^{dHet}$) and double knockout ($R9/p53^{DKO}$) mice. These mice were monitored over 17 months for the development of spontaneous tumours.

Results: RNA-seq analysis identified 945 differentially expressed genes (DEGs) in $R9^{KO}$ mice compared to wild-type (WT) controls. Gene ontology analysis revealed upregulation of several proliferative signalling pathways, including MAPK/ERK, NOTCH, and WNT. Despite enhanced oncogenic signalling, $R9^{KO}$ mice did not develop spontaneous tumours. However, $R9/p53^{dHet}$ mice (n=23) developed sarcomas at an earlier time compared to control $p53^{Het}$ mice (n=18; $p < 0.05$). Moreover, $R9/p53^{dHet}$ mice displayed an altered tumour spectrum, with a higher incidence of soft tissue sarcomas (STS). H&E staining of tumour biopsies revealed increased mitotic activity in sarcomas from $R9/p53^{dHet}$ mice ($p < 0.05$). Analysis of the TCGA-SARC dataset showed that low expression of CTLH complex genes (*MKLN1* and *RMND5B*) was significantly associated with low survival in patient survival ($p < 0.001$).

Conclusions: Our data indicates that loss of RanBP9 alone cannot initiate tumourigenesis. However, the heterozygous loss of RanBP9 and p53 promotes increased STS development. Ongoing efforts identify the mechanism to understand how the loss of CTLH activity contributes to sarcoma development in the absence of p53. Our findings may support the development of anti-cancer therapeutics that activate RanBP9-CTLH complex activity.

Poster #42

Mutational landscape of pure ductal carcinoma in situ and associations with disease prognosis and response to radiotherapy

Noor Rizvi[1], Eliseos J. Mucaki[1,2], Emily L. Salmini[1], Monica Zhang[2], Sabina Trebinjac[3], Ezra Hahn[3], Lawrence Paszat[3], Sharon Nofech-Mozes[4], Michael T. Hallett[1,5,6], Eileen Rakovitch[3] , Vanessa Dumeaux[1,2,5,6]

[1] Department of Biochemistry, Western University, London, Canada; [2] Department of Anatomy and Cell Biology, Western University, London, Canada; [3] Department of Radiation Oncology, Sunnybrook Health Sciences Centre, University of Toronto, Toronto, Canada; [4] Department of Pathology, Sunnybrook Health Sciences Centre, University of Toronto, Toronto, Canada; [5] Department of Oncology, Lawson Research Institute, London Health Sciences Centre, London, Canada; [6] Centre for Translational Cancer Research, Western University, London, Canada.

Background: Ductal Carcinoma in Situ (DCIS) poses significant challenges in breast cancer management due to the absence of reliable markers for predicting progression to invasive disease. Although the typical treatment involves breast-conserving surgery (BCS) followed by radiation therapy (RT), this approach often leads to overtreatment, as not all DCIS cases advance to an invasive stage. Our study aims to use genetic information from DCIS tumors to predict disease progression and RT response, thereby refining clinical decision-making and enhancing patient outcomes.

Methods: We conducted whole-exome sequencing on 147 patients diagnosed with pure DCIS who underwent BCS with or without RT, with matched normal tissue sequenced for all cases. The patient cohort included long-term clinical follow-up and recurrence data. Somatic variants were identified using a deep learning appraoch, and annotated with Ensembl's Variant Effect Predictor (VEP). Mutational signatures and driver genes were analyzed in R using the MutationalPatterns and dNdScv packages, respectively. Allele-specific CNAs were estimated using the ASCAT algorithm, and associations between genetic alterations and 10-year local recurrence outcomes were assessed using survival analysis, with stratification by RT status.

Results: Our genomic profiling revealed that DCIS lesions frequently harbor mutations in canonical cancer drivers such as PIK3CA and TP53, as well as in genes involved in epithelial structure and cell adhesion. However, these alterations were not predictive of recurrence. A distinct subset of early-onset DCIS cases exhibited markedly elevated tumor mutational burden and enrichment of sigantures such as SBS26, SBS7b, and SBS5, although these were not associated with recurrence or clinical subtype. We identified five genes—SH2B2, PDZD8, MYO7A, MUCL3, and DNASE2B—whose mutations were significantly associated with recurrence across both RT-treated and untreated patients. In patients who received RT, mutations in an additional 27 genes, including those involved in cytoskeletal stability (KRT1, CFAP47), DNA repair (REV1), and cellular metabolism (MGAM2, AADACL3), were associated with increased recurrence risk (Fig.1). These mutations were strongly predictive of recurrence within the first five years post-treatment and frequently co-occurred (Fig 1). We observed recurrent losses in cytobands containing key tumor suppressors (CDKN2A, MSH2), adhesion molecules (keratins, EPHA3), and gains in oncogenic regions such as 11q13 and 5p14. Notably, basal-like and high-grade DCIS exhibited higher CNA burden and more pronounced loss in specific cytobands compared to other subtypes.

Conclusions: Our findings uncover the genomic landscape of pure DCIS and highlight key factors that contribute to LR and mediate the adverse effects of RT. While *TP53* and *PIK3CA* mutations play important roles in early tumorigenesis, they do not predict recurrence, emphasizing the need for alternative biomarkers. We identify distinct mutational processes and genetic alterations that disrupt cytoskeletal integrity, cell-cell interactions and cell adhesion, potentially destabilizing the epithelial tissue environment and contributing to recurrence, particularly following RT-induced stress. These findings provide a foundation for understanding the genetic basis of DCIS progression and identifying potential molecular drivers of treatment resistance. Future research will be essential to translate these insights into clinical practice, guiding the development of more targeted therapeutic approaches to improve outcomes for patients with DCIS.

Figure 1. Mutations associated with radiotherapy resistance in DCIS. a An oncoplot showing the distribution of mutations in 29 genes significantly associated with local recurrence in RT-treated patients. Color-coding indicates mutation types; clinical annotations show age, grade, molecular subtype, and recurrence status. **b** Kaplan-Meier analysis of LRFS comparing patients with mutations in at least two of the 29 genes (red) versus those without mutations (blue). **c** Distribution of TMB, shown as number of non-synonymous variants, log2 scale) for lesions with at least one mutation in two genes associated with LRFS colored by recurrence status at 10 years. **d** GO cellular component enrichment network analysis of recurrence-associated genes in RT-treated DCIS. Network visualization shows enriched GO terms (FDR < 0.2) from genes linked to local recurrence following RT. Nodes represent individual GO terms with size proportional to gene count (>2), and edges indicate significant semantic similarity between terms. Node color intensity corresponds to enrichment significance.

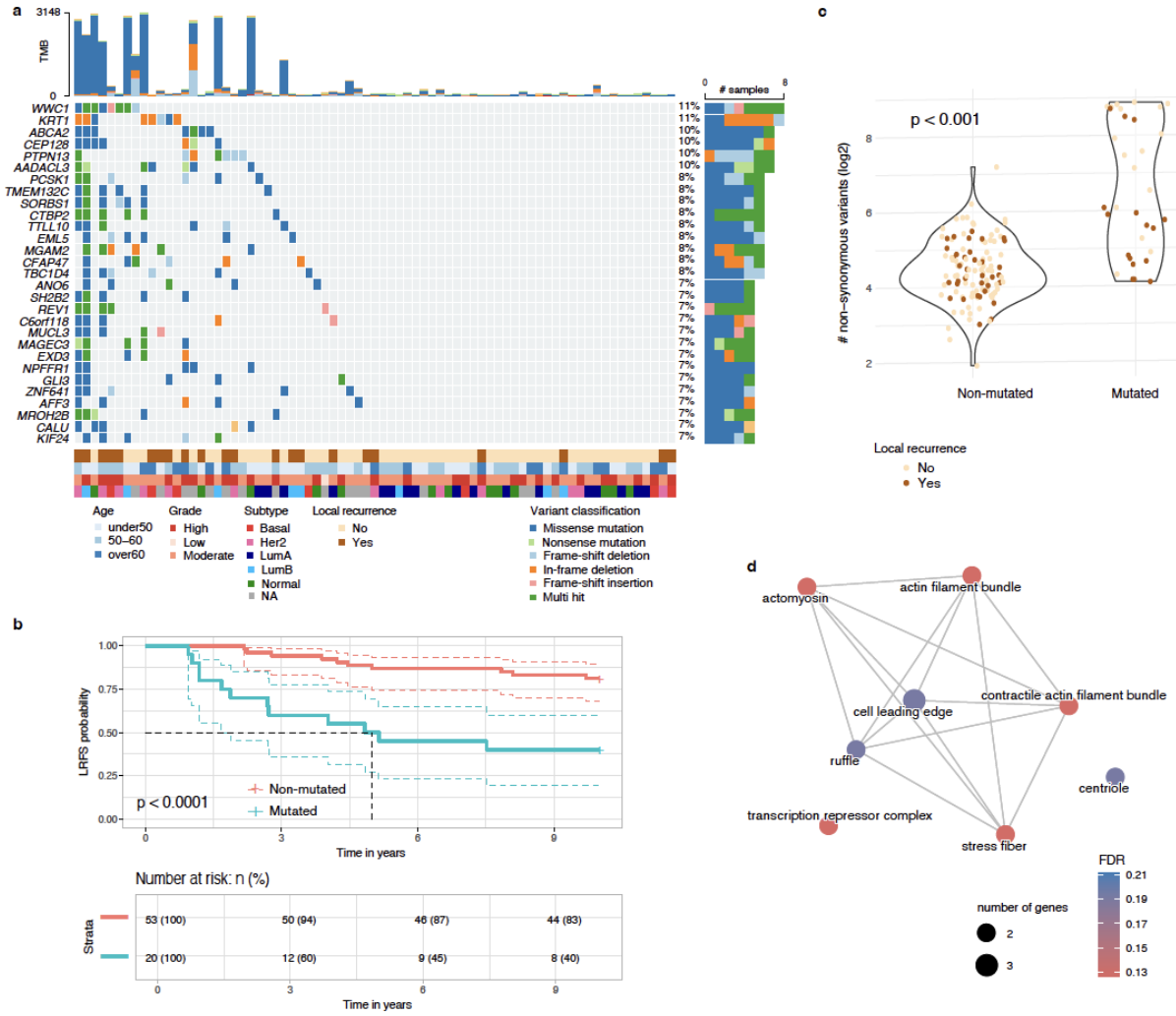

Poster #43

A mechanistic investigation of KRAS inhibitor response in PDAC cells using a multi-omics approach

Fatema Abdullatif[1], Owen Hovey[1], Tyler Cooper[1], Giles Lajoie[1], Teklab Gebregiworgis[1,2]
[1]Department of Biochemistry, Schulich School of Medicine & Dentistry, Western University, London, ON
[2]Department of Oncology, Schulich School of Medicine & Dentistry, Western University, London, ON

Introduction: Pancreatic ductal adenocarcinoma (PDAC) is among the most aggressive solid tumors, with a mortality rate nearly matching its incidence. It is projected to become the second leading cause of cancer-related deaths by 2030. Diagnosis typically occurs at an advanced stage, often after distant metastasis, making surgical resection of the primary tumor ineffective. However, chemotherapy poses major challenges for this disease, leaving limited treatment options for patients with the disease. One of the most common mutations in PDAC are KRAS mutations, present in over 90% of patients. Currently there are some KRAS inhibitors targeting some of the most common mutations, G12C and G12D, however, issues with resistance to these drugs is common. Here, my aim is to elucidate the alterations that occur upon inhibition of mutated KRAS, determining the targets of these drugs and pathways that can be exploited for therapeutic gain.

Methods: Dose response curves for the KRAS G12C (MRTX849) and G12D (MRTX1133) inhibitors were used to determine the concentration of drugs to use for the Mass Spectrometry (MS) and Nuclear Magnetic Resonance (NMR) experiments. Proteomics (n=4) and phosphoproteomics (n=6) were initially completed to map signaling pathway changes following inhibition of mutated KRAS, following that untargeted metabolomics are then conducted to confirm initial findings from the MS experiments, probing for alterations in metabolic profile following treatment (n=5) at 24 hours for cell lysates and media.

Results: Dose response curves for the KRAS inhibitors in pancreatic cancer cell lines are conducted after treatment for 72 hours, and inhibitory concentrations at which around 50% of cells were impacted are identified. The values determined here will be used for treatment of cells used for the MS and NMR experiments. Proteomics analysis shows changes in branched chain amino acid synthesis (BCAA), and we confirmed this with changes via NMR, showing a potential route for targeting.

Conclusions: My goal here is to mechanistically understand the alterations that occur following inhibition of mutated KRAS in PDAC cell lines. Determining altered pathways helps with understanding mechanisms of inhibition and further resistance. KRAS mutations are extremely common in PDAC, and can be exploited for therapeutic advancements, for a disease that is often faced with drug resistance issues.

Poster #44

Characterization of histone deacetylase inhibitor (HDACi) activity on ovarian clear cell carcinoma (OCCC) cell line spheroids

Sylvia Cheng[4], Bart Kolendowski[1,2], Yudith R. Valdes[1,2], Trevor G. Shepherd[1,2,3,5,6], Gabriel E. DiMattia[1,2,4,6]
[1]The Mary & John Knight Translational Ovarian Cancer Research Unit, Verspeeten Family Cancer Centre, London Ontario Canada; [2]LHSC Research Institute, London Health Sciences Centre, London, Ontario, Canada; Departments of [3]Anatomy and Cell Biology, [4]Biochemistry, [5]Obstetrics & Gynaecology, and [6]Oncology, Schulich School of Medicine and Dentistry, Western University, London, Ontario, Canada

Introduction: OCCC is a rare histotype of epithelial ovarian cancer (EOC) with poorer prognosis compared to other EOC histotypes due to resistance to first-line chemotherapeutics, Carboplatin and Paclitaxel. Chemoresistance is due to a unique molecular and genetic profile, as well as intra-peritoneal metastasis through the formation of multicellular cancer aggregates, named spheroids, which attach to peritoneal surfaces to form secondary lesions. Therefore, finding effective therapeutics for OCCC spheroids that target the molecular characteristics of this subtype is key to improving patient outcome. There is interest in targeting the OCCC epigenome as ~50% of OCCC lesions carry truncating mutations in AT-rich interaction domain containing protein 1A (ARID1A). ARID1A loss is associated with changes to global H3K27Ac distribution and histone deacetylase (HDAC) activity, contributing to cancer progression. As such, HDACi's are being investigated for ARID1A-mutant cancers. We aim to determine how HDACi disturbs the OCCC spheroid epigenome and how these changes alter spheroid formation and viability to determine the potential of HDACi's as targeted therapy for OCCC.

Methods: Non-adherent, ultra-low attachment (ULA) plates allowed OCCC cell lines to autonomously form multicellular aggregates, or 3D avascular tumourspheres, that better recapitulate patient tumour morphology relative to traditional 2D culture. Human OCCC cell lines cultured in ULA were treated with HDACi's Entinostat (ENT) and ACY1215 (ACY) and subject to spheroid reattachment, IC50 determination, trypan blue cell counting, and whole cell and acid-extracted nuclear histone lysate collection.

Results: The sensitivity of 15 OCCC cell lines to ENT was correlated with cell line doubling time. Both ENT and ACY treatment increased H3K27Ac levels in both adherent and spheroid OCCC cells in all cell lines tested. The IC50 of ENT was lower than ACY in both KOC-7c and 105C OCCC cell lines, determined using both bulk cell viability and colony forming abilities. KOC-7c spheroids were sensitive to both inhibitors and had a dose-dependent reduction in spheroid cell viability. 105C spheroids displayed increased cell viability and live cell-counts when treated with low micromolar concentrations of ENT and ACY due to a short-term protection from detachment-associated apoptosis. Combination treatment of HDACi with EZH2 inhibitor, EPZ-6438, was not more effective at reducing cell viability than ENT alone in any cell line tested.

Conclusions: These findings suggest that regulation of histone acetylation is critical for OCCC monolayer and spheroid cell viability. HDACi's can alter the epigenome of OCCC cell line spheroids, but OCCC spheroids display varying response to HDACi based on their spheroid characteristics.

Poster #45

Inhibiting TGFβ Signaling using 1,4-DHP in PDAC cells

Andrei Glogov[1], John Di Guglielmo[2]
[1]Physiology and Pharmacology, [2]Oncology

Introduction: Pancreatic Ductal Adenocarcinoma (PDAC) remains a dismal disease to treat, where the 5-year survival rate is ~ 12%. Transforming growth factor beta (TGFβ) plays a paradoxical role in the progression of PDAC, acting as a tumor-suppressor in early stages of disease and a tumor-promoter in later stages by inducing epithelial-mesenchymal transition (EMT), migration and chemoresistance. TGFβ in the tumor microenvironment (TME) also activates cancer-associated fibroblast (CAF) formation, leading to the over deposition of extracellular matrix constituents and cytokines (including TGFβ). This fosters a hypoxic environment that hinders drug penetrance and promotes aggressive tumor behaviour. Thus, we hypothesize that inhibition of the TGFβ Type II Receptor (TBRII) using novel 1,4 dihydropyridine (DHP) compounds will decrease CAF activation and EMT in PDAC cells. Recent work in our laboratory utilizing 1,4 DHP compounds show selective degradation of TBRII, leading to decreased downstream signaling, migration and EMT markers in non-small cell lung cancer cells. However, this has not been investigated in a PDAC context and forms the basis for this research.

Methods: Panc-1 cells (pancreatic carcinoma cells) were treated with DHP followed by TGFβ to assess if these signaling and functional outcomes can be recapitulated in a PDAC context and analyzed via western immunoblotting, immunofluorescent microscopy and invasion/migration assays. Cytotoxicity of DHP was evaluated by an MTT assay to help determine an optimal dosage and safety profile. Pancreatic stellate cells will be treated with DHP to evaluate effects on activation by TGFβ to a CAF phenotype, while CAFs will be treated with DHP to evaluate deactivation or conversion to senescence. This will be evaluated via western immunoblotting, immunofluorescent microscopy, β-Galactosidase Assay and ELISA assay. Lastly, a human organoid co-culture model with CAFs will be used to analyze effects of TGFβ pathway inhibition using DHP in a 3D setting and will be assessed using western immunoblotting, immunofluorescent confocal microscopy and ELISA assay.

Results: Preliminary results show that DHP selectively reduces TBRII protein levels, decreasing canonical SMAD2 phosphorylation and non-canonical P38 phosphorylation in Panc-1 cells. DHP is also capable of inhibiting the increase of EMT transcription factors Snail and Zeb1 in response to TGFβ, while preventing the downregulation of E-cadherin. The MTT assay shows that DHP does not elicit high cytotoxic effects. Under immunofluorescent microscopy, DHP prevents the formation of F-actin stress fibres in response to TGFβ that is seen during EMT.

Discussion: The gold standard for treating PDAC is early detection before metastasis occurs, however better options for patients with unresectable/later stages of disease are still required. The switch to a tumor-promoting role of TGFβ in PDAC progression despite a functional signaling pathway presents a basis for therapeutic investigation. Controlled reduction of CAF activation may lead to improved drug penetrance without promoting aggressive tumor behaviour and overall reduction of tumoral support. On the tumor front, a decrease in EMT in PDAC cells may reduce chemoresistance and motility, restoring sensitivity to current therapeutics.

Poster #46

Identification and functional characterization of the cancer-initiating cell population in human ovarian clear cell carcinoma (OCCC) lines

Blane Gebreyes [4], Bart Kolendowski [1,3], Vasu Bhat [2,3], Yudith R. Valdes [1,3], Trevor G. Shepherd [1,3,4,6,7], Gabriel E. DiMattia [1,3,5,7]

[1]The Mary & John Knight Translational Ovarian Cancer Research Unit, Verspeeten Family Cancer Centre, London Ontario Canada; [2]Translational Breast Cancer Research Unit, Verspeeten Family Cancer Centre, London Ontario Canada; [3]LHSC Research Institute, London, Ontario, Canada; Departments of [4]Anatomy and Cell Biology, [5]Biochemistry, [6]Obstetrics & Gynaecology, and [7]Oncology, Schulich School of Medicine and Dentistry, Western University, London, Ontario, Canada

Introduction: OCCC is a rare histotype of epithelial ovarian cancer that has a poor prognosis if diagnosed at a late stage. One determinant of OCCC mortality is the extent of regional and distant metastases within the peritoneal cavity. Metastasis is responsible for 90% of cancer deaths and can be attributed to a small subpopulation of highly tumorigenic cells with a capacity for self-renewal, known as cancer stem cells (CSCs). Despite making up 0.01-2% of the average tumour mass, these cells play a crucial role in treatment resistance, disease spread, and recurrence.

Methods: RT-qPCR, Western blotting, and FLOW cytometry will be employed in OCCC cell lines to establish a baseline expression profile for well-characterized CSC markers. Select lines will then undergo CSC enrichment through the development of drug-resistant lines or through specialized culture conditions meant to sustain only CSCs. Changes in the expression of well-characterized CSC markers in enriched lines will be investigated relative to the pre-enrichment parental cell line and will be functionally characterized via *in vivo* xenotransplantation.

Results: The ability to proliferate in suspension culture in standard media did not predict a cell line's ability to proliferate in suspension culture using CSC enriching media, nor did it correlate with the expression of ALDH1A1 or the activity of ALDH family members in human OCCC cell lines. Of the well-characterized Yamanaka factors, OCT4 expression showed no association with CSC-related traits or proliferative capacity in CSC culture conditions, whereas SOX2 and NANOG were positively correlated. In the 105C OCCC cell line, the development of resistance to paclitaxel or AZD-8055 is associated with increased expression of CSC markers and enhanced proliferative capacity in CSC culture conditions. However, paclitaxel resistance does not show increased expression of CSC markers and enhanced proliferative capacity in CSC culture conditions in the TOV-21G and OVTOKO OCCC cell lines.

Conclusions: This is the first time human OCCC cell lines have been enriched with CSCs for identification and functional characterization. These results may provide a platform for future studies aimed at understanding how various epigenetic features define an OCCC CSC from a bulk tumour cell and thus potentially identify existing epigenome-targeted therapies which may selectively kill CSCs.

Poster #47

Identification of Optimal Microbiome Donor Profiles to Enhance Immunotherapeutic Response in Melanoma.

Authors: Kelly J Baines[1], Rene Figueredo[2], John Lenehan[2,4], Saman Maleki Vareki[1,2,3,4]

Affiliations: [1] Department of Pathology and Laboratory Medicine, Western University, [2] Department of Oncology, Western University, [3] Department of Medical Biophysics Western University, [4] Verspeeten Family Cancer Centre, Lawson Health Research Institute

Introduction: In 2024, melanoma was projected to account for approximately 11,500 new cancer diagnoses in Canadians and 1,300 deaths, with disproportionately higher mortality in males than in females. Contributing to patient demise is the fact that nearly 50% of advanced melanoma patients receiving anti-programmed death-1 (anti-PD1)-based immunotherapies experience therapeutic resistance. Profiling of gut microbiome composition has linked specific gut bacteria with improved response to immune checkpoint inhibitors (anti-PD1), however it remains undetermined if specific bacteria play a prominent role in the determination of PD1 response.

Methods: Stool samples were collected from responder patients that have received anti-PD1 alone or in combination with anti-CTLA4 with advanced melanoma. To determine if FMT from healthy donors or anti-PD1 responders is superior in sensitizing resistant tumors to anti-PD1 therapy, the microbiomes of 6 healthy donors (3 male and 3 female) and 6 responder patient donors (3 male and 3 female) was engrafted into 6 avatar mice, each. Two weeks after FMT, stool was collected from mice for metagenomic and metabolomic analysis. Following FMT, these animals were inoculated with B16F10 melanoma cells and subsequently administered anti-PD1 treatment. Tumor growth was measured daily, and the tumor microenvironment was compared across microbiome sources via flow cytometry analysis of isolated tumor infiltrating lymphocytes. Cell-free filtrates from donor stool was applied in culture to activated Jurkat (human CD4 T-cells) for 24 hours, and changes to T-cell stimulation and activation was assessed. Flow cytometry will be conducted for activation and apoptosis, and cytokine release will be measured using ELISA.

Results: Preliminary results indicate that FMT from healthy donors offers greater regulation of tumour growth, with possible sex-effects between donor and recipient. In vitro application of cell-free filtrates for 24 hours to Jurkat cells resulted in differential activation between stool donor source, as measured by IL-2 ELISA and CD69 flow cytometric analysis.

Discussion: With the results from this study, we will be able to determine the immunomodulatory properties of each microbiome source on the immune profile within melanoma tumors and their response to immunotherapy, as well as the impact of donor sex on microbial engraftment. This offers improved engraftment and successful of immune refractory cancers.

Poster #48

Developing Novel Potent and Specific Pin1 Inhibitors to Probe the Molecular Mechanisms of Tumour Resistance in Pancreatic Ductal Adenocarcinoma

George Xie[1], Ian Gao[2], Michael Kerr[2], Brian Shilton[1], Shawn Li[1,3], Xiao Zhen Zhou[1,3,4,5], Kun Ping Lu[1,3,5]

[1]Department of Biochemistry, Schulich School of Medicine and Dentistry, Western University
[2]Department of Chemistry, Western University
[3]Department of Oncology, Schulich School of Medicine and Dentistry, Western University
[4]Department of Pathology and Laboratory Medicine, Schulich School of Medicine and Dentistry, Western University
[5]Robarts Research Institute, Schulich School of Medicine and Dentistry, Western University

Pancreatic ductal adenocarcinoma (PDAC) is one of the most aggressive and lethal cancers, projected to become the second-leading cause of cancer death by 2030. PDAC remains to be nearly universally lethal, and is notoriously hard to treat, owing to lack of early detection methods and criteria, and a highly immunosuppressive tumour microenvironment (TME) comprised of a dense network of fibroblasts, stromal cells, and regulatory immune cells which aid in immune evasion. The unique prolyl isomerase Pin1, discovered by our lab, regulates the conformation, activity, and stability of over 70 oncogenes and 30 tumour suppressors. Pin1 is overexpressed in many cancers, where it drives cancer initiation and progression, contributing to 13 of the 14 hallmarks of cancer. Notably, all-*trans* retinoic acid (ATRA) and arsenic trioxide (ATO), are a combination of FDA-approved drugs for treating acute promyelocytic leukemia (APL) which were later discovered to target Pin1. Since Pin1 overexpression drives diverse cancer pathways, including drug resistance, many groups have investigated combination therapies using Pin1 inhibitors and currently approved therapies. We have previously shown that by targeting Pin1, PDAC can be rendered eradicable by current therapies gemcitabine (GEM) and anti-PD-1 monoclonal antibody (mAb) therapy. Inhibition of Pin1 sensitizes tumours to GEM uptake and reshapes the immunosuppressive TME, turning PDAC from immune “cold” to “hot”; however, the precise molecular mechanisms by which Pin1 inhibition disrupts cancer resistance and immune evasion is still unknown. Current Pin1 inhibitors ATRA+ATO suffer from toxicity and off-target effects, limiting their potential to be adopted into clinical use for PDAC, despite being long-approved for treatment of APL. Other described Pin1 inhibitors are not potent enough or have unfavourable chemical moieties. We hypothesize that by developing novel more potent and specific Pin1 inhibitors, we can dissect the mechanisms by which Pin1 inhibition reforms the TME and overcomes drug resistance, while offering a novel therapeutic approach to cure PDAC. Currently, we have discovered three promising chemotypes of Pin1 inhibitors, and we have established a comprehensive array of assays used to guide optimization and further increase potency and specificity. Our most promising lead compound shows low nanomolar affinity, induces rapid degradation of Pin1, and is highly specific for Pin1, while current work is being done on obtaining crystal structures and comprehensively confirming proteome-wide specificity. Using the most promising Pin1 inhibitors with and without GEM+anti-PD-1 mAbs, we will treat syngeneic PDAC mouse models, then investigate effects at a cellular level, using single-cell and spatial omics. These approaches will allow us to finely dissect changes in specific immune cell types compared to PDAC tumour cells and cancer-associated fibroblasts. Furthermore, we will evaluate crosstalk between cells, and how the cellular composition of the TME changes under Pin1 inhibition. By developing the most potent, specific, and clinically relevant Pin1 inhibitors described to date, and by uncovering the molecular mechanisms by which Pin1 inhibition overcomes cancer resistance and immune evasion, this study will pave the way for the first in-human trials to treat PDAC through Pin1 inhibition.

Poster #49

Investigating combination PD1 and TIM3 blockade in an HPV+ head and neck cancer model

Nhi Le[1], Harrison Pan[1], Amir Karimi[1], John Barrett[1,2], Anthony Nichols[1,2]
[1]Department of Pathology and Laboratory Medicine, Schulich School of Medicine and Dentistry, Western University, Canada
[2]Department of Otolaryngology, Head & Neck Surgery, Western University, Canada

Introduction

HPV+ Head and Neck Squamous Cell Carcinoma (HNSCC) is a type of aggressive oral cancer with a low survival rate with more than 50% of HNSCC patients experiencing tumor recurrence and metastasis within 3 years. Immune checkpoint inhibitors have been an important step forward in care, offering better efficacy and lower toxicities than chemotherapy for this type of cancer. Anti-PD1 therapy have been FDA-approved, but the overall response rate still is as low as 15%. Preliminary data suggests that combining other immunotherapy targets such as TIM3 with PD1/PDL1 therapy can yield additive anti-tumor effects, providing rationale for further exploration. We hypothesize that combined PD1 and TIM3 blockade in an immunocompetent HPV+ HNSCC murine model will provide a durable and efficacious response due to alterations in the tumor microenvironment (TME).

Methods

MOC1 cells (HNSCC carcinogen induced syngeneic cell line) are cultured and injected in the flank of immunocompetent C57BL/6 mice. Mice (n=32) are randomized into one of four groups: control, anti-TIM3 only, anti-PD1 only, or combination anti-TIM3 and PD1. Mice will be on treatment over the course of 30 days. Tumor measurements are taken and excised at endpoint for further analysis. Post-experimental analysis includes flow cytometry, immunohistochemistry and single cell RNA sequencing to investigate the tumor microenvironment.

Expected Results

The mice group treated with combined PD1 and TIM3 inhibition will exhibit better tumor control compared to the monotherapy and control groups, observed by greater regression in tumor size during treatment. The TME of tumors treated with combination therapy will experience higher immune cell infiltration compared to monotherapy administration.

Discussion

By evaluating tumor regression and characterizing changes in the tumor microenvironment across the different groups, our findings will provide preclinical evidence to inform the development of novel combination therapies. These results could lay the foundation for future clinical trials aimed at improving treatment outcomes and survival rates for advanced HNSCC patients.

Poster #50

The sex-specific role of Spy1 in the liver stress response and disease.

Milan Lobana[1], Isabelle Hinch[1], Amy Llancari[1], Bre-Anne Fifield[1,2], Lisa A. Porter[1,2,3*]
[1]Department of Biomedical Sciences, University of Windsor, ON, Canada N9B 3P4
[2]WE-SPARK Health Institute, University of Windsor, ON, Canada N9B 3P4
[3]St. Joseph's Health Care London, Lawson Health Institute, ON, Canada N6A 4V2

Introduction: Liver cancer is a leading cause of cancer-related mortality, with hepatocellular carcinoma (HCC) comprising 90% of cases. HCC exhibits a notable sex bias, with males being 3.4 times more likely to develop the disease. Although the mechanisms underlying this disparity remain unclear, liver stress responses such as inflammation and oxidative stress are established contributors to HCC progression. These stress responses are regulated by the cell cycle. Spy1, an atypical cyclin-like protein involved in the cell cycle, accelerates cell proliferation and increases susceptibility to HCC by binding to CDK2. However, its sex-specific role in liver stress responses has not been elucidated. Using a novel Alb-Spy1 mouse model that upregulates Spy1 in both male and female livers, this study investigates the role of Spy1 in the liver stress response induced by the methionine-choline deficient (MCD) diet. We hypothesize that Spy1 overexpression drives sex-specific differences in histopathology, including fat deposition, collagen levels, and inflammation, as well as proliferative and apoptotic markers. This research aims to provide critical insights into the role of Spy1 in sex-specific liver responses, advancing understanding of HCC development and guiding future therapeutic interventions targeting Spy1-mediated pathways.

Methods: Wild-type and Alb-Spy1 transgenic mice on the C57BL/6N background were housed and maintained in the Animal Care Facility at the University of Windsor under regular conditions following the Canadian Council of Animal Care guidelines. Livers were excised at two time points (15 and 65 weeks) and tissues were fixed in either 10% formalin or 4% PFA for microtome and cryo-sectioning, respectively. Histopathological tests including Oil Red O for fat deposition, Trichrome for fibrosis, β-Galactosidase for senescence, and Hematoxylin for nuclear area and immune cell infiltration were conducted. To assess proliferation and apoptosis, Immunohistochemistry was performed.

Results: Various sex and age specific differences were seen. Alb-Spy1 male mice had decreased fat, fibrosis, nuclear area, and senescence, while Alb-Spy1 females had increased immune cell infiltration, fibrosis, and nuclear area. Commonalities seen across both sexes were a ubiquitous increase in proliferation and no alterations in apoptosis with overexpressed Spy1.

Discussion: Spy1 overexpression in males was associated with decreased fat deposition, reduced senescence, lower fibrotic response, and increased proliferation, suggesting Spy1's role in exhausting fat stores to allow cell cycle re-entry to proliferate and repair damage. Due to the decreased fibrosis, Spy1 in males could drive non-cirrhotic HCC susceptibility. In contrast, females exhibited increased immune cell infiltration and fibrosis independent of changes in fat or senescence, proposing a potentially distinct role of Spy1 toward cirrhotic HCC susceptibility. The effects of aging on the above processes was also sex-dependent, highlighting a differential exhaustion rate of mechanisms that protect against HCC development. This study highlights Spy1 as a potential sex-specific regulator of hepatic regeneration and disease development, paving the way for future mechanistic studies to consider hormonal and cell cycle regulation. This study also revealed different pathologies present across sex and age, which emphasize the importance of sex-specific biomarkers and personalized therapy options for patients with liver disease in clinic.

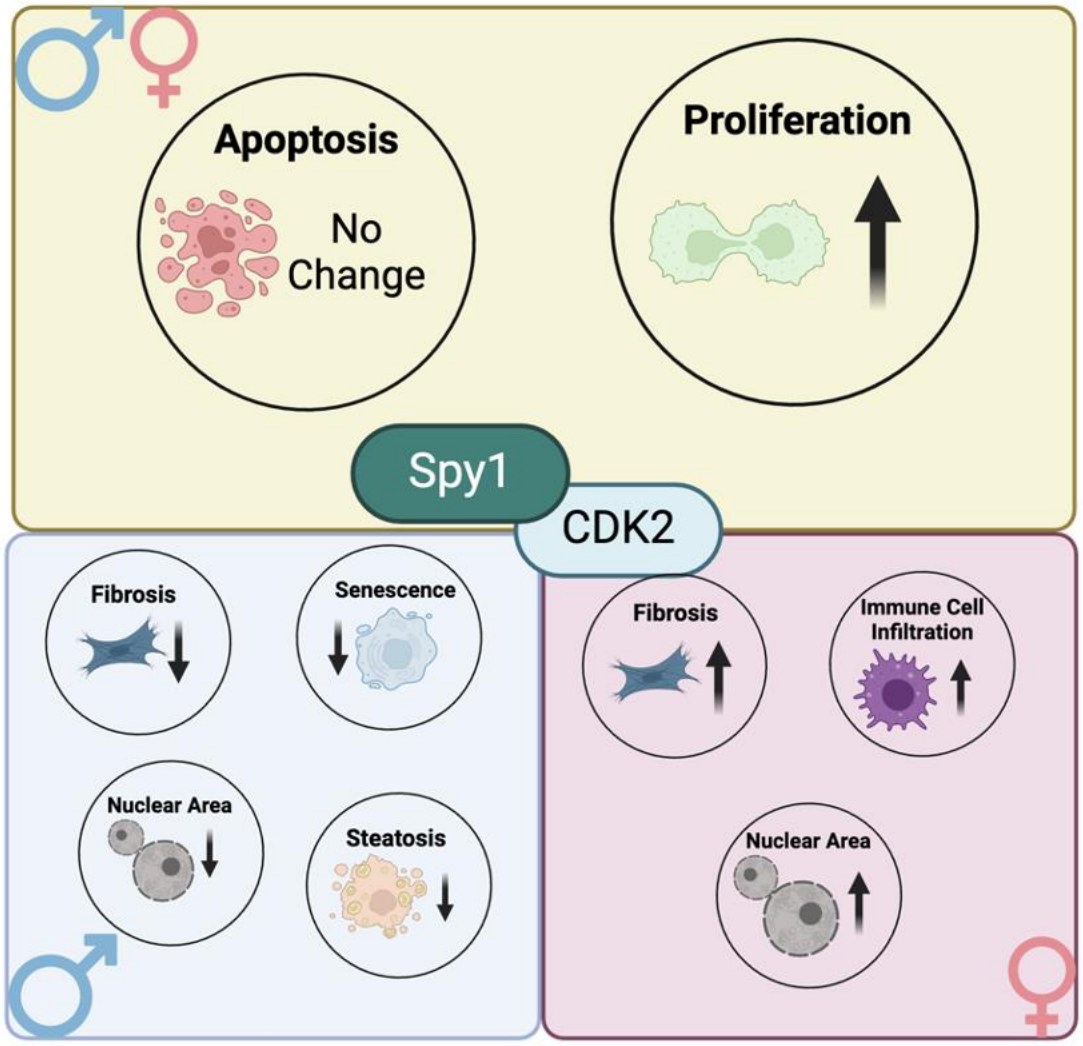

Figure 1: Schematic showing summary of sex-specific differences and commonalities when Spy1 was overexpressed in a diseased hepatic environment. Made in BioRender.

Poster #51

Investigating the Targeted Effects of HA-Conjugated Nanoparticles Against Glioblastoma

Vanessa Riolo [1], Dorota Lubanska[1], Lisa A. Porter [1,2] Simon Rondeau-Gagne[1], Angela Awada[1]
[1]University of Windsor, [2]St. Joseph's Health Care London

Introduction: Glioblastoma (GBM) is a lethal grade IV glioma of the central nervous system. Despite the standard treatments, prognosis remains poor due to several barriers to successful treatment such as the presence of the blood-brain barrier, tumour heterogeneity, and glioma stem cells (GSCs), which are known to increase aggressiveness and hinder therapy response. A notable GSC marker is the CD44 receptor, which is activated by its primary ligand, hyaluronic acid (HA), to promote cancer progression. High CD44 expression is correlated to poor prognosis. Nanoparticle therapies are an emerging field of cancer research that allow for selective targeting of GSC populations. Our lab has shown that HA-Conjugated Nanoparticles (HA-CPNs) can selectively target CD44+ cells, eliciting anti-tumour effects both *in vitro* and *in vivo*. We want to utilize HA-CPNs to target GSC populations within a biologically relevant glioblastoma organoid system, to study their effects on GSC regulation.

Methods: We examined CD44's role in GBM and assessed HA-CPN impacts on CD44 expression in 2D cell cultures and 3D organoids. Using shCD44 and PLKO control, we analyzed proliferation and stemness in GBM cell lines. We then treated cells with HA-CPNs to assess effects on CD44 expression via qRT-PCR and on proliferation. Glioblastoma organoids were generated using U-251 MG cells and matrigel, then treated with HA-CPNs via two delivery methods. Uptake was tracked through fluorescence microscopy using the rhodamine-labeled HA-CPNs. CD44 expression was monitored over time using qRT-PCR and correlated to uptake. We also propose simplified fluorescent CPNs and assessed uptake with flow cytometry, and CD44 expression changes via western blotting.

Results: Through our data, we have shown the essentiality of CD44 within GBM, and that infection with shCD44 results in a significant decrease in proliferation and increase in differentiation. Additionally, HA-CPN treatment demonstrated a decrease in CD44 expression and proliferation of GBM cells in 2D cell cultures. Glioblastoma organoids demonstrate the ability to uptake HA-CPNs into their microtissues in a time and density-dependent manner and seem to impact CD44 expression.

Discussion: We have demonstrated that CD44 plays an essential role in regulating proliferation and stemness, and that treatment with HA-CPNs may decrease CD44 expression within a 3D organoid model. Further investigations must be done to optimize timing and dosage of HA-CPN delivery throughout organoid growth for more significant results. Further studies should also explore the spatial regulation of CD44 and related markers within the 3D tumour, using immunofluorescent staining techniques. This may paint a clearer picture into the GSC regulation occurring within the sections of the tumour. Exploring the use of HA-CPNs and other novel nano-systems can help to improve our understanding of CD44 and its role in regulating GSC dynamics and may open avenues for development of nano-based targeted therapies to improve prognosis for patients in the future.

Poster #52

Examining the role of a pancreas-specific isoform of SPCA2 in pancreatic pathology

Oneeb Hassan[1, 3, 4], Peter Stathopulos[1], and Christopher Pin[1, 2, 3, 4]
[1]Department of Physiology and Pharmacology, [2]Department of Oncology, [3]Baker Centre for Pancreatic Cancer, [4]Verspeeten Family Cancer Centre

Introduction: Pancreatitis is the most significant risk factor for the development of pancreatic ductal adenocarcinoma (PDAC), a highly lethal cancer with a 5-year survival rate of ~12%. Initiation and progression of pancreatitis is affected by calcium (Ca^{2+}) dependent mechanisms. While transient increases in cytosolic Ca^{2+} are crucial for normal exocrine secretion of digestive enzymes, sustained elevation triggers premature enzyme activation, mitochondrial dysfunction, and necrotic cell death leading to pancreatitis. Store-operated calcium entry (SOCE) is a main mechanism for restoring Ca^{2+} levels within the endoplasmic reticulum (ER) and we identified a pancreas-specific isoform of Secretory Pathway Ca^{2+} ATPase 2, termed SPCA2C, that interacts with regulators of SOCE. Over-expression of SPCA2C in HEK293 cells increases cytosolic and ER Ca^{2+} levels but, to date loss of SPCA2C has not been examined in the context of pancreatic pathologies. We hypothesize that loss of SPCA2C will reduce cytosolic/ER Ca^{2+} levels and SOCE activation in the pancreas, thereby decreasing pancreatic injury.

Methods: A mouse model in which the transcriptional start site of *Atp2c2* (gene encoding SPCA2C) was deleted was generated (*Atp2c2*$^{\Delta 24/\Delta 24}$). Pancreatic morphology and expression of cell differentiation markers (insulin, CK19, amylase) were assessed in *Atp2c2*$^{\Delta 24/\Delta 24}$ mice. Expression of the SOCE regulators STIM1 and Orai1 was determined by RNA-seq and immunoblotting. Pancreatic acini were isolated from *Atp2c2*$^{\Delta 24/\Delta 24}$ and wild type littermates, and Ca^{2+} signaling assessed using Fura-2 ratiometric assays. Acute pancreatitis was induced via injection of supramaximal levels of cerulein and pathological severity assessed 8 and 72 hours post-treatment through histological and molecular approaches.

Results: *Atp2c2*$^{\Delta 24/\Delta 24}$ mice showed no differences in gross morphology based on pancreatic weight, histology, or cell differentiation. While *STIM1* and *Orai1* expression was not altered at the transcriptional level, altered protein levels were observed in both untreated and cerulein-treated *Atp2c2*$^{\Delta 24/\Delta 24}$ mice. Isolated *Atp2c2*$^{\Delta 24/\Delta 24}$ acini showed significantly decreased ER Ca^{2+} despite no difference in cytosolic Ca^{2+} and SOCE activation. While no differences in pancreatitis severity was observed 8 hours following cerulein treatment, at 72 hours, *Atp2c2*$^{\Delta 24/\Delta 24}$ mice showed less damage based on reduced inflammation and fibroblast activation compared to wild type mice.

Discussion: These results suggest SPCA2C may be involved in stabilizing the proteins involved in SOCE and maintaining ER Ca^{2+} levels in pancreatic acinar cells, which may decrease the severity of pancreatitis in *Atp2c2*$^{\Delta 24/\Delta 24}$ mice. Further experiments will evaluate the effect of losing SPCA2C on pathological progression in models of PDAC involving $KRAS^{G12D}$.

Poster #53

MetaStruct: A modular framework for scalable and reproducible metagenomics analysis

Behnam Jabbarizadeh[1] and Saman Maleki Vareki [1,2,3,4]

[1] London Regional Cancer Program, Lawson Health Research Institute, London, ON, Canada
[2] Department of Pathology and Laboratory Medicine, University of Western Ontario, London, ON, Canada
[3] Department of Oncology, Western University, London, ON, Canada
[4] Department of Medical Biophysics, Western University, London, ON, Canada

Introduction: The analysis of shotgun metagenomics data remains challenging due to the fragmentation and heterogeneity of data types, spanning microbial taxonomic profiles, gene families, enzymatic pathways, and clinical metadata. Existing bioinformatics pipelines often lack cohesive integration, have inconsistent preprocessing methods, and typically provide limited scalability and reproducibility. Inspired by Seurat's transformative impact on single-cell transcriptomics [1], which unified diverse data types into a cohesive analytical structure, we developed MetaStruct, a modular, object-oriented data structure explicitly tailored to overcome these specific limitations and complexities in metagenomics research.

Methods: MetaStruct is designed to house multi-layered metagenomics data within a single container object. It supports the integration of taxonomic, functional, and clinical metadata, enabling seamless preprocessing, normalization, statistical testing, and machine learning workflows. We implemented modular tools for quality control, diversity analysis, dimensionality reduction, differential abundance testing, and interactive visualization, each featuring customizable parameters and seamless inter-module interoperability. Notably, our differential abundance module supports classical and compositional-aware methods, and our visualization tools enable dynamic exploration through layered metadata integration. MetaStruct was built in R, with compatibility for integration into existing pipelines and cloud-based tools.

Results: We applied MetaStruct across four independent clinical trial cohorts investigating fecal microbiota transplantation (FMT) and cancer immunotherapy. The framework facilitated consistent data management and harmonization across all datasets, enabling seamless switching between cohorts for comparative analysis and hypothesis testing. MetaStruct's modular design streamlined the development of a unified web application that allowed real-time exploration, visualization, and integration of taxonomic, functional, and clinical data. This capacity to interoperate across trials and data types helped uncover cross-cohort patterns and supported the generation of innovative biological insights that would have been difficult to achieve with traditional workflows.

Conclusions: MetaStruct addresses a critical gap in metagenomics by introducing a Seurat-like object system that standardizes and simplifies complex microbiome analyses. By consolidating disparate data types into a unified and extensible structure, MetaStruct enhances reproducibility, accelerates discovery, and opens new opportunities for collaborative microbiome research. Its flexible design and demonstrated utility in interventional studies make it a valuable asset for translational microbiome science.

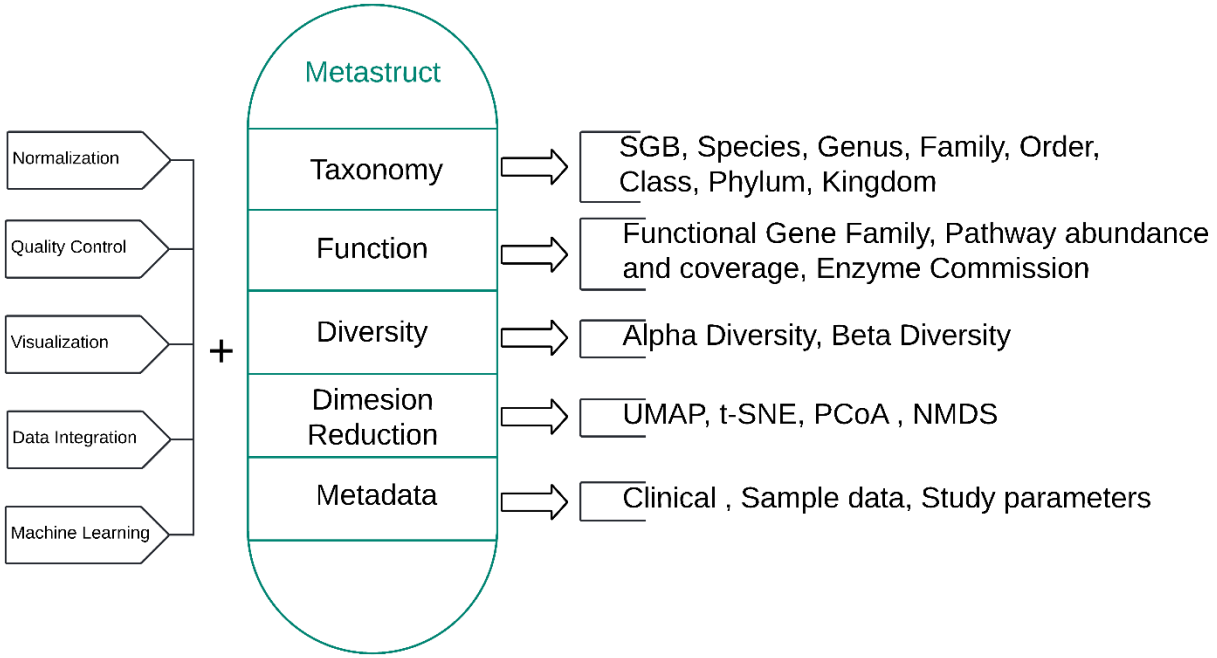

Figure 1 Overview of the MetaStruct framework.

MetaStruct encapsulates multiple layers of metagenomic data, including taxonomy, function, diversity, dimensionality reduction, and metadata, within a unified object-oriented structure.

[1] Hao, Y., Stuart, T., Kowalski, M.H. et al. Dictionary learning for integrative, multimodal and scalable single-cell analysis. Nat Biotechnol 42, 293–304 (2024)

Poster #54

Assessing the Unique Roles of PANX1 Proteoforms in Melanoma

Stephanie E. Leighton[1], Danielle Johnston[1], Kevin Barr[1], Dale W. Laird[1,2], Silvia Penuela[1,3,4]

Affiliations: [1]Department of Anatomy and Cell Biology, Schulich School of Medicine and Dentistry, University of Western Ontario, London, Ontario, Canada, N6A 5C1; [2]Department of Physiology and Pharmacology, Schulich School of Medicine and Dentistry, University of Western Ontario, London, Ontario, Canada, N6A 5C1; [3]Western's Bone and Joint Institute, The Dr. Sandy Kirkley Centre for Musculoskeletal Research, University Hospital, London, Ontario, Canada N6A 5B9; [4]Division of Experimental Oncology, Department of Oncology, University of Western Ontario, London, Ontario, Canada, N6A 5W9

Introduction: Pannexins (PANX1, PANX2, and PANX3) are a family of integral membrane glycoproteins that canonically function to facilitate cellular signaling through the regulated passage of ions and metabolites such as ATP. Among pannexins, PANX1 is the most ubiquitously expressed in mammalian tissue and cell types and disruptions to its expression have been associated with the onset and progression of various cancers, including melanoma. Previously, we have demonstrated that targeting PANX1 via shRNA or pharmacological inhibitors significantly reduced melanoma growth and migration although it is unclear whether this phenotypic change is due to PANX1 or a novel C-terminal PANX1 proteoform (PANX1-25K) which is abundantly expressed in melanoma patient samples at different stages of disease progression.

Methods & Results: Using a CRISPR-Cas9 strategy targeted to the initiating methionine start codon we discovered that PANX1-25K was retained following the genetic ablation of full length PANX1(PANX1-FL) in A375-P cells. Immunofluorescent labeling for PANX1 in PANX1 KO A375-P cells revealed an apparent loss of classical PANX1 cell surface staining yet retained intracellular PANX1 signal. Subsequent subcellular fractionation assays determined that PANX1-25K is cytosolic indicating that this shorter proteoform may have unique cellular functions that differ from PANX1-FL which functions as a large-pore channel at the cell surface. Utilizing bulk RNA sequencing we identified a significant disruption to cell cycle related genes when PANX1-FL was genetically ablated or targeted with spironolactone, a PANX1 pharmacological inhibitor. However, live cell imaging revealed that the targeted deletion of PANX1-FL did not significantly alter the growth or migration of control A375-P cells suggesting that PANX1-FL may not be essential for melanoma cell growth or migration. However, when control and PANX1 KO A375-P cells that harbored the PANX1-25K proteoform were challenged with pharmacological PANX1 inhibitors cell growth was significantly reduced suggesting PANX1-25K may impact cell growth.

Conclusions: Looking forward, we will explore the intracellular function of PANX1-25K in melanoma cells, and test if deleting PANX1-25K influences melanoma cell properties. This investigation will provide foundational knowledge regarding the distinct role(s) of PANX1-FL and PANX1-25K which may have translational implications when considering novel treatment targets for melanoma.

Poster #55

Characterizing PANX1-25K: A Potential Cancer Proteoform with Unique Localization and Stability

Dan Stefan[1], Brooke L. O'Donnell[1,3], Stephanie E. Leighton[1], Danielle Johnston[1], Laszlo Gyenis[2], Silvia Penuela[1]

[1]Department of Anatomy and Cell Biology, Schulich School of Medicine and Dentistry, University of Western Ontario, London, Ontario, Canada, N6A 5C1.

[2]Department of Biochemistry, Schulich School of Medicine and Dentistry, University of Western Ontario, London, Ontario, Canada, N6A 5C1.

[3]Department of Molecular Physiology and Biological Physics, School of Medicine, University of Virginia, Charlottesville, Virginia, The United States of America, 22903

Introduction: The channel forming glycoprotein pannexin1 (PANX1) promotes tumour growth, migration and survival in a diverse set of cancers including breast cancer, melanoma and squamous cell carcinoma. Recently our lab has identified a novel C-terminal alternative translation initiation proteoform of PANX1 with a mass of 25 kDa called PANX1-25K (25K). This novel PANX1 proteoform is prominently expressed in various cancer cell lines and is upregulated in patient-matched squamous cell carcinoma samples relative to non-cancerous skin controls. We hypothesize that 25K plays a necessary role in the tumorigenic advantage canonically attributed to full-length PANX1 (FL) . In order to study the function of 25K, it must first be established as a distinct stable isoform of PANX1. Thus the aim of this study is to uncover basic properties of the novel protein including its localization, sequence, post-translational modification, protein-protein interactors and stability in the cell.

Methods and Results: Co-immunoprecipitation revealed that 25K is able to form complexes with beta-catenin, a key component of the Wnt signalling pathway as well as PANX1-FL. An immunofluorescent microscopy assay with an overexpression construct of 25K indicated that unlike PANX1-FL, 25K primarily localizes intracellularly. In melanoma and breast cancer cells with and without PANX1-FL, a dephosphorylation assay revealed that endogenous 25K is phosphorylated, while mass spectrometry identified 3 sites of N-glycosylation along the 25K sequence. In the same cells, cycloheximide chase-assays revealed that like PANX1-FL, 25K is a long-lived protein with stable protein levels over 16 hours of translation inhibition, independent of PANX1-FL expression. The stability and unique localization of 25K suggest a PANX1-FL independent function for the novel 25K protein.

Discussion: Along with our continuing efforts to knock out and sequence 25K, this work contributes to our understanding of a novel cancer proteoform which could ultimately serve as a therapeutic target or prognostic marker in melanoma and other cancers.

Poster #56

Suppression of the IL-18 pathway by the Human Papillomavirus E7 oncoprotein in head and neck squamous cell carcinoma.

Andris M. Evans[1], Wyatt Anderson[1], Joe S. Mymryk[1,2,3].

Department of Microbiology and Immunology[1], Otolaryngology[2], Oncology[3], Western University, Canada

The incidence of human papillomavirus-positive (**HPV+**) head and neck squamous cell carcinoma (**HNSCC**) is rapidly increasing, such that the incidence in men has surpassed that of women with cervical cancer. Despite generally favourable treatment outcomes for HPV+ compared to HPV-negative HNSCC, roughly 30% of patients still succumb to the disease. Additionally, many survivors experience lifelong treatment-related sequelae. Improved understanding of the effects of HPV in HNSCC is required for the development of effective therapies with fewer adverse consequences. HPV+ HNSCCs retain expression of the E6 and E7 viral oncoproteins, which are critical for tumour growth, survival, and avoidance of the immune system. To aid in viral immune evasion, E7 can disrupt the methylation of several host gene promoters that interfere with HPV infection. One potential target of E7 is IL-18, a pro-inflammatory cytokine with a critically important role in epithelial barrier function. IL-18 activity is antagonized by the soluble IL-18 binding protein (**IL-18BP**). Our analysis of RNA-sequencing data from the HNSCC cohort of The Cancer Genome Atlas shows increased *IL18BP* and reduced *IL18* mRNA levels in HPV+ HNSCC compared to HPV- HNSCC and normal adjacent tissues. This suggests a concerted antagonism of the IL-18 pathway by E7 that affects patients with HPV+ HNSCC. Higher levels of methylation also exist at CpG sites in the *IL18* promoter in HPV+ HNSCC patients. These observations indicate a possible mechanism for transcriptional repression of *IL18* in HPV+ HNSCC. Luciferase reporter assays demonstrate that HPV16 E7 expression alone can repress IL-18 transcription *in vitro*. Enzyme-linked immunosorbent assays also demonstrate that cells expressing HPV E7 have reduced levels of IL-18 protein in cell culture supernatants. Using a panel of point mutants for HPV16 E7, we have identified specific surface-exposed amino acid residues that appear necessary for IL-18 repression. Although HPV16 accounts for approximately 80% of HPV+ HNSCC, we also tested this activity in other oncogenic and non oncogenic alpha HPV types. Our analysis identifies that this repression of IL-18 transcription is generally conserved across E7 from most HPVs, but not all. Future experiments will further investigate the mechanism by which IL-18 is repressed by E7 in the context of HPV+ HNSCC. As E7 is consistently retained in HPV+ HNSCC, this novel viral immune evasion mechanism may also impact the immune response within HPV+ HNSCC tumours. This insight provides valuable information for the development of future therapies for targeted reactivation of the immune response to HPV+ HNSCC.

Poster #57

The Effects of EZH2 Inhibition on Colitis-Associated Colorectal Cancer

Ginnian Leung[1,2], Frederikke Larsen[1,2], Mathieu F. Derouet[1], Liyue Zhang[1], Samuel Asfaha[1]
[1]Department of Medicine, Schulich School of Medicine & Dentistry, Western University, Canada
2Department of Pathology and Laboratory Medicine, London Health Sciences Centre, Canada

Introduction: Colorectal cancer is the second leading cause of cancer deaths in Canada, with chronic gastrointestinal inflammation significantly increasing the risk of colitis- associated cancer (CAC). The molecular mechanism behind this is unknown, but epigenetic changes associated with inflammation are suspected to play a role. Interestingly, both colitis and CAC are linked to the histone methyltransferase EZH2, which contains a SET domain that catalyzes H3K27me3 to repress gene expression. Notably, EZH2 silences transposable elements (TEs), and its inhibition can re-express TEs, inducing a viral mimicry response with anti-tumor effects. This project explores how EZH2 histone methylation affects CAC tumorigenesis and if viral mimicry is involved. We hypothesize that inhibiting EZH2 reduces CAC tumorigenesis by activating a viral mimicry response.

Methods: $Dclk1^{CreERT2}$;$Apc^{f/f}$ mice were crossed to $Ezh2^{SET/SET}$ mice to knockout EZH2 histone methyltransferase activity. To induce CAC, $Dclk1^{CreERT2}$;$Apc^{f/f}$ (control) and $Dclk1^{CreERT2}$;$Apc^{f/f}$; $Ezh2^{SET/SET}$ mice were administered 3 doses of tamoxifen followed by 5 days of 2% DSS. At week 14, colonic tumor number and size were assessed. Tumors were also analyzed for RNA expression of TEs and interferon stimulated genes (ISG). In another experiment, HCT116 and HT29 cells were treated with EPZ-6438 (3uM) or vehicle for 6 days. RNA expression of TEs and ISGs were assessed.

Results: Knockout of the EZH2 SET domain significantly decreased colonic tumor number and the percentage of mice that formed tumors.

Discussion: Deleting EZH2 histone methyltransferase activity significantly reduces CAC tumorigenesis.

Booth #58

Educational Initiatives for Trainees of the CTCR

Mark Njoroge Wanyoike
Isabella Tait
Elaine Whitmore
Evan Xie

Abstract not available for booklet

Poster #59

Clinical Significance of Grade 1 Triple Negative Breast Cancer: A Retrospective Cohort Analysis

Laurice Arayan, MD[3**], Neya Ramanan[1], Mah-noor Malik[1], Sarang Upneja, MD[1], Haniya Farooq[2], Swati Kulkarni, MD[1,3], Rasna Gupta, MD[1,3], John Mathews, MD[1,3], Abdullah Nasser, MD[1,3], Vikas Garg, MD[7], Alina Bocicariu, MD [1,4], Lisa Porter, PhD[5], Bre-Anne Fifield, PhD[5], Rong Luo, PhD[6], Muriel Brackstone, MD[1,7], Caroline Hamm, MD [1,3]
[1]Schulich School of Medicine and Dentistry, Western University, Windsor, (ON), Canada, [2]School of Medicine, University College Dublin, Dublin, Ireland, [3]Department of Oncology, Windsor Regional Hospital, Windsor, (ON), Canada, [4]Department of Pathology, Windsor Regional Hospital, Windsor, (ON), Canada, [5]Department of Biology, University of Windsor, Windsor, (ON), Canada, [6]Department of Mathematics, University of Windsor, Windsor, (ON), Canada, [7]University of Western Ontario, London, (ON), Canada

Introduction: Grade 1 Triple Negative Breast Cancer (TNBC) comprise of histologically low-grade lesions whose natural histories, molecular features, and optimal therapy vary from those of high-grade TNBCs. Here, we describe the clinicopathologic features and outcomes of patients with grade 1 TNBC.

Methods: This is a retrospective descriptive study on grade 1 TNBC patients from two regional cancer programs in Canada seen between January 1, 2004 and December 31, 2022. Demographic data, tumor characteristics, treatment and outcomes of patients with TNBC from the two institutions were collected and analyzed. Recurrence and mortality rates were also determined. Comparison of the American Joint Commission of Cancer (AJCC) staging systems 7 and 8 was completed.

Results: We identified a different pattern of histology for grade 1 TNBC where 17 of 19 (89.4%) patients had infiltrating ductal disease, in contrast to literature which reported either carcinoma with salivary gland like morphology or low grade lesions considered benign as the more common histology pattern. Five had breast cancer recurrence indicating a recurrence rate of 26.3%. Out of the five patients with breast cancer recurrence, one was stage I, three were stage II and one was stage III. All three patients (15.7%) who died from cancer were stage II.

Discussion: TNBC patients with grade 1 tumors in this study were shown to have a different histology from that reported in literature. The study also showed recurrence rate in more than a quarter of the cases. The relapse pattern is not dissimilar to other grades of TNBC and according to this study does not represent a unique subset of TNBC. Ongoing research into the importance of grade in TNBC is needed, with increased understanding of the impact of grade in the management of TNBC.

Poster #60

Title: Dermatomyositis as a Possible Paraneoplastic Syndrome of Metastatic Urothelial Carcinoma

Authors and Affiliations
Amn Marwaha[1], Raman Sambhi[1,2,3], Ricardo Fernandes[1,2,3]
[1]Schulich School of Medicine and Dentistry, Western University, London, Ontario
[2]Division of Medical Oncology, Department of Oncology, Schulich School of Medicine & Dentistry, Western University, London, Ontario, Canada
[3] Verspeeten Family Cancer Centre, Victoria Hospital, London Health Sciences Centre, London, Ontario, Canada

Introduction: Dermatomyositis (DM) is an idiopathic inflammatory myopathy characterized by proximal muscle weakness and cutaneous manifestations, such as Gottren's papules and a heliotrope rash. Paraneoplastic dermatomyositis is a notable subset of dermatomyositis cases as those with DM have a nearly 5-fold risk of developing malignancy. Dermatomyositis associated with urothelial carcinoma is incredibly rare with few cases reported in the literature.

Case: Herein we present a case of a 65-year-old male diagnosed with urothelial carcinoma of the bladder who presented with dermatomyositis at the time of development of metastatic disease, raising the question of possible paraneoplastic syndrome. He presented to the Genitourinary Multidisciplinary Clinic after routine surveillance revealed a 1.7 cm lytic lesion in the right public ramus. The biopsy-confirmed high-grade urothelial carcinoma was subsequently treated with chemoradiation therapy and zoledronic acid. He developed a suspected allergic hypersensitivity reaction after treatment with zoledronic acid therapy. Further bisphosphonate therapy was discontinued and treatment with prednisone and diphenhydramine provided improvement of the symptoms. Repeat cystoscopy, chest, abdomen, and pelvis CT scans demonstrated no tumor recurrence or progression at this time. Several months later, he developed new onset dysphagia, skin rash, significant weight loss and worsening myofascial pain. Bloodwork revealed an elevated CRP (5.4 mg/L), CK (548 U/L), LDH (392 U/L). He was seen by rheumatology, who felt that the clinical picture was consistent with dermatomyositis. Therefore, the patient was treated with prednisone and mycophenolate with improvement of cutaneous and myopathic symptoms. Surveillance pan CT scans revealed disease progression and platinum-based chemotherapy was initiated, followed by maintenance immunotherapy with avelumab. Unfortunately, immunotherapy was discontinued due to dermatomyositis flare. A third-line systemic therapy with enfortumab vedotin was given until further disease progression. The patient proceeded with palliative care and died shortly afterwards.

Discussion: This report highlights a rare case of possible paraneoplastic dermatomyositis in a patient with diagnosis of urothelial carcinoma. Further, dermatomyositis symptoms may signal disease progression in patients with a history of malignancy. Drug-induced dermatomyositis may also be a part of the differential diagnosis for a patient presenting with these symptoms. Ultimately, multidisciplinary management of paraneoplastic dermatomyositis and collective decision-making consistent with the patient's goals of care are critical in the timely diagnosis and management of underlying malignancy.

Poster #61

Creation of an Artificial Intelligence Based Tool for Clinical Trial Matching in HER2-Positive Breast Cancer: A Canadian Study Comparing Manual and Automated Approaches

Laurice Togonon Arayan[1,2], Swati Kalia[1,5], Utkarsh Akhouri[1], Depen Sharma[1,4], Christina Trieu[1,4], Eva Lorena Moreira Vieira[1,5], Tony Kin Wai Hung[1,3], Renee Nassar[1,4], Ria Patel[1], Salah Alhajsaleh[1,4], Anaa Jaet [1,4], Nasong Anthony Luginaah[1,4], Milica Paunic[1], Pratham Gupta[1], Olla Hilal[1], Mahmoud Hossami [1,4], Roaa Hirmiz[1], Megan E Delisle[1,7], Michael Touma[1], Govana Sadik[1,4], Caroline M. Hamm[1,2]

[1]Clinical Trials Navigator, Windsor, ON, [2]Windsor Regional Hospital, Windsor, ON, [3]Hartford HealthCare, Hartford, CT; [4]University of Windsor, Windsor, ON; [5]Western University, London, ON; [6]University of Toronto, Faculty of Medicine, Toronto, ON; [7]University of Manitoba, Winnipeg, MB

Introduction: As cancer treatment become more tailored to individual patients, oncological clinical trials have become increasingly complex. The time required for eligibility determination by AI-based clinical trial matching system was 2 hours versus manual reviewers at 150 hours. In 2019, the Clinical Navigation Program (CTN) was designed in collaboration with people with lived experience (PWLE) to resolve the gap in navigating the search for cancer clinical trials. As of 2023, the CTN program doubled the rates of referral to trials at the Windsor Regional Hospital. To optimize this program, ongoing efforts are focused on expediting the processes within CTN including consideration of use of AI. The proposed study will compare AI programs versus the ongoing CTN program in terms of clinical trial matching.

Methods: Seventeen HER2-positive breast cancer patients, encompassing a range of disease stages and prior lines of treatment, were included in this study. To develop an AI-based clinical trial matching tool, Natural Language Processing (NLP) technique was employed without reliance on structured data. Specifically, the pre-trained *all-MiniLM-L6-v2* model from the SentenceTransformer Python library was utilized. Matching thresholds were predefined, with an inclusion score of ≥0.7 and exclusion score of ≤0.2 based on semantic similarity. An iterative process of comparison and model refinement will be conducted to align the AI tool's matching performance with that of the Clinical Trial Navigator (CTN) team. The control arm consisted of the CTN group's standard practice, wherein trained navigators manually matched patient data to ongoing clinical trials using the continually updated CTN masterlist of actively recruiting HER2 positive breast cancer clinical trials in Canada.

Results: At present, the machine learning model is able to match 1 patient to multiple trials at a rate of 11 seconds in comparison to manual CTN navigators at an average of 3 -4 days. AI is currently able to match clinical trials at a rate of inclusion similarity 0.6 and exclusion similarity 0.3. AI is currently unable to match the CTN manual navigators in terms of clinical trial matching, and is ongoing iterative comparison and training.

Discussion: Ongoing optimization is necessary to evaluate whether the tool effectively matches patients to clinical trials. If successful, the results can be used to eventually integrate AI to CTN processes.

Poster #62

Antibody Drug Conjugates versus Docetaxel for Previously Treated Advanced Non-small Cell Lung Cancer-A Systematic Review and Meta-analysis of Randomized Controlled Trials.

Saqib Khan[1, 2], Laís Marques Eiras[1], Gabriel Boldt[1, 2], Jacques Raphael[1, 2], Daniel Breadner[1, 2]
[1]Schulich School of Medicine & Dentistry, Western University, London, ON, Canada
[2]Verspeeten Family Cancer Centre, London Health Sciences Centre, London, ON, Canada

Introduction: Docetaxel, following progression on immunotherapy and platinum-based chemotherapy, remains the standard of care for advanced non-small cell lung cancer (NSCLC) but offers limited efficacy. Antibody-drug conjugates (ADCs) may improve outcomes in this population. This meta-analysis evaluates the efficacy and safety of ADCs versus docetaxel in previously treated advanced NSCLC through a systematic review and meta-analysis of randomized controlled trials (RCTs).

Methods: Databases [PubMed (MEDLINE), EMBASE and Cochrane Library], clinical trial registries, and proceedings of global oncology conferences from January 2015-November 2024 were screened for phase II/III RCTs comparing ADC (e.g., sacituzumab govitecan, datopotamab deruxtecan, and tusamitamab ravtansine) versus docetaxel. Two researchers independently completed data retrieval and screening work using Covidence. The primary outcomes include progression-free survival (PFS) and overall survival (OS), while the secondary outcomes include objective response rate (ORR), disease control rate (DCR), and adverse events (AEs). The pooled hazard ratios (HR) and odds ratios (OR) were meta-analyzed using the appropriate generic variance and Mantel-Haenszel methods. Random-effect models were used to compute pooled estimates.

Results: Of the 212 records screened, 3 RCTs involving 1597 patients were included (Figure 1). ADCs did not significantly improve PFS (pooled HR: 0.91, 95% CI: 0.73-1.13). For OS, the pooled HR was 0.88 (95% CI: 0.78-1.00, p = 0.06), reflecting a borderline significant trend favouring ADCs, with negligible heterogeneity (I^2 = 0%). Furthermore, subgroup analysis demonstrated a significant OS benefit in the non-squamous cohort (HR: 0.85, 95% CI: 0.74-0.98, p = 0.03). Additionally, no difference was observed in terms of ORR (OR: 1.16, 95% CI 0.54-2.51) and DCR (OR: 1.39, 95% CI: 0.75-2.57). Grade ≥ 3 treatment-related AEs were significantly lower (pooled OR: 0.49, 95% CI: 0.26–0.90, p = 0.02) with ADCs despite high heterogeneity (I^2 =87%).

Conclusion: Our findings report a significant survival benefit in patients with non-squamous NSCLC treated with ADCs compared to docetaxel with a manageable safety profile. However, further research is needed to address heterogeneity, refine patient selection and more mature survival data with predictive biomarkers.

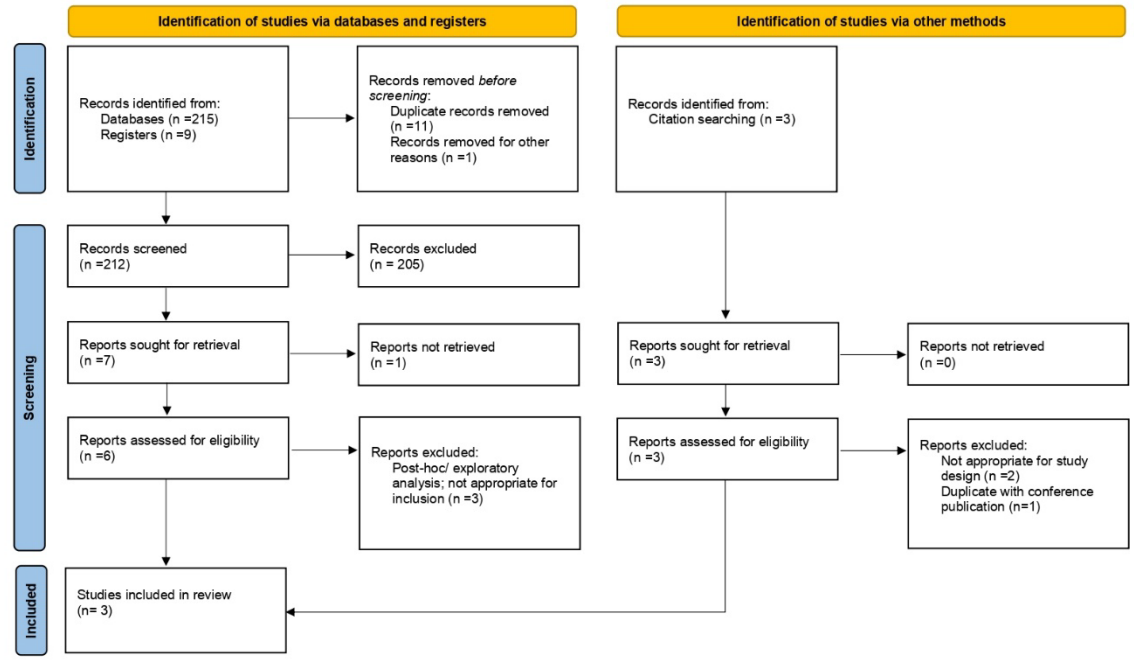

Figure 1: PRISMA 2020 flow diagram.

Poster #63

Orthopedic Interventions and Outcomes in patients with Metastatic Renal Cell Carcinoma - A Systematic Review

Abdulrahman Al Bochi[1], Mohamad Tarek Madani[1], Muhammad El-Kassem[1], Mohammed Fadel[1], Adnan Rajeh[2,3], Gabriel Boldt[4], Ricardo Fernandes[2,3]

[1] Schulich School of Medicine and Dentistry, Western University, London, Ontario
[2] Verspeeten Family Cancer Centre, Victoria Hospital, London Health Sciences Centre, London, Ontario, Canada
[3] Division of Medical Oncology, Department of Oncology, Schulich School of Medicine & Dentistry, Western University, London, Ontario, Canada
[4] Division of Experimental Oncology, Department of Oncology, Schulich School of Medicine & Dentistry, Western University, London, Ontario, Canada

Introduction*:*
The treatment landscape of renal cell carcinoma (RCC)has improved the clinical outcomes and survival leading to increase length of care required for patients with metastatic disease, particularly for bone metastatic disease. The aim of this study is to systematically review and analyze the literature to determine the efficacy and outcomes of orthopedic interventions in comparison with other palliative treatment interventions among patients with symptomatic bone metastasis from RCC.

Methods:
Embase, MEDLINE, and Cochrane were searched from January 1, 2014, until January 30, 2024, for relevant studies assessing the treatment intervention for bone metastatic disease in patient with RCC. Outcome measures of interest included: overall survival, reoperation rates, complication rates, and quality of life.

Results:
Out of 2208 studies screened for inclusion, 15 studies were included in this review. Six studies focused on bone metastasis to the appendicular skeleton, five studies to the axial skeleton, and four studies to both skeleton types. Orthopedic surgical interventions, as well as combination therapies that involve surgical and targeted therapy, resulted in the highest overall survival. Among surgical interventions, complete metastasectomy provided the greatest survival benefit compared to intralesional curettage and stabilization-only procedures.

Conclusion:
Orthopedic surgical interventions, such as complete metastasectomy, have the potential to increase overall survival and improve quality of life for RCC patients with metastatic bone disease compared to non-surgical approaches. Combining surgery with targeted therapy may also pose survival benefits. Nevertheless, the predominance of retrospective data in the literature underscores the need for randomized controlled trials to establish definite treatment guidelines and optimize patient selection for orthopedic interventions.

Poster #64

Standard Chemo-Immunotherapy versus Real-World Protocols: Evaluating Outcomes in Triple-Negative Breast Cancer Neoadjuvant chemo/ immunotherapy

Laurice Arayan[1], Rong Luo, PhD[2], Sneha Mukherjee[3, 4], Swati Kulkarni [1, 4]

[1]Windsor Regional Cancer Program, Windsor, ON, [2]Department of Mathematics, University of Windsor, Windsor, ON, [3]Schulich School of Medicine and Dentistry, [4] Western University, London, ON

Introduction: Different subtypes of breast cancer lead to variations in the treatment approaches to improve the outcomes. About 20% patients present with triple negative breast cancer. Introduction of Pembrolizumab[a] in the neoadjuvant setting and capecitabine[b] in the adjuvant setting highlights the growing importance of research to improve outcome for triple negative breast cancer patients. Cancer Care Ontario has approved the various combinations of chemotherapy regimens with immunotherapy Pembrolizumab. The aim of this study was to compare the tolerance, rates of PCR and outcomes of patients in terms of overall and disease free survival, with various immunotherapy-chemotherapy combinations.

Methods: This study reviewed patients aged 18 years old and above, male and female, who were histologically diagnosed with Triple Negative Breast Cancer and received neoadjuvant and/or adjuvant systemic therapy from January 1, 2021 to December 31, 2024 in the Windsor Regional Cancer Program. Descriptive statistics was used to summarize the demographic and clinical characteristics, PCR rates of the patients. Kaplan-Meier survival analysis will be used to compare disease free and overall survival of the overall population as well as effect of various chemo-immunotherapy combinations in comparison to the chemotherapy used with immunotherapy in the landmark trial KEYNOTE 522. Toxicity data will also be analyzed.

Results: The preliminary report included 89 out of total 160 patients. The cohort of TNBC patients was exclusively female, predominantly postmenopausal, and most commonly presented with cT2 and cN0 tumors. Nearly half had undergone genetic testing and about 45% reported a family history of breast cancer. High-grade tumors (Grade 3) were predominant, consistent with TNBC biology. The majority underwent breast-conserving surgery and received radiation and systemic therapy, with complete pathological response (PCR) achieved in nearly one-third of patients, post-neoadjuvant treatment. Three patients received non-Keynote 522 immunochemotherapy regimen, two were treated with neoadjuvant pembrolizumab, dose dense anthracycline, cyclophosphamide with paclitaxel and, one received pembrolizumab with docetaxel and cyclophosphamide. Despite aggressive treatment, side effects and cancer-related mortality were not very common, with five cancer related deaths and one patient with relapse.

Conclusions: Continued follow up is important for assessing overall and disease-free survival. Additional numbers are needed to draw a more definitive conclusion, especially in cases where an immunotherapy-chemotherapy regimen outside of the Keynote 522 protocol was used. Numbers are small due to single institution database.

Poster #65

Impact of Clinical Trial Navigators on Clinical Trial Accrual through Multidisciplinary Case Conferences: A Pre- & Post-Implementation Study

Christina Trieu[1], Salah Alhajsaleh[1], Anaam Jaet[1], Renee Nassar[2], Mahmoud Hossami[2], Laurice Togonon Arayan[3], Swati Kalia[2], Depen Sharma[4], Roaa Hirmiz[2], Milica Paunic[5], Olla Hilal[6], Anthony Luginaah, Michael Touma[2], Govana Sadik[1], Ria Patel[2], Partham Gupta[6], Megan Delisle[7], Gregory Charalambos Anagnostopoulos[6], Lee McGrath[2], Caroline Hamm[3]
[1]University of Windsor, [2]Clinical Trials Navigator, [3]Windsor Regional Hospital, [4]University of Ottawa, [5]University of Toronto, [6]Western University, [7]University of Manitoba

Introduction: Clinical trial participation improves cancer outcomes but remains limited due to systemic barriers, including lack of awareness, time constraints, and inadequate referral processes. Clinical Trial Navigators (CTNs) offer tailored trial recommendations based on a patient's treatment history and eligibility, have demonstrated potential to increase accrual rates. Embedding CTNs directly into Multidisciplinary Case Conferences (MCCs) may further streamline referrals by engaging with care teams at critical decision points. This study aims to evaluate the impact of CTN integration into MCCs on trial referral and enrollment rates, as well as implementation effectiveness and workflow optimization.

Methods: This hybrid effectiveness-implementation study conducted at the Windsor Cancer Centre, focusing on breast, glioblastoma, and gastrointestinal cancer MCCs. The study includes an initial observational phase to establish baseline referral and enrollment rates through chart reviews. Following this, CTNs will participate in MCCs using updated clinical trial master lists and the "Look Up Trials" app to provide real-time matching support. We hypothesize that CTN integration will increase referral and accrual rates while improving the efficiency of clinical trial discussions. Quantitative data will be analyzed descriptively. In parallel, surveys and structured interviews using the Consolidated Framework for Implementation Research (CFIR) constructs and "Think Aloud" process with MCC participants will capture qualitative feedback on barriers, facilitators, and perceptions of workflow changes. Thematic analysis will be used to analyze qualitative responses.

Results: At the time of submission, the project is in the early observational phase, with research ethics board approval recently obtained. Anticipated outcomes, based on similar prior studies, include a 25% referral rate and 8% accrual rate among approximately 168 patients and 60 physicians. Secondary outcomes will explore iterative process improvements, physician satisfaction, and the utility of digital tools in supporting trial matching.

Discussion: This study is among the first to explore the real-time integration of CTNs into MCCs as a strategy to enhance clinical trial access and coordination. We anticipate that this model will improve referral and enrollment processes while alleviating physician burden and streamlining workflows. Insights from this implementation will inform future scalability across other disease sites and cancer centers. As the study progresses, iterative feedback from participants will guide refinements to optimize both navigator involvement and clinical trial integration into standard cancer care.

Poster #66

A Quality Improvement Initiative to Mitigate Immunotherapy-Related Toxicities among Patients Receiving Immunotherapy using a Novel Grade 2 Toxicity tool

Laurice Arayan[1], Emmanuel Joran Boujeke[2], Tarek A. Elfiki[1], Tiffany Gowanlock[4], Tina Alice Joseph[2], Caroline M. Hamm[1,3], Mina Djuketic[3]
[1]Windsor Regional Cancer Centre, Windsor, ON, [2]Schulich School of Medicine and Dentistry, Western University, Windsor, ON, [3]University of Windsor, Windsor, ON, [4]Windsor Regional Hospital, Windsor, ON

Introduction: Immune checkpoint inhibitors have significantly improved outcomes in triple-negative breast cancer, but immune-related toxicities (IRT) remain a major concern. Guidelines on the management of IRTs have been developed and are in use from the American Society of Clinical Oncology (ASCO) and Cancer Care Ontario- Ontario Health (CCO-OH). However, because of the need to be detailed and extensive, this format makes it more difficult for both front-line health care workers and patients to use. This study aimed to develop and evaluate a novel grade 2 immunotherapy toxicity screening tool designed to identify and prevent progression of IRTs before they result in hospitalization and irreversible organ damage.

Methods: The tool was created using patient and healthcare provider handouts adapted from the CCO Immune Checkpoint Inhibitor Toxicity Management Clinical Practice Guideline (March 2018). A Plan-Do-Study-Act (PDSA) cycle was employed to test, refine, and implement the tool, with iterative changes based on feedback from healthcare providers and patients. Healthcare providers were engaged through team presentations in staff meetings, and the Patient and Family Advisory Committee was also consulted for feedback. Handouts were distributed to patients and healthcare providers, and displayed in chemotherapy suites and clinics. The intervention's effectiveness was assessed through surveys distributed to both groups six months after implementation to gather perceptions and identify barriers to use including ease of use and continued patronage to the tool.

Results: There were 71 survey participants in total, 43 healthcare providers and 28 patients. Results revealed that both patients and healthcare providers found the tool easy to follow and would recommend its continued use. Healthcare providers suggested to add other symptoms to the list including arthritis, which was also corroborated by the patients as missing in the tool. However, some patients and healthcare providers reported that they did not receive the tool during its rollout. Despite this, the tool was considered helpful by both groups in managing IRTs.

Discussion: Ongoing assessment is necessary to evaluate whether the tool effectively reduces the progression of IRTs leading to hospitalization and organ damage, and further refinements may be needed based on continuous feedback from stakeholders.

Poster # 67

Crowdfunding for central nervous system tumors: A cross-national analysis of GoFundMe campaigns in Canada, the United Kingdom, and the United States

Abdulla Elsaleh[1], Ryan Zhao[2,3], Yajur Iyengar[4], Yunyi Zhang, Seth Climans[3,5]

[1]Temerty Faculty of Medicine, University of Toronto
[2]Department of Clinical Neurological Sciences, Schulich School of Medicine and Dentistry, Western University
[3]London Health Sciences Centre
[4]Faculty of Medicine, University of Ottawa
[5]Department of Oncology, Schulich School of Medicine and Dentistry, Western University

Introduction: Tumors of the central nervous system (CNS) impose significant financial, emotional, and logistical burdens on patients and families. While public healthcare systems in Canada and the UK aim to minimize out-of-pocket costs, patients from those countries still turn to crowdfunding platforms like GoFundMe. This study aimed to compare crowdfunding campaigns for brain cancer across Canada (CA), the United Kingdom (UK), and the United States (US) to explore differences in campaign characteristics, funding success, and predictors of financial outcomes.

Methods: We initially extracted 9,026 GoFundMe posts for patients with CNS tumors, of which 8,134 originated from the United States, United Kingdom, or Canada; from this subset, 200 campaigns were randomly selected for detailed content analysis. Descriptive statistics were generated by country. Two multivariable linear regression models were constructed: one for the full sample and one for the 200-case subset. Predictors included country, amount requested, campaign length, patient demographics, treatment type, and tumor subtype. Amount received (in CAD) was the primary outcome.

Results: Campaigns from the US requested the highest average funding (CAD 60,366 ± 1,546,112) but also showed the greatest variability. In contrast, Canadian campaigns received more on average (CAD 27,175 ± 35,119) than UK (CAD 16,763 ± 17,850) or US (CAD 19,187 ± 27,249) campaigns. Supportive care was the most frequently cited reason for crowdfunding in Canadian and UK campaigns, while standard of care requests remained very common across all countries. Requests for alternative or experimental treatments were more frequent in UK (33.3%) and US (28.5%) campaigns compared to Canada (20.0%). The most common tumor type in Canada and the US was adult-type glioma, while UK campaigns most commonly omitted the specific type of brain tumor.
In the full-sample regression model, the only significant predictor of funds raised was the amount requested ($\beta = 0.883$, $p = 0.049$). In the detailed model, tumor types categorized as “Other” were associated with significantly lower funds raised ($\beta = –11,692$, $p = 0.033$). No other demographic or campaign characteristic, inAbcluding country, age, or reason for request, was significantly associated with amount received.

Conclusions: Despite different healthcare systems, patients in all three countries turn to crowdfunding to cover a mix of standard, supportive, and experimental care costs. US campaigns demonstrate higher variability in funding goals, while Canadian campaigns received the most funding on average. However, factors like gender, tumor subtype (except "Other"), or care type were not strong predictors of campaign success. These findings highlight the potential inequities and uncertainties of relying on crowdfunding for critical health needs and suggest that unmeasured factors, such as social reach or storytelling, may play a larger role in determining financial outcomes.

Raltitrexed as a substitute for 5-fluorouracil in combination with pembrolizumab and platinum in a patient with metastatic esophageal squamous cell carcinoma and coronary artery disease: a case report

Matthew Van Oirschot, BASc[1], Saurav Verma, MD[1,2], Daniel Breadner, MD[1,2], Andrea Vucetic, MD[1,3]

[1]Schulich School of Medicine & Dentistry, Western University

[2]Division of Medical Oncology, Verspeeten Family Cancer Centre, London Health Sciences Centre; Schulich School of Medicine & Dentistry, Western University

[3]Department of Radiation Oncology, Verspeeten Family Cancer Centre, London Health Sciences Centre; Schulich School of Medicine & Dentistry, Western University

Abstract

Introduction: Chemoimmunotherapy is the standard treatment for patients with metastatic esophageal squamous cell carcinoma (SCC), for which 5-fluorouracil (5-FU) is commonly part of the chemotherapy regimen. Given that 5-FU has a mean cardiotoxicity risk of approximately 5%, raltitrexed has often been used as an alternative in patients with a history of fluoropyrimidine-associated cardiotoxicity or significant coronary artery disease (CAD). We report the first case, to our knowledge, of the use of raltitrexed in place of 5-FU in combination with pembrolizumab and platinum-based chemotherapy for the treatment of metastatic esophageal cancer in a patient with CAD.

Case: A 75-year-old gentleman with preexisting multivessel CAD was diagnosed with metastatic gastroesophageal junction (GEJ) SCC after presenting to medical attention with a two-month history of worsening chest pain in addition to progressive dysphagia associated with weight loss. Following initial treatment with palliative locoregional radiotherapy to the lower mediastinum, GEJ, and upper abdomen, the decision was made to proceed with palliative systemic therapy. Considering his significant cardiac history, 5-FU was replaced with raltitrexed and combined with carboplatin and pembrolizumab. After a total of 10 months of treatment, the patient presented to hospital with recurrent chest pain and was diagnosed with a non-ST-elevation myocardial infarction. Despite radiographic evidence of stability of his malignancy on systemic therapy, he was not considered to be a candidate for cardiac intervention. He was thus transitioned to a comfort-focused care approach and passed away shortly thereafter, with the cause of death being acute coronary syndrome.

Discussion: Although the patient unfortunately passed away prematurely due to preexisting CAD, there was no evidence of disease progression in the 10 months that he received treatment. In addition to an encouraging progression-free survival, the patient reported an overall improvement in quality of life while on therapy with no signals of toxicity from raltitrexed or immunotherapy. Overall, the present case demonstrates that chemotherapy in combination with immunotherapy for the treatment of advanced esophageal cancer appears to be safe and effective when raltitrexed is substituted for 5-FU, which is of particular relevance due to the many overlapping characteristics of patients with cardiac pathology and esophageal cancer.

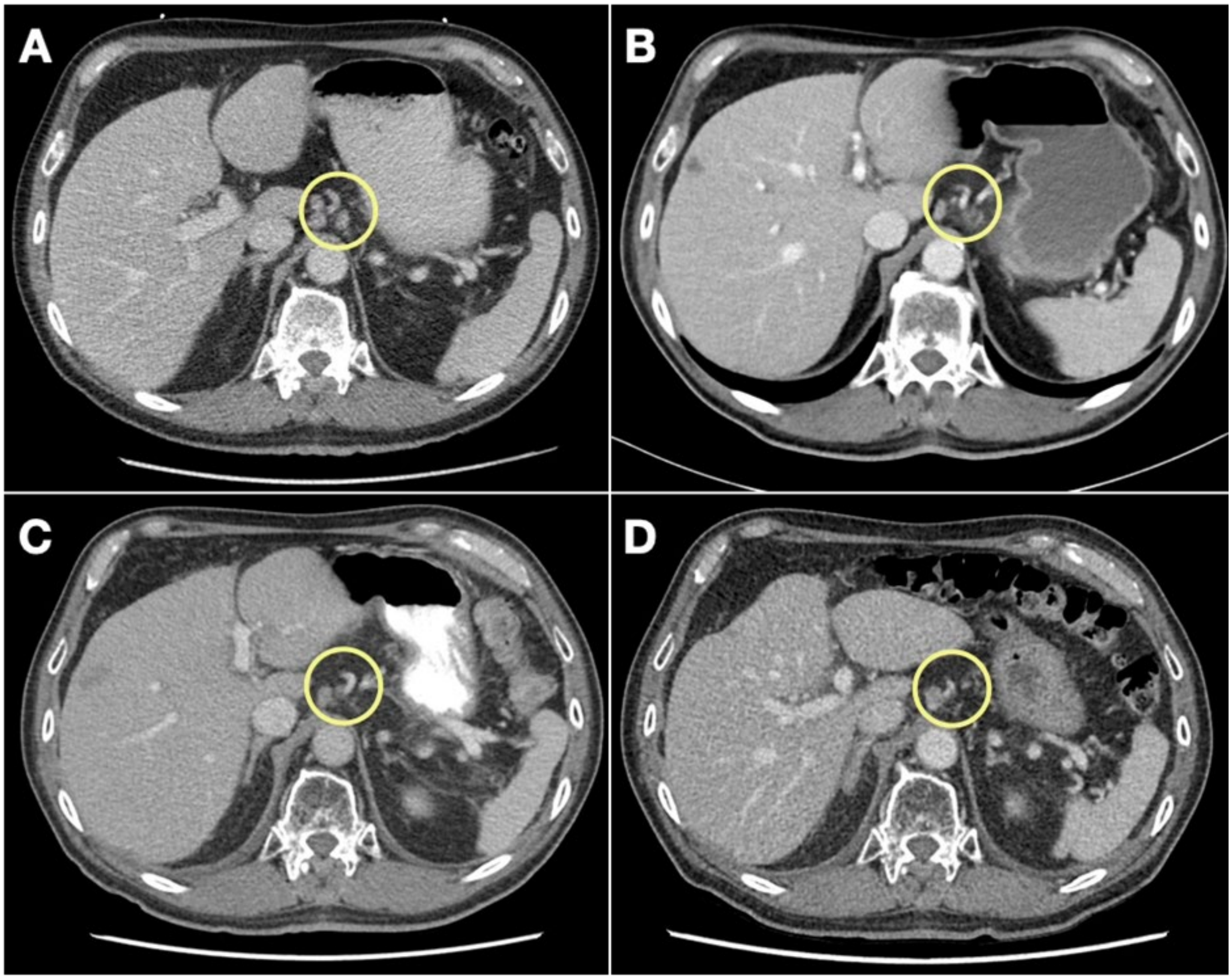

Figure 1. Serial axial computed tomography (CT) images of gastrohepatic lymphadenopathy. (A) Baseline diagnostic imaging in September 2022 demonstrated multiple gastrohepatic lymph nodes. (B) Significant interval reduction in the size of numerous gastrohepatic lymph nodes with almost complete disappearance of the left gastrohepatic node conglomerate in February 2023 after 1 month of chemoimmunotherapy. (C) Mixed response with a small interval increase in the size of a right gastrohepatic lymph node seen in May 2023. (D) Near complete response in the gastrohepatic lymphadenopathy in September 2023 after 8 months of chemoimmunotherapy with the exception of a single slowly growing right gastrohepatic lymph node since February 2023.

Poster #69

The CHemotherapy **A**nd **S**tool Transplantation in **P**ancreatic **D**uctal **A**deno**C**arcinoma (**CHASe-PDAC**) safety trial combining fecal microbiota transplantation using LND101 in combination with gemcitabine and nab-paclitaxel chemotherapy in patients with advanced PDAC

Danial K. Hadi[1], Elena V. Tsvetkova[1,2], Daniel A. Breadner[1,2], Stephen A. Welch[1,2], Seema N. Parvathy[3,4,6], Michael Silverman[3,4,5,6], Saman Maleki-Vareki[1,2,7,8,9], John G. Lenehan[1,2]

[1] Department of Oncology, Western University, London, Ontario, Canada
[2] London Health Sciences Research Institute (LHSCRI), London, Ontario, Canada
[3] Department of Medicine, Division of Infectious Diseases, Western University, London, Ontario, Canada
[4] Division of Infectious Diseases, St. Joseph's Health Care, London, Ontario, Canada
[5] Department of Microbiology & Immunology, Western University, London, Ontario, Canada
[6] Lawson Health Research Institute, London, Ontario, Canada
[7] Department of Pathology and Laboratory Medicine, Western University, London, Ontario, Canada
[8] Department of Medical Biophysics, Western University, London, Ontario, Canada
[9] Ontario Institute of Cancer Research, Toronto, Ontario, Canada

Background: Pancreatic ductal adenocarcinoma (PDAC) is the 3rd leading cause of cancer-related deaths in Canada as of 2024. It has been established that tumors such as PDAC, similar to the gut, have their distinct microbiomes. Bacterial species producing the enzyme cytidine deaminase (CDD), which inactivates gemcitabine commonly used to treat PDAC, represent the dominant class within PDAC tumors. Pre-clinical studies in murine models of PDAC showed that oral FMT from healthy human donors (human-to-mouse FMT) successfully altered the mouse gut and tumor microbial compositions identifying previously unknown crosstalk between the gut and tumor microbiomes. The alteration in the tumor microbial population also led to improved infiltration of CD8+ T cells and a reduction in tumour size. Our hypothesis is that oral FMT will reduce the intratumoral CDD-producing species and increase gemcitabine cytotoxicity and increase CD8+ T cell infiltration of tumors, resulting in improved survival.

Objectives: CHASe-PDAC is a single institution, open-labelled clinical trial to evaluate the safety of combining FMT with standard of care gemcitabine and nab-paclitaxel (GnP) in patients with advanced PDAC. Secondary objectives include measuring progression free survival (PFS), overall survival (OS), the objective response rate (ORR), as well as identifying alterations in the gut microbiota, and measuring changes in the circulating immune cell populations.

Methods: 20 patients ≥18 years with advanced PDAC most appropriate for first-line palliative GnP will be enrolled and treated at the Verspeeten Family Cancer Centre or satellite centres. Patients will receive a single treatment of oral capsule FMT using LND101, containing healthy donor stool as per our local protocol. The first dose of GnP will be administered at least 7 days after FMT to allow microbial engraftment and continue as per standard of care. Patients will provide stool and blood samples at 5 key timepoints (S1-S5) throughout treatment as shown in Figure 1. The primary outcome of safety will be assessed using NCI-CTCAE v5 criteria to ensure toxicity does not exceed that known to occur with GnP. The secondary outcomes of PFS, OS, and ORR will be determined using RECIST 1.1 criteria. Alterations in the gut microbiome composition will be determined using metagenomics and changes in circulating immune cell populations determined by flow cytometry. We will also analyze plasma metabolomic changes before and after FMT.

Results (partial): To date, 2 patients have been enrolled and both completed FMT and received at least 1 cycle of GnP. There have been no toxicities reported from LND101. Side effects associated with therapy post-GnP include only grade 1-2 toxicities such as fever, fatigue, nausea, anemia,

thrombocytopenia, and alterations in hepatic markers (ALT, AST, and alkaline phosphatase). These toxicities are consistent with GnP chemotherapy and there has been no increase in severity. Patient one has received 3 cycles of GnP and the first CT scan to assess response at 3 months has shown an overall reduction in tumour burden.

Conclusions: Combining LND101 with GnP chemotherapy in patients with advanced PDAC has so far been safe and the first enrolled patient has responded to therapy at the time of initial radiographic assessment suggesting no detriment on treatment response.

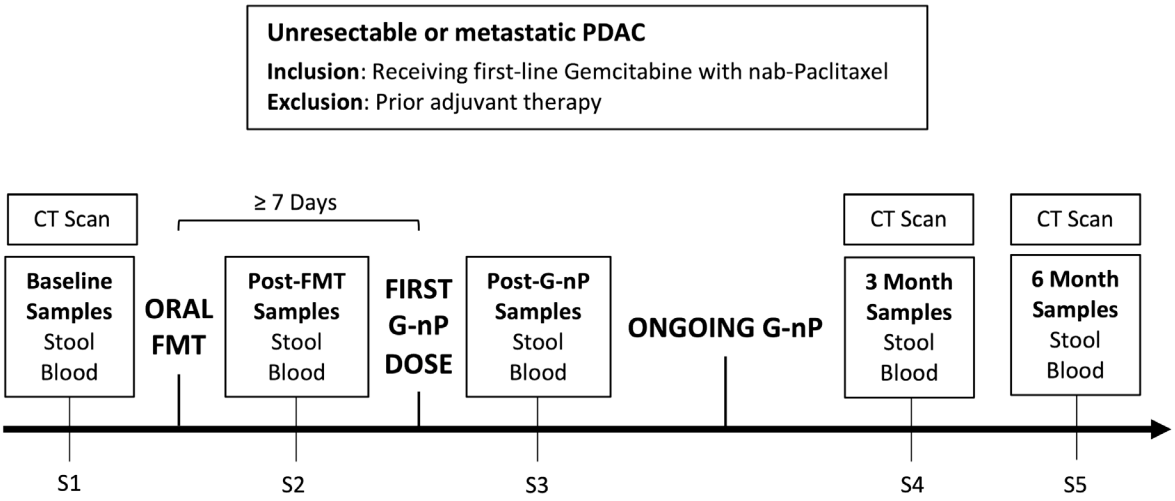

FMT: Fecal Microbiota Transplant; **G-nP:** Gemcitabine with nab-Paclitaxel

Figure 1: Schema of the CHASe-PDAC phase 1 trial assessing the safety of combining oral fecal microbiota transplantation (FMT) using LND101 from healthy donor stool in patients with advanced pancreatic ductal adenocarcinoma receiving first-line palliative gemcitabine and nab-paclitaxel (GnP).

Poster #70

Pediatric-Type Gliomas in Older Adults (>40 years)

Inci Yaman Bajin[1], Morgan Black[1], Kathie Baer[1], Jacob Houpt[2], Qi Zhang[2], Seth Climans[1], Cynthia Hawkins[3], Julie Bennett[4,5], Maria MacDonald[1].
1 Division of Medical Oncology, Western University, Verspeeten Family Cancer Centre, London
2 Department of Pathology, Western University, London
3 Department of Pathology, Hospital for Sick Children, Toronto
4 Division of Hematology/Oncology, Hospital for Sick Children, Toronto
5 Division of Medical Oncology and Hematology, Princess Margaret Cancer Centre, Toronto

Introduction

Pediatric-type gliomas are increasingly recognized in adult populations. Approximately one-third of gliomas in adolescent and young adult patients aged 14–39 years harbour pediatric-type molecular alterations. The frequency of pediatric-type glioma in adults >40 years is unknown. Given the current guidelines, there is a high risk of misdiagnosis of a pediatric-type glioma as molecular glioblastoma (GBM) IDH-wildtype. We hypothesize that a lesser, but still clinically significant, frequency of pediatric-type alterations will be found in adults 40 years and older. These tumours, including pilocytic astrocytoma, diffuse midline glioma (H3 K27-altered), and other gliomas, exhibit distinct molecular and clinical characteristics in adults. Despite their rarity, understanding their behaviour in adults is critical for accurate diagnosis and tailored therapeutic strategies. This study aims to first evaluate the frequency of pediatric-type gliomas in adults >40 years, and the second phase of the study aims to analyze the clinical data, histopathological features, and molecular markers (e.g., BRAF alterations, H3 K27 mutations, FGFR alterations). Here we report the results of the first phase of the study.

Methods

A retrospective analysis was conducted on adult patients (>40 years) to measure the prevalence of pediatric-type gliomas at London Health Sciences Centre between 2012 and 2022. The Southwest Regional Cancer Program (SWRCP) database was investigated with four pathologies: (1) all gliomas, 2) GBM or grade 4 Astrocytoma, 3) IDH mutant glioma, 4) IDH wildtype, non-GBM or Pediatric-type glioma.

Results

Among 1049 adult glioma patients, 167 (16%) were excluded for being <40 years old.
From the remaining 882 patients, 747 GBM patients (84%) were excluded, leaving 145 cases with potential pediatric-type gliomas. From these 145 cases, 9 cases (1%) were already diagnosed with a pediatric-type glioma. Further exclusions removed molecular GBMs, IDH-mutant gliomas and cases with aggressive features (microvascular proliferation/necrosis), leaving 56 cases (6%) with possible pediatric-type glioma. These tumours were histologically grade 2 and 3 IDH-WT gliomas. Tissue samples of these 56 patients are planned to be sent to the Hospital for Sick Children for further molecular analysis.

Conclusion

Pediatric-type gliomas in adults represent a distinct subgroup with unique molecular and clinical features. The correct diagnosis of a pediatric-type glioma in an adult will improve patient care. We identified 56 potential pediatric-type gliomas that were labelled as IDH wildtype GBM using current and past guidelines. Correct diagnosis would allow accurate prognosis and avoid exposure to toxic and unnecessary treatments such as radiation and alkylating chemotherapy. The next phase of this study will involve molecular analysis of the tumour samples of these patients. This study may challenge our standard of care and inform age-stratified, cost-effective, publicly funded molecular testing for pediatric molecular alterations in adults over the age of 40.

Poster #71

The London HPV Immunization Project

Leah Kanee MSc[1], Sukhman Brar MD[2], Caroline McKenna, Allana Simon, Aileen Liang MD[3], Kimya Manoucheri, Taryn Taylor MD PhD FRCSC[4], Ji-Hyun Jang MD MPH FRCSC[5]

[1]Schulich School of Medicine and Dentistry, Western University, London, Canada, [2]Diagnostic and Molecular Pathology, Schulich School of Medicine and Dentistry, Western University, London, Canada [3]Internal Medicine, Schulich School of Medicine and Dentistry, Western University, London, Canada, [4]Obstetrics and Gynecology, Schulich School of Medicine & Dentistry, Western University, London, Canada, [5]Gynecologic Oncology, Schulich School of Medicine & Dentistry, Western University, London, Canada

Introduction: The human papillomavirus (HPV) is one of the most common sexually transmitted infections. While the body can typically clear the infection itself, in a small subset of individuals, persistent high-risk HPV infection has the potential to cause cervical, oropharyngeal, anal, penile, vaginal, or vulvar cancer[1,2]. Of particular interest, more than 99% of cervical cancer cases are caused by persistent high-risk HPV infection[3]. Two HPV vaccinations are currently offered in Canada, GARDASIL® 9 and CERVARIX®, and are protective against high-risk HPV strains known to cause a majority of anal and genital cancers[4]. Although widely available, vaccination rates vary throughout the country, ranging from 57-91%[5]. Barriers to HPV access and uptake have been documented, however, existing literature largely limited to the context of school-aged children. Therefore, the goal of this study is to understand the perceived barriers and facilitators to HPV vaccination in an adult population, particularly among those attending colposcopy clinic in London, ON.

Methods: A convenience sample of study participants were recruited from the St. Joseph's Colposcopy clinic in London, Ontario between June 2021-January 2025. Participants (n=142). Participants were asked to complete a paper survey, which was informed by questions from the validated HPV attitudes and Beliefs Scale (HABS). The survey asked questions about demographic information, cervical cancer screening history, perceptions regarding the HPV vaccine, and perceived barriers and facilitators to HPV vaccination. Survey responses were entered into REDCap, and data analysis was carried out in Excel. Data was stratified by HPV vaccination status, household income, and age.

Results: 142 individuals completed the survey, however 7 entries were excluded due to incomplete data. Of the eligible participants, 83 (62%) participants never received HPV vaccination. Of those vaccinated, 11 (21%) received 1 dose, 14 (27%) received 2 doses, and 26 (50%) received 3 doses. One person did not report vaccination status. When asked if they would be open to receiving the HPV vaccine, the majority of unvaccinated participants at 48 (58%) answered 'definitely yes' or 'probably yes'. Contrastingly, only 10 (12%) indicated they definitely would not receive the vaccine. Among unvaccinated individuals (n=83), the main barriers to HPV vaccination included lack of knowledge (n=34), no recommendation from physician (n=24), concern about side effects (n=19), and lack of financial resources (n=14). The most common facilitators to HPV vaccination included providing information about the vaccine, its purpose, importance, side effects, safety (n=49), explaining HPV vaccine efficacy against cancer (n=30), providing printed materials (n=25), providing information on insurance coverage/cost of vaccine (n=25).

Conclusions: Barriers to HPV vaccination among adult populations persist. However, overcoming these barriers and addressing concerns surrounding vaccination can be achieved through discussions and education on HPV vaccination in health encounters, and information dissemination through various media modalities. Subsidizing vaccine costs should also be considered to address financial barriers to HPV vaccination.

Poster #72

Real-world outcomes of patients with advanced or metastatic HR+/HER2- breast cancer treated with CDK4/6 inhibitors

C. Jia [1, 2], P.S. Blanchette [2, 3, 4], B. Carter [2], K.K. Anderson [1, 5], S.A. Climans [3], D.G.M.M. Mata [3], J. Raphael [3, 6]

[1] Department of Epidemiology and Biostatistics, Western University, London, ON, Canada;
[2] Institute of Clinical Evaluative Sciences Western, London, ON, Canada;
[3] Division of Medical Oncology, London Regional Cancer Program, London Health Sciences Centre, Western University, 800 Commissioners Road East, London, ON, Canada;
[4] Verspeeten Family Cancer Centre, London Health Sciences Centre, London, ON, Canada;
[5] Department of Psychiatry, Western University, London, ON, Canada;
[6] Lawson Health Research Institute, London, ON, Canada;

Introduction: Cyclin-dependent kinase 4/6 inhibitors (CDK4/6i) with endocrine therapy (ET) are standard first-line therapies for hormone receptor-positive (HR+) / human epidermal growth factor receptor 2-negative (HER2-) metastatic breast cancer (mBC). Comparative real-world evidence (RWE) studies are warranted due to a lack of randomized clinical trials directly comparing palbociclib (PAL) and ribociclib (RIBO) effectiveness.

Methods: A retrospective cohort study was conducted in adult (age ≥ 18 yrs) HR+/HER2- mBC who started PAL or RIBO therapy from April 2016 to March 2022 in Ontario, Canada. Study endpoints were (1) factors associated with specific CDK4/6i usage, (2) safety and (3) overall survival (OS), and time on therapy (TOT). Standardized differences (SD) were used to evaluate differences between groups. Multivariable logistic regression models were used to compare factors associated with CDK4/6i usage and Cox proportional hazards models were used to evaluate OS and TOT.

Results: 4,380 and 1,916 PAL- and RIBO-recipients were identified. Increased odds of PAL-receipt were associated with age, time from diagnosis to treatment, and treatment at an academic centre. Increased RIBO-receipt was associated with prior chemotherapy and treatment start after 2020. RIBO-recipients experienced a lower unadjusted incidence of all-cause any-grade anemia, thrombocytopenia, hepatitis and dose reductions; but a higher incidence of treatment discontinuations and switches to an alternate CDK4/6i (SD ≥ 0.10). In our unadjusted 2-year survival analysis, TOT favored PAL vs. RIBO (68% vs 61%; p-value<0.0001 and OS favored RIBO vs. PAL (74% vs. 68%, p-value<0.0001). Multivariable analysis demonstrated an increased overall survival among patients receiving RIBO as compared to PAL (HR=0.78, 95% CI:0.68-0.90, p-value=0.0006).

Conclusions: This study suggests a significant OS difference in favor of RIBO using RWE data from Ontario, Canada. These findings, in addition to safety and prescription factors, may be helpful in the selection of CDK4/6i for patients with HR+/HER2- mBC.

Poster #73

Generative Artificial Intelligence Processing of Pathologist Stream-of-Consciousness Dictation in High-Accuracy Cancer Synoptic Reporting

Kyla Trinh[1], and Matthew Cecchini[1]
[1]Department of Pathology and Laboratory Medicine, London Health Sciences Centre and Western University, London, ON, Canada

Introduction: Standardized synoptic reporting plays a critical role in modern oncology, providing clinicians with the key details and data necessary for patient management. However, the manual generation of these reports entails a time-consuming process for pathologists, often requiring the interruption of microscopic analysis to interact with reporting systems. While dictation software exists, the current available tools often lack flexibility and demand precise phrasing, meaning a limited ability to modify or interpret natural, conversational language. Emerging generative artificial intelligence (AI), particularly large language models (LLMs) that are capable of processing multimodal inputs like natural language audio, presents a promising opportunity to streamline the synoptic reporting process. These AI tools possess the potential to understand and interpret the nuances of conversational dictation and translate unstructured input into formalized reports. This study aimed to evaluate the feasibility of using a LLM, Gemini 2.5 Pro, to automatically generate synoptic cancer reports from pathologist stream-of-consciousness audio dictations, using AI-simulated clinical scenarios as a baseline for comparison.

Methods: Synthetic, clinically relevant, cancer case scenarios (*n* = 4) were developed using ChatGPT 4o, a LLM, ensuring variation in stage and case types. A corresponding structured synoptic report was created in association with each case, serving as the ground truth, the established benchmark used as a representation of the correct interpretation of the case. A pathologist recorded natural stream-of-consciousness audio dictations detailing the findings for each simulated case. Gemini 2.5 Pro processed these recordings, along with the corresponding College of American Pathologists (CAP) cancer protocol template, transcribing the audio and generating formalized synoptic reports. The AI-generated reports were compared against the ground truth to evaluate the extraction of histologic grade, lymph node ratio, tumour size, and TNM staging components, specifically, the primary tumour (T) and lymph node involvement (N) classifications. All parameters were graded for accuracy using a 0-3 scale (3 = perfect match; 0 = major discrepancy indicating diagnostic inaccuracy).

Results: The Gemini 2.5 Pro AI system successfully transcribed the stream-of-consciousness audio dictations, generating a synoptic report for each case. Subsequent evaluation comparing the AI-extracted TNM staging components against the ground truth data from the original synthetic reports demonstrated 100% accuracy in T and N classification. Upon examination of histologic grade, lymph node ratio, and tumour size, comparison between the ground truth and AI-generated synoptic reports yielded 100% accuracy for case-relevant parameters. All features were correctly identified by AI, assigning the appropriate values in the AI-generated synoptic reports, using the information provided in the natural language dictations alongside the respective CAP protocol.

Discussion: The findings demonstrate the high feasibility and accuracy of using advanced generative AI to create synoptic cancer reports from pathologist stream-of-consciousness dictations. The AI-generated synoptic reports achieved high fidelity in classifying parameters, suggesting that LLMs can reliably interpret and structure complex information embedded within conversational speech. This approach holds significant potential to streamline the pathology reporting workflow while maintaining precision in synoptic report production. Further research will explore optimal strategies for integrating such AI tools into routine clinical practice to enhance reporting efficiency.

Poster #74

Clinico-molecular Characteristics and Treatment Patterns in Stage IV NSCLC: A Retrospective Study from Southwestern Ontario

Authors: Sarah Ma[1,2], Jonathan Moroniti[1], Ana Carolina da Cruz[4], Andra Sterea[1], Muhammad Minhas[1], Ravnoor Singh Kang[1], Mehdi Qiabi[1,2,3], Mark Vincent[1,2,3], Michael Sanatani[1,2,3], Jawaid Younus[1,2,3], Daniel Breadner[1,2,3], Phillip Blanchette[1,2,3], Hamid Mithoowani[1,2,3], Diane Logan[1,2,3], Jacques Raphael[1,2,3], Kathie Baer[2,3], Morgan Black[2,3], Robin Sachdeva[5], Saritha Surapaneni[2,3], M. Sara Kuruvilla [1,2,3]

Affiliations:

1. Schulich School of Medicine and Dentistry, Western University, London, ON, Canada.
2. London Health Sciences Centre Research Institute, ON, Canada.
3. Department of Oncology, London Regional Cancer Program, London Health Sciences Center, 800 Commissioners Road East, London, ON, N6A5W9, Canada.
4. Department of Statistical and Actuarial Sciences, Western University, London, ON, Canada.
5. Precision Medicine Group, LLC.

Introduction: Non-small cell lung cancer (NSCLC) remains a leading cause of cancer-related mortality in Canada. Over half of NSCLC patients are diagnosed with advanced disease, with an estimated five-year survival rate below 5% for those with Stage IV. Recent advancements in treatment, particularly immunotherapies such as immune checkpoint inhibitors, hold promise for improving clinical outcomes. However, the real-world implementation and impact of these treatments remain uncertain. This is especially applicable in Southwestern Ontario, Canada, a region with a large, demographically diverse population, distinct socioeconomic patterns, and varying levels of healthcare access. Our study aims to evaluate the emerging clinico-pathologic characteristics, treatment patterns, and clinical outcomes of this population in a real-world setting.

Methods: We conducted a retrospective chart review of serially registered adult patients diagnosed with Stage IV NSCLC at the London Health Sciences Centre from January 1st, 2017, to December 31st, 2020. Data on demographics, clinical characteristics, diagnosis, pathologic features, treatment, toxicity, progression, and survival outcomes were collected. Descriptive statistics were applied, and the data cutoff date was May 4, 2024. The research protocol for this study was reviewed and approved by the local research ethics board.

Results: A total of 523 patients were included in the analysis (median age 69; 48.6% male). Majority were current or former smokers (>85%), and over half (51.6%) had an ECOG performance status of 0-1, while 27.2% had 2 or higher. Autoimmune comorbidities were present in <5% of patients. Histologically, adenocarcinoma was the predominant subtype (69.6%). EGFR and ALK mutations were found in ~11% and <3% of patients, respectively. Among patients with known PD-L1 status, 30.4% were negative, 31.2% were weakly positive, and 38.4% were strongly positive; PD-L1 status was unknown in 23.9% of cases. In terms of treatment, among those who received first-line systemic therapy, 31.2% received single-agent immunotherapy, 17.2% with chemotherapy alone, 33.2% with chemoimmunotherapy, and 18.4% with targeted molecular therapies. Overall, 31.7% received palliative radiation alone, while 11.3% received no treatment. Treatment selection was associated with PD-L1 expression levels (**Figure 1**).

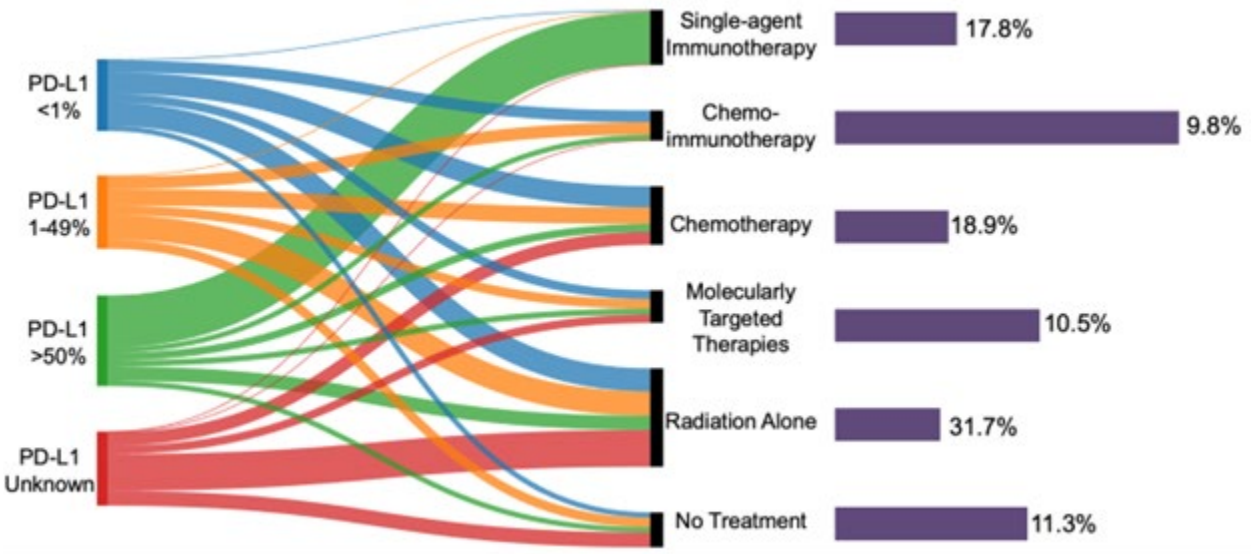

Figure 1: First-line treatment by PD-L1 status in Stage IV NSCLC

Discussion: Lung cancer patients in Southwestern Ontario represent distinct population, as reflected by the demographic and baseline characteristics observed in our cohort. The prevalence of EGFR and ALK mutations mirrors rates seen in early-stage NSCLC in Southwestern Ontario. Despite a high smoking rate (>85%), squamous cell carcinoma accounted for a small minority of patients. First-line treatment decisions were closely aligned with PD-L1 status, with most patients with strongly positive PD-L1 expression receiving single-agent immunotherapy, while those with negative or weakly positive PD-L1 expression predominantly receiving chemotherapy or chemoimmunotherapy. Notably, approximately 40% of patients either received palliative radiotherapy alone or no treatment, highlighting a significant segment of patients not being able to access available systemic therapy. Limitations of this study include missing data and potential regional bias due to geographical restrictions. Future research will focus on clinical outcomes in this cohort.

Poster #75

Integrating Fecal Microbiota Transplantation Clinical Trial Data on a Novel Interactive R Shiny App

Anorin Shadi Ali[1], Behnam Jabbarizadeh[2], and Saman Maleki[1-4]
[1]Department of Pathology and Laboratory Medicine, Schulich School of Medicine & Dentistry, Western University, Canada, [2]London Regional Cancer Program, London Health Sciences Research Institute, London, ON, Canada, [3]Department of Oncology, Western University, London, ON, Canada, [4]Department of Medical Biophysics, Western University, London, ON, Canada

Introduction: Immunotherapy to treat cancer patients remains limited by high rates of primary resistance. Emerging evidence suggests that the gut microbiome plays a role in modulating host responses to immunotherapy. Fecal microbiota transplantation (FMT) has shown promise in overcoming resistance to immunotherapy in recent clinical trials. However, the data generated remain underanalyzed, and cross-trial comparisons are limited due to inconsistencies in data processing and analysis. This project aims to standardize and integrate metagenomic sequencing data from three major clinical trials investigating FMT in melanoma patients, and to develop a novel, user-friendly R Shiny application that facilitates the interactive exploration of taxonomic, functional, and clinical patterns.

Methods: Raw sequencing data from three FMT trials was uniformly processed using a metagenomics pipeline involving MetaPhlAn and HUMAnN. The resulting taxonomic and functional profiles were merged with curated clinical metadata. A modular R Shiny application was developed to enable real-time statistical analysis, including alpha and beta diversity, relative and differential abundance, and pathway coverage. The application supports dynamic filtering, interactive plotting, and hypothesis testing without requiring programming expertise.

Results: The platform offers an accessible and user-friendly interface for analyzing high-dimensional microbiome-clinical data. It revealed patterns such as enrichment of *Ruminococcus* organisms in responders and donor-specific microbial profiles. The app supports granular subgroup analyses and cross-trial comparisons, facilitating translational insights into the enhancement of microbiome-mediated immunotherapy.

Conclusion: This work presents the first interactive tool for harmonized, cross-trial microbiome analysis in the context of FMT and immunotherapy. By democratizing access to complex data and promoting reproducible workflows, it accelerates the identification of microbial features linked to clinical outcomes and supports the development of precision microbiome-based interventions.

Poster #76

Retrospective Analysis of the Impact of Comorbidity Index Scores on Predicting AML 30-day Mortality and Intensity of Induction Chosen

Francesco Vito[1,2], Rufina Ning[1,2], Allyson Jane[1,2], Pedrom Farid[1,2], Dr. Caroline Hamm[1,2]
[1]Schulich School of Medicine & Dentistry, Western University, London, ON, Canada.
[2]University of Windsor, Windsor, ON, Canada

Introduction:
Acute Myeloid Leukemia (AML) is a difficult type of blood cancer to treat and can lead to death early after diagnosis and induction chemotherapy treatment. There are two main broad treatment types: low and high intensity chemotherapy. The treatment type physicians choose for their patients can be influenced by factors such as patient health and age. There are comorbidity scales that can help quantify these factors: HCT-CI (Hematopoietic Cell Transplantation-Comorbidity Index) and CCI (Charlson Comorbidity Index). The primary study aim of this project is to determine if there is any relationship between a patient's CCI/HCT-CI score and both their 30-day mortality after diagnosis and the type of treatment physicians chose for them.

Methods:
This study is a retrospective chart review of all AML patients treated at WRH between March 1st, 2019 to December 31st, 2023 with either low or high intensity chemotherapy treatment. Many different factors were collected: 30-day mortality after diagnosis, type of treatment (high vs low), comorbidities, and demographic factors.

Results:
There was a total of 66 patients diagnosed with AML at WRH who underwent either low or high intensity chemotherapy treatment in the study timeframe. A total of 15 patients (22.7%) received low intensity treatment and 51 patients (77.3%) received high intensity treatment.

The CCI and the HCT-CI were calculated for both those who died within 30 days of diagnosis of AML and those who survived within 30 days of diagnosis. For those who died within 30-days of diagnosis, CCI and HCT-CI values were 6.9 (95%CI 4.63-9.09) and 4.6 (95%CI 2.3-6.9) respectively. For patients who survived within 30-days of diagnosis the CCI and HCT-CI values were 5.4 (95%CI 4.63-6.15) and 2.4 (95%CI 1.77-2.94). There was no statistical difference between the two groups for either comorbidity score. Moreover, the CCI and the HCT-CI were calculated for both patients who underwent low intensity treatment and those who underwent high intensity treatment. For low intensity treatment, the CCI and HCT-CI were 8.3 (95%CI 5.83-10.57) and 4.3 (95%CI 2.48-6.12) respectively. For high intensity treatment, the CCI and HCT-CI were 4.8 (95%CI 4.29-5.31) and 2.1 (95%CI 1.6-2.6) respectively.

Discussion:
First, the results show that although there might be a correlation between a higher HCT-CI and CCI score and higher 30-day mortality after getting diagnosed, this is not statistically significant, and more data is needed. Second, there seems to be a correlation between having higher CCI and HCT-CI scores and receiving low intensity AML treatment. A possible reason for this could be that physicians are more likely to suggest low intensity AML treatment for those with more comorbidities. However, only the CCI scores showed a statistically significant difference with a p-value<0.05.

Conclusion

CCI/HCT-CI scores may be useful in the future for predicting 30-day mortality and guiding what type of treatment a patient gets. However, more data is needed to make any conclusion.

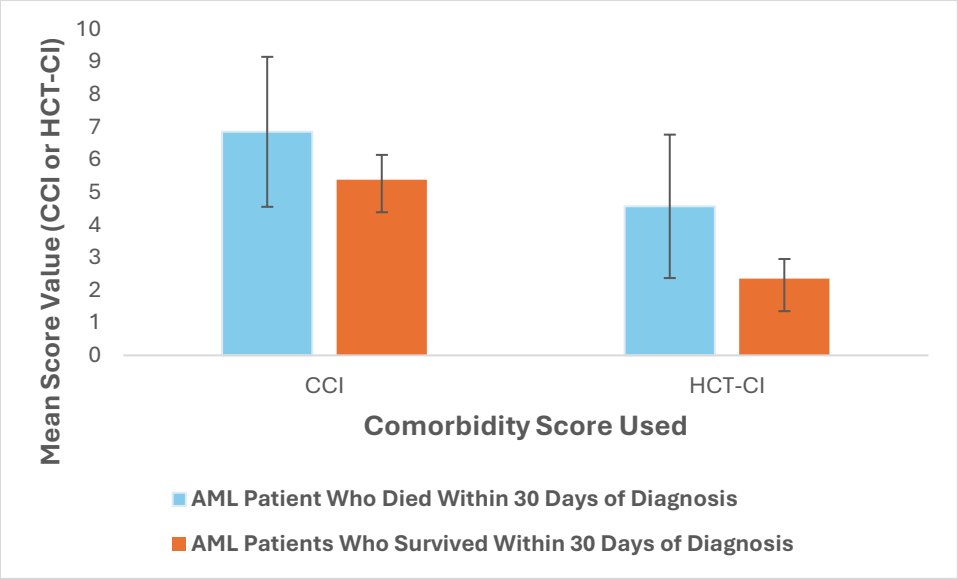

Figure 1: Mean CCI & HCT-CI Score for both patients who died within 30 days of diagnosis and those who survived within 30days of diagnosis. 95% CI shown

Booth #77

Efficacy, Functional Consequences, and Immunomodulatory Effects of Treatment with Naporafenib in Anaplastic Thyroid Carcinoma

Amir Karimi[1,2,3,*], Nachuan (Harrison) Pan[1,2,3,*], Peter Zeng[1,2,3], Sarah EB Ryan[1,2,3], Shengjie Ying[1,2,3], Nhi Le[1,2,3], Halema Khan[2,3], Krista Joris[2,3], Joe S Mymryk[3], John W Barrett[2,3], Anthony C Nichols[2,3]
[1]Department of Pathology and Laboratory Medicine, Schulich School of Medicine & Dentistry, Western University, Canada; [2]Department of Otolaryngology – Head and Neck Surgery, London Health Science Centre, London, ON, Canada; [3]Verspeeten Family Cancer Centre, London Health Science Centre, London, ON, Canada; * These authors contributed equally.

Introduction: With a historical median overall survival of less than 6 months, anaplastic thyroid cancer (ATC) is the most aggressive type of thyroid malignancy. The substantial improvements in patient outcomes due to the addition of RAF inhibitors (RAFis) and MEK inhibitors (MEKi) to the standard of care are marred by the restriction of the efficacy of these treatments to $BRAF^{V600E}$-mutant tumours and the rapid development of treatment resistance. These limitations are attributed to the inability of the conventional RAFis to inhibit MAPK signalling through RAF dimers. Type II RAFis, which are active against RAF dimers, may circumvent treatment resistance in this setting. Data from our lab indicate that the type II RAFi naporafenib may overcome the resistance to conventional RAFis and effectively suppress the viability of ATC cells in several cell line and patient-derived xenograft models of ATC. Here, we investigated the efficacy, functional consequences, and immunomodulatory effects of treatment with naporafenib, alone or combined with the MEKi trametinib, across several *in vitro* and *in vivo* models of ATC.

Methods: Human ATC cell lines were treated in triplicates with 2 µM of DMSO, dabrafenib, and naporafenib, and RNA was extracted after 24 hours of incubation. *In vivo* experiments were carried out using the TBP-3743 immunocompetent model of ATC ($Braf^{V600E}$, Trp53-/-). When the tumour volumes reached $50mm^3$, the mice were randomized and started receiving the treatments via oral gavage and intraperitoneal injections. tumour volumes were measured using a calliper, and the growth rates were compared by linear mixed-effects modelling. Cell type deconvolution and differential expression analysis of the RNA-seq data were performed using mMCP-counter and DESeq2, respectively. Progeny and clusterProfiler were used for pathway analysis.

Results: Molecular profiles of the samples indicated that naporafenib restricts the viability of ATC cells by potent suppression of both MAPK and PI3K/AKT pathways, an effect that might be partially mediated by its off-target inhibition of the RTK EphA2. Moreover, treatment with naporafenib led to enhanced MHC complex assembly and activated interferon signalling in the malignant cells, suggesting modulation of the immunogenicity of these cells. Our trials in the immunocompetent mouse model indicated effective suppression of tumour growth and enhanced immune activity under both naporafenib monotherapy and treatment with the combination of naporafenib and trametinib (NT). Moreover, while monotherapy with anti-Pd1 did not suppress growth or alter the molecular profiles of the tumours, the combination of NT and anti-Pd1 led to a more durable response and was accompanied by enhanced T-cell infiltration and higher immune activity even when compared to treatment with NT alone. Assessment of immune checkpoints suggested a significant increase in the abundance of Ctla4 and Tim3 in response to NT, raising interest in evaluating the combination of blockade of these targets with the NT treatment.

Conclusions: Overall, our results indicate that naporafenib can effectively overcome the resistance to conventional RAFis. Moreover, treatment with NT leads to a remodelling of the immune microenvironment of the tumours that can be modulated with immune checkpoint blockade for an enhanced anti-tumour activity.

Booth #78

Developing the Métis-CTN program: National meeting to co-create a clinical trials navigation pathway for Métis cancer patients

Ria Patel[1], Milica Paunic[2], Bharat Gupta[3], Ibrahim Mohamed[3], Renee Nassar[1], Depen Sharma[4], Christina Trieu[5], Salah Alhajsaleh[5], Anaam Jaet[5], Mahmoud Hossami[1], Laurice Togonon Arayan[6], Swati Kalia[2], Roaa Hirmiz[1], Olla Hilal[3], Anthony Luginaah[3], Michael Touma[1], Govana Sadik[5], Pratham Gupta[3], Lee McGrath[2], Megan Delisle[7], and Caroline Hamm[6]

[1]Clinical Trials Navigator, [2]University of Toronto, [3]Western University, [4]University of Ottawa, [5]University of Windsor, [6]Windsor Regional Hospital, [7]University of Manitoba

Introduction: Clinical trials are fundamental for advancing research by leading to the development of new treatment options and ensuring equitable healthcare outcomes. The Clinical Trials Navigation (CTN) program was established to address the gap in patient access to cancer clinical trials by supporting patients in navigating the trial search process. Since the implementation of the CTN program, 8 patients have self-identified as Indigenous, highlighting the need for a structured and culturally sensitive pathway for Indigenous patients. By implementing a distinctions-based approach, this project aims to develop a Métis-specific clinical trials navigation pathway tailored to the unique needs and values of Métis communities. This abstract outlines the goals and design of a national meeting focused on co-developing this pathway in collaboration with Métis leaders, healthcare professionals, and patients.

Methods: To inform the development of a Métis-specific clinical trial navigation pathway, a national in-person meeting was organized with Métis patients, Indigenous patient navigators, researchers, and clinicians. A combination of participatory methods including empathy mapping, small group storytelling, world-café methodology, and whole group reflection was used to support participant engagement and ensure a space for culturally safe discussion. Participants discussed barriers in accessing clinical trials from a Métis cancer patient perspective and engaged in collaborative discussion to develop solutions. Insights from this meeting will guide the next steps of CTN program modification and implementation, ensuring the pathway reflects the needs and values of Métis communities.

Results: The national meeting held in April 2025 aimed to strengthen relationships among Métis stakeholders to support ongoing collaboration to implement the Métis-CTN. Participants identified several barriers that Métis cancer patients may face along the clinical trial navigation process including mistrust in the healthcare system, financial and logistical challenges, and absence of culturally safe support and environments. To address these barriers, solutions proposed included offering supportive intake procedures, trauma-informed care approaches, and embedding Indigenous Navigators within care teams and clinical trial related discussions. To better support Indigenous Navigators throughout the Métis-CTN pathway, participants emphasized the need for timely access to trial and patient information, accessible contact details, phone scripts, and tailored guidebooks co-developed with the CTN team. These insights will guide the next steps in modifying and implementing the CTN program to reflect the unique needs and values of Métis patients and communities.

Discussion: This national meeting with Métis partners represents a crucial step in identifying the barriers that Métis cancer patients may face when accessing clinical trials. Using a collaborative framework, this meeting will support the development of a shared understanding of solutions the CTN program might provide. Insights gathered through this discussion will inform the design of a culturally safe navigation pathway and will contribute to reconciliation efforts by increasing enrollment of Métis individuals in clinical trials. While the initial focus is on the Métis population, this distinction-based approach serves as a foundation for expanding this pathway for other Indigenous groups.

Poster #79

Connecting Clinical Trials with Patients using Patient Navigation: A Scoping Review

Olla Hilal[1], Yvonne Paglicauan[2], Ria Patel[3], Pratham Gupta[1], Leena Moshref[4], Nicole Askin[5], Carla Epp[5], Anthony Luginaah[6], Renee Nassar[7], Roaa Hirmiz[7], Milica Paunic[8], Mahmoud Hossami[7], Rhonda Abdel-Nabi[7], Kayla Touma[7], Depen Sharma[9], Rija Fatima[7], Emmanuel Akingbade[7], Ibrahim Mohamed[6], Swati Kalia[7], Michael Touma[7], Govana Sadik[3], Laurice Arayan[7], Salah Alhajsaleh[3], Anaam Jaet[3], Christina Trieu[3], Megan Delisle[4,10], Caroline Hamm[3,6]
[1]Department of Medical Sciences, Western University, [2]University of Manitoba, [3]University of Windsor, [4]Department of Surgery, University of Manitoba, [5]WRHA Virtual Library, University of Manitoba, [6]Schulich School of Medicine & Dentistry, Western University, [7]Clinical Trials Navigator, Windsor Regional Hospital, [8]Temerty Faculty of Medicine, University of Toronto, [9]Faculty of Medicine, University of Ottawa, [10]Paul Albrechtsen CancerCare Manitoba Research Institute

Introduction: Patient navigation is a promising strategy to improve access to cancer care, but the evidence supporting its role in increasing access to cancer clinical trials has not been systematically evaluated. This scoping review aims to critically appraise, synthesize, and present the available evidence on the use of patient navigation to increase cancer clinical trial enrollment.

Methods: Nine databases were searched for English peer-reviewed articles from inception through December 21, 2023. Two independent researchers screened titles, abstracts, and full texts and extracted data using standardized forms.

Results: Among the 23 included articles, 18 (78.3%) were observational studies, and only 5 (21.7%) were randomized trials. Fourteen (60.9%) were described as pilot/feasibility studies. Of the observational studies, 13 (56.5%) included a comparator group. Six (26.1%) studies were multi-institutional; 17 (73.9%) were single-center. Twenty-one (91.3%) studies were from the USA; 2 (8.7%) were from Canada. Thirteen (56.5%) focused on equity, all addressing racial/ethnic groups. Seven (30.4%) articles used patient navigation for clinical trials for all cancer types; 14 (60.9%) focused on specific cancers, with 12 (85.7%) primarily addressing breast cancer. Among 21 studies describing navigator qualifications, 4 (17.4%) required professional training (e.g., nurse, social worker), and 17 (73.9%) used community representatives. Education/training for navigators was described in 12 (52.2%) articles. The interventions used most frequently by navigators included education in 19 articles (82.6%) and care coordination in 17 articles (73.9%). Direct clinical trial referrals were unmentioned; logistical and financial assistance appeared in only 2 articles each (8.7%). Navigators in 7 (30.4%) studies directed patients to trials within and outside their center; 16 (69.6%) navigated patients only within their center. Five articles compared enrollment with and without navigation: 4 showed no improvement, and 1 reported improvement with navigation. Five other articles reported enrollment with navigation without a comparison group. Two studies limited to eligible patients reported 80.4% and 86% enrollment in a clinical trial with navigation. Three studies including all interested patients reported enrollment rates of 7%, 22%, and 22.5%.

Conclusions: Evidence on patient navigation for cancer clinical trials is primarily from observational, pilot/feasibility, single-center studies in North America, with a focus on breast cancer. Furthermore, navigator training details are underreported and their interventions' scope is limited. Few studies have examined diverse equity groups. Future research should employ more rigorous designs to evaluate different patient navigation approaches and assess their impact on clinical trial enrollment across a wider range of cancers and patient populations.

Poster #80

Transforming prostate cancer management: The role of nurse-practitioner-led prostate cancer clinics in genitourinary oncology

Matthew Parezanovic[1], Sari Belzycki[1], Branka Vujcic [1], Morgan Black [1], Kathie Baer[1], Ricardo Fernandes [1,2]
[1] Verspeeten Family Cancer Centre, [2]Western University

Introduction: Prostate cancer management continues to evolve with newer treatments and improved clinical outcomes. Androgen receptor pathway inhibitors (ARPIs) have shown life-extending benefit for treatment of locally advanced and metastatic prostate cancer, translating to ongoing surveillance and monitoring for a growing number of patients. Since the 1970's in Canada, nurse practitioners (NPs) have been developing their role, including in oncology, to ease access, coordinate and improve care, and create efficiency in the healthcare system. This quality improvement project evaluates the implementation of a NP-led Prostate Cancer Clinic (NPPCC) at an academic regional cancer centre . The purpose of this retrospective study was to review the impact of the NPPCC model, in terms of clinical metrics including patient volumes, time followed, and patient care management.

Methods: Retrospective data were collected from electronic medical records for patients with a history of prostate cancer treated at the NPPCC at London Health Sciences Centre (London, Ontario, Canada) between July 1, 2016, and November 4, 2024. Inclusion criteria were adult patients (≥18 years) with a confirmed diagnosis of prostate cancer who engaged in at least one NPPCC follow-up visit within the study period. This study was approved by The Western University Health Sciences Research Ethics Board. All Data were stored in a secure, electronic REDCap database hosted by London Health Research Institute. The primary outcome was the volume of patient visits per year. Secondary outcomes included total and annual number of patients referred to clinic, the number and type of electronic prescriptions issued, the volume of electronic genetic tests ordered, number of electronic supportive care referrals made, the duration of follow-up within the NPPCC, and the amount of clinic time reallocated or saved from Medical Oncology clinics. Descriptive statistics were used to summarize study outcomes. Data analysis was performed using IBM SPSS Statistics, Version 29.0.2.0 (IBM Corp., Armonk, NY).

Results: A total of 531 eligible patients were included in this analysis. The mean duration of follow up was 13.9 months (+/- 16.6 months, range 0-68 months). Between November 1, 2023 and November 4, 2024 (one year snapshot with two full-time NPs) there were 990 patients encounters, corresponding to 62 clinic days based on 30 minutes appointments and an 8-hour workday. The annual average clinic time was 240 clinic hours per NP. Of the patients managed, 484 (91.1%) received prescriptions by the NP for ARPIs and 194 (36.5%) received prescriptions for androgen deprivation therapy. Supportive medications (denosumab, acetaminophen-codeine, hydromorphone, mirabegron and tamsulosin) were prescribed to 39% of patients (n=205). Genetic testing was ordered for 35.3% of patients. Additionally, 179 electronic referrals were initiated (33.8%) by the NPs to other specialists or supportive services.

Conclusion: The implementation of a NPPCC model demonstrated substantial improvements in care delivery and clinic efficiency. With over 500 patients managed, and nearly 1,000 patient encounters within a 12-month period, the clinic effectively optimized resource utilization, maintaining a high volume of patients. An average of 240 clinic hours were saved annually from medical oncologists' clinics. The independence and scope of NPs, including physical assessment, ordering and interpreting diagnostic tests, making diagnoses and referrals, and prescription management, highlight their capacity to run independent clinics to manage complex patients with advanced prostate cancer. These findings suggest that a NP-led model can sustain high-quality, guideline-concordant prostate cancer care while improving access and operational efficiency within oncology practices.

Poster #81

A Window of Opportunity for Prehabilitation in Patients with Pancreatic Cancer: Preliminary Descriptive Statistics and Survival Analysis

Erica Lo[1,2], Tania Larsen[1,3], Alison Rushton[1], Anton Skaro[2,4,5]

1. School of Physical Therapy, Department of Health & Rehabilitation Sciences, Faculty of Health Sciences, Western University, London, Ontario, Canada
2. Baker Centre for Pancreatic Cancer, London Health Sciences Centre, London, Ontario, Canada
3. Vascular Surgery & Cardiology, London Health Sciences Centre, London, Ontario, Canada
4. Multi-Organ Transplant Program, London Health Sciences Centre, London, Ontario, Canada
5. Schulich School of Medicine & Dentistry, Western University, London, Ontario, Canada

Introduction: Due to older age, pre-existing comorbidities and complex geriatric issues, many patients with pancreatic cancer are frail. Frailty in this population is associated with decreased treatment tolerance, poorer surgical outcomes, poorer physical function and quality of life, and an increased risk of mortality. The aggressive symptoms associated with disease progression and treatment often contribute to further decline in the functional status of patients, producing additional burdens. However, frailty is emerging as a significant modifiable risk factor, and exercise is a potential therapy to counteract the negative effects of frailty and pancreatic cancer. Further research is needed to support the identification and treatment of frailty in patients with pancreatic cancer.

Methods: This observational longitudinal cohort study aims to investigate the impact of frailty on physical functioning, quality of life, and survival in patients undergoing neoadjuvant therapy and/or surgery for pancreatic cancer. A convenience sample of adults undergoing treatment for pancreatic adenocarcinoma was recruited from the local cancer centre in London, Ontario. Sex, age, body mass index, comorbidities, resectability, Fried Frailty Index, 6-minute walk test (6MWT), and a quality of life questionnaire (EORTC-QLQ30) were collected. The outcome of interest was survival. Baseline measures were used for this analysis. Descriptive statistics were used to report baseline patient characteristics and outcome measures. A Weibull proportional hazards survival analysis was used to investigate the relationship between frailty status and survival.

Results: In this preliminary analysis, 34 participants were included. 44.1% of participants were females and 55.9% were males. The average age of participants was 69 years. Most participants were pre-frail (65.2%), and 60.1% had a poor 6MWT score (< 400 metres). The average score for physical functioning across participants was 93.3% on the EORTC-QLQ30, indicating good physical functioning. Quality of life, emotional functioning, fatigue, pain, and appetite were the most affected compared to other domains in the EORTC-QLQ30. 91.3% of participants reported sufficient activity levels in the Fried Frailty Index. Frailty was found to be associated with survival, with frail patients being at greater risk of mortality.

Conclusions: Most participants at baseline are not yet frail and report high physical functioning and sufficient activity levels, suggesting that baseline status presents a potential window of opportunity for patients with pancreatic cancer to engage in targeted exercise interventions to manage and/or prevent frailty progression. Physical measures are feasible and can inform treatment decision-making to optimize patient outcomes.

Poster #82

Development and evaluation of an ultrasound-compatible gynecological brachytherapy simulator.

Celeste MacDonald[1], David Contella[1], Prakash Hampole[1], Tiana Trumpour[2], Lucas C. Mendez[1], Aaron Fenster[2], Douglas A. Hoover[1], Donna H. Murrell[1]
[1]Verspeeten Family Cancer Centre, [2]Robarts Research Institute

Introduction: Brachytherapy (BT) is a vital component in the treatment of locally advanced cervical cancer, significantly contributing to improved survival outcomes. The technique requires the precise placement of BT applicators, often under ultrasound guidance. Despite its clinical importance, training opportunities for BT are limited due to lack of tools. Studies have shown that trainee confidence and competence in procedural tasks are closely tied to repetition and exposure, which shows the need for accessible and effective simulation-based training. However, existing BT simulators often fall short in anatomical realism or compatibility with standard BT applicators and ultrasound imaging. This project aims to address this through the design and evaluation of a novel, anatomically accurate, ultrasound-compatible simulator specifically developed for gynecological BT training.

Methods: The simulator was constructed based on MRI scans from a publicly available cervical cancer dataset. Organs including the uterus, cervix, bladder, vulva, and rectum were contoured, converted into STL files, and edited using 3D modeling software to create realistic, fillable molds. A cylindrical structure was used for the rectum to accommodate transrectal ultrasound probes. Organs were fabricated using plastisol, enhanced with varying concentrations of softeners, hardeners, and glass microbeads to simulate appropriate tactile feedback and ultrasound contrast. The organs were then cast in tissue-mimicking plastisol and placed in a 3D-printed pelvis to ensure correct anatomical positioning and realistic external features. Five attendees participated in a hands-on workshop using the simulator. Each completed pre- and post-training self-assessment surveys to evaluate their confidence in performing ultrasound-guided intracavitary and interstitial BT procedures on a 10-point Likert scale. A final survey containing 11 questions collected feedback on anatomical accuracy, realism, and overall training utility.

Results: Participants demonstrated increased confidence across both procedural types. Confidence in intracavitary BT improved by an average of 2 points, and interstitial BT by 1.4 points. All participants agreed or strongly agreed that the simulator accurately represented organ size, shape, and placement. Notably, 80% of participants strongly agreed the simulator should be used as a standard component of BT training programs. Participants also emphasized the realistic tactile responses and ultrasound image quality, highlighting its effectiveness.

Discussion: This anatomically accurate, ultrasound-compatible BT simulator offers a novel platform for developing skill in and understanding of gynecological brachytherapy. It fills a critical training gap and provides trainees the opportunity to build skills without risk to patient safety. Positive feedback underscores its value and supports broader integration into radiation oncology education. Future development will aim to expand the simulator's versatility and assess long-term impacts on clinical training outcomes.

Poster #83

Targeted Treatment of Solid Tumors with BRAF Fusions: A Systematic Review

Joseph N. Samuel[1], Saurav Verma[2], Eric Winquist[2], Seth A. Climans[2], Chantel Cacciotti[3], Gabriel Boldt[2], Jacques Raphael [2]
[1]Department of Medicine, Western University, London ON, [2]Verspeeten Family Cancer Centre, Western University, London ON, [3]Department of Pediatrics, Western University, London ON

Background: *BRAF* fusions are uncommon driver alterations in a range of cancers. While the *BRAF* V600E mutation is a recognized target for the BRAF inhibitors, *BRAF* fusions have not yet been investigated as potential targets for treatment in most cancers, and there is limited literature available to help guide treatment for patients with these fusions with targeted therapies, including direct BRAF inhibitors and downstream MEK inhibitors. This systematic review aims to summarize the available literature on the targeted treatment of solid tumors harboring a *BRAF* fusion.

Methods: We conducted a systematic review to delineate the reported efficacy, response rates and survival outcomes, of targeted treatment in patients with a solid cancer harboring a *BRAF* fusion. PubMed, Embase, and Cochrane CENTRAL were searched between 2014 and 2024. Data were extracted to assess the details of efficacy.

Results: A total of 37 studies involving 113 patients with *BRAF* fusion-positive cancer who underwent targeted therapies were included. Most of these studies were case reports and case series (n = 31, 84%), with four clinical trials (11%) that were either phase I or phase II. The review included various cancer types, with central nervous system (CNS) cancers, including gliomas and pilocytic astrocytomas, being the most common (n = 66, 58%), followed by melanoma (n = 20, 18%) and non-small cell lung cancer (NSCLC) (n = 9, 8%). Other cancers (n = 18, 16%) included sarcoma (n = 7), genitourinary (n = 2) and colorectal (n = 1). Among the *BRAF* fusion gene partners, *KIAA1549* was the most frequent (n = 62, 55%), followed by *SND1* (n = 6, 5%) and *AGK* (n = 4, 4%). The targeted therapies used were varied, with MEK inhibitors being used in most patients, selumetinib (n = 36, 32%), followed by trametinib (n = 34, 30%), as well as, binimetinib and cobimetinib. BRAF and pan-RAF inhibitors used included dabrafenib, vemurafenib, tovorafenib and belvarafenib. The response rates were reported for 103 patients, with 2% achieving a complete response (n = 2), 46% showing a partial response (n = 47), and 22% exhibiting stable disease (n = 23). Objective response rate in NSCLC, sarcoma, melanoma and CNS tumors was 88%, 57%, 52% and 41% respectively. Data on survival outcomes was limited.

Conclusions: In conclusion, there is limited data on the efficacy of targeted therapy in solid tumors with a BRAF fusion, with most evidence coming from case reports/series, alongside a few phase I/II trials. While BRAF fusion-positive cancers show varying yet promising responses to BRAF and/or MEK inhibitors, the effectiveness may vary with histology. Given the rarity of these fusions, there is a clear need for international collaboration and innovative trial designs, such as basket and platform trials, to assess targeted treatment strategies more effectively and improve outcomes for these patients.

Poster #84

Adjuvant CDK4/6 Inhibitors in High-Risk Breast Cancer - A Comprehensive Critical Appraisal of the PALLAS, MONARCH-E and NATALEE Trials through The Lens of Research Methodology

Authors:
Raman Sambhi[1, 2], Danilo Giffoni M. M. Mata[1,2,3]

Affiliations:
[1] Division of Medical Oncology, Verspeeten Family Cancer Centre, London Health Sciences Centre, ON N6A 5W9, Canada. Danilo.Giffoni@lhsc.on.ca; Raman.Sambhi@lhsc.on.ca;
[2] Schulich School of Medicine and Dentistry, Western University, London, ON N6A 5C1, Canada.

Abstract not available for booklet

Poster # 85

Is MRI imaging necessary for producing clinically appropriate hippocampal contours for HA-WBRT?

Owen Rodrigues, Melody Qu, Timothy Nguyen, Glenn Bauman, Andrea Vucetic, Shaheer Shahhat, Sympascho Young, Terence Tang, John Patrick, George Rodrigues

Department of Radiation Oncology, London Regional Cancer Program, London Health Sciences Centre, London, Ontario, Canada.

Introduction: To prepare a HA-WBRT plan, a radiation oncologist must contour the two hippocampi which can be time intensive and traditionally requiring access to a fused MRI scan for CT-simulation. This study seeks to assess the clinical appropriateness of hippocampal contours created by an AI-based automatic contouring system (using only CT imaging) to MRI-based clinical consensus and clinician contours. If MRI imaging is considered to be not essential, this can simplify the clinical care path with cost savings which may be important in resource-limited jurisdictions.

Methods: Sixteen anonymized HA-WBRT patients were included within this study. Four types of contours were generated or available for study and included:

1. Consensus based "gold standard" contours generated by use of the STAPLE algorithm with seven RO observers utilizing MR-fused CT-simulation information without access to autocontours.

2. MRI based Limbus AI autocontours (limbus.ai).

3. CT-simulation based (without MRI imaging) Limbus AI autocontours.

4. Clinical contours generated by the treating RO prior to this study (using MR-fused CT-simulation imaging and Limbus AI autocontours).

For each these cases four contours were generated (or clinically available) including both left and right hippocampus as well as their respective PRV (5mm) avoidance contours. Various comparisons between contour generation approaches were conducted using Dice Coefficient analysis and descriptive statistical assessment of the magnitude of over- and under-contouring.

Results: Relevant comparisons between generated and available contours are summarized in table one.

Table 1: Dice coefficient comparisons of clinically treated contours, CT-based and MRI-based autocontours and STAPLE consensus contours.

Comparison	**Left Hippo**	**Right Hippo**	**Left 5mm PRV**	**Right 5mm PRV**
Clinical vs. STAPLE	0.65	0.62	0.82	0.81
Limbus MRI vs. STAPLE	0.68	0.65	0.84	0.81
Limbus CT vs. STAPLE	0.58	0.56	0.79	0.77
Limbus CT vs. Limbus MRI	0.66	0.68	0.83	0.83

Limbus CT vs. Clinical	0.74	0.75	0.86	0.86

A summary of cases where there was more significant over-contouring vs. under-contouring is detailed in table two.

Table 2: Summary of comparisons where there was greater over-contouring versus under-contouring of contour 1 vs. contour 2.

Contour 1	**Contour 2**	**Left Hippo**	**Right Hippo**
Clinical	STAPLE	11/16	12/16
Limbus MRI	STAPLE	10/16	8/16
Limbus CT	STAPLE	12/16	12/16
Limbus CT	Limbus MRI	16/16	15/16
Limbus CT	Clinical	13/16	8/16

Conclusions: Consideration of both the DICE coefficient analysis as well as the over-/under-contouring analysis lead to the following conclusions:

1. Hippo and PRV contours generally have DICE of 0.62-0.65 and 0.81-0.82 when compared to the STAPLE which define a level of acceptability when assessing autogenerated contours.

2. Limbus MRI contours are a clinically acceptable surrogate due to their DICE of 0.65-0.68 (hippo) and 0.81-0.84 (PRV); whereas CT-based Limbus contours are slightly inferior– 0.56-0.58 (hippo) 0.77-0.79 (PRV).

3. Limbus CT based autocontours are consistently over-contoured when compared to STAPLE, MR Limbus, and clinically delivered contours.

Therefore, Limbus CT-based autocontours can be used clinically with the understanding that this may lead to more brain sparing near the hippocampi. Given that known brain metastases near the hippocampal structures is a general contraindication for HA-WBRT, CT-based autocontours without the use of MRI imaging is a reasonable alternative care path particularly in resource-constrained practice environments.

Poster #86

Dosimetric analysis and replanning study of MRI and PSMA-PET guided prostate SBRT-SIB from the ARGOS-CLIMBER phase I/II trial

David DeVries[1], Hatim Fakir[1,2], Andrew Loblaw[3], Aneesh Dhar[1,4], Sherif Ramadan[1,4], Lucas C. Mendez[1,4], Joelle Helou[1,4], Rohann Correa[1,4], Michael Lock[1,4], Matt Wronski[5], John Conyngham[6], Zahra Kassam[7,8], Vibhuti Kalia[7,8], Priscila Crivellaro[7,8], Aaron Ward[2,9], Jonathan D. Thiessen[2,10,11], Ting-Yim Lee[2], David Laidley[12,13], and Glenn Bauman[1,4]

[1]Department of Radiation Oncology, London Health Sciences Centre, [2]Department of Medical Biophysics, Western University, [3]Department of Radiation Oncology, Odette Cancer Center, Sunnybrook Health Sciences Centre, [4]Department of Oncology, Western University, [5]Department of Medical Biophysics, Odette Cancer Center, Sunnybrook Health Sciences Centre, [6]Patient partner, [7]Department of Medical Imaging, St. Joseph's Health Care, [8]Department of Medical Imaging, Western University, [9]Baines Centre for Translational Cancer Research, London Health Sciences Centre, [10]Division of Medical Physics, CancerCare Manitoba, [11]Department of Radiology, University of Manitoba, [12]Department of Nuclear Medicine, St. Joseph's Health Centre, [13]Department of Nuclear Medicine, Western University

Introduction

Prostate cancer often presents diffusely, but may involve focal dominant intra-prostatic lesions (DILs). Stereotactic body radiotherapy (SBRT) is routinely used to treat the entire prostate, but boosting DILs with escalated radiation doses has also been found to be effective and safe. The ARGOS-CLIMBER prospective trial investigated using both multi-parametric magnetic resonance imaging (mp-MRI) and prostate-specific membrane antigen positron emission tomography (PSMA-PET) to identify DILs for dose-boosting using SBRT simultaneous in-field boost (SBRT-SIB). This study answers the following dosimetry-related research questions: 1) what DIL boost doses could be achieved; 2) what impact did target volume, risk stage, and neo-adjuvant androgen deprivation therapy (ADT) have on achievable DIL doses; 3) how do the DIL doses compare to those achieved by a dose-escalated SBRT non-SIB plan; and 4) does allowing high-gradients in DIL boost dose distributions increase dose levels?

Methods

ARGOS-CLIMBER accrued n=50 patients: 32 in Cohort 1 (no neoadjuvant ADT) and 18 in Cohort 2 (three months neoadjuvant ADT). Patient mp-MRI and PSMA-PET datasets were acquired to enable DIL contouring. Five fraction SBRT-SIB treatments were planned to deliver radiation to the whole prostate (35 Gy), seminal vesicles (25 Gy), lymph nodes (25 Gy, possible 35 Gy boost), and DILs (up to 50 Gy dependent on organs-at-risk (OARs) constraints). DIL boosts were designed to minimize dose-gradients to maximize safety for nearby OARs. Target and OAR dose metrics were compared between risk groups and trial cohorts using the Wilcoxon rank-sum test.

A retrospective planning study was also performed for 18 Cohort 1 patients for comparison to the delivered treatment plans. First, a uniform whole-prostate 35 Gy non-SIB plan was developed as a comparison baseline. Second, a dose-escalated uniform 40 Gy plan was developed. Third, new SBRT-SIB plans were developed that allowed high-gradient boosts. Dose metrics were compared to the delivered plan using the Wilcoxon signed-rank test.

Results

DIL volumes were lower for both the high-intermediate risk and neo-adjuvant ADT groups ($p=0.01$, $p=0.03$). Marginally higher DIL boost doses were achievable for the high-intermediate risk group versus the high-very high group (Figure 1a, $p=0.12$). Neo-adjuvant ADT patients achieved significantly higher DIL doses with median gross-tumour volume (GTV) D95 values increasing by 4.8% (Figure 1a, $p=0.005$). Therefore having a lower cancer risk or neo-adjuvant ADT led to having smaller DIL volumes and higher DIL boost doses.

The replanning study showed that SBRT-SIB provides higher DIL doses than both 35 and 40 Gy non-SIB SBRT plans, reaching median GTV D95=42.6 Gy (Figure 1b, $p<0.001$). Allowing high-gradient boosting produced higher DIL doses over standard boosting (Figure 1b, $p=0.004$). SBRT-SIB plans had higher OAR doses, but they remained within constraints. These results show that high DIL doses are possible with SBRT-SIB. High-gradient boosting showed benefit, but the trade-off between treatment outcomes and possible toxicities warrants further research.

Conclusions

This study's dosimetric analysis indicates that SBRT-SIB successfully boosts DILs to higher doses than conventional SBRT techniques, while respecting OAR constraints. Higher boost doses may be possible for high-intermediate risk populations, by employing neo-adjuvant ADT, and by allowing high dose gradients.

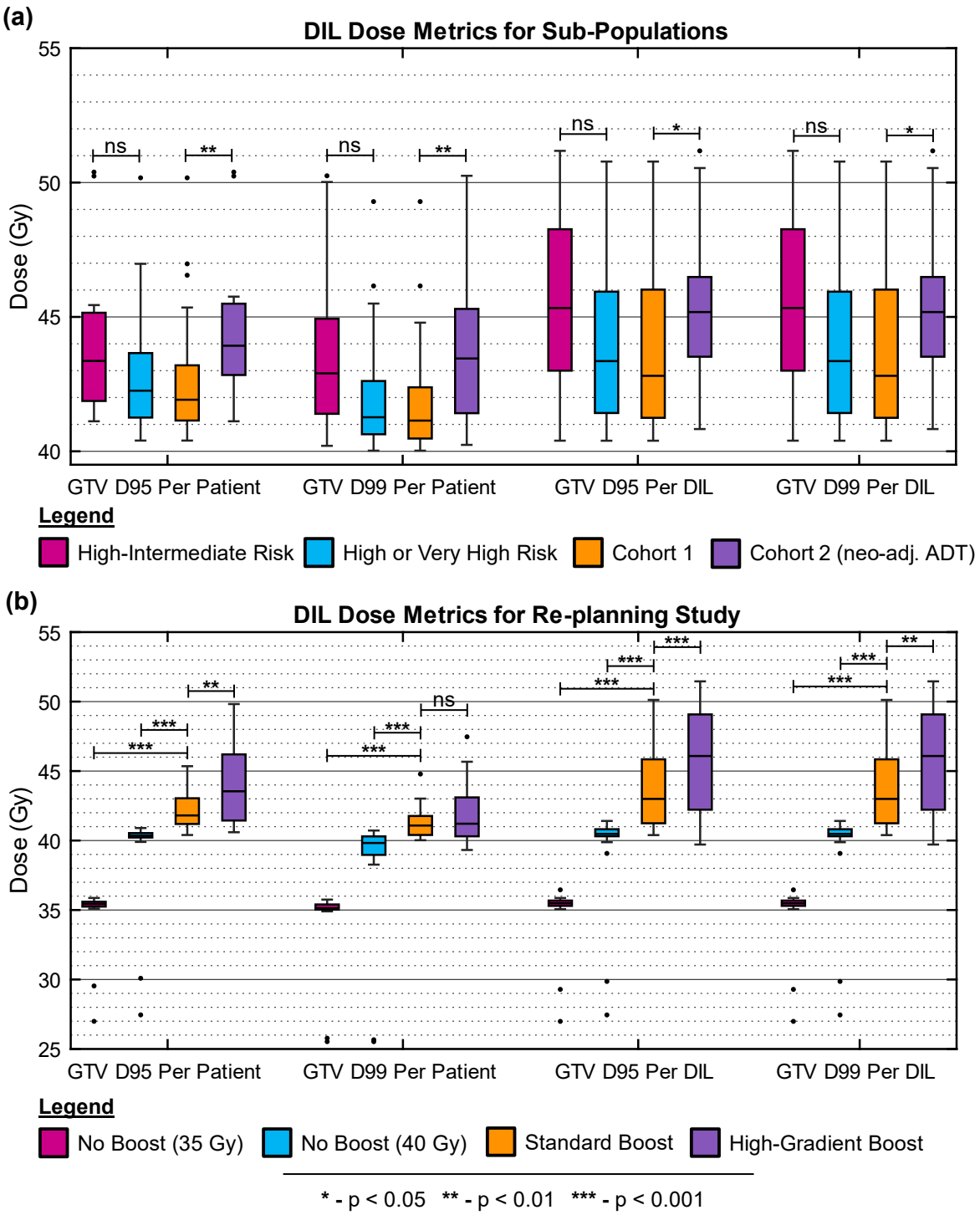

Figure 1: Comparison of DIL target boost doses for (a) risk group and neo-adjuvant ADT sub-populations and (b) different treatment plan techniques. For "Per Patient" analysis, all DIL GTV structures for a patient were aggregated into one structure and dose metrics extracted to provide that patient's metric values. For "Per DIL" analysis, each patient's DILs were analyzed separately to get metric values. Statistical tests used: (a) Wilcoxon rank-sum test (unpaired), (b) Wilcoxon signed-rank test (paired).

Poster #87

Dosimetric Feasibility Study of Stereotactic Body Radiotherapy and High Dose Rate Brachytherapy for Dominant Intraprostatic Dose Boosting

Noah Blackburn-Hum[1], Lucas Mendez[2,3], Joelle Helou[2,3], Rohann Correa[2,3], Aaron Ward[4,5], Hatim Fakir[3,4], Andrew Loblaw[6,7], Glenn Bauman[2,3], Douglas Hoover[2,3,4], David DeVries[3]
[1]*Department of Physics, University of Waterloo, Waterloo, ON, Canada*
[2]*Department of Oncology, Western University, London, ON, Canada*
[3]*Department of Radiation Oncology, London Health Sciences Centre, London, ON, Canada*
[4]*Department of Medical Biophysics, Western University, London, ON, Canada*
[5]*Baines Centre for Translational Cancer Research, London Health Sciences Centre, London, ON, Canada*
[6]*Department of Radiation Oncology, Odette Cancer Center, Sunnybrook Health Sciences Centre, Toronto, ON, Canada*
[7]*Department of Radiation Oncology, University of Toronto, Toronto, ON, Canada*

Introduction

Recent trials have demonstrated that boosting dominant intraprostatic lesions (DILs) has shown improvements to patient outcomes using both conventionally-fractionated, and ultra-hypo-fractionated radiotherapy. Achievable boost doses are limited with stereotactic body radiotherapy (SBRT), however, due to organs-at-risk (OARs) constraints. Combination of brachytherapy and external radiotherapy has shown success for whole-prostate treatment, and so using SBRT plus high-dose rate brachytherapy (HDR-BT) may be more effective at boosting DILs given BT's rapid geometrical dose fall-off. Our study investigates employing high-dose-rate brachytherapy (HDR-BT) with SBRT to enhance DIL boosting.

Methods

A 10-patient subset was selected from the ARGOS trial cohort, in which patients received prostate SBRT with 35 Gy in 5 fractions and SIB to DILs identified via MRI and PSMA-PET. DIL dose escalation was limited by OAR constraints such that a median boost of GTV D_{95}=42.6 Gy was achieved. The delivered ARGOS plans were taken as the baseline for comparison (designated "SBRT-SIB").

The following steps then took place: 1) new SBRT plans were created to simulate delivering a homogenous 30 or 35 Gy in 5 fractions to the prostate, 2) patient trans-rectal ultrasounds (TRUS) acquired during fiducial implantation for ARGOS were used for simulated HDR-BT, 3) BT needles were virtually placed within DILs transferred to the TRUS via deformable registration, 4) single-fraction BT plans were produced to boost DILs to 15 Gy while respecting OAR constraints calculated by subtracting the uniform SBRT plan contributions from the ARGOS trial constraints. Dose metrics were extracted from the SBRT and BT plans separately and summed using EQD2 to get simulated "SBRT 30 Gy+BT" and "SBRT 35 Gy+BT" treatment dose metrics. Comparison to the "SBRT-SIB" treatment dose metrics used the Wilcoxon signed-rank test.

Results

For the patient subset, a median DIL GTV volume of 8.4cc was found (median 31.4% of prostate). Figure 1 shows "SBRT 35 Gy+BT" plans achieved near-equivalent DIL boosts compared to "SBRT-SIB" (change in

median ΔGTV_{D95}=0.7 Gy EQD2 lower, p=1.0), with higher whole-prostate coverage for many patients and similar OAR metrics.

The "SBRT 30 Gy+BT" treatment achieved higher DIL boosts than the "SBRT-SIB" plan, as shown in Figure 1 (median GTV_{D95}=165.2Gy vs 138.1Gy EQD2 respectively, p<0.001). The "SBRT 30 Gy+BT" strategy reduced rectum and bladder dose metrics when compared to the "SBRT-SIB" plan, at the expense of higher urethra doses. Prostate PTV_{D95} coverage was lower compared to "SBRT-SIB" (78.2 vs 91.9 Gy EQD2, p=0.56) and D99 values (70.9 vs 87.8 Gy EQD2, p=0.23), though the clinical impact of this is currently unclear. The change in prostate coverage for "SBRT 30 Gy+BT" was highly variable across patients, likely from the unique size and location of DILs per patient.

Conclusions

SBRT with HDR-BT can provide enhanced DIL boost doses compared to SBRT-SIB. The SBRT 35 Gy+BT strategy did not outperform SBRT-SIB. However, SBRT 30 Gy+BT led to a statistically significant increase in DIL doses and improvement in bladder and rectum dosimetry, without significantly reducing dose to the whole prostate. This suggests that SBRT 30 Gy in 5 fractions with BT boost is a promising treatment regimen.

Figures

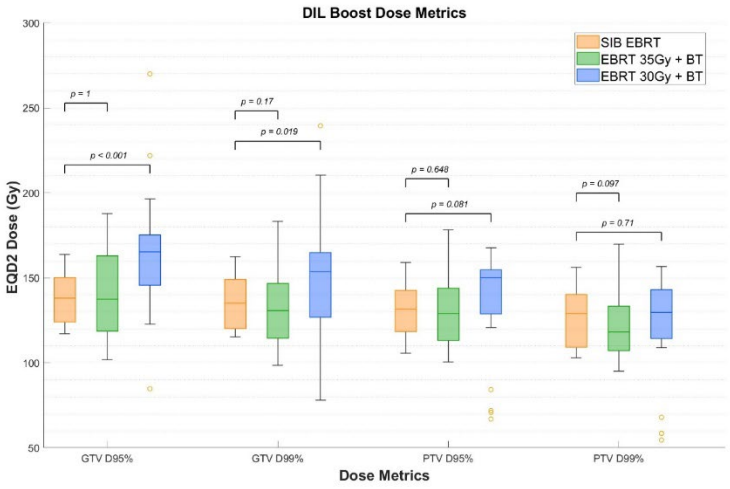

Figure 1: *Comparison of the DIL boost dose metrics across the three treatment schemes. The SBRT DIL PTV margin was 3 or 4 mm, as per the original ARGOS trial protocol [1]. The same PTV was applied for the DILs on the TRUS for the BT plans to account for uncertainty in the transfer of the DIL GTV contours via deformable registration. Most patients had multiple DILs identified, which were combined into a single structure for these dose metrics. Dose metrics per DIL were also analyzed, but are not presented here as they demonstrated similar trends.*

Poster #88

A frame-averaging technique for low-dose volumetric 4D-CT image quality enhancement and motion assessment

Yau T[1,2], Mehrez H[3], S Gaede[1,2]
[1]Department of Medical Biophysics, Western University, [2]London Regional Cancer Program,
[3]Canon Medical Systems

Introduction: Currently, four-dimensional computed tomography (4D-CT) is standard-of-care imaging for thoracic cancers to visualize tumour motion. However, conventional CT scanners are only capable of imaging with a thin axial-field-of-view (aFOV) up to 40mm, making image reconstructions prone to motion artifacts while reproducing only a single respiratory cycle. Comparatively, volumetric 4D-CT (v4D-CT) is capable of imaging with up to a 160mm aFOV, allowing for true dynamic imaging of tumour motion over multiple respiratory cycles free from conventional motion artifacts. However, the extended scan duration and wider aFOV can significantly increase imaging dose to the patient. A low-dose v4D-CT scan may mitigate imaging dose to the patient while allowing for retrospective image quality enhancement via frame-averaging of the 4D dataset. This study investigates the utility of a novel, low-dose, v4D-CT imaging protocol that provides a more robust motion assessment compared to conventional 4D-CT without sacrificing image quality.

Methods: A Catphan 504 phantom and QUASAR motion phantom with Delrin spheres embedded within a cedar insert were imaged on an Aquilion ONE PRISM CT scanner for 1 minute using a 160mm axial-field-of-view and 0.275s rotation time. The Catphan was imaged using an x-ray tube current of 10mA and 300mA, while the QUASAR phantom was imaged at 10mA and 100mA. All Images were reconstructed using a Deep Learning Reconstruction Algorithm with 0.5mm slice thickness. Imaging dose was assessed using a CT dose index ($CTDI_{vol}$). Catphan modules for noise, line-pair resolution, and low-contrast resolution were analyzed. Line-pair resolution was assessed using a modulation transfer function (MTF) and low-contrast visibility was calculated according to the Rose model. The 10mA Catphan images were frame-averaged, and metrics reassessed as functions of number of frames. The QUASAR phantom was imaged during sinusoidal motion with a 2cm peak-to-peak amplitude and a period of 4s. QUASAR inserts were thresholded and the centroid tracked in the 10mA and 100mA scan to verify low-dose motion assessment.

Results: $CTDI_{vol}$ values for the 10mA scans were 28-32mGy, compared to 280mGy and 930mGy in the 100mA and 300mA scan respectively. The extracted motion profiles from the 10mA and 100mA QUASAR phantom datasets were found to be highly correlated ($r^2>0.88$, $p<0.001$). MTFs did not change with frame averaging. CT noise as a function of frames averaged was found to decrease exponentially using a single-term power function ($r^2>0.99$, $p<0.001$), with under 5 frames required to achieve CT noise in the 10mA equivalent to the 300mA scan. Low-contrast visibility scores improved with frame averaging, with no inserts visible initially in the 10mA scan increasing to 8 out of 9 inserts visible in the frame-averaged image.

Conclusion: Motion assessment is feasible using low-dose v4D-CT, with significant image quality improvements observed with retrospective frame-averaging at a fraction of the imaging dose.

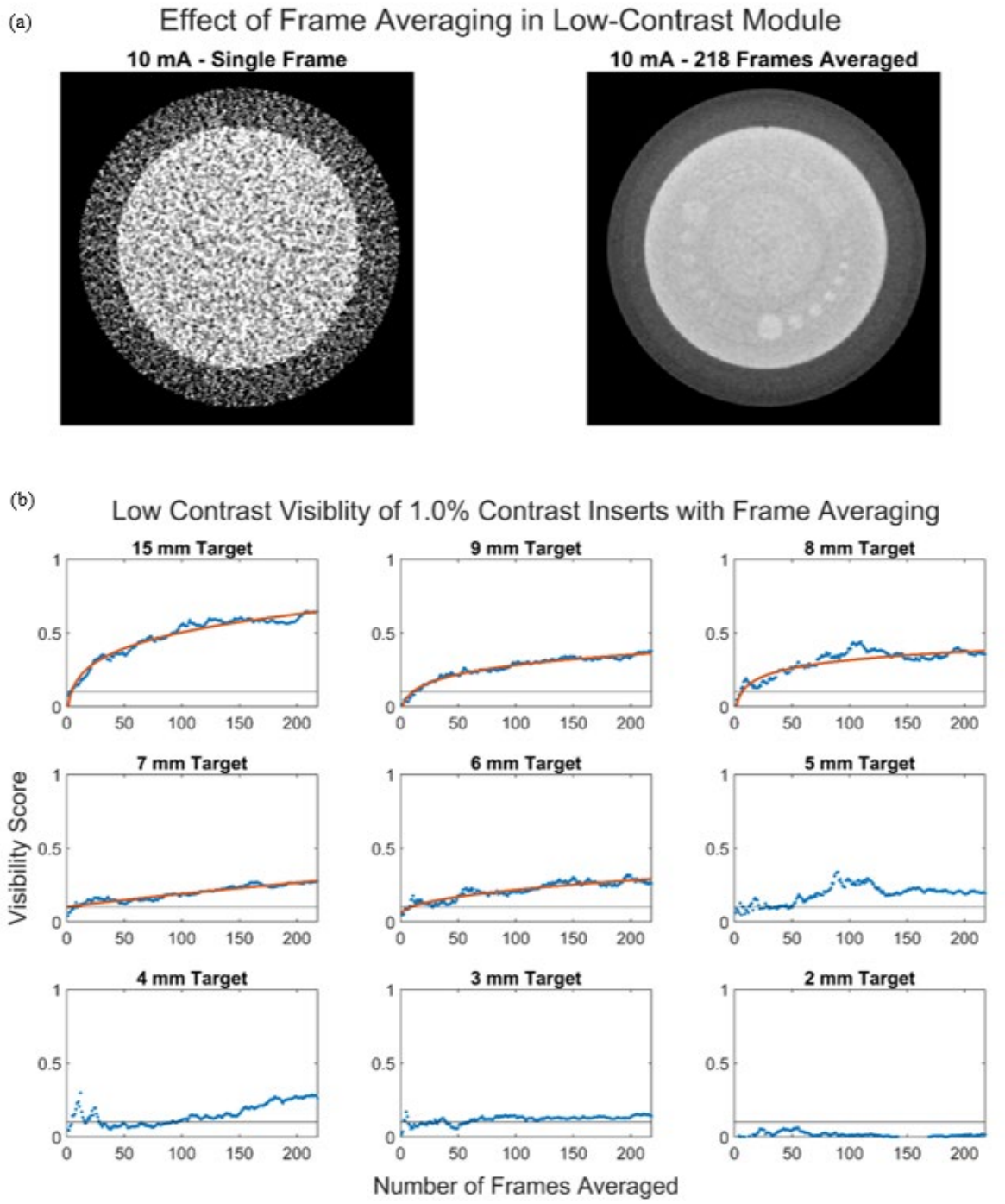

Figure 1: Scans of the low-contrast module before and after frame averaging displayed at a Window Level/Window Width of 20/120 (a). Visibility scores in the 10mA scan as a function of frames averaged is shown in (b), where the horizontal line in each graph identifies the visibility score from the 300mA scan.

Poster #89

The integration of electroanatomic maps into cardiac radioablation treatment planning: A systematic review

Authors: Sarah Konermann, MSc[1], Ian J. Gerard, M.D., PhD[1], Martin L. Bernier, M.D.[1, 2], Tarek Hijal, M.D.[1,2], Gabriela Stroian, PhD[1, 2], Neil Kopek, M.D[1, 2], Joanne Alfieri, M.D.[1, 2], Piotr Pater, PhD[1, 2]
[1]McGill University, Montreal, Quebec, Canada, [2]McGill University Health Centre, Montreal, Canada

Introduction:

Ventricular tachycardia is a life-threatening arrhythmia that can occur secondary to cardiac tumors. Radiation therapy is an emerging treatment modality for this condition. This technique is called cardiac radioablation. Electroanatomic maps are commonly used to delineate clinical target volumes (CTVs) in cardiac radioablation planning; however, radiation oncology treatment planning systems cannot directly integrate electroanatomic data. As a result, various workflows have been developed to guide CTV creation. This systematic review aims to summarize existing protocols for integrating electroanatomic maps into cardiac radioablation treatment planning.

Methods:

A systematic search of PubMed was conducted in January 2024 using relevant keywords. Results were filtered following PRISMA (Preferred Reporting Items for Systematic Reviews and Meta-Analyses) guidelines. Publications were sorted based on their workflow, for example, whether CTV definition is based on a visual comparison of the electroanatomic map to treatment planning images, or whether clinical target volume definition relies on software-based integration of the electroanatomic maps with other images. Software-based methods were further classified by the use of commercial or non-commercial tools.

Results:

The initial search yielded 271 publications, with two additional hand-selected articles added. A total of 85 publications met inclusion criteria and did not meet exclusion criteria. Of these, 53 (62%) describe an unaided side-by-side approach, while 14 (16%) describe a modified side-by-side method, such as using fiducials for guidance. Twenty-five (29%) publications report using software-assisted workflows. Workflow trends remained relatively constant from 2018 to 2023 (Figure 1), with side-by-side comparisons being the most common. Twelve distinct software-based workflows were identified; 10 (83%) of these are compatible with the CARTO electroanatomic mapping system (Biosense Webster, Yokne'am Illit, Israel), and 6 (50%) use 3D Slicer, a free, open-source 3D visualization platform.

Conclusions:

Despite the existence of multiple protocols for integrating electroanatomic maps into cardiac radioablation planning, no standardized approach has been established. As the field evolves, the development of consensus guidelines will be essential to facilitate reproducibility and enable meaningful comparisons across limited clinical datasets.

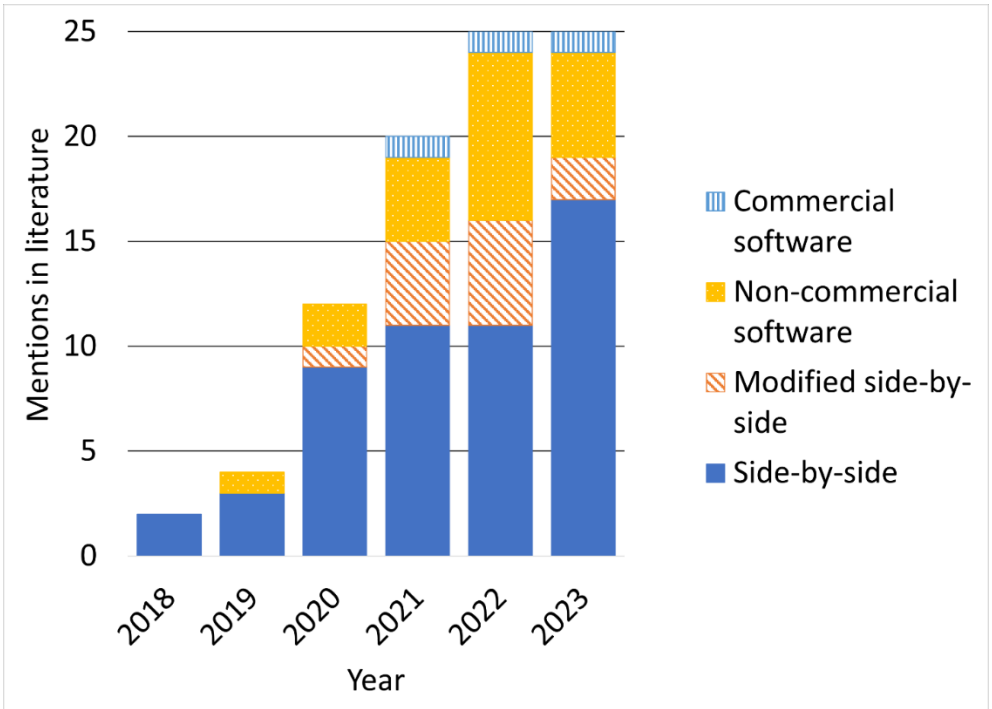

Figure 1: Mentions of clinical target volume definition workflows using electroanatomic maps in literature before January 11, 2024, by workflow type and year published.

Poster #90

A non-invasive artificial intelligence approach to stage esophageal adenocarcinoma

Marcus Milantoni[1], Rahul Nayak[2,3], Richard Malthaner[2,3], Mehdi Qiabi[2,3], & Sarah Mattonen[1,3]

[1]Dept. of Medical Biophysics, [2]Dept. of Surgery Div. of Thoracic Surgery, [3]Dept. of Oncology, Western University

Introduction: Endoscopic resection (ER) provides minimally invasive treatment for managing early stage (T1N0) esophageal adenocarcinoma (EAC). Currently, EAC staging comprises of PET-CT scans to detect metastasis, followed by endoscopic ultrasound (EUS) to assess the tumor size (T stage) and lymph node involvement (N stage). However, EUS is invasive, and has a limited accuracy (30%) in differentiating small superficial lesions suitable for ER. *There is an unmet need to determine the T and N stages directly from the PET-CT scans alone.* Convolutional neural networks (CNNs) offer a promising non-invasive alternative to interpret PET-CT scans, with the potential to stage tumors without the use of EUS. This study aims to assess the efficacy of a CNN based model to classify T and N staging.

Methods: A retrospective study of 164 EAC patients treated with upfront esophagectomy at the London Health Sciences Centre was conducted. Prior to treatment, PET-CT scans were acquired. Ground truth labels were assessed by histopathology of the resected specimen. The dataset was split into 70% training, 15% validation, and 15% testing. Esophageal volumes were auto-segmented, and image pre-processing was applied. A custom 3DConvNeXt model was developed and evaluated using area under the receiver operator characteristic curve (AUC) and accuracy from the unseen testing dataset.

Results: The 3DConvNeXt based model showed strong performance with a validation accuracy of 84%, validation AUC of 0.8, testing accuracy of 84% and testing AUC of 0.72.

Conclusion: The novel 3DConvNeXt model demonstrates potential for classifying EAC based on PET-CT scans alone, with high accuracy in distinguishing superficial lesions suitable for ER. These findings suggest that CNN-based analysis of PET-CT scans could reduce the need for invasive EUS and shorten the time from diagnosis to treatment.

Poster #91

Peptide-based Imaging Agents Targeting Protease-Activated Receptor 2 (PAR2) for Pancreatic Cancer

Cristian Ciciretto[1], Xiao Wen (Kelly) Zhou[1], Lihai Yu[2], Courtney Brooks[2,3], Christopher Pin[1-3], Rithwik Ramachandran[1], John McGuire[1], Len Luyt[1,2]

[1]University of Western Ontario, [2]Verspeeten Family Cancer Centre, [3]Baker Centre for Pancreatic Cancer

Introduction: Pancreatic carcinomas have extremely poor prognoses due to their difficult location, high malignancy, and rapid progression of metastasis. Protease-activated receptor 2 (PAR2) is a proteolytically activated G-protein coupled receptor (GPCR) implicated in a variety of different cancer types including pancreatic cancer, making it an important biological target for diagnostic imaging and therapeutic intervention. Despite this, there are currently no established *in vivo* molecular imaging agents targeting this receptor. One high affinity fluorescent peptide 5-isoxazolyl-cyclohexylalanine-cyclohexylglycine-Ala-Arg-Lys-(Sulfo-Cyanine 5)-NH_2 (**1**; Isox-Cha-Chg-ARK-(Sulfo-Cy5)-NH_2) was designed to target PAR2 for the imaging of prostate cancer cells *in vitro*.[1] This sequence was further modified to incorporate ^{18}F for use in positron emission tomography (PET) imaging.[2] Early *in vivo* studies on wild-type animal models revealed accumulation in multiple organs including the liver, pancreas, and intestines, with predominantly renal clearance.[2] In a new generation of peptides, radiometal-based analogues are being investigated for their therapeutic and diagnostic (theranostic) applications for pancreatic cancer.

Methods: To validate PAR2 as a target for pancreatic cancer, confocal microscopy was conducted on PANC-1 cells using peptide **1**. Cells were incubated with the probe as well as an unlabelled PAR2-targeting peptide to demonstrate receptor selectivity. Five peptides were then designed and synthesized through automated solid-phase peptide synthesis (SPPS). Each peptide had the same binding sequence as **1**, however they were conjugated to a cyclic chelator instead of a fluorescent dye. This allows for coordination of ^{68}Ga for PET imaging, or other radiometals for therapeutic purposes. Each peptide had a linker region between it and the chelator, which consisted of either a hydrocarbon chain or a diethylene glycol chain with zero, one, two, or three glutamic acid residues installed to improve tumor uptake. Peptide radiolabelling with ^{68}Ga was then done through a 30-minute reaction at 85°C.

Results: Peptide **1** bound to the extracellular PAR2 site of PANC-1 cells, which was inhibited upon pre-treatment with high quantities of a non-fluorescent PAR2 inhibitor. Successful peptide radiolabelling was confirmed using reverse-phase high performance liquid chromatography (RP-HPLC), revealing consistent retention times for both the radiolabelled and product standard.

Discussion: Confocal microscopy revealed that **1** was selective for PAR2 within PANC-1 cells, making it a suitable target for PET imaging. To further demonstrate applicability, it is currently being tested using organoid models of pancreatic cancer. Out of the five radiometal-based peptides, those with the highest potencies for PAR2 will move forward for ^{68}Ga radiolabelling and *in-vivo* testing in a PANC-1 xenograft model.

References:

1. LeSarge, J. C.; Thibeault, P.; Milne, M.; Ramachandran, R.; Luyt, L. G. *ACS Med. Chem. Lett.* **2019**, 10(7):1045-1050.
2. LeSarge, J. C.; Thibeault, P.; Yu, L.; Childs, M. D.; Mirka, V. M.; Qi, Q.; Fox, M. S.; Kovacs, M. S.; Ramachandran, R.; Luyt, L. G. *Eur. J. Med. Chem.* **2023**, 246:114989.

Poster #92

Assessment of Therapeutic Efficacy and Biological Effects of ^{225}Ac, ^{177}Lu, and ^{161}Tb in the Treatment of Metastatic Castration-Resistant Prostate Cancer

Shahin Ghaseminejad[1], Danny de Sarno[1], Glenn Bauman[2], Ting-Yim Lee[1]

[1]Department of Medical Biophysics, Robarts Research Institute, and Lawson Research Institute, London, ON

[2]Department of Radiation Oncology, London Health Sciences Centre, London, ON

Introduction: Targeted Radionuclide Therapy (TRT) delivers precise, localized radiation by using radionuclide-conjugated ligands that selectively bind to tumor-specific receptors, maximizing cytotoxic effects while minimizing damage to healthy tissue. It has been accepted as a standard-of-care treatment for neuroendocrine tumors (NETs) and metastatic castration-resistant prostate cancer (mCRPC). The current radionuclide of choice, ^{177}Lu, is a beta emitter. However, alpha emitter ^{225}Ac and Auger electron emitter ^{161}Tb can potentially be more effective because of their higher linear energy transfer (LET) and shorter ranges. The DNA within the nucleus is the primary target, and the desired clinical outcome is achieved by inducing different types of DNA lesions, such as single and double-strand breaks (SSBs & DSBs) and complex DSBs within this molecule, leading to cell death. Depending on the type and range of radiation, DNA lesions are induced both within the source-containing cell and in neighboring cells, a phenomenon known as the crossfire effect. To quantitatively evaluate this effect, we propose the Biological Effective Cell Kernel (BECK), a novel approach for computing DNA breaks from radionuclides in cells. Moreover, we compared the therapeutic efficacy of ^{177}Lu, ^{225}Ac chain, and ^{161}Tb by estimating the number of direct DNA breaks using the BECKs from the corresponding radionuclides.

Methods: An average prostate cellular fraction (CF) of 0.24 was obtained in six prostate cancer patients using CT Perfusion. A cell model was constructed using 20µm diameter spheres with 8µm diameter nuclei and 26µm center-to-center distance, resulting in 0.24 CF. The TOPAS-nBio Monte Carlo Tool was used, and radioactive sources were distributed randomly based on the clinically administered activity within the cytoplasm of a cell, and the Biological Effect Cell Kernel (BECK) was generated by scoring the DNA breaks (DNABs) with the DBSCAN algorithm in the source-containing cell, and the non-radioactive cells at various distances. DNA break maps from self-irradiation and the crossfire from neighboring cells were generated by convolving the BECKs with the cell model's time-integrated activity (TIA). Finally, DNAB maps were used to compare the effective ranges and therapeutic efficacy of the radionuclides.

Results: Self-irradiation double-strand breaks (DSBs) per source were 48, 0.022, and 0.083 for ^{225}Ac, ^{177}Lu, and ^{161}Tb. Complex DSBs showed values of 32, 0.019, and 0.073, respectively. As shown in Figure 1, accounting for the crossfire effect, DSBs increased to 140, 69, and 109 for ^{225}Ac, ^{177}Lu, and ^{161}Tb, and Complex DSBs showed values of 74, 60, and 96. The crossfire contribution was estimated as ~42% for ^{161}Tb, and ~75% for ^{225}Ac and ^{177}Lu. The maximum ranges were also ~85µm for ^{225}Ac, ~150µm for ^{177}Lu, and ~110µm for ^{161}Tb.

Conclusions: ^{225}Ac had ~2000 times the DNABs compared to ^{161}Tb or ^{177}Lu per source. ^{161}Tb is nearly four times more effective than ^{177}Lu in causing DNABs. Treatment of macrometastases (i.e., visible lesions more than 3-5 millimeters) can be expected to be more reliant on crossfire contributions than micrometastases. ^{177}Lu, with the highest crossfire effect and the lowest induced DNABs, is more suitable for macrometastases treatment, while ^{161}Tb or ^{225}Ac are more suitable for micrometastases.

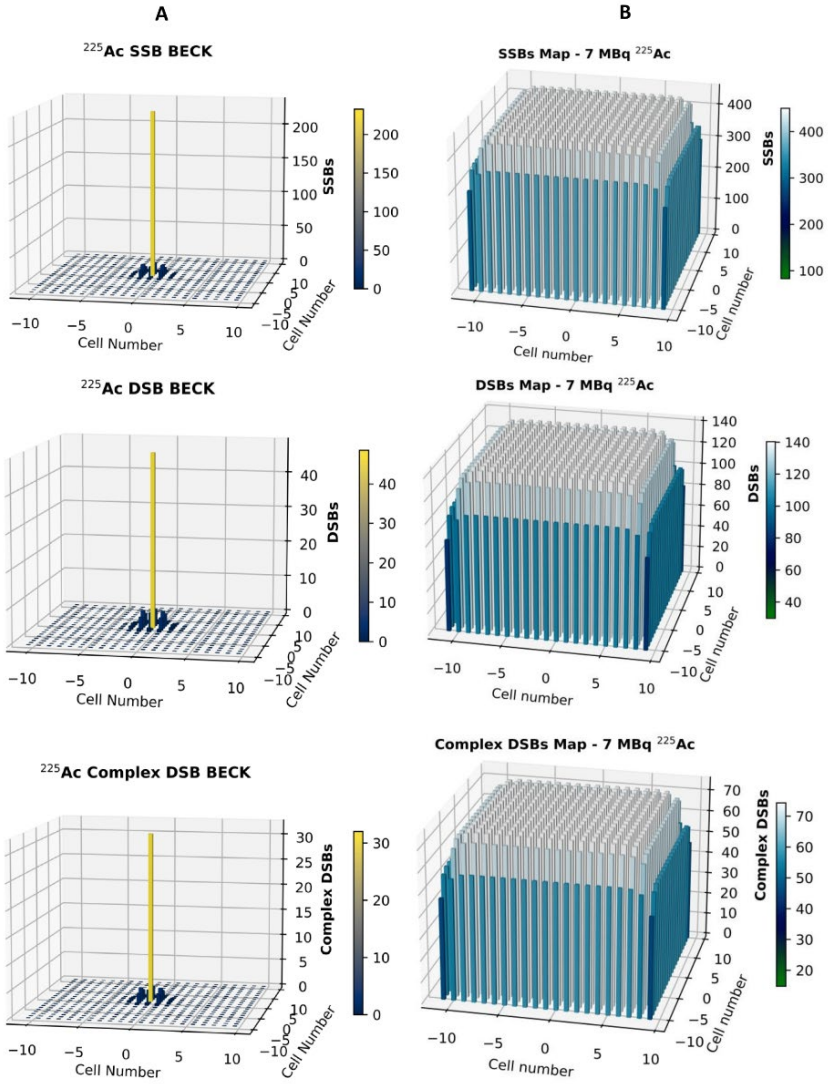

Figure 1. A cross-section of the isotropic 3D Biologic Effect Cell Kernel (BECK) for ^{225}Ac (column A), and the cell model's DNA lesion map obtained by convolving the 3D BECK with the 3D cell model's TIA map (column B).

Poster #93

Simultaneous Assessment of Pulmonary Ventilation and Perfusion Using Dynamic CT Imaging

Ahmed S. Mohamed[1], Stewart Gaede[1,3,4], Ting-Yim Lee[1,2,3,5]

Affiliations:

[1] Medical Biophysics, The University of Western Ontario, London, ON, Canada

[2] Robarts Research Institute, The University of Western Ontario, London, ON, Canada

[3] Imaging Program, Lawson Health Research Institute, London, ON, Canada

[4] Medical Physics, The Verspeeten Family Cancer Centre, London, Ontario, Canada

[5] Medical Imaging, The University of Western Ontario, London, ON, Canada

Introduction: Lung cancer remains the leading cause of cancer-related mortality worldwide, with non-small cell lung cancer (NSCLC) accounting for approximately 80–85% of all cases. Accurate assessment of lung ventilation and perfusion is crucial in NSCLC treatment planning to estimate postoperative lung function, identify non-functional segments for resection, and guide radiation therapy to target cancerous areas while preserving healthy tissue. The conventional method for evaluating ventilation and perfusion involves nuclear medicine ventilation-perfusion (V/Q) scans, which require two separate procedures and have limitations such as low spatial resolution, time-consuming protocols, temporal mismatch between ventilation and perfusion assessments, and qualitative or semi-quantitative evaluation. There is a growing need for a better alternative to the conventional lung V/Q scan. Computed tomography perfusion (CTP) imaging offers high spatial resolution and rapid acquisition but is limited to assessing pulmonary perfusion only. In this study, we are extending our analysis algorithm to simultaneously image lung ventilation and perfusion from a single CT Perfusion scan.

Methods: Four anesthetized pigs in the supine position were mechanically ventilated (3-second breath cycle) and scanned over 40 s using a CTP protocol, acquiring six lung volumes per respiratory cycle (0.5 s intervals) to generate tissue density curves (TDCs). These TDCs—shown in Figure 1—integrate three dynamic components: (1) perfusion (contrast-enhanced pulmonary blood flow), (2) ventilation (cyclic alveolar air-volume changes), and (3) involuntary motion (cardiac/respiratory bulk displacement). To isolate ventilation and perfusion, non-rigid registration was applied to correct motion artifacts, followed by JWL model deconvolution with the pulmonary artery TDC to estimate and subtract perfusion, yielding the ventilation curve. Fourier transform then quantified ventilation amplitude/frequency, while perfusion metrics were derived directly from deconvolution.

Results: The Fourier transform of the ventilation curves revealed a dominant amplitude component at 0.35 Hz in agreement with the controlled ventilation rate of 0.33 Hz. Ventilation amplitude and trough-to-peak values were higher in the posterior lung segments compared to the anterior, consistent with gravitational effects in the supine position favoring posterior lung ventilation due to greater alveolar expansion in dependent regions. Similarly, JWL deconvolution-derived perfusion maps revealed higher posterior perfusion, aligning with gravitational blood flow distribution

Conclusion: This study demonstrates the feasibility of extending CTP analysis to assess lung ventilation and perfusion simultaneously. In the future, we plan to compute voxel-based maps to evaluate ventilation and perfusion at 2-3 mm resolution spanning the whole lung volume captured by the imaging protocol. Validation with stable xenon CT for ventilation and ^{68}Ga-MAA PET for perfusion is also planned.

Fig 1

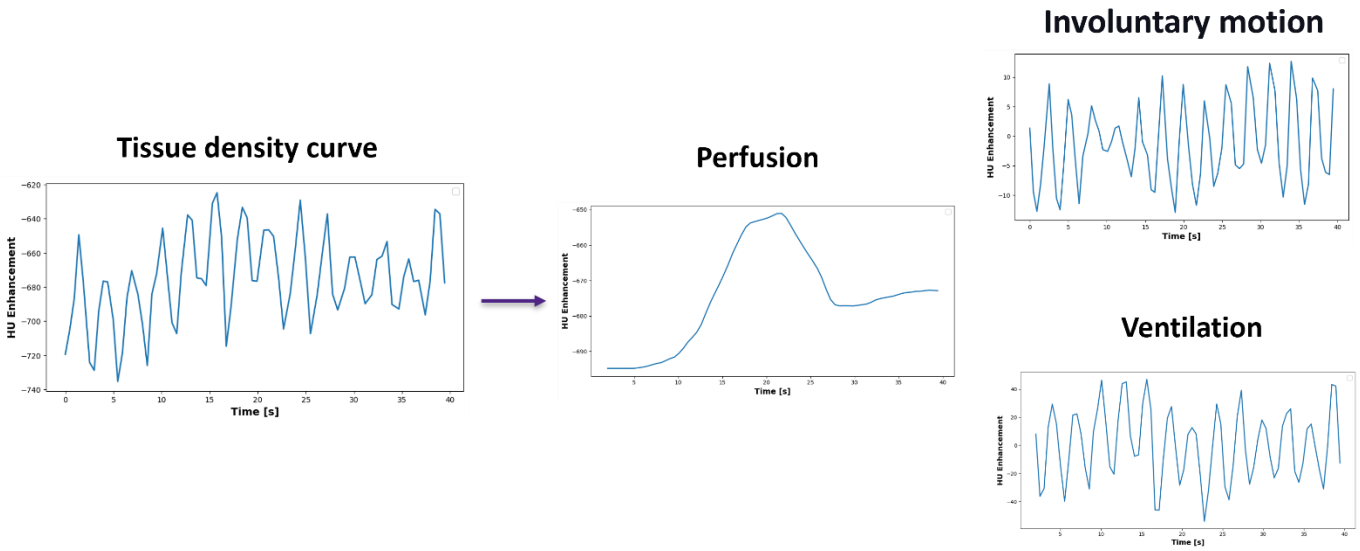

Poster #94

Risk stratification of early-stage non-small cell lung cancer using PET-based radiomics

Christine A. Santiago[1], Viswam Nair[2], Sarah A. Mattonen[1]
[1]Department of Medical Biophysics, Western University, London, Ontario
[2]Clinical Research Division, Fred Hutchinson Cancer Center, Seattle, Washington

Introduction: Lung cancer is the most common cause of cancer death worldwide with non-small cell lung cancer (NSCLC) accounting for 85% of lung cancer patients. Surgery with a curative intent is the standard of care treatment for early-stage NSCLC (stage I-II). However, it is estimated that 30-55% of lung cancer patients will have a recurrence within 5 years after treatment. To prevent recurrence, adjuvant therapy, can be given after surgery such as chemotherapy, radiation therapy, and immunotherapy. However, there is the risk of severe side effects or toxicity. Currently, the decision to give a patient adjuvant therapy depends on several factors such as the stage of the cancer, the patient's age, symptoms, and medical history. To determine the stage and extent of the disease, medical images are taken prior to treatment including computed tomography (CT) and ^{18}F-fluoro-2-deoxy-D-glucose (^{18}F-FDG) positron emission tomography (PET). PET-based radiomics and machine learning can extract information not visible to the human eye and potentially aid in risk stratification. The aim of this ongoing study is to train, test and externally validate a PET-based radiomic model to predict time to recurrence.

Methods: Our dataset included 300 patients with early-stage NSCLC from the Verspeeten Family Cancer Centre who have undergone surgical resection. ^{18}F-FDG-PET scans were performed prior to surgery. The regions-of-interest (ROIs) we analyzed were the tumour and a 1cm expansion of the tumour contoured using a semi-automatic segmentation tool in MIM Software. Radiomic features were extracted using PyRadiomics 3.1.0. Features included shape-based features (n = 14), first-order statistic features (n = 18), and second-order features (n = 73). The clinical features (n = 4) included were age, sex, overall stage, and primary surgery. This resulted in a total of 109 features for analysis. The dataset was split into independent training (70%, n = 210) and testing sets (30%, n = 90). We built a random survival forest to predict time to recurrence in the training set. Concordance was used to measure the model performance in the training and testing cohorts.

Results: The number of patients that had a recurrence was 103 (n = 72 (70%) in the training set and n = 31 (30%) in the testing set). The top performing feature was overall stage, followed by second-order gray level dependence matrix texture features from the peri-tumoural ROI and gray level co-occurrence matrix texture features from the tumour ROI. A concordance of 0.768 and 0.612 was achieved in the training and the testing sets respectively.

Conclusion: These preliminary results demonstrate a PET-based radiomics model can identify patients with low- and high-risk of recurrence. Ongoing work in this study involves a performance comparison to clinical features and increasing the dataset size. Future work includes implementing both diagnostic CTs, analyzing additional regions of interest, and comparing the performance of our machine learning model to a deep learning model. This has the potential to be used as a risk prediction tool to aid clinicians in deciding if a patient would benefit from a more aggressive treatment plan.

Poster #95

Magnetic Particle Imaging Lymphography: assessing superparamagnetic iron oxide nanoparticles for sentinel lymph node detection

Nitara E. Fernando[1,2], Olivia C. Sehl[3], Benjamin D. Fellows[3], and Paula J. Foster[1,2]

[1]Department of Medical Biophysics, University of Western Ontario, London, ON, Canada,
[2]Cellular and Molecular Imaging Group, Robarts Research Institute, London, ON, Canada
[3]Magnetic Insight Inc., Alameda, CA, United States

Introduction: During metastasis, tumour cells drain to nearby lymph nodes, the first of which are named the sentinel lymph node(s) (SLN). SLN biopsy (SLNB) determines if metastasis has occurred. Traditionally, SLNB involves injecting a Technetium-labeled tracer peritumourally, pre-operative imaging with SPECT to locate the SLN, and surgery guided by a gamma probe to remove them. Limitations include short tracer half-life which can make scheduling the SLNB difficult, and radiation dose to patients and healthcare workers. Alternatively, magnetic localization, with superparamagnetic iron oxide nanoparticles (SPIONs) as the tracer and a magnetometer to detect SPIONs in the SLN during surgery can be used, however, this lacks pre-operative imaging.

Magnetic Particle Imaging (MPI) directly detects SPIONs, holding potential for pre-operative imaging in magnetic SLNB. To develop MPI lymphography, it is essential to determine the optimal SPIONs for SLN mapping. Tracer characteristics (size, shape, coating, sensitivity, resolution) play a role in SLN detection. Answering questions related to the timing of SPIO drainage to SLN and the persistence of signal are important for implementation into a clinical workflow. This study assesses the in vivo pharmacokinetics for SLN mapping with MPI in a murine model, using five commercially available SPIONs.

Methods: Sensitivity of each SPION was measured using MPI Relaxometry. Next, the in vivo pharmacokinetics of each SPION was investigated. Nu/nu mice were administered 0.8 mg/kg of SPION **(**n=4 for each; **Table 1)** intradermally to the left footpad, modeling an established drainage pathway from the footpad to the popliteal node (pLN), defined as the SLN in this model. Mice were imaged with MPI 20 min post-injection, to determine a baseline signal, and 4, 24, and 192 hr post injection to quantify signal to the SLN. Full body MPI scans (5.7 T/m, x=13mT, z=20mT) were acquired at each timepoint. The percentage of initial injected dose (%ID) that reached the SLN was determined for each timepoint. At endpoint pLNs and higher echelon nodes (HENs) were excised for ex vivo MPI and histology.

Results: Synomag D has the highest particle sensitivity, as measured with MPI relaxometry (**Figure 1A**). Synomag D also has high signal in the SLN (**Figure 1B, C**). VivoTrax+, which demonstrates higher particle sensitivity than VivoTrax due to its larger iron core sizes (**Figure 1A**), has no detectable drainage to the SLN in vivo (**Figure 1B**). Coating effects were evaluated for Synomag-D (plain, PEG, PEG-Mannose). Sensitivity decreased with PEG and PEG-Mannose coatings, but SLN signal remained similar. However, plain and PEG-coated SPIONs showed higher HEN signal than PEG-Mannose-coated SPIONs. Ex-vivo MPI and histology confirmed SPION presence in SLNs, except for VivoTrax+.

Conclusions: This work is the first to present differences in lymphatic drainage of commercially available SPIONs using MPI. Synomag-D tracers provide higher MPI signal at the SLN and show the potential to detect the echelon nodes. Assessing the status of HENs may help to identify which cancer patients require invasive lymph node dissections. This study highlights the importance of an in vivo assay for evaluating tracers.

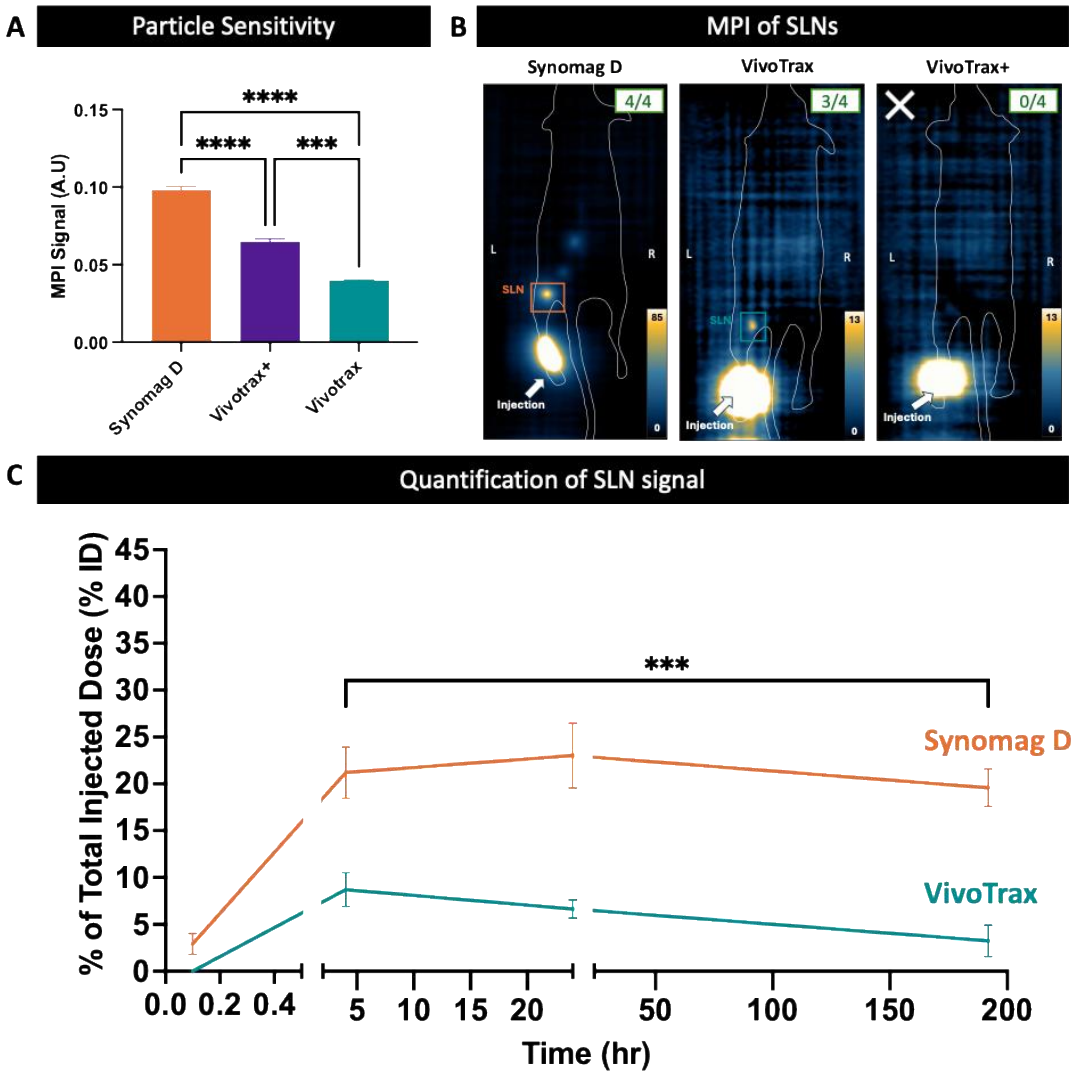

Figure 1. Comparing iron core sizes. (A) Particle sensitivity for MPI was assessed for three core nanoparticles, Synomag-D, VivoTrax, and VivoTrax+ using MPI Relaxometry. (B) A representative MPI for one mouse from each SPION at 4 hours post injection is shown. The arrow denotes the injection site (left footpad) and a box is drawn around the location of the SLN. For Vivotrax+ the SLN was not detected in full body scans, denoted by the white X. On the top right corner of each image, a box with a fraction denotes the number of mice for which MPI signal was detected at the 4 hour imaging time point. For Synomag D, SLN signal was detected for 4/4 mice, for Vivotrax SLN signal was detected for 3/4 mice and for VivoTrax+ 0/4 mice had SLN signal. (C) Signal to sentinel lymph node for each SPION was quantified over time as %ID. Signal in the SLN was not quantifiable for any mice injected with VivoTrax+. %ID for mice administered with Synomag D was significantly higher than those injected with Vivotrax ($p<0.001$).

Poster #96

Characterization of MRI Performance for Radiotherapy and the Potential for Mid-Field MRI

Farley Chicilo[1], Steward Geade[1], Eric Lessard[1]
[1]Vespeeten Family Cancer Program, London Health Sciences Centre, London, ON, Canada

Purpose:

MRI offers superior soft tissue contrast, making it an essential tool in radiation therapy planning. However, accurate planning requires an understanding of image quality limitations, particularly geometric distortion, signal-to-noise ratio (SNR), and spatial resolution, all of which are influenced by magnetic field strength. Many radiotherapy departments do not have access to dedicated MRI simulators and instead rely on shared diagnostic scanners, thereby limiting patient access. Mid-field MRI systems (<1T), such as the 0.55T Freemax, are emerging as cost-effective alternatives due to their reduced siting requirements, lower operational costs, and larger bore sizes [1,2]. These advantages may help expand MRI accessibility in community-based or mobile care settings. However, evaluation is needed to confirm clinical suitability. This study aims to characterize MRI image quality at 1.5T to set a baseline for planned comparisons with a 0.55T system using the Magphan RT phantom, in order to assess changes across field strengths and determine implications for different radiotherapy treatment sites.

Methods:

A modular, liquid-filled Magphan RT phantom (Phantom Laboratory) [3] was scanned using clinical brain and pelvis MRI sequences at 1.5T with adjusted fields of view to ensure full phantom coverage. Smári software was used to assess image quality metrics including geometric distortion, in-plane resolution, SNR, slice thickness, and signal uniformity [4]. The phantom's features, (fiducial spheres, slice thickness ramps, resolution apertures, and uniform background fill) enable evaluation of each metric. Measurements were collected using a 1.5T system over a six-month period to evaluate consistency and serve as a baseline for comparison. Data collection using a 0.55 T system is ongoing.

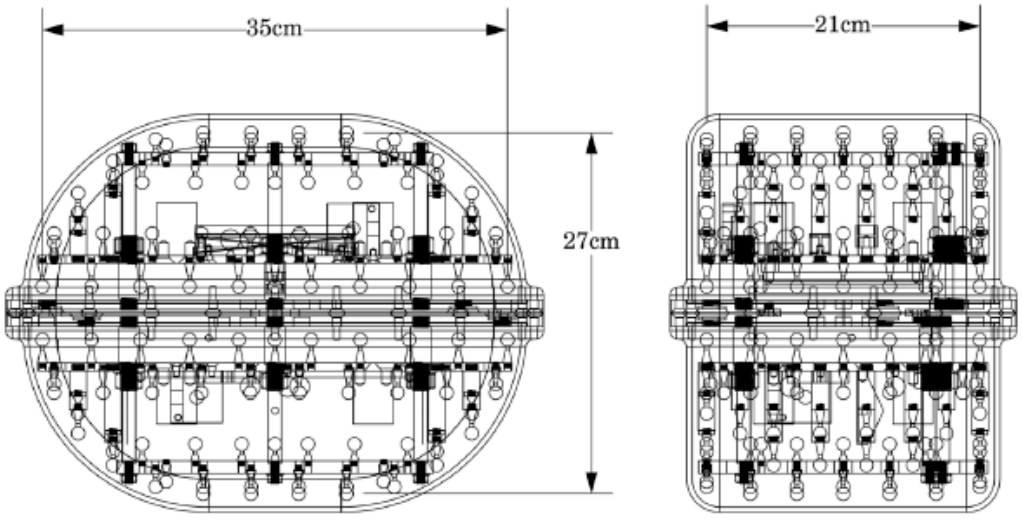

Figure 1 Diagram of Magphan RT [3]

Results:
At 1.5T, image quality metrics were reproducible across a six-month measurement period. Geometric distortion increased radially as expected, while resolution, SNR, slice thickness, and signal uniformity remained within clinical tolerances and showed acceptable variation. These measurements establish a reliable baseline for further comparison. Data collection at 0.55T using the Freemax system is currently underway, with initial imaging protocols in development to enable direct performance comparisons.

Conclusions:
Image quality characterization at 1.5T demonstrates consistency over time and provides a benchmark for evaluating lower field strength systems. Planned assessments at 0.55T aim to quantify the trade-offs between improved geometric accuracy and potential reductions in SNR and resolution, which are expected at mid-field strengths. While protocol optimization and data collection at 0.55T are ongoing, this work lays the groundwork for defining the role of mid-field MRI in radiotherapy planning and guiding future protocol development for broader clinical implementation.

References

1. University of California, San Francisco. "The Promise of Mid-field MRI." UCSF Radiology Blog. Accessed December 11, 2024. https://radiology.ucsf.edu/blog/promise-mid-field-mri

2. Varian Medical Systems. "Breaking Barriers in MRI for Radiotherapy: Henry Ford Health." Varian Blog. Accessed December 11, 2024. https://www.varian.com/resources-support/blogs/breaking-barriers-mri-radiotherapy-henry-ford-health

3. Phantom Laboratory. Magphan RT Phantom Product Guide. Copyright © 2024.

4. Phantom Laboratory. "Magphan Overview.". Accessed December 11, 2024. https://help-smari.phantomlab.com/hc/en-us/articles/360046599934-Magphan-Overview#h_4749ef74-3f19-488e-ae86-ce4fe301d234

Poster #97

Developing an optimization tool for SGRT simulation in silico: a validation study

Haoyue Guo[1, 2], Timothy Yau[1, 3], Stewart Gaede[1, 3], John Patrick[1, 3], Rob Stodilka[1, 3]
[1]Verspeeten Family Cancer Centre, London Health Sciences Centre;
[2]Department of Physics and Astronomy, University of Waterloo;
[3]Departments of Medical Biophysics, Schulich School of Medicine & Dentistry, Western University

Introduction: Surface-Guided Radiation Therapy (SGRT) is an emerging, markerless alternative, technique used for patient setup and motion tracking during external beam radiation therapy. The technique often uses three ceiling-mounted cameras to monitor a user-defined region-of-interest (ROI) on a patient's surface during radiotherapy. However, the ROI must be placed carefully to ensure cameras are unobstructed by linear accelerator (linac) gantry rotation during treatment. ROI placement is challenging since three cameras must be considered simultaneously, which can result in instability during treatment. We have developed a software tool for surface-blockage simulation to guide ROI placement, ensuring camera visibility during complete gantry rotation.

Method: A software was developed to compute SGRT blockage based on knowledge of 3D camera positions, gantry dimensions, DICOM-derived patient surface, and treatment isocenter. A prediction plot was computed to display angles where cameras are blocked by the gantry head. This plot is then used to predict all patient surface points observable by any two cameras at all gantry angles. We validated our method using an in-house, anthropomorphic torso phantom, an AlignRT installation, and a Varian TrueBeam linac. To verify camera blockage prediction, the software was run using the coordinates of the shifted auxiliary cameras and the angles at which the gantry began to block the phantom were noted for each camera pod. To verify the unobstructed patient surface points prediction, ROIs were placed in two locations - one expecting obstructions and one expecting no obstructions. The gantry was then rotated throughout the entire rotational range of 360° to test SGRT fidelity based on the stability of ROI measurements. A deviation within 2° was judged as within the margin of error for radiotherapy.

Results: Experimental results for camera blockage by linac gantry for the symmetrical lateral cameras were 3.5°-106.5° and 356°-251.5°, and simulated results were 3°-105° and 356°-253° respectively. Both experimental and simulated results showed no blockage for the central camera. The measured blockage was within the accepted range of 2 degrees deviation.

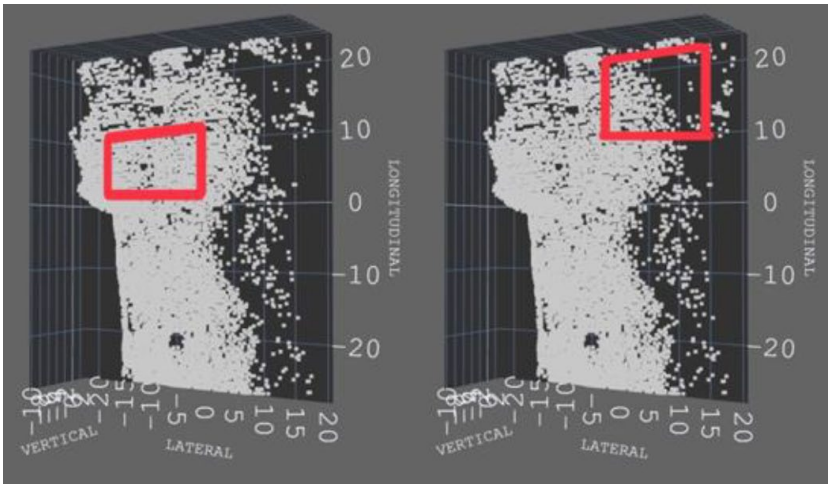

FIG. 2 Unobstructed surface points simulated from the software program

The predicted unobstructed surface points plot in FIG. 2 showed that the center of the chest was dense in points relative to other areas such as the sides of the abdomen, making it an unobstructed area. Comparatively, the empty area to the upper right of the pectoralis major indicates that it was blocked by at least two cameras over some subtended arc, making it an obstructed area. When the ROI was drawn on the center of the chest, AlignRT remained functional for the entirety of the 360° rotation. When the ROI was drawn on the upper right of the pectoralis major, AlignRT stopped measurement from 19°-96°, which is within the simulated blockage angles of 3°-105°.

Conclusions: We created a novel software capable of generating 3D plots of SGRT-camera blockage in real-time (<3 minutes) with an accuracy within 2 degrees. This software will help ROI delineation for SGRT, improving the stability of intrafraction surface monitoring for external beam radiotherapy.

Poster #98

Ongoing Perfusion and Glucose Metabolic Rate Imaging Study using ^{18}F-FDG PET to Differentiate Brain Metastasis Outcomes Post Stereotactic Radiosurgery

Danny De Sarno[1], Melody Qu[2], Glenn Bauman[2] and Ting-Yim Lee[1,2]
[1] Medical Biophysics, Western University, [2] Oncology, London Health Sciences Centre (LHSC)

Introduction: Brain metastases (BMs) affect up to 40% of cancer patients. Standard care involves stereotactic radiosurgery (SRS) with serial MRI for follow-up after treatment. MRI-based post-SRS assessment has variable accuracy, particularly distinguishing treatment related changes from tumor progression. While amino acid PET tracers outperform MRI in making this distinction, their cost and limited availability restrict use. We propose an alternative: dynamic FDG-PET to simultaneously measure glucose metabolic rate (GMR) and perfusion via a novel deconvolution method. Although FDG alone is inferior to amino acid tracers with semi-quantitative SUV analysis due to high background uptake in normal brain tissue, we hypothesize that combining GMR with cerebral blood flow (CBF) will improve diagnostic precision. Specifically, we will test using the metabolic-perfusion ratio (MPR = GMR/CBF) to differentiate post-SRS outcomes: unchanged MPR indicates recurrence, decreased MPR reflects treatment effect, and increased MPR suggests pseudo-progression—critical distinctions for guiding further therapy.

Methods: The ongoing BrainMets trial (single-arm phase II diagnostic study) will test our hypothesis by enrolling 70 patients with brain metastases (BMs) treated via SRS or fractionated stereotactic radiotherapy (FSRT). Each participant will undergo dynamic FDG-PET imaging at three critical timepoints: baseline (pre-treatment), 10 weeks post-treatment, and at suspicion of recurrence (triggered by routine MRI) or 12-month follow-up. Scans will be performed on the OMNI Legend PET/CT (GE Healthcare) at high temporal resolution (2-second intervals) to simultaneously quantify glucose metabolic rate (GMR) via Patlak analysis (adjusted for blood glucose levels) and cerebral blood flow (CBF) using our bespoke flow-modified 2-tissue compartment model (F2TCM). These metrics will generate the metabolic-perfusion ratio (MPR = GMR/CBF) for both tumor and contralateral regions. Tumor states (recurrence, pseudo-progression, or necrosis) will be determined through clinical follow-up or biopsy when available. Finally, receiver operating characteristic (ROC) analysis will compare the diagnostic accuracy of our MPR approach against standard clinical measures including MRI to assess its potential as a superior tool for guiding post-SRS clinical decisions.

Results: So far, we have recruited 2-patients into the trial and both have had their baseline scan. The mean$\pm$stdev GMR, CBF and MPR in the primary brain lesion were 3.2 ± 1.7 $\mu mol/min/100g$, 11.4 ± 1.0 $mL/min/100g$, and 0.29 ± 0.18 $\mu mol/mL$ respectively. The mean$\pm$stdev GMR, CBF and MPR in the region contralateral to the tumor were 8.4 ± 6.5 $\mu mol/min/100g$, 62.6 ± 70.9 $mL/min/100g$, and 0.21 ± 0.14 $\mu mol/mL$ respectively. No statistical significance can be drawn yet due to the limited number of patients analyzed. Importantly, a 34-43% increased MPR in the tumor compared to the contralateral normal brain indicates a mismatch in supply (perfusion) and demand of oxygen (GMR) suggesting potential tumor hypoxia.

Discussion: Accurate assessment of treatment response and disease progression is challenging for BMs. Using dynamic FDG PET to determine perfusion and glucose uptake may address this challenge. This research has the potential to inform clinical decision-making and improve patient outcomes.

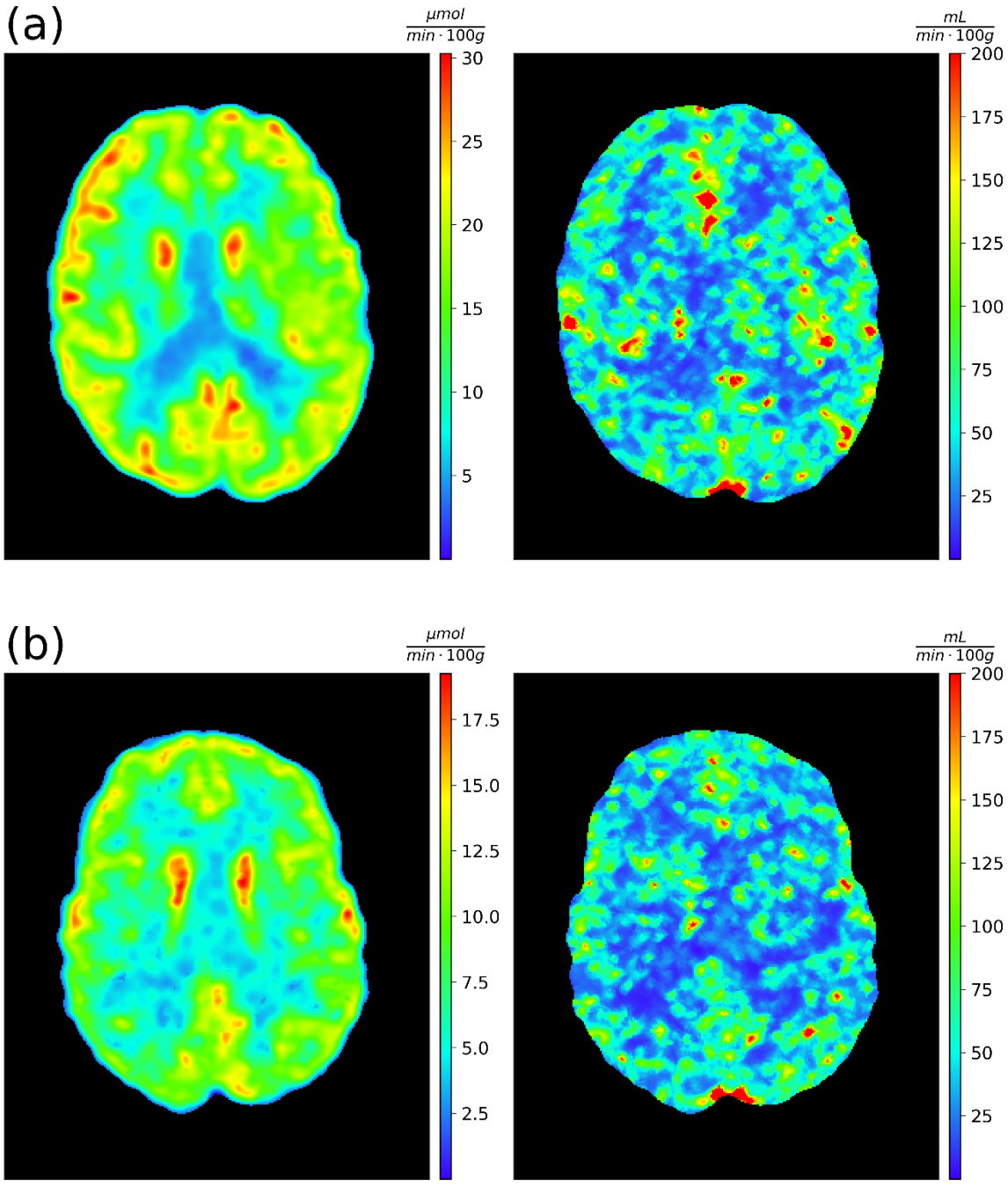

Figure 1. Functional maps for brain metastases. (a) patient 1 and (b) patient 2. Left map: glucose metabolic rate (GMR), Right map: cerebral blood flow (CBF)

Poster #99

Mathematical Modelling of In-vitro Live Cell Imaging to assess Radiation Sensitivity of Pancreatic Ductal Adenocarcinoma

Sophie Heinrich[3], Ye Shen[1,2,7], Christopher Pin[1,2,5,6,7], Eugene Wong[3,4,5]

Departments of [1]Physiology and Pharmacology, [3]Physics & Astronomy, [4]Medical Biophysics,[5]Oncology, and [6]Paediatrics, Schulich School of Medicine and Dentistry, University of Western Ontario, [7]Baker Centre for Pancreatic Cancer, [2]Verspeeten Family Cancer Center, London, Ontario, Canada

Introduction: The most prevalent type of pancreatic cancer is pancreatic ductal adenocarcinomas (PDAC), which develop in the pancreatic ducts. Currently, PDAC tumours are the third leading cause of cancer death in Canada. To gain insights, mathematical models have been used to describe these mechanisms and predict cancer cell behaviour. In this study, we aimed to develop a mathematical model to describe the growth dynamics of patient-derived PDAC cells in-vitro to assess their radiation sensitivity. Specifically, we aimed to extract patient-specific radiation sensitivity parameters based on longitudinal live cell imaging over 3 days. The goal is to test using extracted patient-specific radiation sensitivity to facilitate the development of personalized treatment plans.

Methods: A compartment model was established with three populations, representing proliferating (G1/S, G2/M) and death (removed) cells. To distinguish the different compartments, we analyzed PDAC cells at different stages in the cell cycle using live cell-imaging (Sartorius IncuCyte S3 Live Cell Analysis System), which imaged PDAC cell growth hourly over 3 days. Radiation sensitivity was assessed in three patient-derived 2D PDAC cell lines (PDAC021T, PDAC001T, and PDAC013T) with a dose of 4 Gy.

Specifically, for cell cycle analyses, cell images were analyzed using the OpenCV Python library, enabling detailed examination of individual nuclei in live-cell imaging. This analysis yielded metrics including average integrated saturation and nuclear area, which informed the identification of cell cycle stages (G1/S, G2/M) based on DNA content estimates (haploid vs. diploid). We then employ the population of cells in each cell cycle in the PQS model to extract cell growth and death rates in irradiated versus unirradiated cells.

Results: Based on the ratio of the total cell count at day 3, PDAC021T is identified to be most resistant to radiation, PDAC001T is the most sensitive, while PDAC013T is intermediate. After 4 Gy of radiation, the carrying capacity in the model dropped to 70% in the resistant line compared to 30% for the sensitive line. The cell division rate (G2/M to G1) increased by 43% while the G1/S to G2 rate decreased by 72% in the sensitive line. On the other hand, the cell division rate (G2/M to G1) decreased by only 2% while the G1/S to G2 rate increased by 2% in the resistant line. The extracted parameters from the cell cycle model indicated that the average time spent in G1/S increases post-radiation treatment for the radiation sensitive line, but remain practically unchanged in the resistant line.

Discussion: Our data shows that the mathematical compartmental modeling can distinguish patient-specific cell growth differences with or without radiation treatment. Further refinement and additional cell line testing is needed, but this initial work showed promise in using longitudinal live cell imaging for assessing patient-specific radiation sensitivity. Live cell imaging is becoming commonly available and such mathematical analyses will add value to tracking total cell counts. Work is underway to compare results from this approach against clonogenic assay (current gold standard) which is a simpler assay, with a different endpoint (ability to form clonogens rather than growth/death), but lacks cell cycle information.

Poster #100

Evaluating Lung Lesion Approximation for Workflow Optimization in AI-Assisted SABR Planning for Metastatic Cancer

Jiahai Zhou[1,3], Edward Wang[1,3], Sarah Mattonen[1,2,3]
[1]Department of Medical Biophysics, [2]Department of Oncology, Western University, London, ON, Canada
[3]Baines Imaging Research Laboratory, Verspeeten Family Cancer Centre, London, Ontario, Canada

Introduction:

As metastatic disease progresses, patients often develop multiple lung lesions. Stereotactic ablative radiotherapy (SABR) delivers high-dose radiation to treat these lesions simultaneously, offering survival benefits. Currently, creating a suitable radiation plan takes roughly 8 to 24 hours depending on treatment complexity primarily due to the number and location of targets. Radiation oncologists do not know whether a treatment plan can be created for a given patient. After multiple attempts, it may be found that a patient can not be treated with SABR. This leads to wasted resources and delays the patient in receiving alternative therapies. The Mattonen Lab previously developed an artificial intelligence (AI) model for real-time dose prediction in SABR, which can potentially reduce planning time. However, the model still requires expert manual tumour segmentations as input, which are time-consuming to create. We hypothesize that sphere approximations of tumours will decrease radiation oncologist effort while maintaining accurate dose predictions, expediting treatment eligibility assessments and dose escalation analysis. By optimizing this workflow, we aim to improve SABR planning efficiency and expand patient access to timely treatment.

Methods:

This study utilizes multi-lesion lung cancer cases (n = 125) from the Verspeeten Family Cancer Centre, curated without exclusion based on sex, race, age, or gender to ensure broad applicability. The aforementioned model was previously trained with 80% of the multi-lesion plans with CT scans, an initial dose estimation, and anatomical structure segmentation as inputs and serves as the foundation for this study. For the remaining 20% of plans, the planning target volumes (PTVs) were replaced with spherical approximations determined by three methods: (1) average centroid distance, (2) maximum centroid distance, and (3) volume-matched radius. The dose predictions made using the spherical approximation methods were compared to using the original PTVs via the maximum dose delivered to the healthy organs (heart, esophagus, chest wall, trachea, spinal canal and great vessels), mean absolute error (MAE), gamma analysis, and percentage of lung volume receiving ≥20 Gy (lung V20). Statistical significance was assessed with a two one-sided t-test (TOST).

Results:

As shown in Figure 1, the maximum dose to organs at risk (OARs) is highly consistent across all methods. MAE, gamma pass fraction, and lung V20 are also highly consistent across all methods. TOST also establishes non-inferiority across all OARs.

Discussion:

The strong similarity in dose prediction performance between spherical approximations and actual tumour contours supports streamlining segmentation for patient eligibility assessment. This optimized SABR treatment planning workflow holds significant potential in reducing labor costs before patient eligibility is confirmed and enabling medical specialists to focus on improving treatment outcomes. When combined with future semi-

automated lesion segmentation tools, this method could further minimize manual workload and accelerate the planning process.

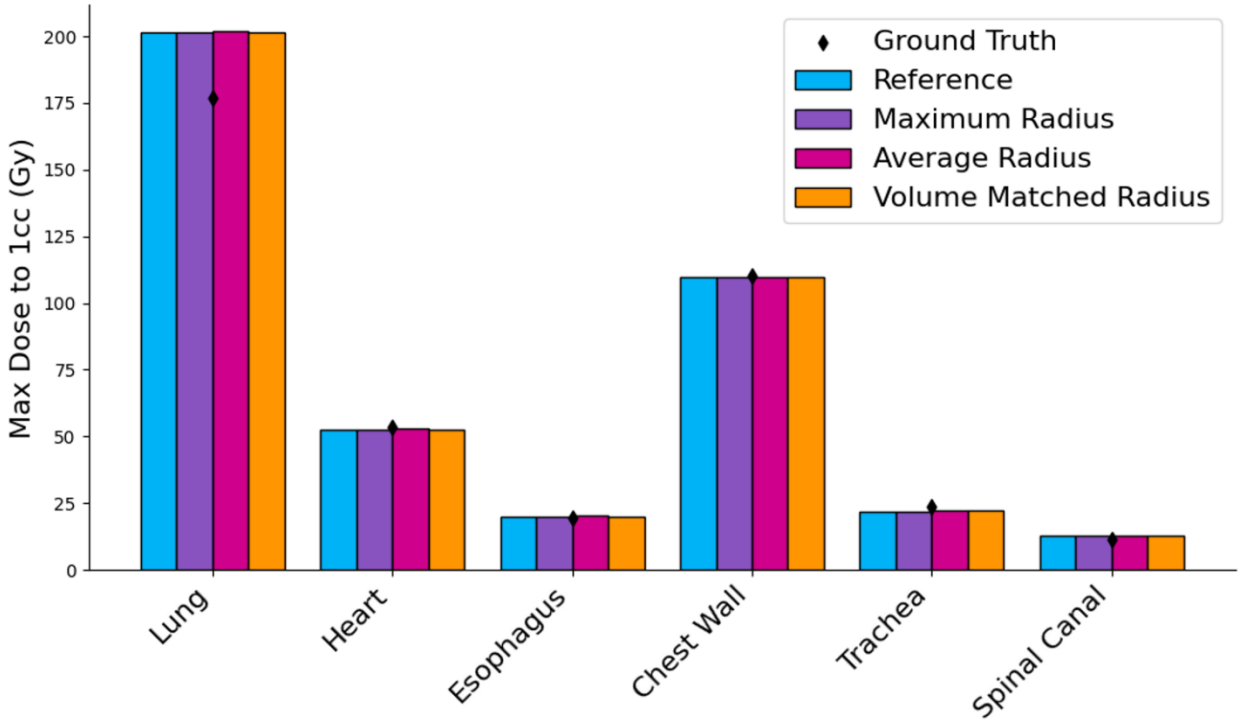

Figure 1. Bar plot comparing maximum dose (Gray) delivered to each organ at risk (OAR) across dose distributions generated using spherical approximations and the original PTV segmentation

Poster #101

Harnessing Eye-Gaze as a Novel Input Modality for Measurement and Quantification in Digital Pathology

Alana Lopes[1], Aaron D. Ward, PhD[1,2], and Matthew Cecchini, MD[3,4]
[1]Departments of Medical Biophysics, [2]Oncology, and [3]Pathology, Western University, London ON, Canada
[2]Department of Pathology and Laboratory Medicine, London Health Sciences Centre, London ON, Canada

Introduction: Pathologists diagnose disease through microscopic examination and analysis of tissue samples. Accurate and timely pathology reporting is critical in oncology, guiding clinical management, prognosis assessment, and therapeutic decision-making. Precise measurement and enumeration of specific histologic features directly inform tumor grading and staging to support clinical decisions. Traditionally, pathologists evaluate tissue on glass slides under a microscope; however, pathology is increasingly transitioning to digital assessment using scanned slides. The standard computer mouse is the most common input modality for a digital interface; however in the context of digital pathology, this input modality may be inefficient for image assessment. The use of eye-tracking technology for pathologists to interact with and assess digital pathology images is potentially a more efficient input modality for digital pathology. The objective of this pilot study was to assess the capability of eye-gaze as an input modality by comparing the accuracy and efficiency of eye-gaze-based measurements and enumeration to mouse-based measurements and enumeration, in the context of digital pathology.

Methods: Eight hematoxylin and eosin-stained whole-slide images from six cases of head and neck squamous cell carcinoma (HNSCC) were digitized using a Grundium Ocus 40 scanner. Three measurement tasks were performed per case: tumor-to-margin distance, depth of invasion, and nerve diameter (18 measurements total). For one case, enumeration of mitotic figures was performed. A single pathologist completed measurements and enumeration in two separate sessions, one week apart: first using a standard mouse and subsequently using eye-gaze input captured by a Tobii Pro Fusion eye tracker. For each method, measurement and enumeration points were marked by pressing a keyboard button at the mouse cursor or gaze location. Accuracy and completion times were compared between the two modalities. The System Usability Scale (SUS) was used to assess subjective impression of the user interface in both sessions and qualitative feedback was subsequently provided by the pathologist for each modality.

Results: The average percent difference and standard deviation between mouse-based measurements and eye-gaze-based measurements was (-0.4 $\pm$ 5.4)%, where a negative value indicates the eye-gaze-based measurement was smaller than the mouse-based measurement. Similarly, the average and standard deviation of time to perform the measurements was (3.4 $\pm$ 2.8)s and (7.1 $\pm$ 4.8)s, for mouse- and eye-gaze, respectively. Enumeration of mitotic figures was completed in 144.0s and 154.8s when using mouse and eye-gaze, respectively, with one additional mitotic figure being counted with eye-gaze. The SUS score was 75% and 55% for the first and second session, respectively, indicating the mouse-based input was more user-friendly. Feedback from the pathologist revealed eye-gaze was difficult to use for precision tasks (i.e., measurements), but was optimal for enumeration tasks.

Conclusions: This pilot study demonstrates the feasibility of eye-gaze as an input modality for measurement and enumeration in digital pathology. Ongoing work seeks to optimize the user-interface for eye-gaze and to expand this study with additional observers.

Poster #102

Evaluation of a Commercial Deep-Learning-Based Contouring Software for CT-Based Gynecological Brachytherapy

Haechan J Yang[1,3], John Patrick[2], Jason Vickress[2], David D'Souza[2], Vikram Velker[2], Lucas Mendez[2], Maria Mansur Starling[2], Aaron Fenster[3], Douglas Hoover[2]
[1]Schulich School of Medicine and Dentistry, Western University, London, Ontario, Canada,
[2]Department of Radiation Oncology, London Health Sciences Centre, London, Ontario, Canada,
[3]Robarts Research Institute, Western University, London, Ontario, Canada

Introduction: High-dose-rate (HDR) brachytherapy is important for managing gynecological cancers. As part of brachytherapy planning, surrounding organs must be segmented, which is time-consuming and prone to interobserver variability. AI-based segmentation has previously shown enhanced efficiency for external beam radiotherapy; however, the presence of applicators makes it more challenging in brachytherapy. Our objective is to evaluate Limbus Contour, a newly released commercial deep-learning based auto-contouring software, for use in HDR gynecological brachytherapy.

Methods: We collected 30 gynecological brachytherapy CT datasets (19.5–28 Gy in 3–4 fractions) from the Verspeeten Family Cancer Center from January 2018 to December 2022. Clinical and AI-generated contours for bladder, bowel, rectum, and sigmoid were obtained. Five patients were randomly selected for retrospective manual re-contouring by four radiation oncologists. Contouring was repeated 2 weeks later with the AI contours as the starting point ("AI-assisted" approach). Comparisons amongst clinical, AI, AI-assisted, and manual retrospective contours were made using Dice similarity coefficient (DSC) and unsigned difference in the highest dose delivered to 2cc of organ (D2cc).

Results: DSC between clinical and AI contours was 0.92, 0.79, 0.62, 0.66 for bladder, rectum, sigmoid, and bowel, respectively. The mean unsigned D2cc difference was lowest for the rectum and sigmoid (0.21 Gy/fraction) and highest for bowel (0.38 Gy/fraction). The agreement between fully automated AI and clinical contours was generally not different compared to agreement between AI-assisted and clinical contours. AI-assisted interobserver agreement was better than manual interobserver agreement across all organs and metrics (Figure 1). AI-assisted contouring significantly reduced contouring time compared to manual approach (7.7 ± 3.4 vs. 14.1 ± 4.6 minutes per patient, $p < 0.001$)

Conclusions: The agreement between AI or AI-assisted contours against the clinical contours was similar to manual interobserver agreement. Implementation of the AI-assisted contouring could enhance clinical workflow by reducing both contouring time and interobserver variability.

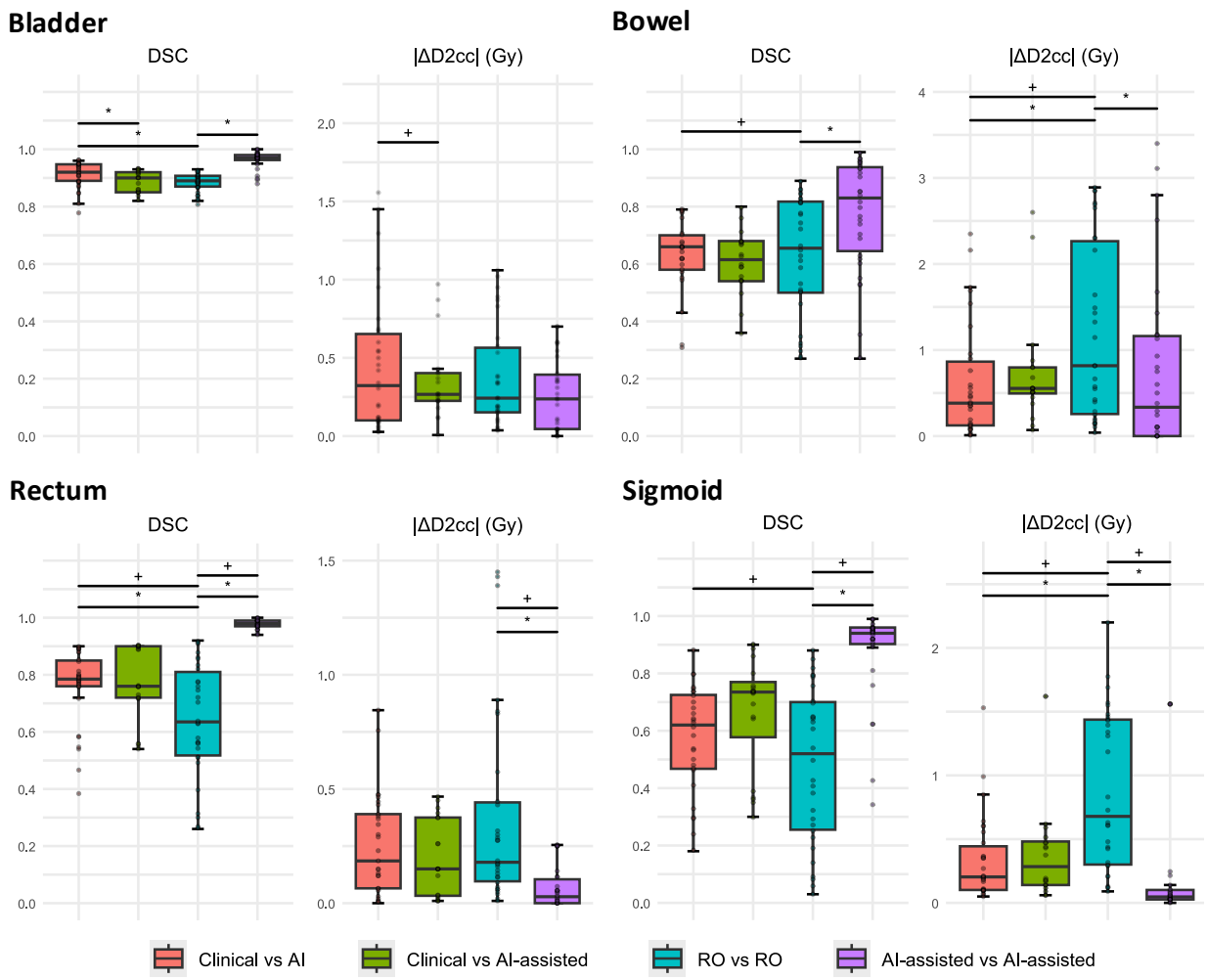

Figure 1: Dice similarity coefficient (DSC) and unsigned difference in the highest dose delivered to 2cc of organ (|ΔD2cc|) between clinical, AI, AI-assisted, and manual retrospective (RO) contours. Statistically significant differences in mean values are indicated by an asterisk (*) and differences in variances are indicated by a plus sign (+).

Poster #103

Non-Invasive Imaging of SynNotch-Engineered NK-92 Cells Targeting a Highly Tumor-Specific Antigen in Ovarian and Pancreatic Cancer

Alexa Smith[1,2], Anthony Arena[2,3], Ying Xia[2], John Kelly[2], Trevor Shepherd[4,5], John A. Ronald[1,2]

[1]Western University Department of Medical Biophysics, [2]Robarts Research Institute, [3]Western University Department of Microbiology & Immunology, [4]Verspeeten Family Cancer Centre, [5]London Health Sciences Centre

Introduction: High-grade serous ovarian carcinoma and pancreatic ductal adenocarcinoma are among the most lethal malignancies, with five-year survival rates below 50%, underscoring the urgent need for more effective treatments. Chimeric antigen receptor (CAR) T cell therapy has transformed hematologic cancer treatment by engineering T cells to eliminate malignant cells. Researchers have attempted to adapt CAR therapies for solid tumors; however, translation remains challenging due to antigen heterogeneity, an immunosuppressive tumor microenvironment, and on-target off-tumor effects. A major limitation in adoptive cell therapy is the inability to track therapeutic cells *in vivo*, making it difficult to evaluate responses, efficacy, and toxicity. To address these challenges, we are developing Synthetic Notch (synNotch)-engineered Natural Killer (NK-92) cells targeting Alkaline Phosphatase Placental Like-2 (ALPPL2), a recently described highly tumor-specific antigen. NK-92 cells have been clinically tested, demonstrating promising efficacy and safety. The SynNotch system is a synthetic receptor that, upon antigen recognition, releases a transcription factor to drive the controlled expression of transgenes of choice. To allow tracking of synNotch NK-92 cells *in vivo*, we previously engineered this system to induce expression of reporter genes for fluorescence imaging (FLI), bioluminescence imaging (BLI), and magnetic resonance imaging (MRI) for preclinical and clinical applications. This strategy aims to enhance the precision and therapeutic potential of engineered cell therapies for ovarian and pancreatic cancer.

Methods: To confirm ALPPL2 expression in target cells, Western blot (WB) and immunohistochemistry (IHC) were performed on three ovarian and two pancreatic cancer cell lines. Lentiviral transduction was used to engineer NK-92 cells with response elements encoding imaging reporters: dTomato for FLI, Firefly luciferase (FLuc) for BLI, and organic anion-transporting polypeptide 1B3 (OATP1B3) for MRI. A second transduction integrated the ALPPL2-specific SynNotch receptor. Engineered NK-92 cells were co-cultured with target cells at varying NK-to-cancer cell ratios. Antigen-dependent immune activation was assessed 24 hours post-co-culture using FLI and BLI.

Results: WB and IHC confirmed ALPPL2 expression in ovarian cancer cell lines SK-OV-3, Caov-3, EFO-27, and pancreatic cancer cell lines Panc-1 and Capan-1. These findings aligned with RNA-seq data, which showed ALPPL2 transcript levels of 0.2, 2.2, 6.9, 21.2, and 268.9 TPM, respectively. FLI qualitatively confirmed dTomato expression in synNotch-engineered NK-92 cells following co-culture with all target cell lines. BLI confirmed FLuc expression, with synNotch NK-92 cells co-cultured with low-antigen-expressing ovarian cancer cells showing a maximum radiance of 4.4×10^4 p/s/cm^2/sr, while those with high-antigen-expressing pancreatic cancer cells exhibited significantly higher radiance at 5.2×10^6 p/s/cm^2/sr. In contrast, control NK-92 cells (naïve or response element-only) generated minimal signal ($p < 0.0001$).

Discussion: This theranostic system combines advanced imaging and immune engineering for real-time monitoring of cellular therapies. By tracking localization, persistence, and tumor interactions, it aims to optimize efficacy, reduce toxicity, and guide adaptive treatments. For further clinical translation, we will utilize the human MRI reporter gene, OATP1B3, that selectively takes up a

gadolinium contrast agent. Future work will focus on integration of therapeutic transgenes and performing *in vivo* modeling with patient-derived xenografts (PDX) to evaluate clinical applicability.

Poster #104

POWER (Precision Oncology at Western University): Evaluating clinical impact of comprehensive genomic profiling of solid tumors in patient management

Pratibha Bhai[1,3], Jacob P. Turowec[1,3], Lee-Anne Pickard[4,5], Sadegheh Haghshenas[3], Karimi Karim[3], Haley McConkey[2,3], Stephanie Santos[1,3], Jennifer Kerkhof[1,3], Morgan Black[4,5], Daniel Breadner[4,5], Matthew Cecchini[1,2], Christopher Howlett[2], Laila Schenkel[1,3], Emilie Lalonde[1,3], Veera Panuganty[4,5], Jacques Raphael[4,5], Ana Lohmann[4,5], Eric Winquist[4,5], John Lenehan[4,5], Paul Stewart[4,5], Elena Tsvetkova[4,5], Mark Vincent[4,5], Ricardo Fernandes[4,5], Glenn Bauman[4,5], Stephen Welch[4,5#], Bekim Sadikovic[1,2,3#]

[1]Molecular Genetics Laboratory, Pathology and Laboratory Medicine, London Health Sciences Centre, London, Ontario, Canada

[2]Department of Pathology and Laboratory Medicine, Schulich School of Medicine and Dentistry, Western University, London, Ontario, Canada

[3]Verspeeten Clinical Genome Centre, London Health Sciences Centre, London, Ontario, Canada

[4]Department of Oncology, Schulich School of Medicine and Dentistry, Western University, London, Ontario, Canada

5 Verspeeten Family Cancer Centre, London Health Sciences Centre, London, Ontario, Canada

Objectives: Molecular profiling of solid tumors is essential in oncology practice, guiding access to molecularly matched therapies. Targeted molecular testing in the province of Ontario follows an indication-based ordering system and many patients are not eligible for CCO (Cancer Care Ontario) approved tumor specific genetic testing based on the stringent criteria, who may benefit from a genetic test and get eligibility for clinical trials and off label drugs. We aimed to assess patients with advanced solid tumors through the POWER (Precision Oncology at Western University) study, first of its kind Canadian study, prospectively assessing impact of expanded Pan-cancer NGS testing on patient management, in real-world oncology practice and evaluate the overall health system impact.

Design & Methods: 554 adult patients (≥18 years) with advanced solid tumors were subjected to Ion Torrent™ Oncomine™ Comprehensive Assay v3 (ThermoFisher). Pre-test and post-test questionnaire assessing the impact of test results on patient management was completed by referring physician.

Results: 79% of patients had clinically relevant variants, and 28% experienced changes in treatment eligibility. Additionally, 18% of patients got eligibility to clinical trials and off-label therapy and 19% (31/162) patients previously tested by tumor-specific panels, experienced management changes when tested through POWER. This study showed broader health system impact: access to safer treatment options (14.5%), change in management (17.6%), treatment sequence changed (17.3%), MOH (Ministry of Health) formulary treatment saved (12.5%).

Conclusion: These results underscore the benefits of Pan-cancer NGS testing over tumor-specific panels in guiding personalized treatment decisions, optimizing patient care, and enhancing healthcare delivery in oncology.

Poster #105

Identifying novel epigenomic DNA methylation biomarkers in myeloid malignancies

Carolyn Lauzon-Young[a,b], Sadegheh Hagshenas[b], Jennifer Kerkhof[b], Jessica Rzasa[b], Michael Levy[b], Karim Karimi[b], Cyrus Hsia[c], Benjamin Chin-Yee[c], Bekim Sadikovic[a,b]
a Department of Pathology and Laboratory Medicine, Schulich School of Medicine & Dentistry, Western University, London, Ontario, Canada
b Verspeeten Clinical Genome Centre, London Health Sciences Centre, London, Ontario, Canada.
c Pathology and Laboratory Medicine, London Health Sciences Centre, London, Ontario, Canada.

Background: Myeloid malignancies represent a diverse group of hematologic malignancies that pose significant diagnostic challenges. Despite advancements in next-generation sequencing (NGS) and standard of care methods a significant portion of patients lack definitive diagnosis. The presence of genetic variants of unknown significance (VUS) complicates diagnostic interpretation of NGS, creating barriers to providing optimal treatment. Our laboratory is recognized as a global expert in developing disease biomarkers called episignatures from DNA methylation profiles. We have pioneered the application of EpiSign technology in clinical settings worldwide to assist in rare disease diagnosis. I hypothesize that myeloid malignancy subtypes exhibit unique episignatures that can be elucidated to deliver novel and clinically relevant diagnostic solutions that significantly enhance patient care and ultimately improve treatment outcomes.

Objectives: My primary objective is to identify myeloid malignancy subtype specific DNA methylation episignatures by adapting the EpiSign discovery pipeline to the disease model of blood cancer.

Methods: DNA is obtained from peripheral blood and bone marrow samples of patients with clinically diagnosed myeloid malignancies including acute myeloid leukemia (AML), myelodysplastic neoplasms (MDS), myeloproliferative neoplasms (MPN), and myelodysplastic/myeloproliferative neoplasms (MDS/MPN); along with undiagnosed samples with clinically relevant genetic mutations, and proliferative/hypoproliferative benign disorders. DNA methylation levels are evaluated using the Illumina Infinium EPIC bead chip arrays. The clustering of cases and controls is examined with Euclidian clustering and multidimensional scaling. A support vector machine (SVM) classifier is used to evaluate the sensitivity and specificity of the biomarker for each cohort.

Results: Preliminary evidence revealed distinct DNA methylation patterns capable of separating types of myeloid malignancies from unaffected controls, and from other types of myeloid malignancies. Episignatures within myeloid malignancy subtypes present significant overlap using current methodologies and require further refinement.

Conclusions: Preliminary evidence from clinically diagnosed samples indicates DNA methylation episignatures can be used to categorize and stratify different myeloid malignancy types, enabling more accurate diagnostic classification of myeloid malignancies.

Special Thank You

Pamela Taylor

Jessica Da Silva

London Health Sciences Foundation

Thank you to our Sponsors

Gold

AstraZeneca

GSK

Lilly

NOVARTIS

Silver

abbvie

AMGEN

Bristol Myers Squibb

Daiichi-Sankyo

AstraZeneca

EMD SERONO

Eisai

Knight

Pfizer Oncology

RECORDATI RARE DISEASES

SERVIER

Bronze

IPSEN Innovation for patient care

Johnson&Johnson Innovative Medicine

Roche

Takeda Better Health, Brighter Future